

**Biodegradation of mono- and poly
aromatic hydrocarbons in a
contaminated aquifer originating from a
former Pintsch gas factory site**

Laboratory and field investigations

Johannes (Johan) Antonius van Leeuwen

Environmental Hydrogeology Group
Utrecht University
Utrecht studies in Earth Sciences No. 225

The examination committee:

Prof. dr. ir. T.J. Heimovaara

Technische Universiteit Delft – Delft, The Netherlands.

Prof. dr. ir. H.H.M. Rijnaarts

Universiteit Wageningen – Wageningen, The Netherlands

Prof. dr. F. Coulon

Cranfield University – Cranfield, England, The United Kingdom

Prof. dr. R. Meckenstock

University of Duisburg-Essen, Duisburg-Essen, Germany

Dr. H. Passier

Deltares – Utrecht, The Netherlands

ISBN: 978-90-6266-580-1

Geprint door: Ipskamp printing

© 2021, Johannes (Johan) Antonius van Leeuwen

All rights reserved. No parts of this publication may be reproduced in any form, by print or other means, without written permission by the author.

Author contact: johanvanleeuwen@yahoo.com

Biodegradation of mono- and polycyclic aromatic hydrocarbons in a contaminated aquifer originating from a former Pintsch gas factory site

Laboratory and field investigations

Biologische afbraak van mono- en polycyclische aromatische koolwaterstoffen in verontreinigd grondwater afkomstig van een voormalige vetgasfabriek

(met een samenvatting in het Nederlands)

Proefschrift

ter verkrijging van de graad van doctor aan de
Universiteit Utrecht
op gezag van de
rector magnificus, prof.dr. H.R.B.M. Kummeling,
ingevolge het besluit van het college voor promoties
in het openbaar te verdedigen op
woensdag 17 februari 2021 des middags te 12.45 uur

door

Johannes Antonius van Leeuwen

geboren op 30 juni 1971
te Deil

Promotor:

Prof. dr. ir. S.M. Hassanizadeh

Copromotoren:

Dr. N. Hartog

Dr. J. Gerritse

Dit proefschrift werd (mede) mogelijk gemaakt met financiële steun van Stichting Bodemsanering NS (SBNS) en instituut voor toegepast onderzoek Deltares.

*“Not all chemicals are bad, without chemicals such as hydrogen and oxygen
there would be no way to make water, a vital ingredient in beer”!*

Quote: Dave Berry

How it came to this...

As a kid I never took anything for granted asking questions how things could be or wondering why things are the way they appear to be. Currently I see the same thing with my own beloved kids, Aafke and Bauke, who are just as curious. However, while my children are happy and performing well in school, for me this has always been a struggle. I guess I never suited the system and although judged as a friendly and helpful kid, my performance at school has never been what parents or a teacher wanted to see, with bad grades along the way. Struggling along, in the end I dropped out during my bachelor's degree education. While my curiosity never died, I took the path of the working man in soil remediation through my dear friend Henk Versteegh who introduced me into this field of work. I started working as an apprentice field worker and soon worked myself up through the ranks to consultant and project leader in *in-situ* remediation and wastewater treatment. After several years in the business, I was initiating site assessments and remediation efforts for the Dutch railways. In this position, while working on several innovative projects at SBNS, Prof. Dr. Ir. S.M Hassanizadeh approached me, asking if I would be willing to prepare a guest lecture for the environmental hydrogeology course at Utrecht University. Arranging excursions, providing lectures and getting familiar with the science behind my profession was as much interesting as an eye opener. It felt like coming home, as if my curiosity from childhood was reborn, asking questions along the way. However, soon I found that these highly appraised and acknowledged scientists did not seem to have all the answers. When asking a question on three-phase flow someone said: "*Johan why don't you look into this subject yourself if you want to know the answer to this?*". Although I took a different direction into biodegradation of tar and learned how to brew beer along the way, I am very thankful for that answer and of everyone involved in the process that followed. First, I had to finish my BSc in civil engineering, and I accomplished it thanks to Ernst Rob, who supervised me during my work and thesis. After this, the dean of Earth Sciences

agreed that I could enroll as a PhD student as long as I would successfully complete the two most difficult courses the faculty provided at the time. This was thought of as a test of competence, and one of those turned out to be one of Majids courses! Prof. Ruud Schotting revealed himself as “the Master of Mathematics Teaching” and if it was not for him, it would still all be Greek to me. Even my curiosity towards DNAPL flow in the saturated subsurface was part of one of the courses, where absorbing the theory behind the subject felt as a great joy. Hereby I thank and extend my sincere gratitude to everyone that had part in achieving the effort towards this dissertation and that I inevitably forgot to mention.

Special thanks go to my promotor, Majid Hassanizadeh, who is the one that looked beyond my lack of education in the start, but somewhere saw opportunity and potential for achieving an intensive PhD research. I am very grateful for the opportunity you enabled and the trust in me working as an independent researcher. Also, I would like to thank my co-promotor Niels Hartog, who had the harsh job of shaping me into a scientist as daily supervisor. Thanks for the perseverance and wonderful discussions we had on hypotheses, data interpretations and common things in our daily work life as dads or employees of a research institute. I am very grateful to my co-promotor Jan Gerritse, who introduced me into the world of microbiology and experimental laboratory work. It was a wonderful experience when I curiously walked into the office as a client from the Dutch railways and asked for progress on microcosms. Instead of answering the question, you taught me how to do analysis on the gas chromatograph and how to interpret the results myself. This was definitely the kickstart for my sincere interest in experimental work, and lots more of collaborative work not included in this thesis with you followed after that.

During the years of doing research, I supervised several Msc and Bsc students that I was fortunate to work with. Stefanos Gkekas was the first and although our extensive work together during his internship and Msc thesis research did not

make it into this dissertation we fruitfully explored the wonderful world of two-phase flow, performing laboratory experiments and field tests on the mobility and recovery of tar as a function of temperature. After Stefanos, Thomas Wagner, Panos Panagiotis, Olaf Brock, Pim Zaremba, and Alex Hockin followed. Special thanks go to Alex, who worked with me during her internship and Msc research. Our work on enhanced bioremediation of pure phase Pintsch gas tar led to a chapter in this dissertation.

Colleagues from Deltares such as Fredericke Hannes who was always helpful in teaching me laboratory work and Marcelle van der Waals with whom I share a common research interest. Andre Cinjee, Rob van Galen and Erik van Vilsteren cannot be forgotten either for field work, or questions and help on LC analysis or ordering chemicals. Hilde Passier helped me focus and approach my research as a common project. Special thanks go to Hanneke van der Klis, who hired me as a researcher at Deltares, you supported me and arranged time to focus on the hardest part of all, finishing the writing. Special thanks go to Dik Welkers and Auke Oostra from the Dutch ministry of environment, who doubled my research budget that kickstarted this PhD research.

I would like to thank my colleagues at Utrecht university, Veerle, Thomas, Matthijs, Alraune, Suzanne, Hamed, Tang, Mandana, Enno, Vahid, Lifei, Jan, Gillian and Annuska. My special regards to Amir and Reza for the opportunity to travel with you during the geology field trip in Iran, which was truly an amazing and wonderful experience.

My gratitude goes to my parents Annie en Piet van Leeuwen, who always were proud and supportive, wondering which path I took in life. I will never forget how my dad Piet, always and often said to me: *“Johan you can achieve anything in life, as long as you really want to do it”*. I came to learn that this became a big part in making choices in life and taking on challenges.

Last but not least my greatest and deepest gratitude goes to my beloved wife Maaïke Salverda, for her understanding and sheer endless support on this important but also demanding quest. You talked me out of the ‘valley of shit’ and have given me the strength to fulfill this all; your endless patience, inspired and guided me through the jungle survival mission that is called a PhD research. Thank you very much dear!

Johan van Leeuwen

Utrecht

September 2020

Table of Content

1	<i>General introduction</i>	25
1.1	BACKGROUND.....	25
1.2	FATE AND TRANSPORT OF TAR IN THE SATURATED SUBSURFACE	27
1.3	WATER SOLUBLE PINTSCH GAS TAR COMPONENTS	30
1.4	REMEDICATION OF AROMATIC HYDROCARBONS	31
1.5	BIOLOGICAL DEGRADATION OF AROMATIC HYDROCARBONS	32
1.6	ENHANCED BIOREMEDIATION	36
1.7	RESEARCH OBJECTIVES:.....	40
1.8	THESIS OUTLINE	40
2	<i>The dissolution and microbial degradation of mobile aromatic hydrocarbons from a Pintsch gas tar DNAPL source zone</i>	43
2.1	INTRODUCTION	44
2.2	MATERIAL AND METHODS	46
2.3	RESULTS	56
2.4	DISCUSSION	65
2.5	CONCLUSIONS.....	74
2.6	ACKNOWLEDGEMENTS.....	75
2.7	SUPPLEMENTARY INFORMATION.....	76
3	<i>Enhanced source-zone biodegradation of Pintsch gas tar: The impact of substrate stimulation</i>	83
3.1	INTRODUCTION	85
3.2	MATERIAL AND METHODS	89
3.3	RESULTS AND DISCUSSION.....	93
4	<i>Anaerobic degradation of benzene and other aromatic hydrocarbons in a tar-derived plume: nitrate versus iron reducing conditions</i>	123
4.1	INTRODUCTION	125
4.2	MATERIAL AND METHODS	128
4.3	RESULTS AND DISCUSSION.....	135
4.4	CONCLUSIONS.....	151
4.5	ACKNOWLEDGEMENTS.....	152
4.6	SUPPLEMENTARY INFORMATION.....	153
5	<i>In-situ biostimulation and bioaugmentation of nitrate-reducing aromatic-hydrocarbon-degrading microbial communities</i>	159
5.1	INTRODUCTION	160

5.2	MATERIAL AND METHODS	163
5.3	RESULTS.....	169
5.4	DISCUSSION.....	186
5.5	CONCLUSIONS	191
5.6	ACKNOWLEDGEMENTS	192
5.7	SUPPLEMENTARY INFORMATION	193
6	<i>Discussion, conclusions and outlook</i>	195
	<i>Curriculum Vitae</i>	201
	<i>References</i>	203

Notations

The following table explains the used symbols in this study.

Symbol	Definition	Dimension
C_t^i	Equilibrium concentration of component i	
C_{aq}^i	Aqueous concentration of component i	
$C_t^{i,o}$	Initial concentration of component I in the tar	
C_{aq}	Aqueous concentrations	
k	permeability	m/d
K_{tw}^i	Tar to water partitioning coefficient	
M_t	Mass of the tar	
V_{aq}	Water volume	
M_{total}	Total mass of mono aromatic hydrocarbons	
K_{NW}	NAPL to water partitioning coefficient	
K_{NW}^{pred}	Predicted partitioning coefficient	
M_{total}^i	Total mass of component i	
V_{tar}	Volume of the tar	mL
ε	Isotope enrichment factor	
δ^{13C}	Isotopic signature for $\delta^{13C}/\delta^{12C}$	
δ^2H	Isotopic signature for δ^2H/δ^1H	
$\delta^HX(t)$	Lambda value at interval t	
H	Heavy isotope	
L	Light isotope	
X	Element	
Λ	Slope of linear regression for 2-D plot of δH^2 versus δC^{13}	

Summary

The focus of this research was on intrinsic and stimulated biodegradation of aromatic hydrocarbons in a Pintsch gas tar contaminated aquifer at a former manufactured gas plant. As a first step pure phase Pintsch gas tar samples from the subsurface have been analyzed for their chemical composition and physical properties. After determining the partitioning of tar components to the groundwater, intrinsic biodegradation has been studied *in-situ* under source and plume conditions. We next investigated potential for biostimulation and bioaugmentation through laboratory experiments and field-tests.

Tar is a relatively common contaminant in the subsurface. Manufactured gas plants have had a considerable contribution to this problem in the past in the urbanized environment. Pintsch gas is a type of manufactured gas, which was produced from gasoil instead of the more commonly used coal. Tar was produced as a by-product during gasification and most often discarded on site or in the close surroundings of the manufactured gas plant in an open pit or ditch. Tar as a by-product from coal gasification is well researched in the past decades. Although an estimated 10% of the total manufactured gas plants consisted of gasoil gasification, barely any studies on this type of source for contamination are performed. To assess the behavior of pure phase Pintsch gas tar in the subsurface, we analyzed its viscosity, density and interfacial tension. It was found that the tar closest to the entry point to the subsurface the least viscous (18.6 cP) was, the density (1.03 kg/m³) and the interfacial tension the lowest. Samples several tens of meters from the point of entry were determined at ± 40 cP, en 1.06 kg/m³ respectively. This indicates that the tar has biologically and or physically has weathered while being in the saturated subsurface for decades.

Another important part on the impact of Pintsch gas tar is the chemical composition. Tar genuinely exists of hundreds or more specific compounds, but primarily consists of cyclic aromatic hydrocarbons. These cyclic aromatic hydrocarbons are divided in mono- and poly cyclic aromatic hydrocarbons (MAHs and PAHs). MAHs such as benzene, toluene, ethylbenzene and xylenes (BTEX) are more water-soluble than PAHs such as naphthalene. While heavier molecular weight PAHs such as acenaphthylene or phenanthrene do barely dissolve in water or not at all. The water-soluble aromatic hydrocarbons are known to form large, contaminated groundwater plumes.

By means of GCxGC-TOFMS analysis on Pintsch gas tar we detected 948 individual hydrocarbon compounds, with PAHs being the most abundant. Naphthalene made up 21% of the tar composition, which is considerably more than the known 10% on average in coal tar. In addition, it was found that the content of benzene, toluene and xylenes (6.7 wt%) was considerably higher than that of coal tar (0.5 wt%). Moreover, less documented tar components were detected such as styrene, cumene and indene. These findings implicate that Pintsch gas is different to coal tar, it potentially is more mobile in the subsurface. Moreover, the chemical composition differs to coal tar, containing more volatile organics, which means potentially larger and prolonged fluxes to the bypassing groundwater.

For some compounds that make up the composition of tar such as toluene and xylenes it is known that they biodegrade relatively well under anaerobic conditions. For others such as benzene, naphthalene and phenanthrene much less is known and more specifically at nitrate reducing conditions. In this work we studied indications for intrinsic biodegradation within the source zone in the vicinity of the dense non aqueous phase liquid (DNAPL). One of the assessed parameters are metabolites produced from aromatic hydrocarbons by micro-organisms under anaerobic conditions.

When MAHs and PAHs are metabolized by anaerobic bacteria, new hydrocarbon compounds are formed also known as metabolites. These metabolites are usually more hydrophilic, although still toxic, than their mother compound due to for instance addition of fumarate or a carboxyl group. On one hand metabolites are an indication of active biodegradation however, if they are not further metabolized, they can remain as newly formed contaminants. During our investigations we detected 123 individual metabolites formed through biodegradation of Pintsch gas tar compounds. A substantial amount of the detected metabolites is carboxylated compounds from indene, naphthalene and other PAHs. These carboxylated compounds are indicators for active biodegradation in the vicinity of the DNAPL and can only be formed under anoxic conditions. That these metabolites have been formed in the subsurface and do not originate from the feedstock for the gasification process is plausible, due to the temperature ($\pm 700 - 1000^{\circ}\text{C}$) of the Pintsch gas process. Carboxylated hydrocarbon compounds would thermally be destroyed within this temperature range. That these carboxylated metabolites are extracted from the tar itself indicates that, after being formed in the groundwater they (partly) partition into the neighboring tar and can act as biological indicators not only from groundwater samples but also from pure phase tar samples.

In this research we detected nine carboxylated indene compounds, that we proposed as metabolites in the biodegradation pathway for indene through the carboxylation pathway.

When aromatic hydrocarbons are biodegraded at intrinsic conditions, this is called natural biodegradation. Sometimes natural biodegradation rates are sufficient to control contaminated groundwater plumes. In other cases, it is an option to stimulate biodegradation by means of addition of acceptor such as sulphate or nitrate. When micro-organisms are inoculated to the contaminated groundwater or sediment this is called bio-augmentation. In this research we

performed biostimulation and bio-augmentation test at the laboratory and subsequently at the field scale.

From microcosms we learned that biostimulation is feasible under groundwater plume as well as source zone conditions. Nitrate additions in general have a positive effect on bio degradational effects. However, at plume conditions benzene is degraded relatively well, while under source zone conditions virtually no degradation for benzene was observed. Remarkable is that under source zone conditions PAHs were biodegraded in the amended microcosms and the largest degradation was observed for the nitrate plus acetate amended microcosms. A possible explanation is that nitrate additions cause an expected growth of biomass, but relatively slow growing benzene degraders are outcompeted over faster growing naphthalene or phenanthrene degrading organisms. Moreover, nitrate additions possibly induce outcompetition between nitrate (NRB) and sulphate (SRB) reducing microbial groups.

Natural biodegradation in contaminated groundwater plumes is well understood for many contaminants under sulphate- or iron reducing conditions. However, especially the effect of nitrate on benzene degradation is still underexposed. From our investigations we found that benzene degraded relatively well at the fringes of the groundwater plume. Moreover, benzene biodegrades well in areas where nitrate is available in the surrounding groundwater downgradient as well as at the upgradient flank of the source zone. At the downgradient fringe benzene concentrations are relatively low compared to the upgradient flank of the source zone. Furthermore, at the downgradient fringe benzene is mostly found in conjunction with naphthalene and the composition is far less complex than on the flank of the source zone, where a large number of tar constituents are present due to mass transfer from the DNAPL to the aqueous phase. Still at these upgradient high concentration source zone conditions benzene is observed to biodegrade well in combination with nitrate presence.

Biostimulation and bio-augmentation field-tests show that high concentrations of added nitrate result in stimulated biodegradation. However, the adaptation of the micro-organisms to nitrate reducing conditions can be one year or more, specifically for benzene. This might be caused by slow growing benzene degraders that are known for doubling times of weeks or even months. It was concluded that dynamics caused by recirculation of non-amended anoxic groundwater only, did not contribute to extra biodegradation. From the field tests we see that biostimulation with nitrate can be an option for increased biodegradation of benzene and could be a feasible remediation option, although relatively long lag times were observed before anaerobic degradation could be determined under amended nitrate reducing conditions.

Biodegradation of aromatic hydrocarbons in contaminated aquifers offers us opportunities for bioremediation. Biostimulation of benzene degrading micro-organisms using nitrate is a useful option to the existing arsenal of remediation techniques. Biodegradation and biostimulation at source zone conditions in the vicinity of DNAPL is useful knowledge and could lead to new more sustainable ways of source zone remediation. However, more research would be necessary to come to such an approach. For instance, it is unknown if biostimulation of DNAPL impacted soil could lead to mobilization of the DNAPL and or larger fluxes of water-soluble hydrocarbons as a result of hydrophobic matrix loss due to more bioactivity.

Samenvatting

In dit onderzoek is de intrinsieke en gestimuleerde biologische afbraak van Pintsch gasteer componenten in de water verzadigde bodem onderzocht.

Als eerste stap zijn de compositie en de fysische eigenschappen van Pintsch gasteer monsters uit de bodem geanalyseerd op een voormalige Pintsch gasfabriek in Amersfoort. Aanvullend is de natuurlijke afbraak *in-situ* onderzocht van de wateroplosbare Pintsch gasteer componenten. Vervolgens zijn de mogelijkheden voor bio-stimulatie en bioaugmentatie onderzocht in laboratorium- en veldexperimenten en meer specifiek onder nitraat reducerende omstandigheden. De experimenten zijn uitgevoerd onder omstandigheden zoals worden aangetroffen in zowel de bronzone waar pure fase teer aanwezig is als ook in de grondwaterpluim waar alleen opgeloste teer componenten aanwezig zijn.

Teer is een relatief veelvoorkomende verontreiniging in de bodem. Gasfabrieken hebben in het verleden een aanzienlijke bijdrage gehad aan bodemverontreiniging met teer in het binnenstedelijk gebied. Pintsch gas is een type lichtgas, dat werd geproduceerd uit gasolie in plaats van de veelgebruikte steenkool. Het afvalproduct van de gasproductie, de teer werd meestal op het fabrieksterrein of in de directe omgeving gedumpt in een open kuil. Op gasfabrieken met teer afkomstig van steenkool, is relatief veel onderzoek uitgevoerd. Van de teer geproduceerd bij Pintsch gasfabrieken is nog nauwelijks iets bekend, terwijl $\pm 10\%$ van de gasfabrieken dit productieproces gebruikte. Om het gedrag van pure Pintsch gasteer fase te kunnen inschatten in de bodem, is de viscositeit, soortelijke massa en oppervlaktespanning vastgesteld. Het blijkt dat dicht bij het lozingspunt de teer het minst visceus (18.6 cP), de soortelijke massa het kleinst (1.03 kg/m^3) en het oppervlaktespanningsverschil met water het geringst is. Andere

teermonsters, verder van het lozingspunt zijn respectievelijk minder visceus, zwaarder en meer hydrofoob. Dit geeft aan dat er vertering heeft plaatsgevonden van de teer in de bodem.

Een ander belangrijk onderdeel is de chemische samenstelling van de Pintsch gasteer. Teer bestaat uit honderden en soms zelfs meer specifieke chemische componenten, maar voornamelijk uit cyclische aromatische koolwaterstoffen. De cyclische aromatische koolwaterstoffen worden onderverdeelt in vluchtige- en polycyclische aromatische koolwaterstoffen (VAK en PAK). De vluchtige aromatische koolwaterstoffen, waaronder benzeen, toluen, ethylbenzeen en xylenen (BTEX), zijn relatief goed wateroplosbaar. De poly aromatische koolwaterstoffen zijn veelal slecht of niet wateroplosbaar. De wateroplosbare stoffen vormen door grondwater stroming vaak grote pluimen met grondwaterverontreiniging.

Door middel van GCxGC-TOF-MS analyse hebben we 948 verschillende teercomponenten gedetecteerd in de Pintsch gasteer. Van dit aantal is het grootste deel polycyclische aromatische koolwaterstoffen. Naftaleen is in grote mate aanwezig, en maakt 21% (w/w) uit van het totaal. Bij koolteer is dit hoofbestanddeel $\pm 10\%$. Ook is gebleken dat ten opzichte van koolteer (0.5 wt%) een relatief groot aandeel (± 6.7 wt%) bestaat uit vluchtige aromatische koolwaterstoffen, zoals benzeen, toluen en xylenen (BTX). Maar ook minder bekende en beschreven componenten een belangrijk aandeel hebben in de samenstelling zoals: styreen, cumeen en indeen.

Dit betekent dat Pintsch gasteer een vloeibare teer is, die zich relatief makkelijk door de bodem kan verplaatsen. Dit betekent ook, dat er veel wateroplosbare componenten in deze teer aanwezig zijn, wat maakt dat er potentieel een grote en langdurige flux naar het grondwater kan optreden.

Van sommige teercomponenten is bekend dat ze redelijk tot goed afbreken onder anaerobe omstandigheden zoals toluëen, ethylbenzeen en xylenen van andere componenten zoals benzeen, naftaleen en fenantreen is veel minder bekend met name onder nitraat reducerende omstandigheden. In dit onderzoek hebben we aanwijzingen bestudeerd voor natuurlijke afbraak in de bronzone op de voormalige Pintsch gasfabriek, door middel van onder andere metabolieten onderzoek.

Als cyclische aromatische koolwaterstoffen worden afgebroken door micro-organismen, ontstaan er nieuwe chemische stoffen of afbraakproducten, de zogenaamde metabolieten. Deze metabolieten zijn meestal meer hydrofiel dan de moedercomponent en beter oplosbaar in water, maar nog wel giftig. Metabolieten worden vervolgens onderdeel van de verontreinigde grondwaterpluim. Enerzijds zijn metabolieten een indicator voor actieve biologische afbraak, maar als metabolieten niet verder worden afgebroken kunnen zij een extra verontreiniging vormen. In dit onderzoek hebben we 123 individuele metabolieten gedetecteerd, afkomstig van anaerobe afbraak van moedercomponenten uit de Pintsch gasteer. Veel van de gedetecteerde metabolieten zijn gecarboxyleerde teercomponenten. Deze gecarboxyleerde cyclische aromatische koolwaterstoffen zijn een indicatie van actieve biologische afbraak en hebben zich alleen kunnen vormen door anaerobe afbraak wat inherent is verbonden aan carboxylering. Dat de gecarboxyleerde metabolieten, zich ook daadwerkelijk in de bodem hebben gevormd is aannemelijk, omdat het Pintsch gas proces plaats vindt op $\pm 700 - 1000^{\circ}\text{C}$ en onderhavige gecarboxyleerde moleculen thermisch vernietigd zouden worden bij deze hoge temperatuur. Dit geeft aan dat hoewel de moedercomponent meer hydrofiel is geworden (deels) oplost in de teer en een aanwijzing is, dat in de nabijheid van de teer afbraak plaats vindt. In dit onderzoek zijn metabolieten, niet alleen aangetroffen in het grondwater waar zij worden gevormd door biologische processen, maar ook geëxtraheerd uit de pure fase teer. Dit betekent,

dat gevormde metabolieten in het grondwater, ondanks dat ze meer hydrofiel zijn geworden (deels) oplossen in de teer.

In dit onderzoek zijn negen nog niet eerder gepubliceerde gecarboxyleerde metabolieten van indeen gedetecteerd. Met behulp van de gedetecteerde metabolieten hebben we een afbraakroute voorgesteld voor anaerobe afbraak van indeen via het carboxyleringsmechanisme.

Als aromatische koolwaterstoffen stoffen intrinsiek worden afgebroken onder natuurlijke omstandigheden, wordt dit 'natuurlijke afbraak' genoemd. Soms is dit voldoende om de verontreinigde grondwaterpluim te beheersen. In andere gevallen kan de biologie worden gestimuleerd door het toevoegen van acceptor, substraat en/of micro-organismen. Als er acceptor of substraat wordt toegevoegd wordt dit bio-stimulatie genoemd en als er micro-organismen worden geïnoculeerd is dit bioaugmentatie. In dit onderzoek hebben we bio-stimulatie en bioaugmentatie experimenten uitgevoerd op laboratoriumschaal en aanvullend opgeschaald naar experimenten in het veld.

Uit de in het laboratorium geprepareerde microcosms is gebleken, dat stimuleren van anaerobe biologische afbraak mogelijk is zowel onder grondwaterpluim-, als bronzone condities. Stimulatie met nitraat laat positieve resultaten zien. Opmerkelijk is dat onder grondwaterpluim condities VAK relatief goed afbreken, maar onder bronzone omstandigheden niet. Onder bronzone omstandigheden vindt er biologische afbraak plaats van de twee en drie ringige PAK-verbindingen. Deze afbraak van PAK's vindt het meeste plaats in de met nitraat gestimuleerde microcosms in combinatie met acetaat. Hierbij moet worden opgemerkt, dat soms langere tijd geen nitraat in de microcosms aanwezig was, omdat dit was verbruikt. Hierdoor heeft sequentieel aanvullend sulfaat- en ijzerreductie en methanogenese kunnen plaatsvinden. Methaan is ook in significante hoeveelheden gemeten in de kopruimte van de microcosms.

Natuurlijke afbraak in de pluimzone is voor veel verontreinigingen een goed onderzocht onderwerp onder sulfaat- en ijzer reducerende condities. Echter met name het effect van nitraat op benzeenafbraak in het grondwater is nog onderbelicht. Uit dit onderzoek is gebleken dat benzeen aan de randen van de verontreiniging goed afbreekt. Benzeen breekt goed af, daar waar nitraat aanwezig is, zowel stroomafwaarts in de pluim als aan de stroomopwaartse zijde van de verontreiniging, in de bronzone. Aan de randen van de verontreinigde grondwaterpluim, zijn de concentraties stroomafwaarts relatief gering en is veelal alleen naftaleen en benzeen aanwezig in combinatie met nitraat. Echter uit dit onderzoek blijkt tevens dat benzeen goed afbreekt dicht bij de bronzone waar de concentraties in het grondwater relatief hoog zijn van alle wateroplosbare teercomponenten en nitraat aanwezig is.

In dit onderzoek is bio-stimulatie en bioaugmentatie als experimenten in het veld bestudeerd. Nitraat blijkt bij hoge concentraties van verontreiniging in het grondwater een stimulerend effect te hebben op de afbraak. Echter de vertraging waarmee dit optreedt kan een tot twee jaar duren, met name voor benzeen. De oorzaak hiervoor zit hem waarschijnlijk vooral in het feit dat benzeen afbrekers langzame groeiers zijn met soms verdubbelingstijden van weken tot maanden. Geconcludeerd is dat de veroorzaakte dynamiek van alleen rondspoelen van anaeroob grondwater, niet voor extra afbraak zorgt. In de veldexperimenten is vastgesteld dat biostimulatie van benzeenafbraak met nitraat een goede oplossing kan zijn als saneringsmethodiek, echter geduld moet worden betracht vooraleer de anaerobe afbraak onder nitraat reducerende omstandigheden op gang komt.

Biologische afbraak biedt veel mogelijkheden om bodemverontreinigingen af te breken. Dat benzeenafbraak door middel van nitraat additie gestimuleerd kan worden is een mooie aanvulling op het bestaande saneringsarsenaal. Dat biologische afbraak in de bronzone waar pure fase teer aanwezig is, kan worden

gestimuleerd is een belangrijke ontwikkeling richting een nieuwe saneringstechniek. Om tot een saneringsmethode te komen is vervolgonderzoek nodig, waarbij onder andere de mobilisatie van de teer door micro-organismen wordt bestudeerd, maar ook naar de effecten van preferente afbraak van PAK-verbindingen. Een bijkomend (negatief) effect zou kunnen zijn, dat door preferente afbraak van PAK's de VAK's in de waterfase worden geforceerd door verkleining van de hydrofobe matrix en daardoor een grotere flux ontstaat van opgeloste VAK's in het grondwater.

1 General introduction

1.1 Background

In the Netherlands 60% of the drinking water is derived from groundwater aquifers, this is more than 750 billion liters of groundwater every year (Geudens and Grootveld, 2017). Another 180 billion liters are applied for industrial and agricultural use (Vewin, 2008). In 60% of European cities with more than 100.000 citizens, groundwater is used at a faster rate than it is replenished (DobrisAssesment, 1995). At a world level, 33% of the world's fresh water supply is being derived from aquifers (Statistics Canada, 2009) and world population is ever increasing, the UN estimates that by the year 2050 there will be an additional 3.5 billion people on the planet and more and more people start living in the cities. This means water as a whole and groundwater from aquifers in specific is becoming an ever-scarcer commodity. While the need for groundwater increases, the quality of groundwater decreases due to human activities.

Contaminants enter the subsurface through waste disposal, spills and application of chemicals (McCarthy and Zachara, 1989), this poses a serious threat for sufficient drinking water supplies in the future. Aquifers for drinking water supply are generally recharged by groundwater infiltration of rain and surface water. Air, surface and subsurface pollutants can potentially reach groundwater aquifers by aqueous transport. Especially Non Aqueous Phase Liquid (NAPL) chemicals, which are used in urban and industrial areas, have the potential for serious long-term contamination of groundwater (Kueper et al., 2003). This is due to their limited, but still much higher than drinking water standards solubility and significant migration potential.

NAPL chemicals are used in large quantities for industrial use, particularly since the 1940s there are numerous NAPL contamination sites in North America and Europe (Mercer, 1993). DNAPLs such as chlorinated solvents; creosotes, coal tar, pesticides and chlorobenzenes are fluids that are immiscible with-, and denser than water. DNAPLs can migrate as a separate phase liquid into the unsaturated and saturated soil. Some NAPLs consist of one chemical compound such as perchloroethylene, but more often they consist of complex chemical mixtures like tar. Tar typically is a DNAPL consisting of hundreds of aromatic hydrocarbon components (Birak and Miller, 2009). Tar as a waste product was widely disposed of on manufactured gas plants (MGP) in the late 19th and early 20th century. In Europe alone more than 6500 MGP have been active and in the US approximately 33,000 – 54,000 sites have been estimated on former manufactured gas plants and creosote sites combined (Hatheway and Group 2012; Thomas and Brinckerhoff 2014). The composition of tars is highly variable (C. Gallacher et al., 2017; McGregor et al., 2012) due to a number of differing processes, mostly due to the retort oven design, type of feedstock and the temperature conducted during processing (Johnston et al., 1993). An estimated 5 to 10 % of all MGP were Pintsch gas plants (Hatheway and Group, 2012). Pintsch gas is a type of manufactured gas plant, that produces lighting gas from oil rather than coal as feedstock. Pintsch gas was used extensively in the lighting of railway coaches (American Scientific, 1898), (Figure 1-1). The composition of Pintsch gas varies mainly on the temperature of the production process and the type of feedstock oil. With increasing production temperature, higher percentages of benzene and toluene are formed (Egloff, G & Twomey, 1916). Due to the type of feedstock

and the specific Pintsch gas process, this type of waste tar potentially holds a

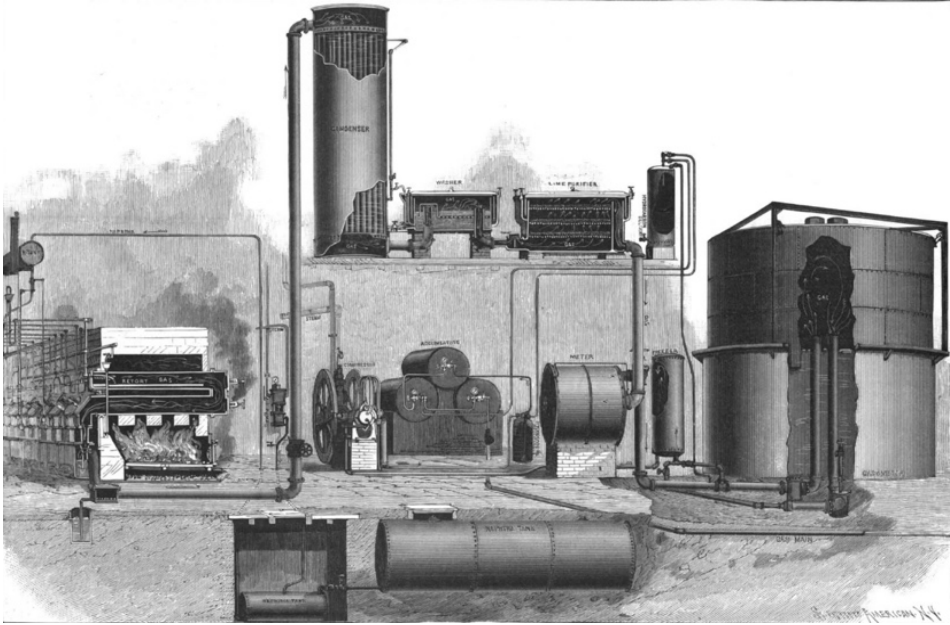


Figure 1-1: *Arrangement of Pintsch gas plant. From: Scientific American July 9, 1898.*

greater portion of volatile aromatic hydrocarbons compared to coal tars. Although Pintsch gas tar is different to coal-tars to the best of our knowledge research has only been reported once on the subject (Wanior and Ripper, 1993).

1.2 Fate and transport of tar in the saturated subsurface

The composition of the tar determines its physical properties such as density, viscosity and interfacial tension (Volkman et al., 1936). These are important parameters related to migration into the saturated subsurface as a separate phase liquid. Other parameters governing movement through the subsurface are the amount of tar, porosity, pore size, capillary pressure and wettability (Mercer, 1993). These parameters vary spatially in the subsurface due to lithological heterogeneity and inherent spatial soil variability (Elkateb et al., 2002). Due to soil heterogeneity DNAPL distribution is typically also heterogeneous. At the former Amersfoort Pintsch gas factory-site it was found that distribution of the

liquid tar was based on heterogeneities of the soil not noticeable with the naked eye (Figure 1-2). Only slightly finer grains or slightly more silt causes smaller pore radii and can act as capillary barriers. On the other hand, slightly coarser-grained soil with larger pores can provide preferential pathways or traps for pooled liquid tar. These pools form long-term sources for groundwater contamination.

Due to varying properties of DNAPL and soil heterogeneity, it's presence, quantity, distribution and potential migration rate should be characterized at each

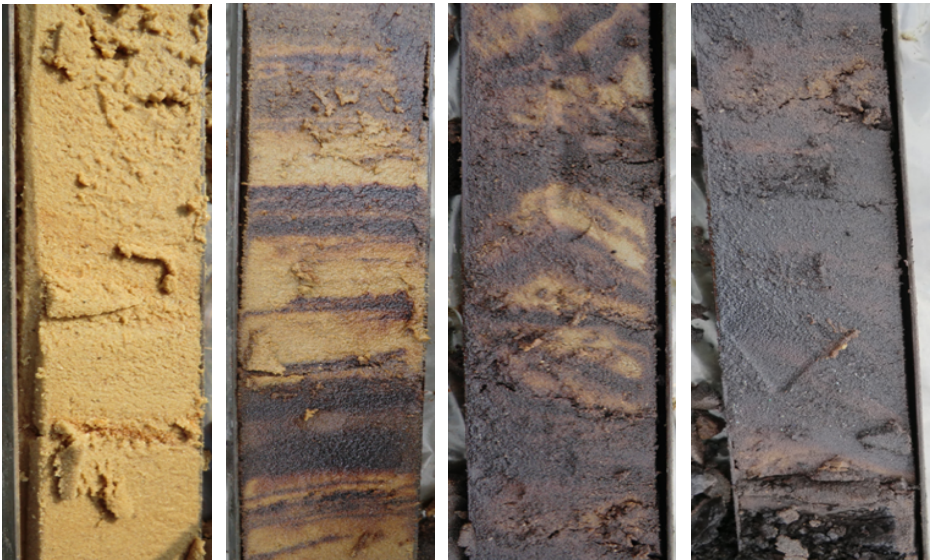


Figure 1-2: DNAPL distribution due to relatively small soil heterogeneity. Drill cores from Amersfoort Pintsch gas factory site. From left to right: Sand containing no DNAPL; Horizontal DNAPL layering (dark sections); High DNAPL saturation with smaller enclosures containing no DNAPL (light sections); Nearly full saturated DNAPL pool zone.

site individually. Envisioning distribution of DNAPL in the subsurface is usually performed by creating a site conceptual model (Figure 1-3).

Once Pintsch gas tar has invaded the saturated subsurface, water soluble aromatic hydrocarbons from the complex mixture start to dissolve into the surrounding groundwater and forms a contaminant plume. Generally, the effective solubility of single compounds is reduced due to the partitioning of multiple components.

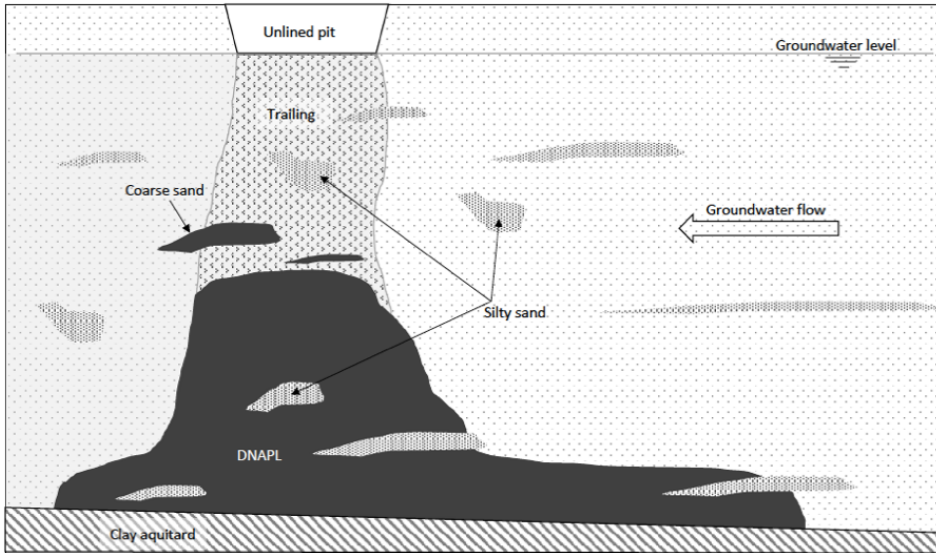


Figure 1-3: Site conceptual model, representing DNAPL distribution. Representing Pintsch gas tar DNAPL distribution at the Amersfoort site.

Dissolved concentrations of aromatic hydrocarbons in the groundwater are also dependent on the NAPL distribution. Where larger pools with smaller tar to groundwater contact surface, will have relatively less excretion or partitioning of water-soluble compounds compared to droplets and ganglia that have more tar to groundwater contact surface. As distribution of the tar has an effect on local groundwater concentrations it is desirable to have an understanding of the distribution at the smallest possible scale.

While using conventional drilling and sampling methods can be assessed at the decimeter or centimeter scale for NAPL distribution, camera footage can be assessed at the millimeter scale. One way of obtaining subsurface camera footage is by use of a camera cone penetration test probe. At the Amersfoort MGP site it was found that tar droplets in the trailing path tend to be relatively small and

spatially relatively far apart compared to the more saturated parts of the source zone (Figure 1-4).

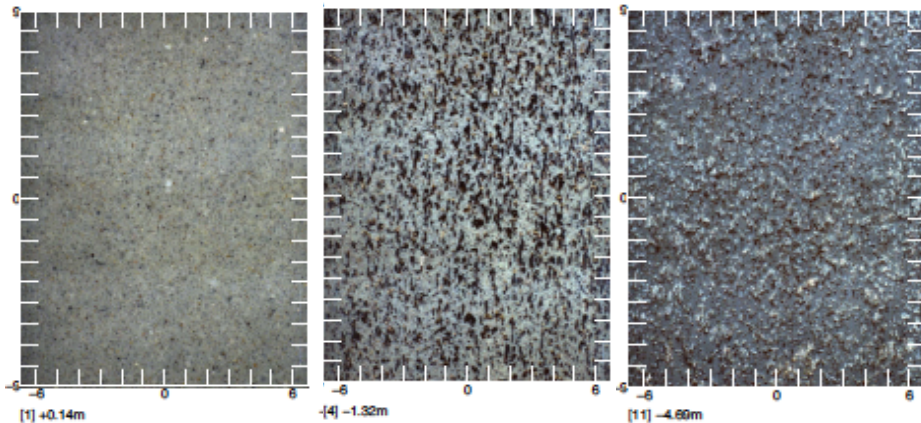


Figure 1-4: Pintsch gas tar distribution at the millimeter scale (12 x 18 mm). Photos are taken by a camera cone penetration test probe at the Amersfoort site. From left to right relatively small droplets left from the DNAPL trailing at ± 6 (+0.14 nieuw amsterdams peil (NAP) meter below ground surface (mbgs). Moderate DNAPL saturation at ± 7.30 (-1.32 NAP) mbgs and on the right fully DNAPL saturated soil, containing visible gas bubbles at ± 10.6 (-4.6 NAP) mbgs..

1.3 Water soluble Pintsch gas tar components

Once DNAPL invaded the saturated subsurface, the water-soluble compounds start partitioning into the surrounding groundwater, forming contaminated groundwater plumes (Peters and Luthy, 1993). Processes that mainly reduce the actual removal of the dissolved contaminants in the groundwater plume are due to retardation through adsorption to the soil matrix, dilution through dispersion and biodegradation by microorganisms (Aronson and Howard, 1997; Micic et al., 2007; Oka et al., 2011; Rogers et al., 2002; Wiedemeier, Todd H.; Rifai, Hanadi, S.; Newell, Charles J.; Wilsdon, John, 1999). At tar contaminated sites, besides the commonly reported BTEX in groundwater, other aromatic hydrocarbon compounds such as styrene, trimethylbenzenes, ethyltoluenes, indene, naphthalene, methylnaphthalenes and methylindenes, are encountered (Micic et al., 2007; Schirmer et al., 2006; Zamfirescu and Grathwohl, 2001), (Figure 1-5

and table 1). While adsorption and dispersion play an important role in the decrease of contaminant concentrations, generally biotransformation is the

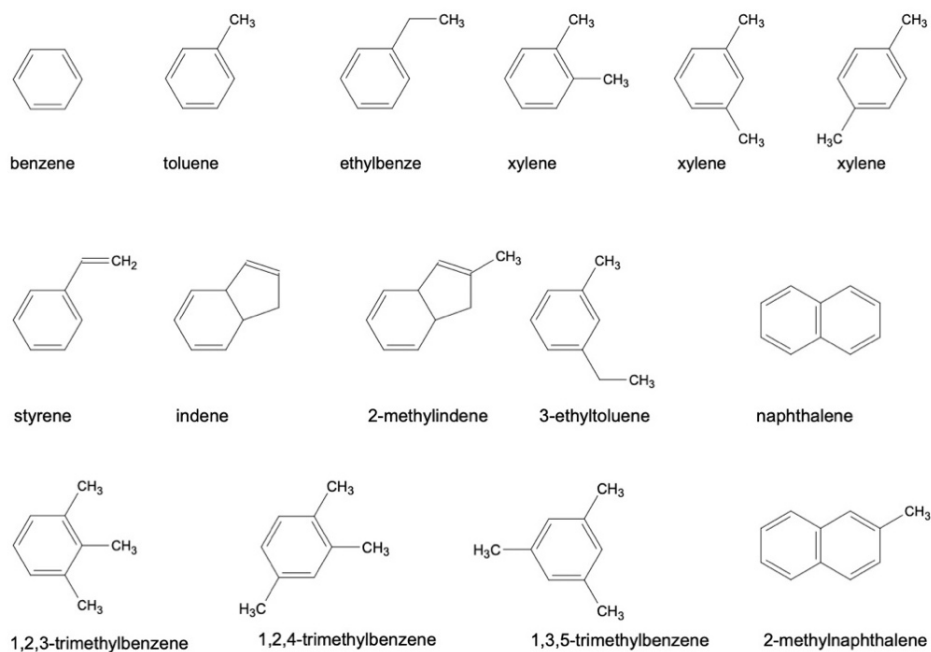


Figure 1-5: Molecular structures of most prominent water-soluble Pintsch gas tar constituents.

dominant attenuation process for BTEX and PAH (Rittman, Bruce E.; Barden, Michael J.; Lovley, Derek; Luthy, Richard G.; Mackay, Douglas M.; Bekins, Barbara, A.; Firestone, Mary K.; Lester, Stephen; Madsen, Eugene; McCarthy, Perry L.; Poeter, Eileen; Scifield, Robert; Warrick, Arthur W.; Wilson, John, 2000).

1.4 Remediation of aromatic hydrocarbons

Remediating these sources for groundwater contamination from the subsurface can be achieved through different techniques such as: dig and dump, pump and treat, steam injection, chemical oxidation, natural attenuation and bioremediation. Dig and dump is a blunt fast measure, however the amount of trucking through densely populated areas and dumping the contaminated spills elsewhere is not

particularly sustainable. Moreover, DNAPLs tend to migrate deeper into the subsurface than can be removed by an efficient dig. Pump and treat used in remediation, does hardly remove the NAPL as source of the groundwater contamination, and in most cases only prohibits extending of contaminated plumes. Other remediation techniques such as steam injection and chemical oxidation are intensive and relatively expensive techniques that hardly can be assessed as cost effective (Kaliampakos et al., n.d.; U.S. Department of Defense, 2009; USEPA, 1998). Less intensive and therefore cheaper and more sustainable techniques are favorable to address the extent of the problem such as natural attenuation or bioremediation.

1.5 Biological degradation of aromatic hydrocarbons

Biodegradation by natural populations of micro-organisms represents one of the primary mechanisms for destruction of hydrocarbon compounds in the environment (Leahy and Colwell, 2019).

Aerobic bacteria use oxygen during biodegradation to destruct hydrocarbons and cells convert them into CO_2 and H_2O . Oxygen availability is limited in groundwater and therefore quickly depletes due to microbial activity. When oxygen is not available, bacteria use nitrate (NO_3^-), iron (Fe^{3+}), manganese (Mn^{4+}), sulphate (SO_4^{2-}) or carbon dioxide (CO_2) to degrade organic compounds. The amount of energy micro-organisms obtain from reduction or oxidation varies per redox pair and each species of bacteria has differing enzymes to take advantage of different redox pairs. Within the natural groundwater conditions various terminal electron acceptors are present which are sometimes used in a specific order according to their decreasing redox potential (mV), (Figure 1-6).

Manganese and iron are generally readily available in the subsurface for microbial use. When Mn^{4+} and Fe^{3+} have been reduced, sulphate can serve as an electron acceptor and

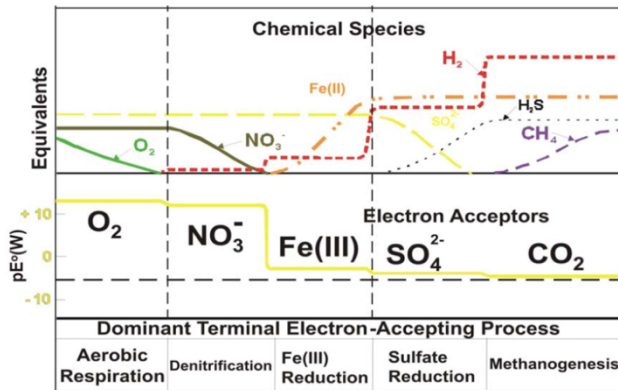


Figure 1-6: Dominant terminal electron acceptors (EPA, 2013)

is converted to sulfide (S^{2-}). However, the lower the redox potential of the acceptor, the slower the reactions and therefore it takes microbes more time to convert hydrocarbon contaminants under iron reducing circumstances for example than during denitrification.

Biodegradation of one or multiple monocyclic aromatic hydrocarbons compounds has been shown to occur in laboratory and field studies under both oxic and anoxic conditions (da Silva and Corseuil, 2012; Edwards and Grbic-Galic, 1994; Gibson et al., 1968b; Gieg et al., 2009). Biodegradation rates range widely and depend mostly on the molecular structure of the contaminant and the terminal electron-accepting processes (Foght, 2008; Meckenstock et al., 2016, 2015). Complex mixtures of aromatic hydrocarbon compounds in groundwater systems often lead to sequential attenuation of the individual components (Suarez and Rifai, 1999). Biodegradation rates for some compounds might increase, in different redox zones, while they decrease for others (Suarez and Rifai, 1999; Swartjes et al., 2011). Moreover, in complex mixtures, co-metabolism can enhance biodegradation of certain recalcitrant compounds (Swartjes et al., 2011). In contrast, certain compounds can inhibit biodegradation due to toxicity (Swartjes et al., 2011).

Benzene in particular is a known human carcinogen, has a high solubility and is known to be persistent in anaerobic environments (Vogt et al., 2011). While field studies have shown that under oxic conditions benzene biodegrades faster than toluene, ethylbenzene or xylenes (Alvarez et al., 1991; Suarez and Rifai, 1999), under anoxic conditions biodegradation of benzene is generally slower than other aromatic compounds (Weelink et al., 2010). Biodegradation of benzene under suboxic nitrate-reducing conditions has been observed (Coates et al., 2002a; Vogt et al., 2011), but its occurrence has been erratic in the laboratory as well as at the field scale (Suarez and Rifai, 1999). It has been suggested that benzene biodegradation in shallow aquifers is actually enabled by the presence of low oxygen concentrations, along the fringe of the contaminant groundwater plumes (Aronson and Howard, 1997). Nonetheless, to date a variety of bacteria using nitrate as electron acceptor and capable of benzene degradation, have been isolated in a pure culture (Vogt et al., 2011). More recently, laboratory studies showed strictly anaerobic degradation of benzene or naphthalene under nitrate reducing conditions related to *Peptococcaceae* (members of the order *Clostridiales*) and benzene carboxylase genes (*abcA*) (Atashgahi et al., 2018; Cupples, 2016; Kleemann and Meckenstock, 2011; van der Waals et al., 2017; van der Zaan et al., 2012; Vogt et al., 2011). To our knowledge, no studies have been published on the relevance of *Peptococcaceae* and the presence of benzene carboxylase genes (*abcA*) throughout contaminated plumes at the field scale.

Polyaromatic hydrocarbons (PAHs) consist of multiple fused aromatic rings and are formed during the incomplete combustion of organic matter at high temperatures (Haritash and Kaushik, 2009). The stability of aromatic rings make PAHs more difficult to biodegrade (Meckenstock and Mouttaki, 2011). Moreover, PAHs that have larger molecular weight are less soluble in water; this means they are more persistent in the environment (Meckenstock and Mouttaki, 2011).

Degradation of MAH and PAHs in plume zones has been shown under methanogenic, nitrate and sulfate reducing conditions (Chakraborty and Coates, 2004; Gieg and Suflita, 2002; Meckenstock et al., 2016). Toluene is generally considered the most readily degraded MAH component under all reducing conditions (Foght, 2008). While several pure strains of toluene-degrading bacteria have been found, pure isolates of benzene-degrading cultures are rare; generally a consortia of bacteria are present (Atashgahi et al., 2018; Dou et al., 2010; Foght, 2008; van der Zaan et al., 2012). Low molecular weight PAHs are relatively more volatile and soluble in water and therefore are more readily biodegraded than high molecular weight PAHs (Ghosal et al., 2016).

Mono- and poly aromatic hydrocarbons are often conjointly present in source zones at tar contaminated sites, and competitive inhibition and co-metabolism can affect the degradation rates (S. W. Chang et al., 2002; Dean-Ross et al., 2002; Meckenstock et al., 2004; Phelps and Young, 1999a; Safinowski and Meckenstock, 2006). Co-metabolism is thought to be particularly important for biodegradation of high molecular weight PAHs (≥ 4 -rings) (Meckenstock et al., 2016; Safinowski et al., 2006). Studies have also shown that multiple MAHs and PAHs can be degraded by a common enzyme system in bacteria (Balachandran et al., 2012; Stringfellow and Aitken, 1995a). Heterocyclic PAHs, commonly found in petroleum and coal-derived tars, have also been shown to be co-metabolized by the same enzyme system as naphthalene, inhibiting naphthalene degradation (Annweiler et al., 2001b; Meyer and Steinhart, 2000).

Biodegradation has shown to occur in water dissolved contamination, and it is assumed that degradation cannot take place directly in the nonaqueous phase but will be indirect (Fountain, 1998). Biodegradation in the vicinity of the DNAPL is complex due to continuous mass transfer to the aqueous phase and partitioning of water dissolved components back into the DNAPL (Figure 1-7). Therefore biodegradation studies in general aim for plume conditions. However DNAPL containing source zones do not exist of 100% DNAPL saturated pores and water pockets or enclosures will remain potentially sustaining contaminant

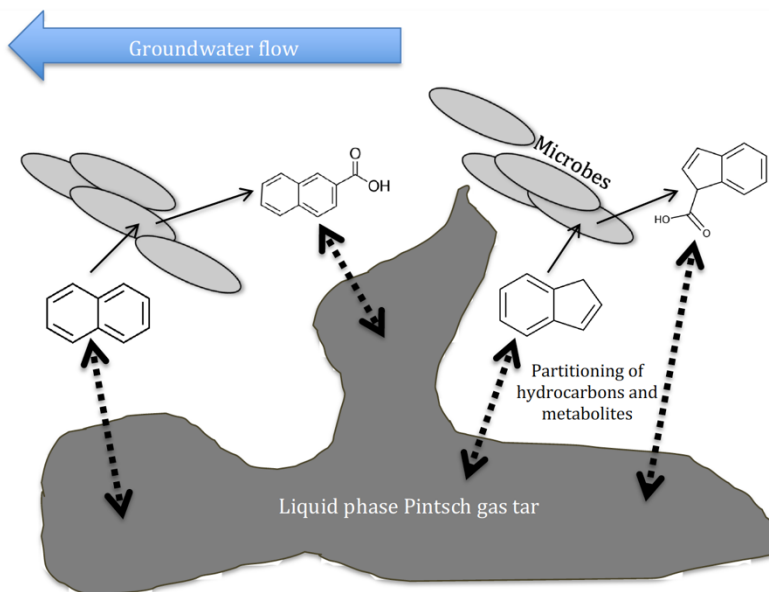


Figure 1-7: Aromatic hydrocarbons and their metabolites partitioning from DNAPL into bypassing groundwater

degrading microbial culture (Meckenstock et al., 2014). Few studies have examined the potential for source zone degradation of hydrocarbon contaminated sites (Müller et al., 2017; Ponsin et al., 2014; Ramos et al., 2013).

1.6 Enhanced bioremediation

The addition of electron acceptors to a contaminated site is known as biostimulation or enhanced bioremediation. Most aromatic hydrocarbons in

general can be removed from groundwater by natural attenuation, however, enhanced biodegradation is generally faster and can be more efficient (Farhadian et al., 2008). Enhanced biodegradation supports the natural biodegradation processes by addition of extra terminal electron acceptor and nutrients (biostimulation) and or competent degrading microorganisms (bioaugmentation) to the contaminated aquifer (Scow and Hicks, 2005). Nitrate and sulfate are commonly used additives in field-scale enhanced biodegradation tests (Istok et al., 1997; Langenhoff et al., 1996; Ponsin et al., 2014; Schreiber and Bahr, 2002; Sublette et al., 2006).

Adding nitrate is an attractive option due to the low cost and relatively high solubility as compared with oxygen (solubility of nitrate and oxygen at 1 bar and 25°C per 100ml: 91.2 g and 4 mg respectively). Manganese and iron are generally readily available in the subsurface for microbial use. However, the lower the redox potential of the acceptor, the slower the reactions and therefore it takes microbes more time to convert hydrocarbon contaminants. The reduction rates of nitrate are also high when compared to manganese, iron or sulphate reducing circumstances.

Enhanced biodegradation of monoaromatic hydrocarbons (MAH) within the contaminant plume can be a good strategy, however as long as the source zone is not affected the flux of contaminants can last for decades or longer.

In situ bioremediation techniques such as biostimulation and bioaugmentation are more complicated to perform at field scale rather than laboratory scale testing due to heterogeneity of the subsurface. To overcome heterogeneity effects, impact prospects of engineered bioremediation can typically be tested by push-pull tests. In a push-pull test, *in situ* microbial activities are determined by injection of a test solution, containing a tracer and one or more reactive solutes. If lag times prevail at a contaminated site, the result of a one well injection and extraction test can be affected by groundwater flow. In such situation well to well recirculation tests are more suitable than single well push-pull tests (Ponsin et al., 2014).

Within a tar source zone in conjunction with MAH additionally polyaromatic hydrocarbons (PAH) are present. Enhanced biodegradation of MAH and PAHs can be achieved through stimulation with additional electron acceptors, substrates or both. Stimulated biodegradation of MAHs and PAHs been shown under nitrate- and sulfate-reducing conditions (Al-Bashir et al., 1990; Ambrosoli et al., 2005; T.P.A. Bregnard et al., 1996; B. V. Chang et al., 2002; Coates et al., 1997; John D. Coates et al., 1996; Durant et al., 1995; Eriksson et al., 2003; Meckenstock et al., 2016). MAH degradation has been shown under chlorate reducing conditions (Chakraborty and Coates, 2004; Solís-González and Loza-Tavera, 2019; Weelink et al., 2010). However, to the best of our knowledge, no studies showing PAH degradation under chlorate-reducing conditions have been reported. Enhanced biodegradation of MAHs and PAHs by stimulating co-metabolism has been shown through the addition of substrates, including, for example, acetate, succinate, glucose, lactate and methanol (Ambrosoli et al., 2005; Maillacheruvu and Pathan, 2009; Teng et al., 2010; Vaidya et al., 2018, 2017; Yuan and Chang, 2007; Zhang et al., 2015a). The addition of acetate, alone or in combination with an electron acceptor, can enhance the degradation of benzene, toluene, naphthalene, acenaphthene, fluorene, phenanthrene, anthracene, and pyrene (Ambrosoli et al., 2005; T.P.A. Bregnard et al., 1996; Coates et al., 2002b; Ebihara and Bishop, 2002; Liu et al., 2017; Maillacheruvu and Pathan, 2009; Mittal and Rockne, 2008; Rahman et al., 2018; Zhang et al., 2017, 2015a). Enhancement with acetate is believed to be primarily caused by co-metabolism and has been shown to depend on the specific reducing conditions (Yuan and Chang, 2007).

Limited studies have shown enhanced PAH degradation using succinate as a substrate, alone or in combination with an electron acceptor. Succinate has been shown to enhance the degradation of naphthalene, acenaphthylene, fluorene, phenanthrene, anthracene, pyrene and benzo(a)pyrene (Burd and Ward, 1996;

Teng et al., 2010; Vaidya et al., 2017). Few studies have investigated the biodegradation of natural mixtures of PAHs from hydrocarbon contaminated sites (e.g. coal-tar or creosote) (Eriksson et al., 2000; Rothermich et al., 2002) and in most cases only one of MAHs or PAHs are measured.

Source zone biostimulation was previously considered infeasible as the high concentration of aqueous phase contaminants were thought to be toxic to microbes (Langevoort, 2009). It is not known to what degree source zone degradation is taking place, nor the possible effects of source zone biostimulation with alternative electron acceptors or substrate. The interaction of hydrocarbons is important to consider for in-situ bioremediation technologies, in particular for source zones where high concentrations of complex mixtures of MAHs, PAHs, and hetero-cyclic hydrocarbons are present. Few studies have examined the potential for source zone remediation of hydrocarbon contaminated sites through biostimulation (Müller et al., 2017; Ponsin et al., 2014; Ramos et al., 2013).

1.7 Research objectives:

The objectives of this research were to gain a better chemical and microbial understanding of natural processes at tar contaminated sites, containing a large extension of DNAPL in the source zone and Pintsch gas tar in specific. The following research questions were addressed:

- How the composition of Pintsch gas tar differs from known coal tars composition and this effects partition to water characteristics?
- What is the effect of nitrate presence on biodegradation in the aquifer on Pintsch gas tar compounds and benzene in specific?
- Does biodegradation occur at source zone conditions and can it be enhanced?

1.8 Thesis Outline

This thesis is organized in six chapters, with four chapters (chapter 2 – 5) as stand-alone manuscripts.

Chapter 1: An introduction to the problem of liquid tar as dense non aqueous phase liquid (DNAPL) and Pintsch gas tar in specific in the saturated zone, biodegradation of tar constituent in the subsurface and enhanced bioremediation complications.

Chapter 2: presents the composition and water-soluble characteristics of Pintsch gas tar. This chapter shows how Pintsch gas tar is different to coal tars by looking at density, viscosity, primary components and amount of light molecular aromatic hydrocarbons. Additionally, it is described how metabolites originating from the tar indicate biodegradation in the vicinity of the DNAPL in the subsurface and a novel anaerobic biodegradation pathway through carboxylation for indene is proposed.

Chapter 3: demonstrates the potential for enhanced bioremediation in source zones by indigenous species to the contaminated aquifer. Long term microcosm

experiments were conducted in the laboratory with sediment from a Pintsch gas factory tar contaminated site. The sediment which was sampled from a source zone area contained a complex mixture of mono- and polycyclic aromatic hydrocarbons. Microcosms were prepared using several acceptors such as nitrate, sulfate, chlorate and succinate and acetate were added as substrate.

Chapter 4: is dealing with natural attenuation of Pintsch gas tar contaminated groundwater plumes in a nitrate containing aquifer. The occurrence and extent of anaerobic degradation of aromatic hydrocarbons was investigated in the contaminant plume using molecular, isotopic and microbial analysis. Variations in composition and concentrations of the complex contaminant mixture were studied by looking at dispersion, adsorption and biodegradation processes in the source-, plume- and fringe zone of the iron and nitrate reducing plume.

Chapter 5: incorporates an enhanced biodegradation field test of BTEX and other water-soluble aromatic hydrocarbons. The described well to well recirculation setup, suited the long lag times for adaptation of the indigenous culture to nitrate reducing conditions. The efficacy of biostimulation by injection of nitrate, and bioaugmentation by addition of a benzene degrading culture harvested from a chemostat in the laboratory are presented. The effects of biostimulation and bioaugmentation are assessed using several strategies including geochemical analysis, microbial and molecular methods, tracer test, and compound specific isotope analysis.

Chapter 6: Presents a general discussion and conclusions on this research, including suggestions for future work.

2 The dissolution and microbial degradation of mobile aromatic hydrocarbons from a Pintsch gas tar DNAPL source zone

Published as:

Van Leeuwen JA, Hartog N, Gerritse J, Gallacher C, Helmus R, Brock O, Hassanizadeh SM, The dissolution and microbial degradation of mobile aromatic hydrocarbons from a Pintsch gas tar DNAPL-source zone, Science of the Total Environment, vol. 722 (2020), article number 137797

Abstract

Source zones containing tar, a dense non-aqueous phase liquid (DNAPL), can contaminate groundwater for centuries. A common occurrence of tar is at former Pintsch gas factories. Little is known about the composition and fate of contaminants dissolving from Pintsch gas tar DNAPL. In this study, we determined the composition and water-soluble characteristics of mobile aromatic hydrocarbons and metabolites from biodegradation in the DNAPL contaminated groundwater at a former Pintsch gas tar plant. We assessed the factors that determine the fate of the observed groundwater contaminants. For the collected tar samples, density (1.03 – 1.06 kg/m³) and viscosity (18.6 – 39.4 cP) are relatively low compared to other coal tars. Analysis showed that phenanthrene is the primary component rather than naphthalene, and that the Pintsch gas tar contains a relatively high amount of light molecular aromatic hydrocarbon compounds, such as benzene, toluene, ethylbenzene and xylenes (BTEX). Less commonly reported components, such as styrene, ethyltoluenes, di-ethylbenzene, 1,2,4,5-tetramethylbenzene, were also detected in water extracts from Pintsch gas tar. Moreover, 47 relatively hydrophilic specific metabolites were found to be present within the tar samples. Metabolites present within the tar suggest biodegradation of mobile aromatic Pintsch gas tar compounds occurred near the DNAPL. Based on eleven detected suspect metabolites, a novel anaerobic biodegradation pathway is proposed for indene. Overall, our findings indicate that Pintsch gas tar has higher invasive- and higher flux properties than most coal tars due to its relative low density, and viscosity, high content of water-soluble compounds.

2.1 Introduction

Former manufactured gas plants (MGPs) are major sources of groundwater contamination (Birak and Miller, 2009). In Europe, around 4500 former MGPs, exist (Thomas and Brinckerhoff, 2014) and in the US the estimated number on

former MGP sites ranges from 1000 to 2650 (Hatheway and Group, 2012). Pintsch gas is a specific type of oil gas, that was used extensively in the lighting of railway coaches (American Scientific, 1898). Liquid phase tar is a waste product formed during the gasification process at MGP sites. Its presence in the subsurface is usually due to leakage from pipes, tanks, and storage chambers, or deliberate dumping (Thomas and Churchill, 2014). Once in the subsurface, both residual- and pool zone tar can act as a groundwater contamination source for decades or even longer (Kueper et al., 2003). Tars are complex mixtures consisting of hundreds of hydrocarbon compounds (Peters and Luthy, 1993). The composition of tars is in general highly variable due to differences in gasification processes, especially the type of feedstock, retort oven design, and the processing temperature (C. Gallacher et al., 2017; Johnston et al., 1993; McGregor et al., 2012; McRae et al., 1999). Our knowledge of composition of tars is rather limited (Bruce et al., 1991; Electric Power Research Institute, 1993). With increasing production temperature, higher percentages of benzene and toluene are formed (Egloff, G & Twomey, 1916). An estimated 5 to 10 % of all MGP were Pintsch gas plants, mostly situated at railway sites (Hatheway and Group, 2012). However, research into this type of contamination is nearly nonexistent (Wanior and Ripper, 1993).

The aim of our study was to gain a better understanding of Pintsch gas tar and its potential environmental impact on the saturated subsurface. Therefore, we determined the composition and physical properties of the Pintsch gas tar as dense non aqueous phase liquid (DNAPL) from a contaminated site in detail. We investigated partitioning behavior of the water-soluble hydrocarbons leaching from the tar into groundwater from multiple tar samples, and dilution effects due to potentially caused by heterogeneity in tar distribution. Moreover, we looked into hydrocarbon compounds produced from biological activity at pooled tar zone conditions. Leading to insight of its impact on groundwater quality, and the potential for degradation. We determined the water-soluble components by

partitioning experiments on liquid phase tar and analyzed potential metabolites formed by anaerobic biodegradation. The overall aim of the study was to gain a better understanding of the risk posed by sites contaminated by Pintsch gas tar.

2.2 Material and Methods

2.2.1 Site description

The field site in this study is a former manufactured gas plant (MGP) located adjacent to the central railway station in the city of Amersfoort, the Netherlands (Figure 2-1). From 1910 to 1958, the factory produced lighting gas via the Pintsch gas process, and the by-product tar was dumped onsite in unlined pits. The site is situated at a geological transition area, where horizontal sand, peat on loam, and gravel layers shift into a more vertical glacial moraine pushed formation to the south.

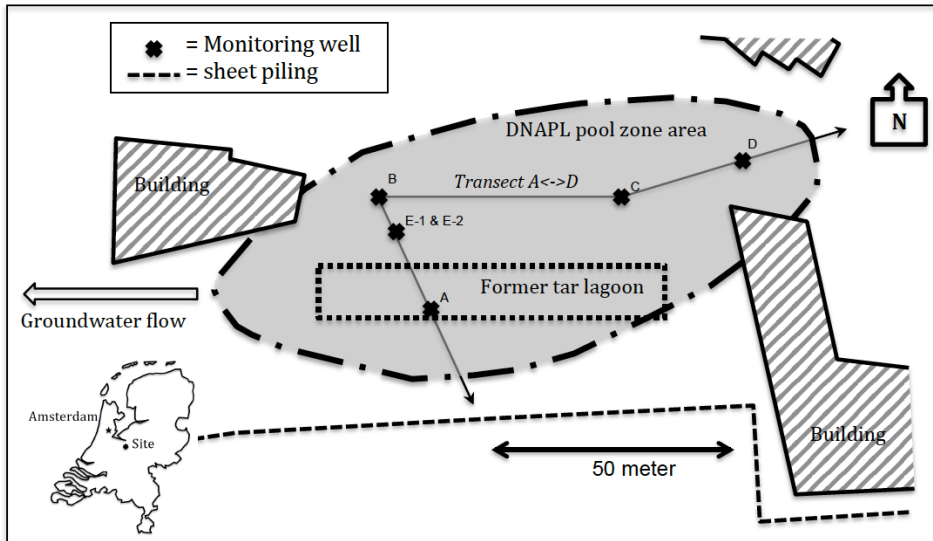


Figure 2-1: DNAPL pool zone area visualizing monitoring well locations for sampling. The DNAPL source zone covers an area of approximately 4500 m² and visualized by the gray area.

The aquitard at 12 meters below ground surface (mbgs) consists of a peat on loam layer thinning from north to south and is found less than 50 cm in thickness at the

west domain of the source zone area, resulting in probable loss of integrity of the aquitard (Figure 2-2). The source zone is considered the pool zone and residual zone combined. In the pool zone saturation of tar is large enough for the DNAPL to potentially flow as a single phase. In the residual zone saturation of the tar is relatively small and the liquid tar is entrapped, therefore not considered mobile. The source zone covers areas of $\pm 4,500 \text{ m}^2$ that contains the pooled and residual tar estimated at 2.8 million liter and 250,000 liters respectively. Residual tar is present below the former tar lagoon over a soil volume of $\pm 16,500 \text{ m}^3$, which extends above the pooled tar zone (Figure 2-1 and Figure 2-2). The extent of the pooled tar zone is approximately $11,000 \text{ m}^3$ of soil volume at the bottom of the shallow aquifer, where the tar has spread in the north-eastward dipping direction of the underlying thin aquitard.

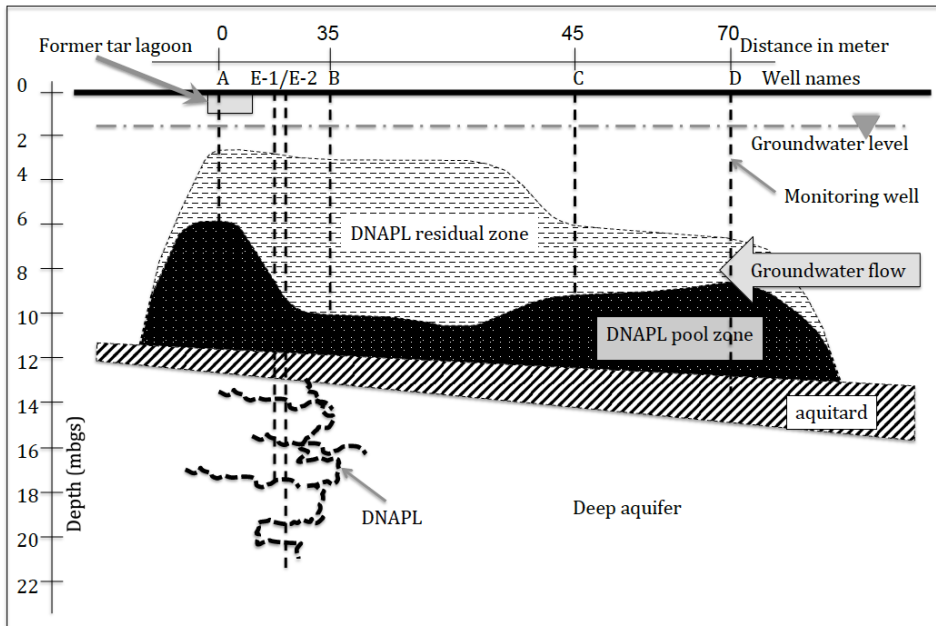


Figure 2-2: *Transect A<->D source zone is considered the pooled Pintsch gas tar (black area) plus the DNAPL residual zone (striped area) above the pooled Pintsch gas tar, residual and pool height can be interpreted from meter below ground surface (mbgs).*

In the year 2000, an engineered hydrogeological barrier was created by constructing two vertical steel sheet pile walls. The hydrogeological barrier forms a funnel-and-gate system in the shallow unconfined aquifer (Figure 2-2). Its main purpose is containment of the source and pool zone area and treatment of the groundwater plume by aeration. The direction of groundwater flow in the shallow aquifer is towards the southeast and shifts at the hydrogeological barrier towards the south-west. As a result, the groundwater interacts with the upgradient DNAPL. The bulk of the DNAPL is situated below the former tar lagoon and is regarded the point of entry in the subsurface and recognized as the source of the pool zone (Figure 2-2). From the source the DNAPL spread along the dipping aquitard towards the north. DNAPL was also detected in the deep aquifer, suggesting leakage through the confined clay/peat layer. In most monitoring wells within the pool zone area, the measured tar heights varied from 0.3 to 6 meters from the bottom of the well. Outline of the pool zone is given in (Figure 2-1).

2.2.2 Field work

Prior to our research, 40 boreholes have delineated the DNAPL containing pool zone. The wells were placed on the clay/peat aquitard. Pool height was monitored 20 times over a 19-month period. DNAPL monitoring well A is situated directly under the former tar lagoon, where the bulk of the liquid tar is present and the subsurface is saturated with tar from 6 to 12 meter below ground surface. This well is considered to hold the least weathered composition on site. Weathering was relatively low, due to the high pore saturation of tar and therefore relatively low tar to groundwater contact. The other three wells chosen for sampling represent the gravity driven migrated liquid tar over along the dipping aquitard towards the north. To gather tar for experimental use from the deep aquifer, two monitoring wells E-1 and E-2 were selected (17 and 21 mbgs) in the deep aquifer. A reference well was chosen. (not shown in Figure 2-1). Reference well, pb323,

was situated 140-meter up gradient from the source zone. Groundwater was collected from the reference well to determine the background composition of contaminants and metabolites, and for use in the partitioning experiments. DNAPL levels in monitoring wells were measured using a Solinst interface probe model 122. The liquid phase tar was sampled using a peristaltic Watson-Marlow 604 U/R pump, through low-density polyethylene (LDPE) tubing from the bottom of monitoring wells at a flow rate of ± 1 L/hr. At this rate, 10 to 60 L liquid phase tar could be obtained per sampling well without extracting any groundwater.

Four Pintsch gas tar samples from four monitoring wells within the DNAPL pool zone were sent to SGS laboratories in Rotterdam, The Netherlands, to analyze viscosity, density and water content. Analyses were performed according to ASTM D7042, D4052 and D1744 standards, respectively.

2.2.3 Pintsch gas tar composition

One liquid phase tar sample, extracted from well A, was analyzed by comprehensive two-dimensional gas chromatography combined with fast time of flight mass spectrometry (GCxGC-TOFMS). A LECO (St. Joseph, Michigan) time of flight mass spectrometer on a model Pegasus 4D was connected to an Agilent 7890A gas chromatograph equipped with a LECO thermal modulator. The TOF ion source was fixed at 200°C and masses between 45 and 500 μm were scanned at a 200 spectra/second rate. The detector voltage was set at 1700 V and the applied electron ionisation voltage at 70 eV.

The sample was prepared by accelerated solvent extraction (ASE) as described by (Christopher Gallacher et al., 2017); it was sealed and stored at 4°C prior to analysis. Dichloromethane, used as solvent for extraction of the Pintsch gas tar sample, was purchased from Fisher Scientific (Loughborough, U.K.). D₁₀-Phenanthrene from Sigma-Aldrich (Gillingham, U.K.) was purchased as calibration standard. Calibration standards were prepared using a standard

mixture containing all 16 EPA PAHs, purchased from Thames Restek (Saunderton Bucks, U.K.). Four deuterated PAHs were purchased from Sigma-Aldrich (Gillingham, U.K.). Extraction from the tar sample was performed using an ASE 350 Accelerated Solvent Extraction system (Dionex, Camberley, UK) and 10-mL stainless steel extraction cells. A comprehensive description of the sample preparation prior to analysis is given in supplementary information.

All standards and extracts were analyzed with the primary oven temperature programmed to be at 75°C for 1 minute, increasing by 12°C/min to 120°C, then increasing by 3°C/min to 310°C, and held at this temperature for 10 minutes. The secondary oven and modulator temperatures were programmed at a 20°C higher offset relative to the primary oven. The modulation period was 6 seconds with a 1.3 second hot pulse time and a cool time of 1.7 seconds. The injection port temperature was 250°C, with a split ratio of 50. One microliter of sample was injected for each run using an MPS2 twister auto-sampler (Gerstel). Helium was used as the carrier gas, with a flow rate of 1.0 mL/min.

We used as primary column a mid-polar TR-50 MS (30 m x 0.25 mm i.d. x 0.25 µm film thickness) was (Thermo Scientific, Loughborough). As secondary column, a non-polar Rtx-5SilMS column (1.5 m x 0.25 mm i.d. x 0.25 µm film thickness) was used, supplied by Thames Restek. The columns were connected via a Thames Restek Press-tight connector.

The chromatograms were processed using LECO ChromaTOF software (Version 4.50.8.0) to search for and identify all peaks with a signal-to-noise (S/N) ratio greater than 10 according to (Christopher Gallacher et al., 2017), which is the limit of quantification. Signal to noise was set at this ratio to avoid mass phantom peaks, which potentially hide other peaks for identification. Statistical analysis was carried out using Microsoft Excel (Version 14.3.7), Minitab version 16 and Matlab R2013a. All peak areas were normalized by dividing the peak area by the sample weight and then the D₁₀-Phenanthrene peak area and taking the fourth root of the normalized value. Fourth root data formation is required as without data

pre-processing the large range of peak intensities within the dataset results in small peaks contributing less towards the principal components regardless of their chemical importance. Taking the fourth root also allows the analysis to focus on the presence/absence of contaminants rather than their concentration, and so relates the data to the primary production method used instead of changes in relative concentration, which may have occurred due to environmental factors.

2.2.4 Bench scale partitioning tests

To study the potential environmental impact of Pintsch gas tar on groundwater, two partition tests were performed. The first test was conducted to study differences in partitioning behavior on several Pintsch gas tar samples obtained from the pool zone on site. Maximum saturation for water soluble tar compounds was conducted by the method described by (Linda S Lee et al., 1992), which lead to choosing a 1:4 tar to water ratio in the experiment.

The second partition test was performed to mimic dilution effects from tar components into groundwater, due to heterogeneity in distribution of tar in a pool zone. Accordingly, tar was exposed to increasing water volumes and the water-soluble fraction of hydrocarbons of the DNAPL quantified. Approximately 2 mL of Pintsch gas tar, 12 mL of shallow aquifer, sampled at a location 175-meter upgradient unimpacted groundwater, and 2 mL of 0.5 g/L mercury chloride (HgCl_2) were added to a 20-mL glass vial with 4 mL headspace and sealed with a Grace silicone, PTFE lined magnetic gold cap. The unimpacted groundwater contained 24.1 mg/L nitrate, 35.0 mg/L sulphate, and 0.1 mg/L manganese (III). No BTEXN above detection limit of $<10 \mu\text{g/L}$ were identified. To produce equilibrium conditions for the dissolving tar components, the vials were rotated top over bottom on a Labinco 528 test tube rotator at 9 rpm and 12°C for 4 weeks. Then, the samples were placed upside down in a vial rack and kept for 7 days in the dark at 12°C according to the procedure proposed by (Peters and Luthy, 1993). After equilibration, $2 \times 1.5 \text{ mL}$ of aqueous phase was sampled and placed

in clean 2-mL glass vials for further gas and liquid chromatography analysis. From the 2 mL vials, 100 μ L subsamples were diluted in 12 mL demineralized water in 20-mL vials capped with PTFE-lined silicone septa for GC-MS headspace analysis.

Concentrations for BTEX partitioned into the water phase were used to determine the content originating from the tar sample for each of the detected monoaromatic hydrocarbon (MAH) components by calculating partition coefficient for each compound. Calculations are based on the method outlined in (Rixey, 1999). The method assumes linear partitioning, where the equilibrium concentration of component i in the tar C_t^i and its aqueous concentrations C_{aq}^i can be related by their partitioning coefficient K_{tw}^i :

$$K_{tw}^i = \frac{C_t^i}{C_{aq}^i} \quad (1)$$

Also, a mass balance of component i gives:

$$V_t (C_t^{i,0} - C_t^i) = V_{aq} C_{aq}^i \quad (2)$$

where M_t is the mass of the tar, $C_t^{i,0}$ is the initial concentration in the tar, C_t^i is the concentration in the tar following the dissolution in the aqueous phase, V_{aq} is the water volume in the test bottle. C_{aq}^i is the aqueous concentration of component i . Combining equations 1 and 2 gives:

$$\frac{1}{C_{aq}^i} = \frac{1}{C_t^{i,0}} \left(\frac{V_{aq}}{M_t} \right) + \frac{K_{tw}^i}{C_t^{i,0}} \quad (3)$$

The experiment is repeated with different volumes of water in different test. Then, if a straight line can be fitted to the plot of $1/C_{aq}^i$ versus V_{aq}/M_t , from the slope, $1/C_t^{i,0}$, and the y-intercept, $K_{tw}^i/C_t^{i,0}$; K_{tw}^i and $C_t^{i,0}$ can be determined.

To quantify the most soluble tar components (MSTC), three bottles of 100 mL, one bottle of 2 L and one bottle of 10 L (Schott, VWR) were prepared; all tests were done in duplicate. Also, two 1-L bottles in duplicate were prepared as control samples, where one sample contained only groundwater and no tar, and the second one was filled with demineralized water and tar. Groundwater

mixtures were prepared with the tar from well A, which is considered to be the most obtainable unaltered tar from the site. Six bottles containing groundwater from unimpacted reference well pb323 and with the tar ratio of water to tar being 10:1, 21:1, 43:1, 360:1, 722:1 and 3613:1. HgCl_2 was added at 25 mg/L to inhibit any biodegradation processes. The bottles were sealed with butyl rubber stoppers. The bottles were stirred with a magnetic bean at 150 rpm during five weeks in a dark constant temperature room at 12°C. Subsequently stirring, was stopped and the bottles were kept at the same conditions for seven days for equilibration. To prevent tar contamination during later sampling procedure, 150 mm long steel syringe needles containing stylet wires were placed through the stoppers. Syringes were placed on the inserted needle to prevent any air water interaction.

2.2.5 Aromatic compound analysis by GC-MS

To quantify the volatile mono-aromatics in the liquid phase tar, a GC-MS analysis method was developed. The following solvents were tested for extraction: hexane, methanol, acetone, and dichloromethane (DCM). After preliminary testing, 100 mL of each solvent was added to 2 grams of tar in 100-mL borosilicate bottles with butyl rubber/PTFE lined septa. Methanol and hexane did not dissolve all the tar, and soot or carbonaceous sorbents were still visible as black particles. DCM appeared to dissolve the butyl rubber septa and did not dissolve all the soot. In literature, often a mixture of hexane and DCM is mentioned as extraction solvent (Ghosh et al., 2000; Hodges and Richardson, 1996; Jonker and Koelmans, 2002; Jonker and Smedes, 2000; Lee, 2000). Testing a hexane-DCM mixture showed no proper mix with the water phase and therefore was not suitable as solvent. Based on the least solvent volume required to fully dissolve the tar including the soot, acetone was chosen as solvent.

Acetone extract injection volume was 10 μL , with a split ratio of 1:6. The temperature program was set at: start 40°C hold for one min., then to 200°C at 10°C/min. and third step to 300°C at 20°C/min. and hold 1 min. A Varian ms-

column was employed, type VF-624, with dimensions 30 m x 0.25 mm x 1.40 μm film thickness. Helium was used as carrier gas at 1 mL/min., and the injector temperature was set at 250°C. For mass spectrometer, a Shimadzu QP-2010 plus was employed, mode EI/scan at a mass range of 29-300 amu. Deuterated compounds were used to show a high enough signal outside the natural mass distribution. Benzene-d₆, toluene-d₈, ethylbenzene-d₁₀, 1,3,5-trimethylbenzene-d₁₂ and naphthalene-d₈ were purchased from Sigma-Aldrich and used as internal standards. External standards, containing all relatively good water-soluble components from Pintsch gas tar were prepared as solutions in methanol as 2, 20, 50, 100 and 200 mg/L.

Gas chromatographic analyses of headspace analyses were performed on water samples from the tar to water partition tests on a Shimadzu GC-2010 and a PAL auto sampler. The same GC-MS method as for the acetone extracts was used. Injection volume was 250-500 μL , with a split of 1:5 – 1:10. Samples were collected from monitoring wells A, B, C, D, E-1 and E-2 at the site (Figure 2-1) and a GC-MS method was developed. The water samples were prepared and stored as described in section 2.2.

2.2.6 Metabolite analysis using LC-qTOF-MS

Analysis on metabolites was performed using liquid chromatography quadrupole time of flight mass spectrometry (LC-qTOF MS). To assess metabolites from mobile tar component degradation a target list was compiled. Subsequently, a method was developed for qualifying all targeted metabolites. For analysis, samples fixated with HgCl_2 at 25 mg/L to inhibit any biodegradation processes and were stored at -26°C for a maximum of 180 days. Prior to analysis 1.5 mL, from the field sample was filtrated and transferred into a 1.5 mL screw topped vial (VWR; cl. Gl. 32 x 11.6mm). Sample preparation is described in detail in the supplementary information. For quantification, a standard mix was prepared containing 2-Naphthoic acid, DL-benzylsuccinic acid, cinnamic acid, benzoic

acid, 4-hydroxy benzoic acid and 1-H-indene-3-carboxylic acid. First, 1 g/L stock solutions were prepared by dissolving 10 mg of those compounds in 10 mL methanol. From the stock solutions, a mixture was prepared and used to make standard series containing; 1, 5, 10, 25, 50, 100, 200 and 500 $\mu\text{g/L}$ of each compound. A hybrid quadrupole orthogonal accelerated time-of-flight mass spectrometer, in combination with a Bruker maXis 4G mass spectrometer (MQ0201G053, Bruker Daltonics, Bremen, Germany), was used with a mounted HD collision cell for higher maximum resolution and sensibility on low molecular compounds (<200 m/z). The Shimadzu Nexera UHPLC system contained a SIL-30A autosampler, binary pumping system (LC-30AD) and a column oven (CTO-20AC) Shimadzu, Kyoto, Japan (Prantle 2014). An Acquity UHPLC CSHC18 column (150mmx2.1 mm; 1.7 mm; Waters) was used. Electrospray ionization (ESI) was used to produce ions from macromolecules and compounds measured in negative ionisation mode. A pre-run of 8 minutes was used for equilibration of the LC column, and sodium acetate (CH_3COONa), (0.25 mM in 1:1 Isopropyl alcohol (IPA): H_2O) used as calibration liquid. MS-MS fragments for the standards and suspects were searched by using Auto MS-MS data. Broadband CID (bbCID) was then used for suspect screening and quantification. A full description of the developed method is given in the supplementary information.

For data acquisition and analysis, first, retention times of the standards were searched, based on their calculated exact masses, by using a software program DataAnalysis Compass IsotopePattern (omicX). Then, recovery of the reference compounds was calculated from the spiked samples and MS-MS fragments were searched in DataAnalysis, using Mol-files from Chemspider. In the second phase, all data generated, including exact masses, retention times, and MS-MS fragments (and in some cases also ion ratios), were used to produce an automatic screening method in TASQ. Settings can be found in the description given in the supplementary information.

All different topics for data acquisition and the method applied are included in Figure 2-3.

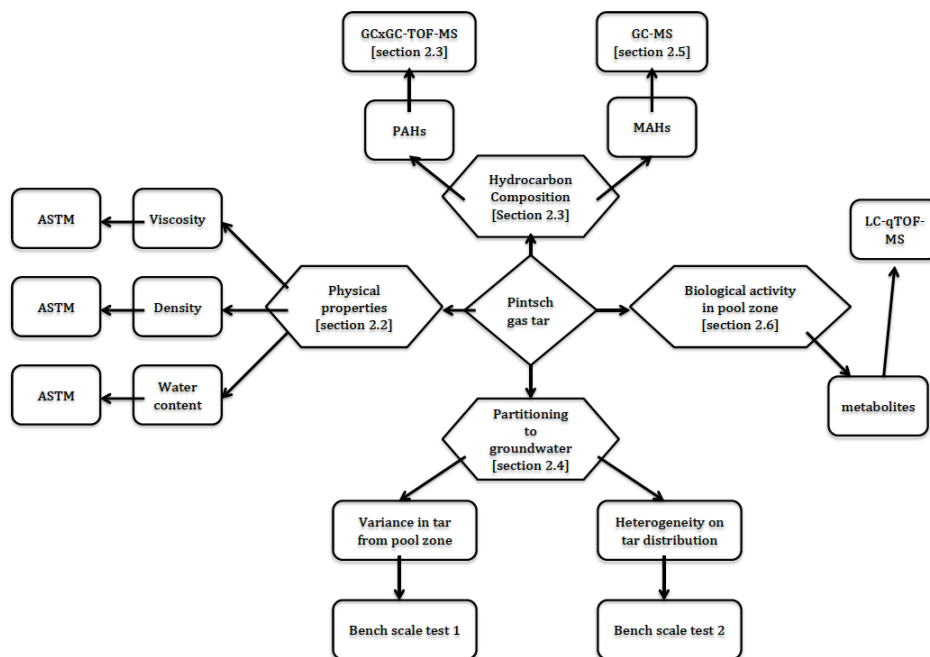


Figure 2-3: Overview methods.

2.3 Results

2.3.1 Pintsch gas tar composition

The Pintsch gas tar sample with the lowest viscosity and density was found closest to the former tar lagoon (Figure 2-2, monitoring well A, Table 2-1). At this sample location, the pool height (6 meter) is also the largest at the site, suggesting that the least altered tar is present here. In this tar sample, a total of 946 individual compounds were detected by GCxGC-TOFMS analysis. The large number of detected compounds illustrates the chemical complexity of the tar. This tar sample contained 57% polycyclic aromatic hydrocarbons (PAHs), 22% polycyclic aromatic sulphur heterocycles (PASH), 12% aliphatic compounds and

alkylated PAHs, 6% polycyclic aromatic oxygen heterocycles (PAOH) and 2% polycyclic aromatic nitrogen heterocycles (PANH). A complete list of all detected components can be found in Supplementary information.

Table 2-1: *Physical properties for Pintsch gas tar samples, collected from wells A,B,C,D.*

Well Sample	A	B	C	D
Distance from entry point (m)	0	25	45	70
Viscosity (cP)	18.56	31.58	34.52	39.41
Density (kg/L)	1.0308	1.0498	1.0576	1.0593
Water content (% wt)	0.0800	0.0660	0.0580	0.0650

The primary compound was phenanthrene with 26,2 g/kg, followed by naphthalene, with 20,9 g/kg. A total of 57 alkylated benzenes ranging between C₉H₁₂ and C₁₃H₂₀ were detected within the sample with the largest number of isomers containing C₁₂H₁₈ with 17 isomers detected. The lightest volatile aromatic compound by molecular weight was found to be styrene. BTEX were not detected by the GCxGC-TOFMS, due to the analysis method. The distribution of alkanes larger than C₁₁, indicates a pattern similar to Diesel (Figure 2-4).

A relatively small number of 15 PANHs were detected, all in the form of 3- and 4-ring heterocycles. A total of 49 compounds representing PAOHs were found, with the lowest molecular weight PAOH being anisole (C₇H₈O) and the highest

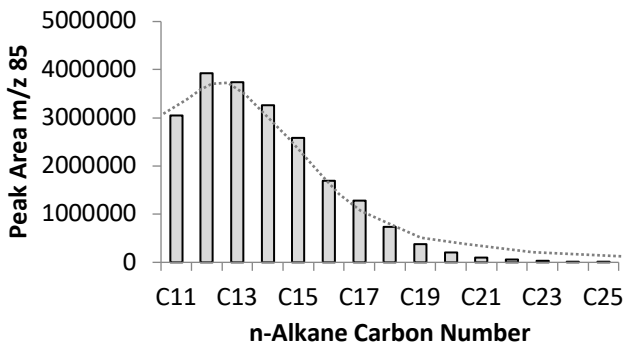


Figure 2-4: *n-alkane distribution pattern of Pintsch gas tar (sample well A) and reference distribution pattern Diesel represented as a dotted line from (Coulon et al., 2004)*

molecular weight PAOH being three benzenobisbenzofuran isomers (C₁₈H₁₀O₂). A large number of PASHs were detected with a total of 203 PASHs ranging from benzenethiol (C₆H₆S)

to benzo[4,5]triphenylono[1,12-bcd]thiophene ($C_{20}H_{10}S$), phenanthro[3,4-b]thiophene, benzo[2,3]phenanthro[4,5-bcd]thiophene. No terpenes, such as hopanes or steranes that are known biomarkers in oil, were detected in the Pintsch gas tar sample. Since BTEX could not be detected by the GCxGC-TOFMS, due to the analysis method, additional analyses were performed by GC-MS.

The additional analysis for water soluble compounds revealed light molecular hydrocarbon compounds from the Pintsch gas tar (Figure 2-5). Toluene (33.86 g/L) was the most abundant followed by xylenes (19.51 g/L) and benzene (13.3 g/L), (Figure 2-6). Benzene, xylenes and toluene (BXT) content in our Pintsch gas tar sample was 6.7 wt%, which is relatively high compared 0.5 to 1 wt% for coal tars (Linda S Lee et al., 1992; Peters and Luthy, 1993).

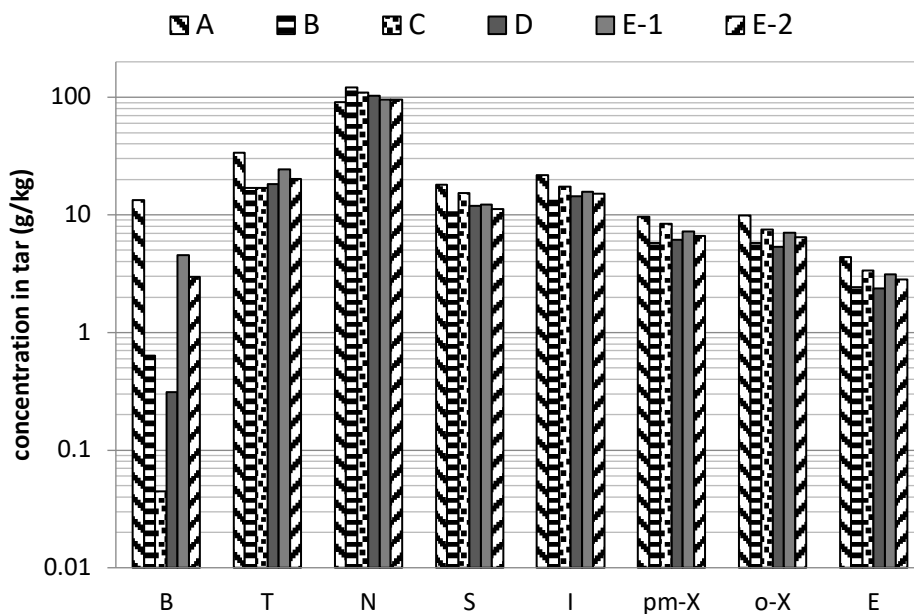


Figure 2-5: Water soluble compounds in Pintsch gas tar, using acetone extraction and GC-MS analysis. In figure B for benzene; T for toluene; N for Naphthalene; S for Styrene; I for Indene; pm-X for para-/meta-xylenes; o-X for ortho-xylene; E for ethylbenzene; 2-MI for 2-methylindene; 1,2,4-TMB for 1,2,4-trimethylbenzene; 1-MN for 1-methylnaphthalene and 2-MN for 2-methylnaphthalene.

2.3.2 Partitioning of tar to water from several samples across the pool zone

To assess the consistency of tar composition after decades of presence in the aquifer and variation in partitioning between samples, four liquid phase tar samples from different parts of the source zone in the shallow aquifer (A, B, C and D, Figure 2-1 and Figure 2-2) revealed 12 monoaromatic hydrocarbon components (Table 2-2). Benzene, toluene and naphthalene were highest in the water phase (Figure 2-6).

Table 2-2: Calculated $\log K_{tw}$ and initial concentrations of water-soluble hydrocarbon compounds within the tar, using (Rixey et al.), * $\log K_{ow}$ values from national center of biotechnology.

	$\log K_{tw}$	$\log K_{ow}$	Solubility in water	A	B	C	D	E-1	E-2
compound	calculated	Lit.*	mg/L	(mg/L)	(mg/L)	(mg/L)	(mg/L)	(mg/L)	(mg/L)
Benzene	2.3	2.1	1790	9649.2	409.9	61.9	436.4	4704.3	4348.8
Toluene	3.0	2.7	520	36418.0	33183.1	25075.2	31203.7	34276.4	37206.1
Ethylbenzene	3.5	3.2	150	6190.2	6660.5	7128.6	5730.7	6701.0	7556.9
m/p-xylene	3.5	3.2	170	22948.8	25737.8	28882.5	23956.0	24597.5	28199.6
styrene	3.0	3.1	300	10436.9	12316.2	13544.9	11250.4	11235.3	12750.3
o-xylene	3.5	3.0	180	11427.9	12550.8	12891.1	9980.0	12084.0	13717.9
3-ethyltoluene	4.1	3.6	40	4567.1	4988.9	4815.9	4133.3	5261.1	6143.5
1,2,4-trimethylbenzene	4.2	3.8	60	16681.3	18636.9	17572.2	15035.4	19188.3	22592.8
1,2,3-trimethylbenzene	4.2	3.7	60	6641.2	6917.5	6318.1	5381.4	7188.0	8731.9
indene	3.5	2.9	20	21170.5	25968.8	25464.1	21255.6	24675.1	32692.6
2-methylindene	4.0	2.6	20	9064.2	9364.8	8255.3	7646.7	9233.5	10534.2
naphthalene	4.1	3.3	30	221150. 2	243693. 4	289798. 6	274428. 5	236276. 9	244929. 1
total				376345. 3	400428. 7	439808. 4	410437. 9	395421. 5	429403. 7

Additionally, in the water extracts from two samples from the deep aquifer (E-1 and E-2), iso-propylbenzene, also known as cumene, and 1,2,4,5-tetramethylbenzene were identified. Water extracts from the four tar samples from the pool zone (A, B, C, D) show a decrease for benzene and toluene concentration.

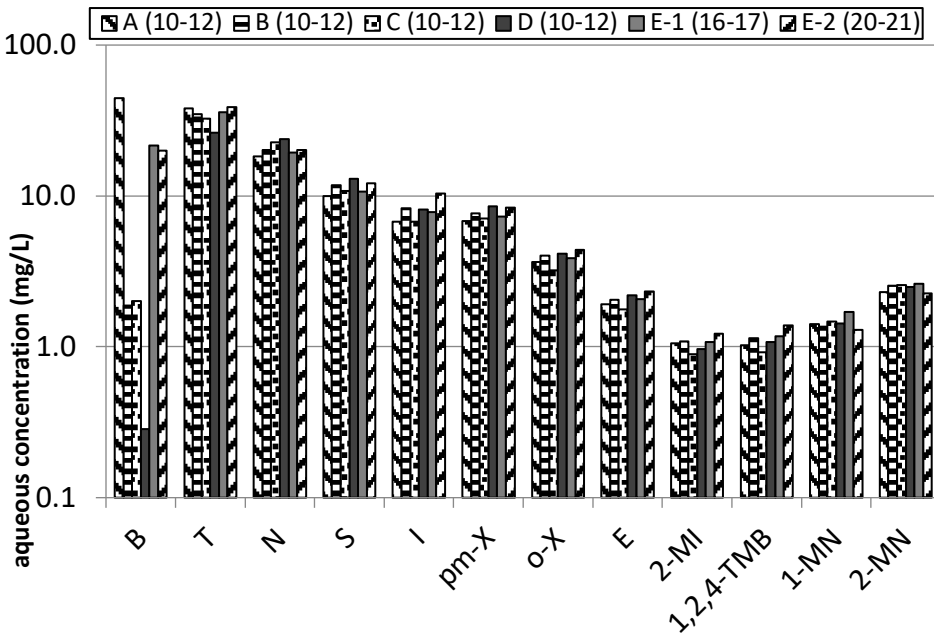


Figure 2-6: Individual tests for water soluble hydrocarbon compounds partition test (tar : water = 1:4) tar collected from 6 monitoring wells A, B, C, D, E-1, E-2. In figure B for benzene; T for toluene; N for Naphthalene; S for Styrene; I for Indene; pm-X for para-/meta-xylenes; o-X for ortho-xylene; E for ethylbenzene; 2-MI for 2-methylindene; 1,2,4-TMB for 1,2,4-trimethylbenzene; 1-MN for 1-methylnaphthalene and 2-MN for 2-methylnaphthalene.

The decrease in benzene corresponds to an increasing distance from the former tar lagoon (Figure 2-6). Benzene decreased from 44.3 mg/L in the water extract from well sample A to 3 mg/L in extract from sample D, 70 meters from the entry point of the DNAPL source. Moreover, concentrations of relatively water-soluble components, such as styrene, indene, xylenes and ethylbenzene, did not decrease

in the extracts from downstream samples (Table 2-2 and Figure 2-6). Naphthalene increased in concentration from 18.2 mg/L at well A up to 23.9 mg/L at the pool fringe at 70 meters towards the pool fringe (Figure 2-6). The further the sample was taken from the former lagoon, the higher the naphthalene concentration.

2.3.3 Dilution effects of aromatic hydrocarbons partitioning to the groundwater

Before composition changes in the contaminated groundwater plume on site can be assessed on transport or degradation effects, a tar-water dilution experiment was executed (Figure 2-7). The least altered tar obtained from well A (Figure 2-2) was exposed to increasing water volumes (tar : water ratios, v : v). In the tar water extracts, 18 lower molecular weight aromatic hydrocarbon components were detected by GC-MS analysis. Benzene was the lowest molecular weight aromatic hydrocarbon compound and 1- and 2-methylnaphthalene were the heaviest detected aromatic components. In addition, compounds that are not commonly associated with tar contaminated sites were detected, such as styrene, ethyltoluenes, diethylbenzene, 1,2,4,5-tetramethylbenzene and methylindenes. Changes in aromatic hydrocarbons leaching from the tar into the increasing groundwater volumes were observed (figure 4). In samples with water to tar ratio of 10:1 and 21:1, approximately similar total concentrations of dissolved aromatic hydrocarbons, 63.4 mg/L and 64.9 mg/L, respectively, were found, which indicates maximum dissolved hydrocarbons in the water phase.

Concentrations and composition of the water-soluble hydrocarbons changed at more diluted tar to water >43:1 up to 3613:1 (Figure 2-4). The total concentration of detected hydrocarbons dropped from 64.9 mg/L to 23.3 mg/L for water : tar ratio 21:1 to 3613:1. Benzene showed the largest aqueous concentration decrease when diluted, followed by toluene, styrene, indene, naphthalene, xylenes and ethylbenzene. For methylindene and 1,2,4-trimethylbenzene, no concentration changes were detected. Dissolved 1- and 2-

methylnaphthalene concentrations increased, from 0.3 mg/L and 0.6 mg/L to 0.6 mg/L and 1.0 mg/L respectively, when more groundwater was present (Figure 2-7).

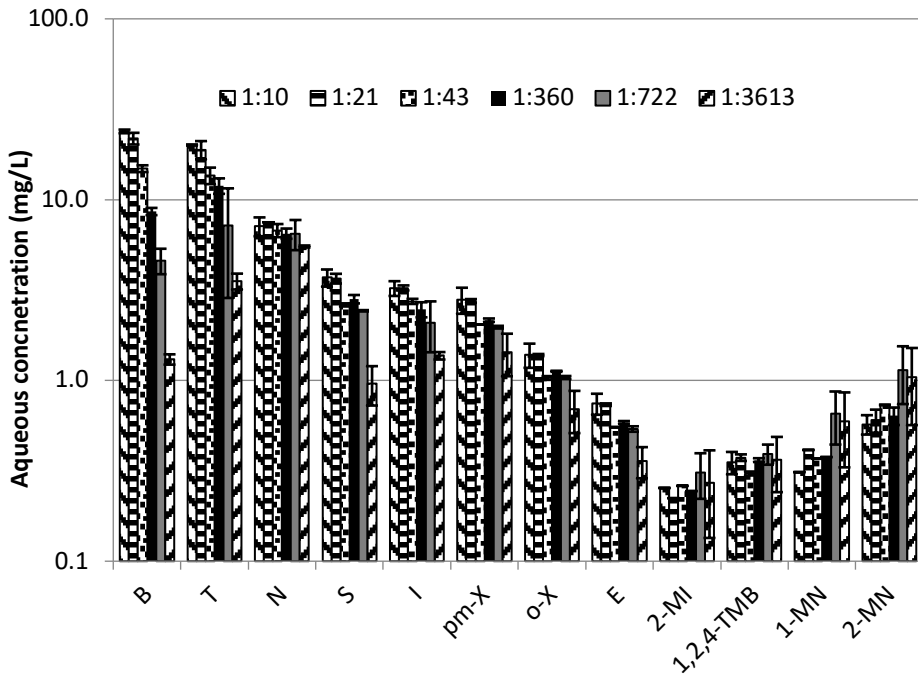


Figure 2-7: Individual tests for water soluble hydrocarbon compounds partition test at increasing water volumes, for the most original tar collected from well A at presumed historical entry point. In figure B for benzene; T for toluene; N for Naphthalene; S for Styrene; I for Indene; pm-X for para-/meta-xylenes; o-X for ortho-xylene; E for ethylbenzene; 2-MI for 2-methylindene; 1,2,4-TMB for 1,2,4-trimethylbenzene; 1-MN for 1-methylnaphthalene and 2-MN for 2-methylnaphthalene.

2.3.4 *Metabolites detected from Pintsch gas tar*

To assess the occurrence of biodegradation, water samples from the tar/water partition vials were screened for suspected metabolites. In total, 123 suspected metabolite compounds including isomers were detected from the tar extracts. In the groundwater reference sample upgradient, 16 metabolites were detected. A comprehensive list of the detected metabolites is given in Supplementary information. Of the total detected metabolite compounds, 118 were qualified, and 5 were quantified using standards. In well A, the highest number of metabolites and their isomers were detected (92 compounds). The number of metabolites decreased gradually towards the fringe of the pool zone from 86 in well B and 87 in well C to 83 in well D. The samples from the deep aquifer revealed 85 in sample from well E-1 and 84 in E-2 metabolites including isomers.

Furthermore, we detected fatty acids and dicarboxylic such as: butyric-, valeric-, fumaric-, succinic-, 3-OH-isovaleric-, octanoic-, adipic-, cinnamic-, nonanoic-, quinolinic- and hippuric acid. These compounds were not detected in the reference sample. These compounds are known fermentation products of hydrocarbons (compounds can be found in the comprehensive target list in the supplementary information).

The following metabolites were quantified: butyric, cinnamic, benzoic, 1H-indene-2-carboxylic- and 2-naphtoic acid. Also, 1-H-Indenecarboxylic acid was detected in all samples ranging from 0.8 to 1.2 µg/L. In the sample from well C, located 45 meters from the former tar lagoon, the highest concentrations for Benzoic acid (309.5 µg/L), cinnamic acid (3.0 µg/L) and 2-naphtoic acid (6.6 µg/L) were detected. The upstream groundwater reference sample revealed no butyrate, cinnamic acid, 1-H-indenecarboxylic acid nor naphtoic acid. However, benzoic acid was detected at a relatively low concentration of (14.7 µg/L), 15 times less than the lowest concentration of 231.7 µg/L in the six tar extracts.

Other detected suspect metabolites were phenyl-, benzyl- and methylbenzyl succinic acid, ethylmalonate, acetylphenol, butylmalonate, isopropylmalic acid. The occurrence of 1H-indene-2-carboxylic acid as a signature metabolite of indene degradation has been confirmed using an internal standard. Additionally, we found carboxylated indene compounds: indene carboxylic acid, indyl methyl succinic acid, 1-H-indene-2-carboxylic acid, 1H-indene-3-carboxylic acid, dihydro-2-indenoic acid, tetrahydro-2-indenoic acid, octahydro-2-indenoic acid, dicyclononane-2-carboxylate, cis-2-carboxycyclohexylacetic acid, dihydromethyl-2-indenoic acid and heptahydromethyl-2-indenoic acid. These new, tentatively identified indene related compounds, we hypothesized as intermediates in the anaerobic biodegradation pathway (Figure 2-8).

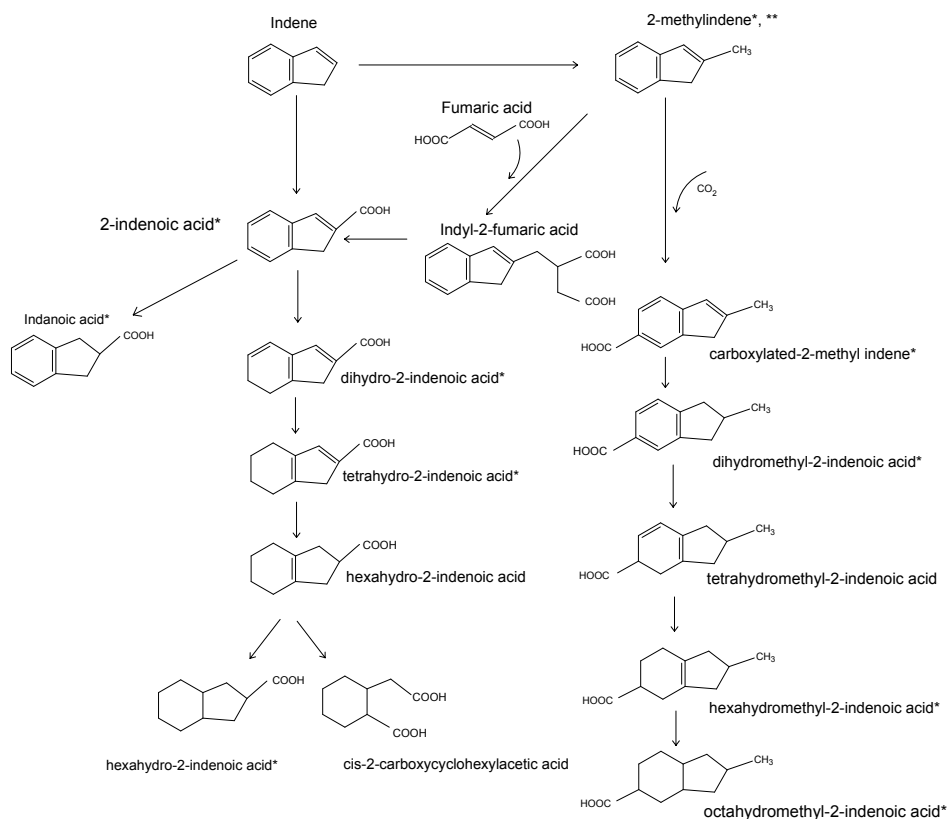


Figure 2-8: Hypothesized anaerobic indene biodegradation pathway; * = detected compound, ** = possible metabolite but can also be originating from Pintsch gas tar.

2.4 Discussion

2.4.1 Composition of Pintsch gas tar

In the analyzed Pintsch gas tar, the most dominant compound was found to be phenanthrene, while in coal tar this is commonly naphthalene (Brown et al., 2006)(Electric Power Research Institute, 1993). The detected n-alkane distribution is most similar to diesel as can be seen from figure 7, (Coulon et al., 2004; Kaplan et al., 1997). The n-alkane distribution suggests that the original feedstock has been similar to diesel oil. The absence of hopanes and steranes in the Pintsch gas tar suggests that the feedstock was a refined product and supports

that diesel-like oil has been used. An alternative possibility is that the Pintsch gas production process itself could be responsible for loss of hopanes and steranes due to the high temperatures involved. Although hardly any alkylated benzenes were expected to be present within Pintsch gas tar in relation to the production process (Lunge, 1909), we found that alkylated benzenes make up a notable group of compounds. In addition, 15 compounds of PANHs were detected in the form of heterocycles; this is a relatively small number and likely due to a low nitrogen content in the feedstock oil (<0.5%) compared to coal tar (> 0.5 – 2%) (Burchill et al., 1983). Our findings indicate that Pintsch gas tar contains a relatively high content of BTX and other mono-aromatic hydrocarbons compared to known coal tars (Brown et al., 2006; Electric Power Research Institute, 1993). BXT in tar is usually close to 0.5 wt% (Peters and Luthy, 1993). Due to relatively high concentrations partitioning into the water phase, it was calculated that BTEX and naphthalene make up 36.5 wt% of the most unaltered tar found on the site. The naphthalene content in Pintsch gas tar ($\pm 21\%$) is relatively high compared to coal tar (10.5%) (D’Affonseca et al., 2011). High BTEX concentrations can also be substantiated as benzene and toluene were the main components of the lighting gas produced by the Pintsch gas process (Butterfield, 1904). The weight percentage of mono aromatic compounds in tar is important because they affect the viscosity of the tar (Electric Power Research Institute, 1993). The tar samples obtained in this study, northside in the former tar lagoon, show a higher viscosity than found at the entry point, where the bulk of the DNAPL is situated directly underneath the former tar lagoon. This suggests more depletion of BTEX from the migrated tars in this study (Table 2-1).

2.4.2 Physical properties and partitioning behavior

The tar-water extraction experiment shows the highest concentrations of benzene and toluene in the water phase. Benzene and toluene concentrations decreased at increasing water volumes. Naphthalene and 2-methylnaphthalene show a reversed

pattern (Figure 2-7). The tars sampled from different parts of the pool zone, however, show different partitioning behaviour after extraction with water. Samples from the shallow aquifer show benzene and toluene decrease along the path of migration over the dipping aquitard, as seen in the dilution experiment. Since groundwater flow is opposite to the dipping direction of the aquitard, this indicates that the tar is more depleted due to dissolution along the tar migration path. Since the farther the tar is situated from the former tar lagoon, the higher the water to tar ratio is (v/v), the dilution experiment simulates the field situation. While this is true for benzene and toluene, it is not for other constituents such as styrene, indene, xylenes and ethylbenzene. Concentrations of these constituents decreased with increasing water volumes (Figure 2-7) as expected from partitioning calculations, but this was not observed in the samples from the pool zone (Figure 2-6), with distance from the tar lagoon. Viscosity of the tar samples ranged from 9.72 to 18.25 cP at 25°C, which is relatively low compared to values given in the literature for coal tar samples, ranging from 34 to 6000 cP at 40°C (L. S. Lee et al., 1992; Peters and Luthy, 1993). This points to the dissolution of mono-aromatic compounds along the migration path of tar. Another explanation could be that due to biodegradation of benzene and toluene in the water phase, their dissolution is enhanced. Thus, the most soluble aromatics are more rapidly depleted. When compounds dissolve from tar into surrounding groundwater, changes occur in partitioning behaviour, and concentration of benzene and toluene become 2 to 5000 times lower (Bruce et al., 1991). However, our study shows that Pintsch gas tar is less viscous and contains higher amounts of volatile aromatic hydrocarbons, and therefore could show different weathering characteristics.

Determination of tar composition, using acetone extraction, showed higher concentrations of all water-soluble components compared to calculated weight percentages using Raoult's law. The mass fractions were, higher for the lightest molecular weight compound, benzene, up to four times as high for methylindene.

A similar effect has been described by (Peters and Luthy, 1993), where naphthalene concentrations were in line with Raoult's law predictions, but higher molecular compounds, such as phenanthrene and pyrene, showed higher concentrations. Ideal behaviour is not necessarily expected from tar and an acceptance factor of two is accepted for field-scale approximation of partitioned concentrations due to significant errors (Linda S Lee et al., 1992). Due to the specific characteristics of Pintsch gas tar, the less ideal behaviour could be greater for higher molecular weight components. Characterization of tars is known to be difficult due to the large number of constituents. Different extracts from tar generally have the same functional groups but in different concentrations depending on the solvent used. This is due to the variance in ability of a solvent to extract certain functional groups (Guillén et al., 1991). Solvents with a high density and small viscosity tend to produce more reproducible data. However, there is no simple relation for extraction yield and the ability of a solvent to interact with a tar. Extraction yields for coal tar with different solvents, may show a difference of up to 14% for hexane, 20% for ethanol, 49% for acetone and 64% for dichloromethane (DCM) (Guillén et al., 1991). For Pintsch gas tar, acetone was chosen as the solvent due to its ability to dissolve the total tar mass, without leaving soot, which did occur with hexane, ethanol, and DCM.

2.4.3 Biodegradation indicators within the source zone

It is known that anaerobic hydrocarbon degradation of crude oil is a common process in oil reservoirs (Aitken et al., 2004). Presence of biomarkers and compound specific signature metabolites extracted from crude oil is one line of evidence for the occurrence of anaerobic biodegradation (Bian et al., 2015). Therefore, presence of 118 detected metabolites detected in our shallow aquifer Pintsch gas tar samples suggest active biodegradation is occurring in the source zone. The sample considered holding the most original tar at the point of entry at the tar lagoon come from the pooled tar. From this sample 92 metabolites were

detected. In the three samples taken from the shallow aquifer towards the fringe of the source zone, 92, 86 and 83 individual metabolites were detected. These samples were taken more upgradient relative to the groundwater flow and towards nitrate and sulphate surroundings. In the two deep aquifer tar samples, 85 and 84 metabolites were identified. The samples in the deep aquifer were on the upgradient side where nitrate is present. These results show that liquid phase tar samples collected from both the shallow and the deep aquifer hold a variety of metabolites, and more metabolites have been detected in the proximity of nitrate-reducing groundwater conditions. Although most metabolites had a high confidence score and off targeted and detected metabolites appear at a similar retention time in different samples, the identification of metabolites is not definite as the interpretation is based only on MS/MS fragmentation, rather than reference standards (Krauss et al., 2010). Reference standards are unfortunately not available for most detected metabolites. Therefore, the identified metabolites were divided into known signature metabolites, and suspected- and proposed metabolites. Adipic acid was detected in the tar extracts. It is a dicarboxylic acid known from nylon production in the industry and is rarely found in the environment (Musser, 2003). Hippurate, another suspect metabolite, may indicate toluene, benzene or benzoic acid degradation and is reported in urine of workers exposed to toluene (Hasegawa et al., 1983). Quinolinic acid is known from the kynurenine metabolic pathway towards production of nicotinamide adenine dinucleotide (NAD⁺). Although the detected fatty acids or dicarboxylic acids could originate from natural organic carbon sources, they have been not detected in the upgradient reference sample. Therefore, it is likely that they are related to biodegradation of hydrocarbons.

Detected phenylglyoxylic acid is a metabolite of phenylacetate (Tischler and Kaschabek, 2012). Phenol is the parent compound of phenylacetate and also a suspected metabolite from anaerobic benzene degradation (Tischler, 2015). Although, phenylacetate was not detected in our samples, the absence of a

metabolite does not necessarily mean that the contaminant is not biodegraded. Phenol and phenylacetate might have a higher water solubility than the parent compound and these metabolites may well have higher potential decay rates than the parent compound. As a consequence, the concentration of the metabolite can well be below the detection limit.

Several detected compounds are qualified as suspected metabolites. Phenylacetaldehyde is a known intermediate formed from 2-phenylethanol, which is known to be formed from styrene (Tischler and Kaschabek, 2012). Styrene was found in all our analysed samples. Another detected compound, benzene acetic acid (or phenyl acetic acid), could have potentially been formed from phenylacetaldehyde. This suggests benzene acetic acid production may be the next step in the degradation of styrene. Therefore, we hypothesize that the presence of hydroxyphenylacetic acid, phenylacetaldehyde and benzene acetic acid forms an indication of anaerobic Styrene degradation at this site.

Indene carboxylic acid, a suspect metabolite for indene degradation (Callaghan, 2013), was found in 3 out of the 6 extracted tar samples varying from 2.1 – 2.5 µg/L. Indanoic acid was also detected and both compounds were described as metabolites from anaerobic indene degradation (Callaghan, 2013). Furthermore, additional compounds were detected that, due to their molecular structure, could be potential metabolites in a degradation pathway, through carboxylation of indene. Indene carboxylic acid was identified and is described as possible first intermediate in degradation step from indene or from 2-methylindene (Callaghan, 2013; Safinowski, 2005). Indyl methyl indene succinic acid was also identified and has, to our knowledge, not been proposed to date as a metabolite. Indyl methyl succinic acid we propose as a metabolite in the indene degradation pathway by carboxylation (Figure 2-8). Additionally, other indene related compounds were detected from the tar extracts, from these compounds, we propose a metabolic pathway starting with carboxylation of indene (Figure 2-8).

The metabolites suggest that indene is reduced stepwise before ring cleavage occurs. This is a similar pathway as for naphthalene degradation following the carboxylation pathway (Meckenstock et al., 2000).

2-Naphtoic acid (2-NA) concentrations in tar extracts varied from 9.3 to 24.9 $\mu\text{g/L}$, and benzoic acid (BA) from 83.2 to 246.2 $\mu\text{g/L}$ (Figure 2-9). These concentrations are relatively high compared to 0.4 - 33.6 $\mu\text{g/L}$ found in contaminated groundwater plumes (Jobelius et al., 2011b; Ohlenbusch et al., 2002). This could suggest that these metabolites accumulated from the groundwater into the tar at this site. The highest concentrations of BA were found in tar extracts from well B and D. These wells are situated to the north from the former tar lagoon, where groundwater from upstream, containing nitrate and sulfate in the non-impacted reference well, meets the fringe of the DNAPL. This indicates biodegradation of mono-aromatic compounds, including toluene and/or benzene, at the upstream DNAPL fringes. The highest NA and Indene carboxylic acid (ICA) concentrations were detected in well A and C situated towards the middle of the pool zone, where less or no nitrate and sulphate is present in the surrounding groundwater.

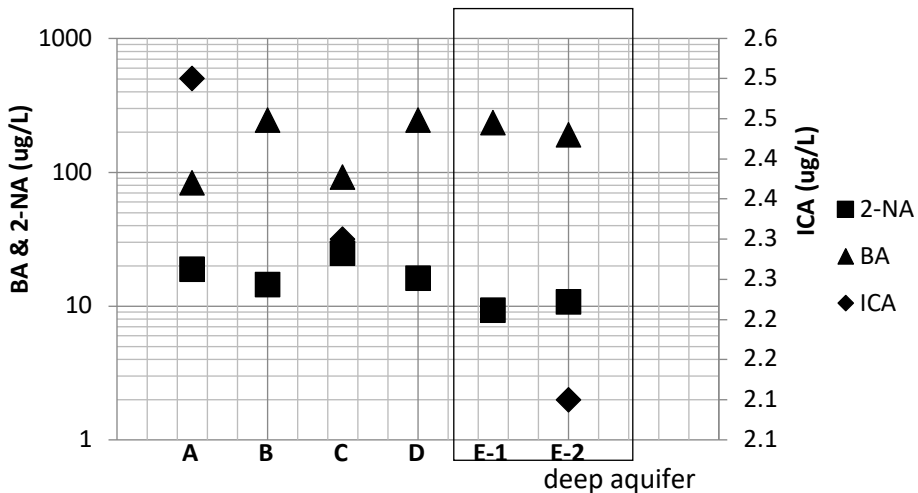


Figure 2-9: Aqueous concentration of metabolite concentration for BA (benzoic acid), ICA (indene carboxylic acid), 2-NA (2-naphtoic acid) from Pintsch gas tar samples.

Metabolites found in the tar extracts could serve as biomarkers. But other known biomarkers, which are commonly detected in crude oil, such as hopanes or steranes (Wang, 1999), were not detected in the Pintsch gas tar. The detected metabolites were extracted from tar samples that had been resident in the subsurface for 60 to 100 years. Possible explanations are 1) metabolites were formed during the invasion of the subsurface and remained within the tar over decades. Or 2) biodegradation in the source zone is active and metabolites are formed in the vicinity of the tar and once formed in the groundwater these metabolites dissolve into the tar. Or 3) metabolites originate from the feedstock prior to the Pintsch gas process.

All detected metabolites could potentially originate from crude oil, distilled feedstock, or the Pintsch gas tar itself. However, it is unlikely that carboxylated hydrocarbon compounds would have survived the distillation process from crude oil to feedstock (diesel/gasoil), as temperature during production would have been 700 - 1000°C (Butterfield, 1904). Benzoic and naphthoic acid, carboxylated compounds detected at the highest concentrations from the Pintsch gas tar samples, are known to be thermally destroyed at, respectively, 530-762°C and 305-410°C (Brzyska and Kula, 1995; Winter et al., 1969). Therefore, it is likely that the abundance of carboxylated metabolites indicate biodegradation of hydrocarbons in the source zone. The metabolites could be formed at the tar-water interface and/or in groundwater in the vicinity of the pure phase tar. Where parent compounds dissolve from the DNAPL into the aqueous phase, their molecular composition is altered by microbial activity. Biodegradation intermediates have been transported downstream by groundwater advection outside of the source zone. Intermediates may also remain in the source zone, because they (re-) dissolve from adjacent groundwater into the tar as they are still relatively hydrophobic. The production of acids, seen in shallow petroleum reservoirs, is similar to those seen in surface oil seeps and laboratory biodegradation experiments (Head et al., 2003). Even in a relatively high-

saturated tar contaminated source zone, there is residual water, which acts as a microbial habitat. When the sum of all detected metabolites is compared to the sum of the water-soluble mono- and polyaromatic hydrocarbon concentrations (Figure 2-10), the least metabolites are present in the tar at the location of the former tar lagoon, where the water-soluble hydrocarbons have the highest concentration. In the wells situated to the north where acceptor from upgradient meets the pool zone, the metabolites are more abundant and water-soluble hydrocarbons have lower concentrations. More biomarkers in relation to available acceptors, suggests alteration of the tar composition by biodegradation towards the tar pool fringe. Tar samples from the second aquifer show relatively higher sum of metabolites than the samples north of the pool in the shallow aquifer and show higher concentrations of soluble hydrocarbons, which suggests less altered tar from the shallow aquifer is leaking into the deep aquifer, through the relatively thin aquitard. Moreover, this suggests more bioactivity.

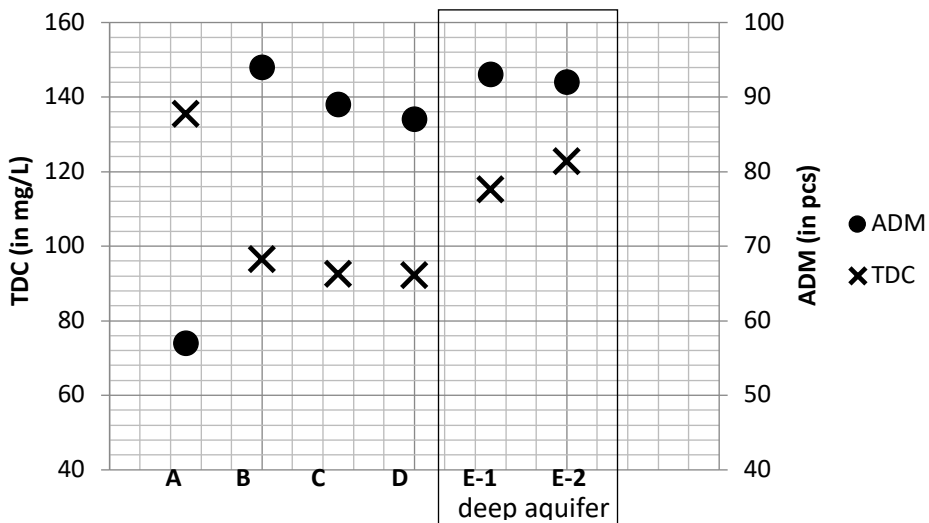


Figure 2-10: Sum aqueous concentration of all detected metabolites and isomers (ADM) and total aqueous concentration of 18 detected water-soluble hydrocarbon compounds (TDC).

More bioactivity could be explained by a smaller amount of tar in the deep aquifer, which means a lower tar to water ratio. Moreover, the larger groundwater velocity in the deep aquifer, contributes more acceptor from upgradient for biodegradation.

The geochemical and biological conditions at the investigated former Pintsch gas plant are representative for other contaminated sites. Therefore, we suggest that the detected metabolites from biodegradation at source zone conditions also occur at other hydrocarbon contaminated sites. Partitioning of contaminants from multi-component DNAPL into the aqueous phase and re-dissolving of their slightly less hydrophobic metabolites back from the aqueous phase into the DNAPL is feasible and demonstrates the complexity of assessing degradation processes within a source zone.

2.5 Conclusions

Although Pintsch gas tar produced from oil can be mistaken for coal tar, we found that phenanthrene is the most abundant constituent rather than naphthalene and holds a high monocyclic aromatic hydrocarbon content. Also, n-alkane distribution shows high similarity to Diesel. Its low viscosity and low density originate from a relatively high content of monocyclic aromatic compounds. Therefore, tar produced by the Pintsch gas process potentially has relatively high invasive properties in the subsurface and partitioning characteristics to the groundwater. Mono aromatic hydrocarbon (MAH) compounds, such as styrene, ethyltoluenes, diethylbenzene, trimethylbenzenes and 1,2,4,5-tetramethylbenzene, are not commonly reported at tar contaminated sites, however, these compounds are present within Pintsch gas tar. These MAHs are soluble in groundwater, partition from the tar into groundwater and potentially are present in contaminant plumes.

The abundance of biomarkers found within Pintsch gas tar samples from the researched site, suggests active anaerobic biodegradation at pool zone conditions. Anaerobic biodegradation within the source zone could occur at the tar water fringe, in pockets of groundwater within the DNAPL saturated area. Most detected metabolites are related to mono- and poly cyclic aromatic hydrocarbons, such as: benzene, toluene, ethylbenzene, xylenes, styrene, trimethylbenzenes, naphthalene and indene. A considerable amount of indene related metabolites was detected, that can be associated to the anaerobic biodegradation by the carboxylation pathway. From these ten indene related metabolites, an anaerobic carboxylation pathway is hypothesized. Other possible anaerobic biodegradation pathways for indene and individual reactions would be subject for future work.

While biotransformation of the parent compounds takes place in the water phase, the formed metabolites, although more hydrophilic after transformation, dissolve at least partially into the liquid phase tar. These metabolites present in the tar can be used as biomarkers for active biodegradation at pool zone conditions.

2.6 Acknowledgements

We thank Stichting Bodemsanering NS (SBNS), for funding the research on partitioning experiments, and metabolite screening on LC-qTOFMS. Also, we like to thank the Scottish Funding Council (SFC) Glasgow Research Partnership in engineering, the University of Strathclyde, WSP and national Grid property from funding support on the GCxGC MSTOF analysis of the Pintsch gas sample. Andre Cinjee (Deltares) and Patrick Broekhuizen (Aveco de Bondt) we thank for their assistance in the field work and Fredericke (Deltares) for her assistance in the laboratory.

2.7 Supplementary information

Table S2.7.1: *Metabolite target list*

	Formula	Parent compound	M-H (z=-1)	MS-MS fragments	Source
Metabolate					
1-naphthoic acid (isomer)	C11H8O2	<i>naphthalene</i>	171,045153	127,055	Zhang et al. 2000
2,3-dihydroxynaphthalene	C10H8O2	<i>naphthalene</i>	159,045153	131.0497; 141.034	(new) identified
2,3-naphthalenedicarboxylic acid	C12H8O4	<i>naphthalene</i>	215,034982	171,0438	(new) identified
2-carboxycyclohexylacetic acid	C9H14O4	<i>naphthalene</i>	185,081932	141,0914	Annweiler et al. 2002
2-ethylhexanol	C8H18O	<i>styrene</i>	129,128489	X	Tischler 2015
3-o-toluoyl propionic acid (isomers 1-4)	C11H12O3	<i>o-xylene</i>	191,071368	X	Morasch et al. 2004
4-aminobenzoic acid	C7H7NO2	<i>aniline</i>	136,040402	X	Schnell and Schink 1990
4-hydroxy benzoic acid	C7H6O3	<i>phenol</i>	137,024418	93,034	Tsai et al. 2009, Focht 2008
acenaphthenoic acid or biphenyl-carboxylic acid (isomers 1-3)	C13H10O2	<i>Acenaphtene / biphenyl</i>	197,060803	153,0705	Safinowski et al. 2006
acenaphthyl methylsuccinate (isomers 1-2)	C17H16O4	<i>acenaphtene</i>	283,097583	X	Morasch et al. 2011
acenaphthyleneic acid (isomers 1-2)	C13H8O2	<i>acenaphthylene</i>	195,045153	X	Safinowski et al. 2006
adipic acid	C6H10O4	<i>e.g. phenol</i>	145,050632	83.05;101.061; 127.04	Bakker 1976
benzoylactic acid (isomers 1-3)	C9H8O3	<i>ethylbenzene</i>	163,040068	119,0502	Callaghan 2013
butyric acid (or butanoic acid)	C4H8O2	<i>Alkanoate</i>	87,045153	X	Bian et al. 2015
carboxylated methyl indene (isomers 1-4)	C11H10O2	<i>indene</i>	173,060803	X	(new) identified
decahydro-naphthoic acid	C11H18O2	<i>naphthalene</i>	181,123403	X	Annweiler et al. 2002
dimethyl-benzoic acid (isomers 1-9)	C9H10O2	<i>trimethylbenzene</i>	149,060803	105,0707	Cozarelli et al. 1990
dimethyl-naphthoic acid (isomers 1-5)	C13H12O2	<i>dimethylnaphthalene</i>	199,076453	155,086	Gieg and Suflita 2002
fluoreneic acid (isomers 1-2)	C14H10O2	<i>fluorene</i>	209,060803	165,0706	(new) identified
fumaric acid	C4H4O4	<i>metabolic intermediate</i>	115,003682	X	-
hexadecanoic acid (or palmitic acid)	C16H32O2	<i>short chain alkanes</i>	255,232954	X	Xin-Yu et al. 2015
hexahydro-naphthoic acid (isomers 1-10)	C11H14O2	<i>naphthalene</i>	177,092103	133,102	Annweiler et al. 2002
hydroxy-naphthoic acid (isomers 1-3)	C11H8O3	<i>naphthalene</i>	187,040068	X	(new) identified
hydroxyphenylacetic acid (isomers 1-7)	C8H8O3	<i>styrene</i>	151,040068	107,0502	Tischler 2015
indanoic acid (isomers 1-2)	C10H10O2	<i>indane</i>	161,060803	117,07	Safinowski et al. 2006
indenoic acid (isomers 3-4, 1 and 2 in quantified)	C10H8O2	<i>indene</i>	159,045153	115,0553	Safinowski et al. 2006

data)					
<i>indyl methyl succinic acid</i>	C14H14O2	<i>indene</i>	213,092103	X	(new) identified
<i>malonic acid</i>	C3H4O4	<i>cinnamic acid (?)</i>	103,003682	X	Thies Thiemann
<i>methyl benzoic acid or benzeneacetic acid (isomers 1-7)</i>	C8H8O2	<i>m-xylene/styrene</i>	135,045153	91,0553	Tischler 2015
<i>methylbenzylsuccinic acid (isomers 1-6)</i>	C12H14O4	<i>o-xylene</i>	221,081932	105,071; 177,0921	Beller, 2000
<i>methyl-naphthoic acid (isomers 1-6)</i>	C12H10O2	<i>naphthalene</i>	185,060803	141,0704	Safinowski et al. 2006
<i>nicotinic acid</i>	C6H5NO2	-	122,024752	X	Young Soo Keum 2008
<i>octadecanoic acid (or stearic acid)</i>	C18H36O2	<i>short chain alkanes</i>	283,264254	X	Xin-Yu et al. 2015
<i>octahydro-2-naphthoic acid</i>	C11H16O2	<i>naphthalene</i>	179,107753	X	Annweiler et al. 2002
<i>p-cresol</i>	C7H8O	<i>phenanthrene</i>	107,050238	X	Tsai et al. 2009
<i>phenanthroic acid (isomers 1-3)</i>	C15H10O2	<i>phenanthrene</i>	221,060803	177,0706	-
<i>phenol (isomers 1-4)</i>	C6H6O	<i>fluorene/benzene</i>	93,034588	X	Tsai et al. 2009
<i>phenylacetaldehyde (isomers 1-3)</i>	C8H8O	<i>styrene</i>	119,050238	X	Tischler 2015
<i>phenylethanol or ethylphenol (isomers 1-2)</i>	C8H10O	<i>styrene</i>	121,065888	X	Tischler 2015
<i>phenylglyoxylic acid (isomers 1-2)</i>	C8H6O3	<i>phenylacetate</i>	149,024418	105,0345	Tischler 2015, Leibman 1975
<i>propionic acid</i>	C3H6O2	<i>carboxylic acid metabolism</i>	73,029503	X	-
<i>pyruvic acid</i>	C3H4O3	<i>metabolic intermediate</i>	87,008768	X	-
<i>succinic acid</i>	C4H6O4	<i>metabolic intermediate</i>	117,019332	X	-
<i>tetrahydro-naphthoic acid (isomers 1-2)</i>	C11H12O2	<i>naphthalene</i>	175,076453	X	Annweiler et al. 2002
<i>trimethylbenzoic acid (isomers 1-6)</i>	C10H12O2	<i>tetramethylbenzene</i>	163,076453	119,086	-
<i>valeric acid</i>	C5H10O2	-	101,060803	X	-

Table S2.7.2: Metabolites detected per tar sample

sample / well name	A	B	C	D	E-1	E-2	reference
filter depth (in mbgs)	10-12	10-12	10-12	10-12	16-17	20-21	8-9
Target compound	score according to Schymanski et al.						
Methylglyoxal	+++	+++	+	+++	+++	+++	
2-methyl 2-hydroxy-propanal		+++	+++		+++		
Butyrate	183.6	171.9	221.5	182.6	247.7	188.1	
Methylmalonate semialdehyde	++++	++++	+	+	++++	++++	
T-butyl formate	+	+++	+	+	+	+	
Valeric acid	+++	+++	+++	+++	+++	+	
Valeric acid	+++	+++	+++	+++	+++	+++	

P-cresol - isomer 1	+++	+++	+++	+	+	+++	
P-cresol - isomer 2	+						
Fumaric acid - isomer 1	++++	++++	++++	++++	---		
Succinic acid or 2-formyl-2-hydroxy-propionate - isomer 1	+++	+	+++	+++	+++	+++	
Succinic acid or 2-formyl-2-hydroxy-propionate - isomer 2	++++	++++	++++	++++	++++	+	++++
3-OH-isovaleric acid - isomer 1	+++	+	+++	+++	+++	+++	
Benzoic acid	306.5	240.5	309.5	282.1	244.5	231.7	14.6
Ethylmalonate - isomer 1	++++	+		---		---	
Ethylmalonate - isomer 2	+				+		++++
Acetylphenol - isomer 1	+++	+++	+++	+	+	+	
Methyl benzoic acid or Acetylphenol - isomer 1	++++	++++	++++	++++	++++	+	
Methyl benzoic acid or Acetylphenol - isomer 2	++++		++++			+	
Methyl benzoic acid or Acetylphenol - isomer 3	++++	++++	++++	++++	++++	+	
4-hydroxy benzoic acid	---	---	---	---	---	---	
Octanoate - isomer 1	+++	+++	+++	+	+++	+	+++
Octanoate - isomer 2					+++		+++
Adipic acid	+++	+++	+++	+++	+++	+++	+++
Cinnamic acid	1.5	1.9	3.0	1.4		1.0	
Indenediol - isomer 1		+++	+++		+++		
Indenediol or styrene carboxylic acid - isomer 1	+	+	+		++++		
Indenediol or styrene carboxylic acid - isomer 2	+++	++++	++++	+		+	
Indenediol or styrene carboxylic acid - isomer 3	+++	++++	++++	+	+	+	
Indenediol or styrene carboxylic acid - isomer 6						---	
Indenediol or styrene carboxylic acid - isomer 7	+	+	++++	+	++++	+	
Phenylglyoxylic acid	++++	++++	++++	++++	+	+	
Phenylglyoxylic acid	++++	++++	++++	++++	++++	++++	
Dimethyl-benzoic acid or Benzylacetate - isomer 1	++++	+	++++	+	++++	+	
Dimethyl-benzoic acid or Benzylacetate - isomer 1						+	
Dimethyl-benzoic acid or Benzylacetate - isomer 2	++++	++++		+	++++	+	+
Dimethyl-benzoic acid or Benzylacetate - isomer 3	++++	++++	++++	++++	++++	+	
Dimethyl-benzoic acid or Benzylacetate - isomer 4	++++	++++	++++	++++	++++	++++	
Dimethyl-benzoic acid or Benzylacetate - isomer 5	++++	+	++++	++++	++++	+	

Hydroxyphenylacetic acid	++++	++++	+	++++	++++	+	
Butylmalonate - isomer 1	+++	+++	+++	+	---	+++	+++
Butylmalonate - isomer 2	---	+		+	+	---	
Butylmalonate - isomer 3	+	+++	+	+	---	+	+++
Nonanoate - isomer 1	+++	+++	+++	+	+++	+	+
Nonanoate - isomer 2	+++	+++	+++	+++	+++	+	+++
1H-indene-2-carboxylic acid	1.0	0.8	0.8	0.9	1.2	0.8	
1H-indene-2-carboxylic acid - isomer 1	++++	+	++++	+	+	+	
1H-indene-2-carboxylic acid - isomer 2	+++	+++	+++			+	
Dihydro-2-indenoic acid - isomer 3	++++	++++	++++	+	+++	+	
Dihydro-2-indenoic acid - isomer 4	+++	++++	++++	+	+++	+	
Dihydro-2-indenoic acid - isomer 5	++++	++++	+++	+	+	+	
Benzoylacetic acid	++++	++++	++++	++++	++++	+	
Benzoylacetic acid, P-coumaric acid or Hydroxycinnamate - isomer 1	++++	++++	++++	++++	++++	+	
Benzoylacetic acid, P-coumaric acid or Hydroxycinnamate - isomer 2	++++	++++	+	++++	++++	++++	
Benzoylacetic acid, P-coumaric acid or Hydroxycinnamate - isomer 3	++++	++++		++++	++++	++++	
Benzoylacetic acid, P-coumaric acid or Hydroxycinnamate - isomer 4	++++	++++	++++	++++	++++	++++	
Benzoylacetic acid, P-coumaric acid or Hydroxycinnamate - isomer 5	++++	+	++++	++++	++++	++++	
Benzoylacetic acid, P-coumaric acid or Hydroxycinnamate - isomer 6			+				
Tetrahydro-2-indenoic acid, Phenylbutyrate or Trimethylbenzoic acid - isomer 1	+	+	++++	+	+	+	
Tetrahydro-2-indenoic acid, Phenylbutyrate or Trimethylbenzoic acid - isomer 2			++++	++++			
Tetrahydro-2-indenoic acid, Phenylbutyrate or Trimethylbenzoic acid - isomer 5		+			+	+	
Tetrahydro-2-indenoic acid, Phenylbutyrate or Trimethylbenzoic acid - isomer 6				+			
Tetrahydro-2-indenoic acid, Phenylbutyrate or Trimethylbenzoic acid - isomer 7	+++	+++	++++		+++		
Tetrahydro-2-indenoic acid, Phenylbutyrate or Trimethylbenzoic acid - isomer 8	++++	+	+		+	---	
Tetrahydro-2-indenoic acid, Phenylbutyrate or Trimethylbenzoic acid - isomer 9	+		++++				
Tetrahydro-2-indenoic acid, Phenylbutyrate or Trimethylbenzoic acid - isomer 10			---				
Tetrahydro-2-indenoic acid, Phenylbutyrate or Trimethylbenzoic acid - isomer 11				+		+	
Tetrahydro-2-indenoic acid, Phenylbutyrate or Trimethylbenzoic acid - isomer 12			---		+		
Quinolinic acid - isomer 2	+	---	+		+	++++	
1-naphthoic acid	++++	++++	++++	++++	++++	+	
2-naphthoic acid	5.7	4.2	6.6	6.4	3.3	3.5	

2-isopropylmalic acid - isomer 2		---			+		
Dihydromethyl indenoic acid, Tetrahydro-naphthoic acid or 2,3-dihydro-1H-indene-acetic acid - isomer 1			+++		+		
Dihydromethyl indenoic acid, Tetrahydro-naphthoic acid or 2,3-dihydro-1H-indene-acetic acid - isomer 5	++++	+++			++++		
Dihydromethyl indenoic acid, Tetrahydro-naphthoic acid or 2,3-dihydro-1H-indene-acetic acid - isomer 6	++++	++++					
Dihydromethyl indenoic acid, Tetrahydro-naphthoic acid or 2,3-dihydro-1H-indene-acetic acid - isomer 9	+++						
Hippurate - isomer 1					---		
Hippurate - isomer 2	---	---	---	---		---	
Hippurate - isomer 5	++++				++++	+	
Hippurate - isomer 6	+++				+++	+++	
4-Hydroxyphenylpyruvate - isomer 1	++++	++++	++++	++++	++++	++++	
Octahydro-2-naphthoic acid or Hexahydromethyl indenoic acid	+++				+	+	
Naphthaleneacetic acid or methyl-naphthoic acid - isomer 4						---	
Naphthaleneacetic acid or methyl-naphthoic acid - isomer 10	+		+	+			
Naphthaleneacetic acid or methyl-naphthoic acid - isomer 5	++++	+	++++				
Naphthaleneacetic acid or methyl-naphthoic acid - isomer 7	++++	++++	++++	+	++++	+	
Naphthaleneacetic acid or methyl-naphthoic acid - isomer 8	++++	+	+	+	+	+	
2-carboxycyclohexylacetic acid	++++	++++	++++	++++	+	+	+
3-o-toluoyl propionic acid - isomer 1	+	+	+	+		+	
3-o-toluoyl propionic acid - isomer 10		++++		++++	+++	+	
3-o-toluoyl propionic acid - isomer 11	+++	++++	++++	++++	+++	+	
3-o-toluoyl propionic acid - isomer 12		+		++++	+	+	
3-o-toluoyl propionic acid - isomer 13	++++	++++	+	+	++++	+	++++
3-o-toluoyl propionic acid - isomer 14				+	++++	+	
3-o-toluoyl propionic acid - isomer 15		++++					
3-o-toluoyl propionic acid - isomer 16	+++	++++			++++	+	
3-o-toluoyl propionic acid - isomer 17	+	+	+	+	+		---
3-o-toluoyl propionic acid - isomer 3	++++	++++	+++	+++	+++	+++	
3-o-toluoyl propionic acid - isomer 4	+++	+++	+++	+++	+++	+	
3-o-toluoyl propionic acid - isomer 6	+	+	++++	++++	++++	++++	
3-o-toluoyl propionic acid - isomer 7	+		+	++++	+	+	

Phenylsuccinic acid - isomer 1	++++	++++	++++	++++	++++	++++	
Phenylsuccinic acid - isomer 2	++++	++++	++++	++++	+	++++	
Benzylsuccinic acid - isomer 1	++++	++++		++++	++++	++++	
Benzylsuccinic acid - isomer 2			++++				
Benzylsuccinic acid - isomer 3	+			+	+	+	
Benzylsuccinic acid - isomer 4	+	++++	++++	++++	+++	+++	
3-naphthalenedicarboxylic acid - isomer 1			+	---			
3-naphthalenedicarboxylic acid - isomer 3	---						
C10H18O5 - isomer 1	+++	+++	+	+++	+++	+++	
C10H18O5 - isomer 2	+++	+++	+++	+++	+++	+++	
Methylbenzylsuccinic acid - isomer 1					---		
Methylbenzylsuccinic acid - isomer 2		---	+++				
Methylbenzylsuccinic acid - isomer 3	---	+	++++	+	---	+	
Methylbenzylsuccinic acid - isomer 4	+	+	+	+		++++	
Methylbenzylsuccinic acid - isomer 5	++++	++++	++++	++++	++++	++++	
Indyl methyl succinic acid - isomer 1	+++	+	+++	+++	+++	+++	
Indyl methyl succinic acid - isomer 2	+++	+++	+++	---	+++	+++	
Naphthyl-2-methyl-succinate - isomer 1	+	---			---	---	
Naphthyl-2-methyl-succinate - isomer 2	---	---	+	+	---	---	
2-(1-methyldodecyl)succinate or 2-(2-methyltridecyl)malonate - isomer 1	+++	+++	+++	+++	+++	+++	+++
2-(1-methyldodecyl)succinate or 2-(2-methyltridecyl)malonate - isomer 2	+++		+++	+++	+++	+	+
2-(1-methyltetradecyl)succinate or 2-(2-methylpentadecyl)malonate - isomer 1	+++						+++

Detected metabolites within Pintsch gas tar extracts sampled from wells in the source zone area, scoring is according to Schymanski et al. + = confirmed structure; ++ = probable structure; +++ = tentative candidate; ++++ = unequivocal molecular formula; 183.6 = exact mass in µg/L.

3 Enhanced source-zone biodegradation of Pintsch gas tar: The impact of substrate stimulation

A version of this chapter is currently prepared to submit for publication

*Alexandra E. Hockin, Johan A. van Leeuwen, Jan Gerritse, Niels Hartog,
S. Majid Hassanizadeh*

Abstract

as higher fluxes of MAHs, is necessary to understand and effectively remediate. To evaluate the potential for enhanced bioremediation in source zones, long term microcosm experiments were conducted with sediment containing a complex mono- and polycyclic aromatic hydrocarbon mixture from a former manufactured gas plant. Experiments were conducted under multiple reducing conditions; nitrate, nitrate-acetate, nitrate-succinate, sulfate and chlorate. A mass balance of hydrocarbons after 4 years showed substantial degradation of PAHs in nitrate-acetate and nitrate-succinate microcosms compared to the unstimulated microcosm. Under nitrate-acetate conditions, on average 51% of low- and 15% of high-molecular weight PAHs were degraded above natural field conditions. In general, PAH degradation decreased with increasing molecular weight. However, the notable exception was naphthalene, with only 7% loss above natural field conditions in the microcosm stimulated with nitrate and acetate. Gene copies for nitrate- (*narG*) and nitrite-reducing (*nirS*) bacteria were elevated in microcosms stimulated with nitrate and a substrate, more so than for stimulation with nitrate alone. Signature metabolites for toluene, naphthalene and indene were found in all microcosms, including the sterile control indicating source zone degradation in-situ. Anions measurements suggest co-metabolism may be an important mechanism for hydrocarbon degradation. Stimulation increased degradation for all monoaromatic hydrocarbons with the exception of benzene, which was degraded up to 5 times more under natural, unstimulated conditions. This study demonstrates the potential for stimulated source zone degradation by indigenous, anaerobic microorganisms using nitrate and acetate. However, though stimulation resulted in an higher overall loss of hydrocarbons, stimulation also inhibited the degradation of soluble monoaromatic hydrocarbons, including benzene, which were more favorably degraded under natural, in-situ conditions. Further research on source zone stimulation and the possible downgradient effects, such source zones by enhanced biodegradation.

3.1 Introduction

Many former industrial sites are contaminated with petroleum hydrocarbons. Common sources of contamination include leaking underground storage tanks, pipelines, waste pits, as well as accidental spills during transportation (Alvarez and Illman, 2006). Petroleum hydrocarbons consist of several hundred compounds; two groups of particular concern are mono-aromatic hydrocarbon (MAHs) and polycyclic aromatic hydrocarbons (PAHs), due to their risk to public health and persistence in the environment (Meckenstock et al., 2016).

MAHs are relatively soluble and can cause extensive contaminant groundwater plumes (Alvarez and Illman, 2006). Benzene in particular is a known human carcinogen, has a high solubility and is persistent in anaerobic environments (Vogt et al., 2011). PAHs consist of multiple fused aromatic rings and are formed during the incomplete combustion of organic matter at high temperatures (Haritash and Kaushik, 2009). The stability of aromatic rings make PAHs more difficult to biodegrade (Meckenstock et al., 2016). Moreover, PAHs that have larger molecular weight are less soluble in water; this means they are more persistent in the environment (Meckenstock et al., 2016). When hydrocarbons are spilled in the environment, they may exist as a separate, non-aqueous phase liquid (NAPL) (Ward, 2015). The presence of a NAPL results in the slow, continuous release of contaminants to passing groundwater, creating large contaminant plumes which can persist for decades (Ward, 2015).

Degradation of MAH and PAHs in plume zones has been shown under methanogenic, nitrate and sulfate reducing conditions (Chakraborty and Coates, 2004; Essaid et al., 2011; Gieg and Suflita, 2002; Gray et al., 2010; Griebler et al., 2004; Meckenstock et al., 2016; Morasch et al., 2011). Toluene is generally considered the most readily degraded MAH component under all reducing conditions (Foght, 2008). While several pure strains of toluene-degrading

bacteria have been found, pure isolates of benzene-degrading cultures are rare; generally a consortia of bacteria are present (Dou et al., 2010; Foght, 2008; van der Waals et al., 2017; van der Zaan et al., 2012). Low molecular weight (LMW) PAHs are relatively more volatile and soluble in water and therefore are more readily biodegraded than high molecular weight (HMW) PAHs (Ghosal et al., 2016).

Often, MAH and PAH are present in the environment in mixtures, where competitive inhibition and co-metabolism can affect the degradation rates (S. W. Chang et al., 2002; Dean-Ross et al., 2002; Meckenstock et al., 2004; Phelps and Young, 1999b; Safinowski et al., 2006). Co-metabolism is thought to be particularly important for biodegradation of HMW PAHs (≥ 4 -rings) (Meckenstock et al., 2016; Safinowski et al., 2006). Studies have also shown that multiple MAHs and PAHs can be degraded by a common enzyme system in bacteria (Balachandran et al., 2012; Stringfellow and Aitken, 1995b). Heterocyclic PAHs, commonly found in petroleum and coal-derived tars, have also been shown to be co-metabolized by the same enzyme system as naphthalene, inhibiting naphthalene degradation (Annweiler et al., 2001a; Meyer and Steinhart, 2000).

Enhanced biodegradation of MAH and PAHs can be achieved through stimulation with additional electron acceptors, substrates or both. Stimulated biodegradation of MAHs and PAHs been shown under nitrate- and sulfate-reducing conditions (Al-Bashir et al., 1990; Ambrosoli et al., 2005; Thierry Pierre Alain Bregnard et al., 1996; B. V. Chang et al., 2002; Coates et al., 1997; J D Coates et al., 1996; Durant et al., 1995; Eriksson et al., 2003; Meckenstock et al., 2016). MAH degradation has been shown under chlorate reducing conditions, (Chakraborty and Coates, 2004; Solís-González and Loza-Tavera, 2019; Weelink et al., 2010) however, to the best of our knowledge, no studies showing PAH degradation under chlorate-reducing conditions have been reported. Enhanced

biodegradation of MAHs and PAHs by stimulating co-metabolism has been shown through the addition of substrates, including, for example, acetate, succinate, glucose, lactate and methanol (Ambrosoli et al., 2005; Liu et al., 2017; Maillacheruvu and Pathan, 2009; Teng et al., 2010; Vaidya et al., 2018, 2017; Yuan and Chang, 2007; Zhang and Lo, 2015). The addition of acetate, alone or in combination with an electron acceptor, can enhance the degradation of benzene, toluene, naphthalene, acenaphthene, fluorene, phenanthrene, anthracene, and pyrene (Ambrosoli et al., 2005; Thierry Pierre Alain Bregnard et al., 1996; Coates et al., 2002b; Ebihara and Bishop, 2002; Liu et al., 2017; Maillacheruvu and Pathan, 2009; Mittal and Rockne, 2008; Rahman et al., 2018; Zhang et al., 2017, 2015b). Enhancement with acetate is believed to be primarily caused by co-metabolism and has been shown to depend on the specific reducing conditions (Yuan and Chang, 2007). Limited studies have shown enhanced PAH degradation using succinate as a substrate, alone or in combination with an electron acceptor. Succinate has been shown to enhance the degradation of naphthalene, acenaphthylene, fluorene, phenanthrene, anthracene, pyrene and benzo(a)pyrene (Burd and Ward, 1996; Teng et al., 2010; Vaidya et al., 2017).

Most degradation studies have focused on single component or artificial mixtures of MAH and/or PAHs. Fewer studies have investigated the biodegradation of natural mixtures of PAHs from hydrocarbon contaminated sites (e.g. coal-tar or creosote)(Eriksson et al., 2000; Rothermich et al., 2002) and in most cases only one of MAHs or PAHs are measured. The interaction of hydrocarbons is important to consider for in-situ bioremediation technologies, in particular for source zones where high concentrations of complex mixtures of MAHs, PAHs, and hetero-cyclic hydrocarbons are present. Few studies have examined the potential for source zone remediation of hydrocarbon contaminated sites through biostimulation (Müller et al., 2017; Ponsin et al., 2014; Ramos et al., 2013). Source zone biostimulation was previously considered infeasible as the high

concentration of aqueous phase contaminants were thought to be toxic to microbes (Langevoort, 2009). However, measurements from a former manufactured gas plant in Amersfoort (Netherlands) detected higher counts of hydrocarbon degraders in the bacterial population in the source zone than in the plume zone. Specifically, high concentrations of sulfate- and nitrate-reducing bacteria and metabolites for anaerobic toluene degradation (benzylsuccinic acid) were found within the source zone (Leeuwen et al., 2020). Upstream measurements showed a constant supply of electron acceptor rich groundwater to the source zone, suggesting potentially favorable conditions for source zone degradation. It is not known to what degree source zone degradation is taking place, nor the possible effects of source zone biostimulation with alternative electron acceptors or substrate. The source zone is from a former Pintsch gas factory and contains a complex mixture of 980 compounds. The tar in this site differs from other coal-tar or creosote contaminated sites due to the high concentrations of both BTEX and PAHs, as well as heterocyclic and oxygenated hydrocarbons. As a result, the mass of the tar on site is slightly higher than water and can be classified as a dense non-aqueous phase liquid (DNAPL).

In this study, we investigated the ability to stimulate microbial degradation in the source-zone for a complex, multi-component hydrocarbon DNAPL using different electron acceptor-substrate combinations. Microcosms were prepared using source zone contaminated sediment and groundwater from the Amersfoort site with added electron acceptors and substrate pairs. To assess enhanced bioremediation, stimulated microcosms were compared with those under unstimulated conditions for hydrocarbon concentrations, anion consumption, metabolite concentration, and DNA.

3.2 Material and Methods

3.2.1 *Microcosm preparation*

Microcosms were prepared anaerobically in an inflatable glove bag filled with N₂/CO₂ (95%/5%) gas which was run over a glass column of hot (350 °C) copper flakes to remove any trace oxygen. Microcosms were prepared in triplicate in 200-ml glass serum bottles with butyl/PTFE lined septa (VWR, Netherlands). Microcosms contained 40 g of source-zone sediment from borehole A005 (depth: 9.5-10 m) and groundwater from well A003A (Figure 3-1). Concentrations of contaminated groundwater are given in Supporting Information (Table S3-1). Control microcosms (S-Con) were prepared to account for abiotic transformations in bottles and sterilized with 100 mg/L NaN₃, 100 mg/L HgCl₂ and autoclaved at 121 °C for 20 minutes. To compare the performance of stimulated microcosms against the natural field conditions, an unstimulated set of microcosms (U-Con) were prepared without added electron acceptors or substrates. Microcosms were stimulated with anaerobic, 1M stock solutions of nitrate, nitrate-succinate, nitrate-acetate, sulfate and chlorate (Table 3-1). Microcosms were then inverted (septa down) on a shaker at 100 rpm in a climate chamber at 20 °C and dosed with additional electron acceptors and/or substrate as needed, see Table 3-1. Microcosms were measured regularly for anions and cations in the first year of operation; hydrocarbons, metabolites and DNA were analyzed after three years and a total extraction of the microcosms was performed after four years (see detailed methods below).

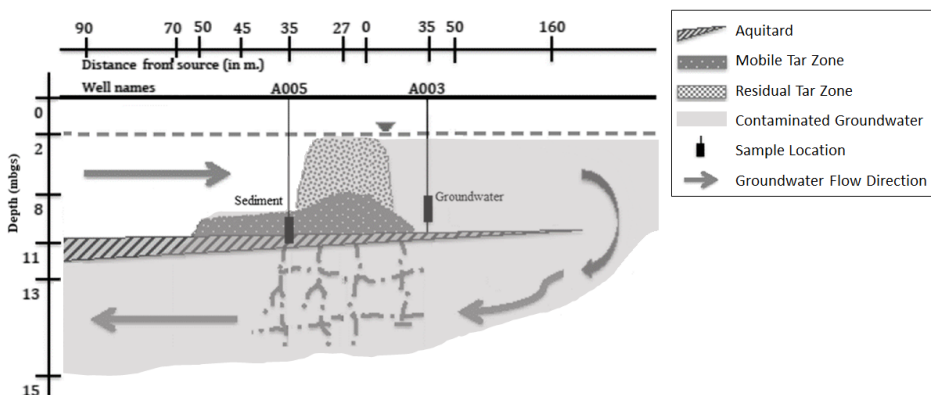


Figure 3-1: Location of samples used for microcosm experiments. Contaminated sediment from source zone well A005 and contaminated groundwater downstream of source zone well A003 (adapted from van Leeuwen et al. (Leeuwen et al., 2020))

3.2.2 Hydrocarbons Analysis

Microcosms were extracted with acetone to quantify the total mass of hydrocarbon, the mass of MAHs and PAHs. Prior to extraction, hydrocarbons were measured in the headspace and aqueous phase using a gas chromatograph (GC). Hydrocarbon concentrations were compared to determine the relative degradation of MAHs and PAHs between the treatments.

PAHs were measured using liquid, cool on-column injection with a HP 6890 series GC system and Agilent CP-Sil 5 CB column (0.32 mm x 30 m), equipped with a FID (COC-GC-FID). Peaks were identified using an Agilent 7890B GC with an Agilent 5977 MSD and a CP-Sil 5 CB column (0.32 mm x 25 m). Aqueous MAH concentrations were measured on an Agilent 7890A GC with a 5975C MSD and a Grace AT-624 column (0.25 mm x 60 m). Headspace MAHs and methane concentrations were measured on an Agilent 6850 GC-FID (flame ionized detector) equipped with an Agilent HP-1 columns (0.32 mm x 30 m), as described previously (Leeuwen et al., 2020). See SI for detailed description of the extraction protocol and temperature settings for the PAH and MAH analyses.

While the septa of all bottles remained tight, one replicate of the NO₃ microcosm leaked during the experiment and was discarded. In addition, when the bottles were measured the septa were punctured and it is possible methane gas could have escaped due to overpressure, a potential source of error.

The relative loss of hydrocarbons was calculated in reference to the U-Con microcosm. Masses were also normalized to the mass of 1,2,4-trimethylbenzene (124-TMB) in each microcosm to account for initial differences in concentration of tar in the microcosms and to make direct comparisons between masses in the microcosms.

3.2.3 Partitioning Calculations

Given the measured aqueous concentrations (C_{aq}) and the total mass (M_{total}) of MAHs in the microcosms after extraction, the mass of each MAH in the tar sample was calculated (Eq. 1). The mass of volatiles in the gas phase was negligible and therefore not included in the mass balance. The volume of tar left in the microcosm, to account for the observed C_{aq} and the M_{total} remaining in the microcosm, was calculated using eq. 2, where K_{NW} is the NAPL-water partitioning coefficient obtained from partitioning microcosm experiments performed on pure-phase tar from the same well as the residual sediment used in the microcosms (Leeuwen et al., 2020). The predicted partitioning coefficient (K_{NW}^{pred}) to account for the observed C_{aq} and M_{total} was calculated assuming the total mass of tar lost was equal to the total loss of hydrocarbons in the microcosm.

$$M_{total}^i = M_{aq}^i + M_{tar}^i \quad \text{Eq. 1}$$

$$V_{tar} = \frac{M_{tar}^i \cdot V_{aq}}{K_{nw}^i \cdot M_{aq}^i} \quad \text{Eq. 2}$$

Table 3-1: *Electron acceptor and substrate dosing schedule for stimulated microcosms*

Electron Acceptor-Substrate	Microcosm Abbr.	May 2014	Sept. 2014	March 2015
Sterile (Control)	S-Con	100 mg/L HgCl ₂ + 100 mg/L NaN ₃	-	-
Unstimulated (Control)	U-Con	-	-	-
Nitrate	NO ₃	10 mM NaNO ₃	-	-
Nitrate-Succinate	NO ₃ -S	10 mM NaNO ₃ + 2mM C ₄ H ₆ O ₄	2 mM C ₄ H ₆ O ₄	10 mM NaNO ₃ + 2 mM C ₄ H ₆ O ₄
Nitrate-Acetate	NO ₃ -A	10 mM NaNO ₃ + 4mM CH ₃ COO ⁻	10 mM CH ₃ COO ⁻	10 mM NaNO ₃
Sulfate	SO ₄	10 mM Na ₂ SO ₄	-	-
Chlorate	ClO ₃	10 mM NaClO ₃	-	-

3.2.4 Anion Analysis

Microcosms were measured regularly in the first 400 days of operation for anion concentrations (acetate, bromide, chlorate, chloride, chlorite, fluoride, formate, fumerate, nitrate, nitrite, phosphate, succinate and sulfate) using a Dionex ICS-1500 equipped with an IONPAC AS14 anion exchange column and an A SRSs-Ultra 14 mm suppressor (Dionex Corporation, Sunnyvale CA, USA).

3.2.5 Semi-Quantitative Metabolite Analysis

Microcosms which showed activity (loss of added electron acceptors) in the first 400 days were also sampled for metabolites and DNA analysis. The SO₄ and ClO₃ microcosms showed no activity and were therefore not measured. Aqueous phase metabolites were measured using liquid chromatography quadruple time-of-flight mass spectroscopy (LC-qTOF-MS) as previously (Leeuwen et al., 2020). Briefly, 1-ml aqueous samples from microcosms were filtered with 0.2- μ m polypropylene

syringe filter (Acrodisc 13, Pall, Netherlands) directly to 2-ml LC vials (VWR, Netherlands). Standards for quantification of 1H-indene-2 carboxylic acid, 1H-indene-3-carboxylic acid, 2-naphthoic acid, sodium benzoate, benzylsuccinic acid and (trans)cinnamic acid were created in a dilution series. Semi-quantification of metabolites was performed for all suspects as described earlier by van (Leeuwen et al., 2020).

3.2.6 DNA Extraction and qPCR Analysis

DNA analyses were performed on aqueous phase samples from all microcosms except the SO₄ and ClO₃ microcosms, which showed no loss of sulfate or chlorate in the first 400 days. From the microcosms, 1 ml of the aqueous phase was centrifuged at 10,000 rpm for 10 minutes, after which the pellet was dissolved in 100 µL supernatant. The genes for total bacterial 16S rRNA, *Peptococcaceae* 16S rRNA, benzene carboxylase (*abcA*) and benzylsuccinic acid (*bssA*) nitrate-reducing bacteria (NRB) were analyzed, as previously described (van der Waals et al., 2017). The gene *bssA* for sulfate-reducing bacteria (SRB) were targeted using primers SRBf and SRBr (Beller et al., 2008). Nitrite reducing bacteria were targeted by the *nirS* gene using primers nirS4F and nirS6R (Braker et al., 1998). Nitrate reducing bacteria were targeted by the *narG* gene using primers narGGF and narGGR (López-Gutiérrez et al., 2004). The primers used and thermal amplification profiles are found in SI; Table S2.

3.3 Results and Discussion

Biodegradation in the microcosms was examined along three lines of evidence: 1) changes in contaminant concentration (hydrocarbon mass balance, presence of metabolites), 2) changes in geochemical conditions (electron acceptor, substrate concentrations) and 3) changes in microbial conditions.

3.3.1 Hydrocarbon Mass Balance

The masses of hydrocarbons were normalized to the mass of 124-TMB in each of the microcosms and to the mass of each component in the U-Con microcosm, representing natural field conditions. By normalizing the masses to 124-TMB, we account for any initial differences in the amount of tar in the sediment added to the microcosms and can make direct comparisons between masses in the microcosms (Figure 3-2). Raw measured masses for PAH and MAH are found in the SI; Tables S3-3 and S3-4. Normalizing to the U-Con microcosm shows the effect of enhanced loss of hydrocarbons above the loss observed under natural field conditions. Within the S-Con microcosm, not all tar was fully extracted from the glass bottle, even after repeated flushing with acetone. The S-Con was autoclaved in the sterilization process and this may have resulted in the strong sorption of tar and likely the loss of MAHs as a result of the increased temperature and pressure in the autoclave. As a result, the initial total mass of MAHs and PAHs was not reproducible. All other microcosms were fully extracted.

Total hydrocarbons were lower in the stimulated microcosms compared to the U-Con microcosm (Figure 3-3). However, the remaining masses varied little between the U-Con, SO_4 and ClO_3 microcosms (Table S3-3 and S3-4) and therefore the SO_4 and ClO_3 microcosms are not discussed further. NO_3 -S and NO_3 -A showed a decrease in total mass and PAHs compared to the U-Con microcosm (Figure 3-3). Stimulation with NO_3 was the least effective of the treatments while stimulation with NO_3 -A was the most effective of the treatments. Overall, MAHs varied little between the microcosms, regardless of treatment.

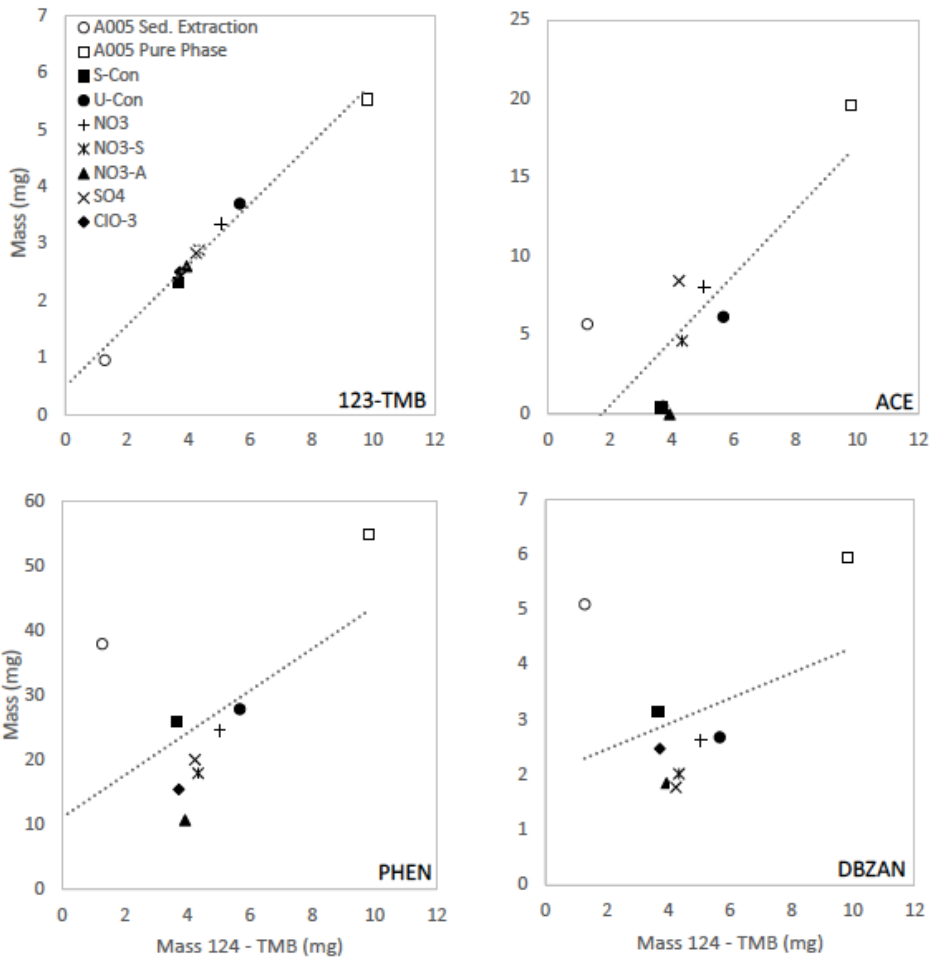


Figure 3-2: Mass of 1,2,4-trimethylbenzene(124-TMB) versus mass of: 1,2,3-trimethylbenzene (123-TMB), acenaphthene (ACE), phenanthrene (PHEN) and dibenz(a,h)anthracene (DBZAN) for the microcosms, residual sediment used in the experiments from well A005 and pure phase tar from well A005 demonstrating the consistent ratio of 123-TMB to 124-TMB in both laboratory and field conditions. Dashed line shows the linear trend line.

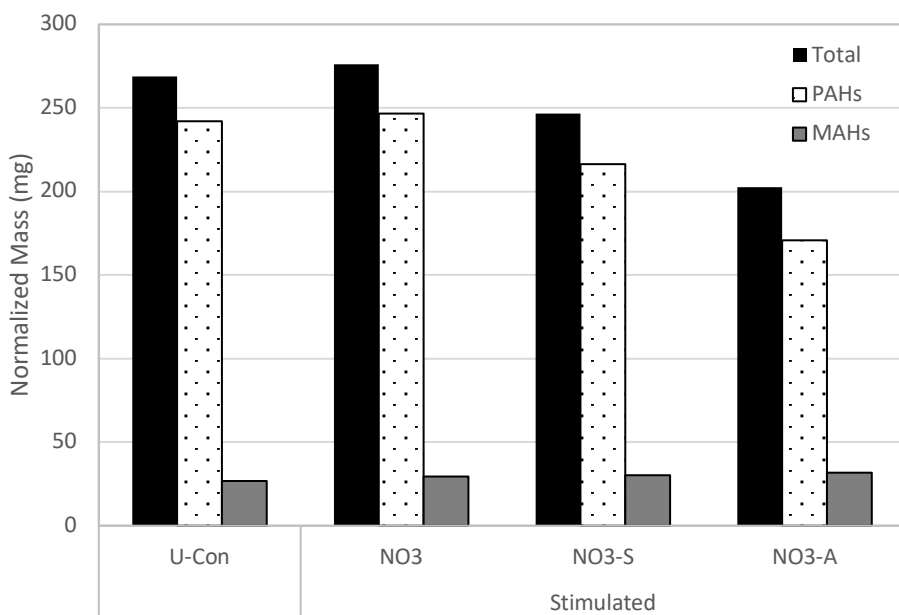


Figure 3-3: Normalized mass of total hydrocarbons, PAHs and MAHs.

3.3.2 Loss of PAHs

The relative loss of PAHs was calculated in reference to the U-Con microcosm. PAH concentrations in the aqueous phase were below the detection limit for all PAHs with the exception of naphthalene. Within the NO₃-S and NO₃-A microcosms there was detectable loss of most PAHs, including HMW PAHs (Table S3-3). The most substantial loss of PAHs was in the NO₃-A stimulated microcosm, with 29% of the sum of PAHs in the microcosm (Figure 3-3). Stimulation with NO₃-S resulted in loss of 11% of PAHs, while stimulation with NO₃ resulted in no additional loss above the unstimulated conditions (Figure 3-3). These results are in keeping with previous studies which found that stimulation with nitrate and a substrate to be more effective at PAH removal than stimulation with nitrate alone (Ambrosoli et al., 2005; Thierry Pierre Alain Bregnard et al., 1996; Langenhoff et al., 1996; Mittal and Rockne, 2008). The addition of co-substrates is expected to increase the number and activity of PAH-degrading microorganisms and may enhance enzymatic activity, leading

to increased degradation of PAHs, either through the direct use of substrates or the decomposition of substrates to form co-metabolic substrates (Ambrosoli et al., 2005; Teng et al., 2010).

3.3.3 Loss of LMW vs. PAHs

In the NO₃-S and NO₃-A microcosms, the LMW PAHs were, in general, lost more than the HMW PAHs (Figure 3-4). However, naphthalene was the exception, with only 7% loss in the NO₃-S microcosm and no loss above unstimulated conditions in the NO₃-A microcosm. This loss is in comparison to an average 51% loss of other LMW PAHs in the NO₃-A microcosm.

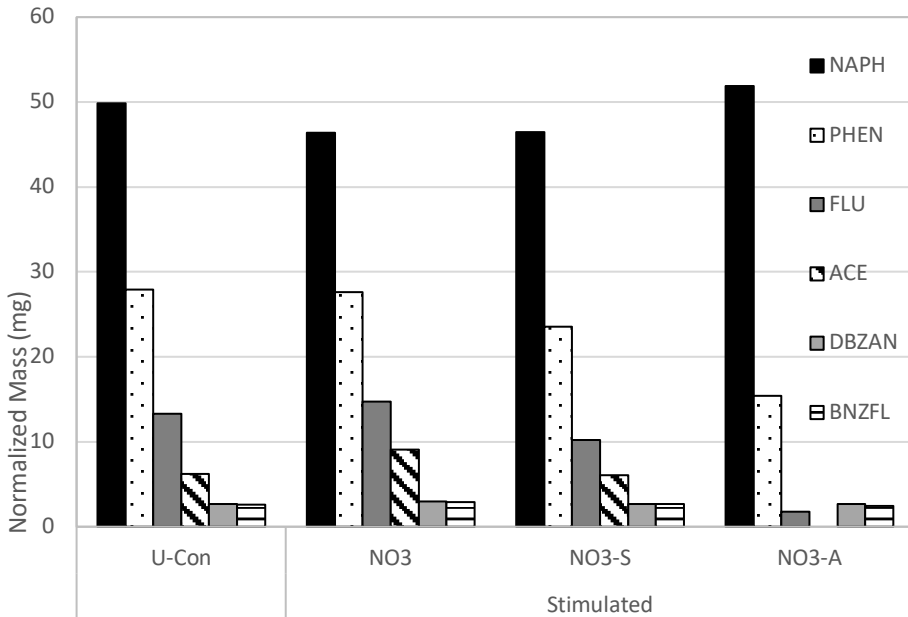


Figure 3-4: Normalized mass of select PAHs remaining in the microcosms after 4 years, listed in the order of decreasing mass remaining in the U-Con microcosm. NAPH = naphthalene, PHEN = phenanthrene, ACE = acenaphthylene, DBZAN = dibenz(a,h)anthracene, BNZFL = benzo[*b*]fluoranthene.

Thus far, the relative recalcitrance of naphthalene with respect to the degradation of LMW PAHs has been found in literature under sulfate reducing conditions (Rothermich et al., 2002). A possible explanation for the lower

naphthalene loss could be the competitive inhibition or co-metabolism of naphthalene, which has been shown by others (Annweiler et al., 2001a; Meyer and Steinhart, 2000; Safinowski et al., 2006). LMW and HMW PAHs have been shown to be degraded by different groups of microorganisms (Zhou et al., 2008). The type of co-substrate used has been shown to affect PAH degradation, as co-substrates influence the structure and diversity of microbial communities (Liu et al., 2017; Zhang et al., 2015b; Zhang and Lo, 2015). The use of different co-substrates therefore can result in differences in the type and rate of PAH degradation.

3.3.4 Loss of MAHs

In contrast to the loss of PAHs, MAHs varied little between the microcosms, with the exception of benzene and ethylbenzene (Figure 3-5). Notably, at the end of the four-year experiment, the U-Con microcosm had the lowest aqueous phase benzene and ethylbenzene concentrations and lowest total benzene mass remaining (Figure 3-5). This result was unexpected as benzene is generally considered recalcitrant under anaerobic conditions and degradation has been shown to be stimulated under a variety of redox conditions. (Meckenstock et al., 2016) The addition of acetate has also been shown to increase benzene degradation in other studies. (Coates et al., 2002b; Müller et al., 2017; Ramos et al., 2013; Teng et al., 2010) The removal of benzene and ethylbenzene appears to have been inhibited by stimulation with additional electron acceptors and substrates.

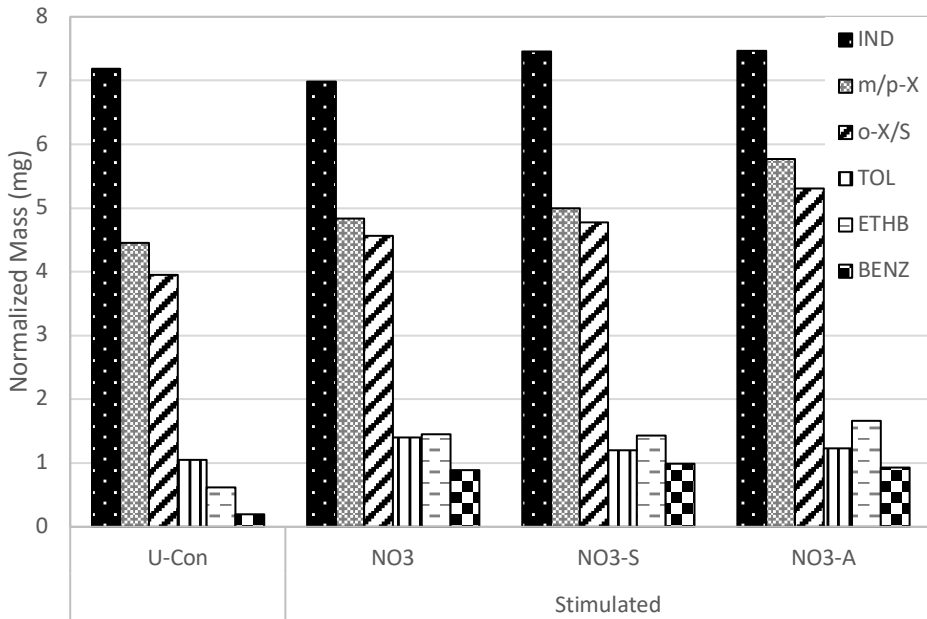


Figure 3-5: Normalized mass of select MAHs remaining in the microcosms after 4 years. Listed in order of decreasing mass remaining in the U-Con microcosm. IND = indene, m/p-X = m/p-xylene, o-X/S = o-xylene/styrene, TOL = toluene, ETHB = ethylbenzene, BENZ = benzene.

3.3.5 Partitioning Calculations

The observed aqueous concentrations of benzene and ethylbenzene in the U-Con microcosm cannot be accounted for by the partitioning coefficients of the pure-phase tar from van Leeuwen et al. (Leeuwen et al., 2020). The average volume of tar to account for the observed aqueous concentration and remaining total mass in the microcosms was calculated from the average volumes, not including benzene and ethylbenzene, due to the above mentioned deviations from the other volatiles. The volume of tar remaining in the microcosm would have to be much larger to account for the very low concentrations observed in the aqueous phase (Table S3-5). In contrast, in the NO₃ and NO₃-S microcosms the aqueous concentrations measured would be expected for a lower total tar volume. Finally, the NO₃-A microcosm, which had the highest overall mass loss, would have to

have the largest volume of tar remaining to account for the observed aqueous concentration and remaining total mass of benzene.

Another possible explanation for the observed aqueous concentration and total mass ratios is changes to the partitioning coefficients (K_{nw}). We would expect an increase in the K_{nw} to result in lower aqueous concentrations, all other things being equal. The calculated K_{nw} deviates from the predicted K_{nw} of the pure-phase tar given by van Leeuwen et al. (Leeuwen et al., 2020) for the microcosms (Figure S3-1). The calculated partitioning coefficients were, in general, lower than the predicted coefficients. The results suggest that stimulation changes the partitioning coefficients of the tar components. Changes in partitioning coefficients can result from leaching of components from the tar (weathering/flushing), (bio)degradation and changes in the liquid phase stability of tar components. (Ghoshal et al., 2004; Lee et al., 1998; Liu et al., 2009; Mahjoub et al., 2000; Peters et al., 2000) However, the changes in partitioning still cannot fully explain the aqueous concentration in relation to remaining mass for benzene in the U-Con microcosm and the reasons for the changes in partitioning should be explored in future research.

3.3.6 *qPCR*

The gene copies per ml for *bssA* (NRB), *Peptococcaceae* 16S rRNA and *abcA* were below the detection limit in all of the microcosms. The NO₃-S and NO₃-A microcosms had higher total bacteria (16S rRNA) and gene counts for nitrite-reducing (*nirS* gene) and nitrate-reducing bacteria (*narG* genes) compared to the control and NO₃ microcosms (Figure 3-6). This corresponds well with the increased overall loss of hydrocarbons in microcosms with substrate over the NO₃ microcosm. The NO₃ microcosm also had slightly elevated total bacteria and *narG* gene copies compared to the S-Con and U-Con microcosms (Figure 3-6). The results suggest that addition of nitrate stimulates growth of nitrate-reducing bacteria and the addition of nitrate with a substrate stimulates the

growth of nitrite reducing bacteria. Addition of co-substrates has been shown to promote the growth of hydrocarbon degrading microorganisms (Ambrosoli et al., 2005; Liu et al., 2017; Yuan and Chang, 2007).

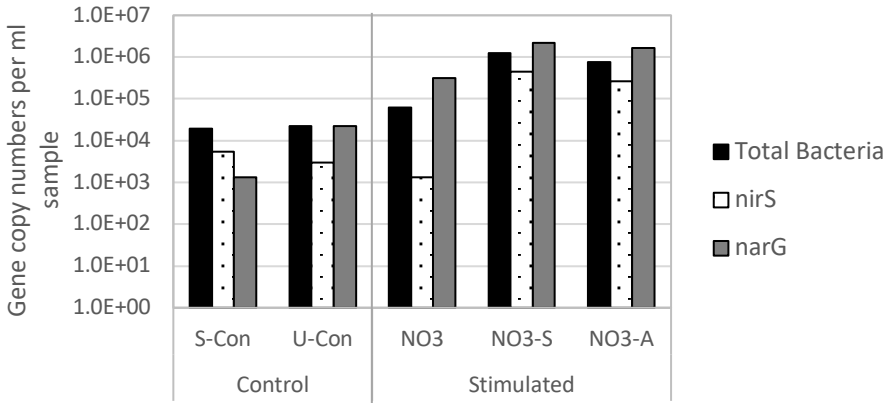


Figure 3-6: qPCR results for total bacteria (*16S rRNA*), *nirS* and *narG*. All samples were below the detection limits for *Peptococcaceae 16S rRNA*, *abcA*, and *bssA* (NRB) (not shown).

Methane was detected in the headspace of all microcosms except for the S-Con. Methane concentrations varied little between the microcosms, in the range of 2.2-2.4 mg/L (Table S3-6). Previous field measurements found methanogenic archaea present in groundwater samples from heavily contaminated source zone wells (Brock, 2016; Raptis et al., 2015). Moreover, methanogenic archaea were found in wells with nitrate and sulfate reducing conditions, which may indicate overlapping redox zones or micro-niches (Bauer et al., 2008; Meckenstock et al., 2015). Hydrocarbon degradation under methanogenic conditions has been widely shown (Annweiler et al., 2001a; Berdugo-Clavijo et al., 2012; B. V. Chang et al., 2002; Dolfing et al., 2009; Maillacheruvu and Pathan, 2009; Qin et al., 2017; Sharak Genthner et al., 1997; Yuan and Chang, 2007; S. Zhang et al., 2012; S. Y. Zhang et al., 2012).

3.3.7 *Metabolites*

The sum concentration of metabolites in the U-Con were 14% higher than in the S-Con (Figure 3-7). This suggests active degradation of hydrocarbons and possible accumulation of metabolites as a result of electron acceptor depletion or slower degradation rate of metabolites compared to parent compounds in the U-Con (Figure 3-7). The lower sum concentration of metabolites in the stimulated microcosms (NO₃, NO₃-S and NO₃-A) could be a result of continued degradation of metabolites. Similarly low concentrations of metabolites, despite evidence of increased degradation has been previously.(Caldwell and Suflita, 2000; Jobelius et al., 2011b)

Benzoic acid, a possible metabolite of benzene, toluene, ethylbenzene and phenol, was the single most abundant metabolite in the microcosms (Table S3-7). Signature metabolites for toluene (benzylsuccinic acid), naphthalene (2-naphthoic acid) and indene (1H-indene-2-carboxylic acid) were found in all treatments and are indicative of toluene, naphthalene and indene degradation (Table S3-7). Metabolites for fluorene, phenanthrene and acenaphthylene were found in all microcosms, including the S-Con (Figure 3-7). Metabolite concentrations from the S-Con suggest source-zone degradation of MAHs and PAHs in-situ, which was also supported by field measurements in source zone wells.(van Logtestijn, 2017) The presence of metabolites provides only qualitative evidence of biodegradation and the quantity of metabolites found depends on both the rate of degradation of the parent compound and that of the metabolite, with supposedly recalcitrant metabolites being found at higher concentrations than relatively easily degraded ones.(Beller, 2002; Jobelius et al., 2011b)

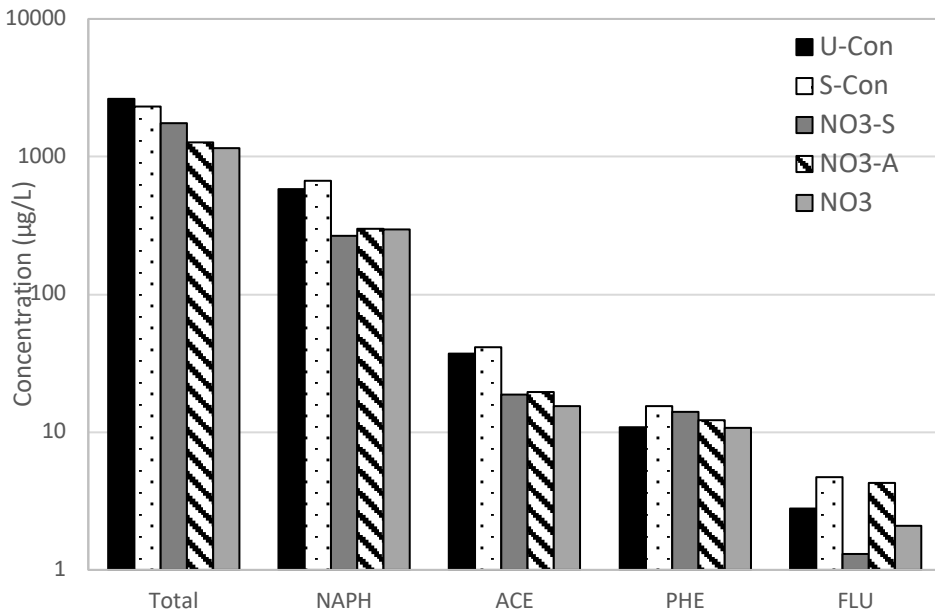


Figure 3-7: Semi-quantitative concentrations of select metabolites for PAHs in aqueous phase of microcosms. Total = total sum of all metabolites measures in the microcosm, NAPH = naphthalene, ACE = Acenaphthylene, PHE = Phenanthrene, FLU=Fluorene.

3.3.8 Anions

No substantial changes in nitrate were observed in the NO₃ microcosm despite measured losses of hydrocarbons (Figure S4). However, nitrate reduction by succinate and acetate was observed in the NO₃-S and NO₃-A microcosms (Figure 3-8 and Figure 3-9). The succinate consumed within the NO₃-S microcosm can be accounted for stoichiometrically for the nitrate and nitrite which was consumed coincident with the succinate. However, the acetate consumed after the second dose (day 118) in the NO₃-A microcosm cannot be accounted for stoichiometrically by the nitrite consumed. Approximately 2.5 times more acetate was consumed than could be predicted for the nitrite consumed in the same interval. A likely explanation is the co-metabolism of acetate with the observed PAH degradation in the NO₃-A microcosm, as shown by others (Ambrosoli et al.,

2005; Liu et al., 2017; Yuan and Chang, 2007; Zhang et al., 2015b; Zhang and Lo, 2015).

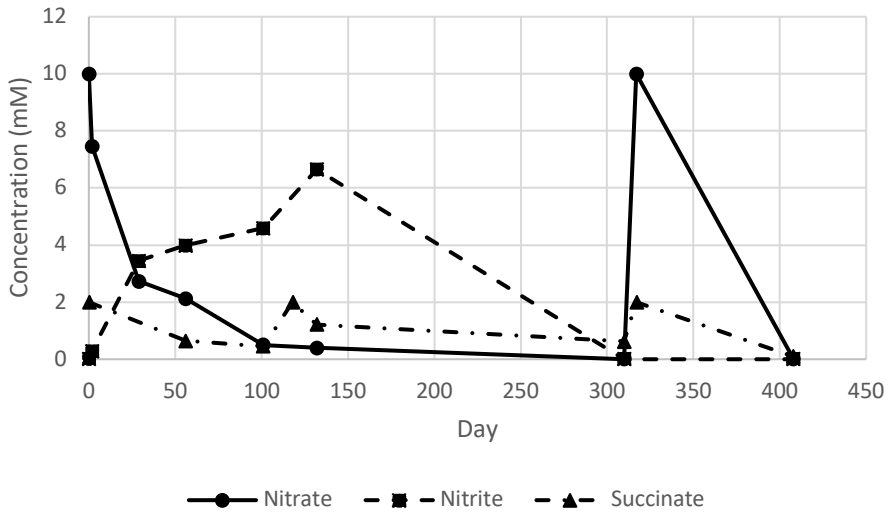


Figure 3-8: Anion concentration over time for the $\text{NO}_3\text{-S}$ microcosm. Arrows indicate when the microcosms were dosed.

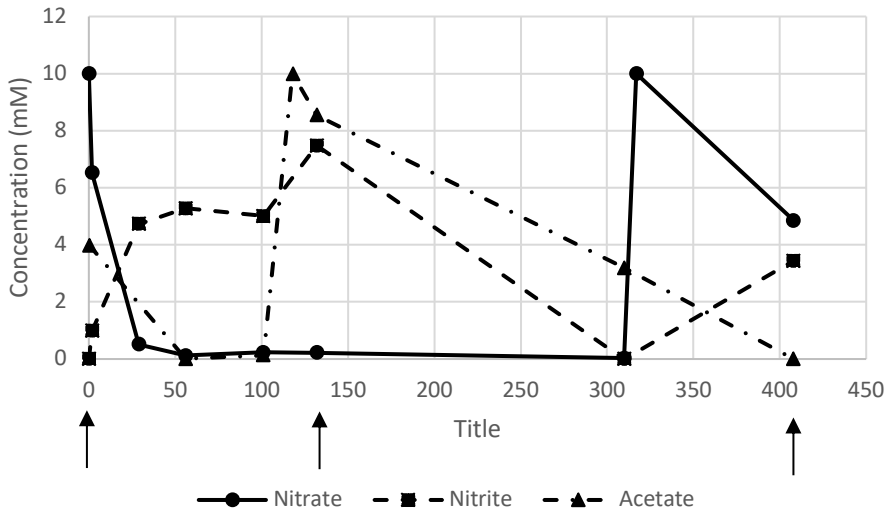


Figure 3-9: Anion concentration over time for the $\text{NO}_3\text{-A}$ microcosm. Arrows indicate when the microcosm was dosed.

The lack of nitrate reduction in the NO_3 microcosm, and the worse performance of the NO_3 microcosm compared to the NO_3 -S and NO_3 -A microcosms, as well as the presence of methane in the microcosms (Table S3-4) suggests that methanogenesis may be the dominant mechanism for tar component degradation within the microcosms. Within the U-Con microcosm, the background concentration of nitrate and sulfate from the groundwater cannot account for the loss of benzene observed (Figure S3-4). Furthermore, the added nitrate in the NO_3 -A microcosm can only account for at most 60% the observed loss of tar components, if the reaction with acetate is excluded.

3.3.9 Implications for source zone remediation

This research highlights the capacity of indigenous microorganisms to anaerobically degrade hydrocarbons when stimulated with nitrate and a substrate. Stimulation with nitrate and a substrate was found to be more effective than stimulation with nitrate alone. Stimulation with NO_3 -A enhanced PAH degradation by 29%, on average above unstimulated conditions. HMW (5-, 6-ring) PAHs showed degradation in microcosms stimulated with nitrate and acetate. Though it was not possible to definitively prove in this research, it is hypothesized that PAHs were degraded by co-metabolism with acetate, which has also been shown by others (Ambrosoli et al., 2005; Liu et al., 2017; Yuan and Chang, 2007; Zhang et al., 2015b; Zhang and Lo, 2015).

Though stimulation resulted in greater overall tar degradation, the aqueous concentration and total mass of benzene were lowest in the unstimulated microcosm. Changes in the partitioning behavior of tar components, specifically benzene and ethylbenzene, were observed though could not be explained by the calculated remaining tar volumes. These results suggest that source zone biostimulation with a substrate could result in a net loss of NAPL at the risk of releasing more soluble tar components (e.g. benzene and other MAHs) to the

groundwater, increasing plume zone concentrations and extent. In addition, the degradation of benzene in the source zone suggest that methanogenic conditions may be more important than previously thought. Further research on source zone stimulation and the possible downgradient effects, such as higher fluxes of MAHs, is necessary to understand and effectively remediate these zones by enhanced biodegradation.

Supplementary material

Detailed Methods for PAH and MAH analysis

One replicate of each microcosm treatment was successively extracted with acetone. The first volume of acetone was added through the septa to the closed microcosm to reduce losses due to volatilization. Subsequently the septa were removed, and acetone added with a glass pipette, for a total volume of 550 ml. After each acetone addition, the microcosms were capped, shaken vigorously and the supernatant liquid decanted into a glass 1-L bottle. Total hydrocarbons were calculated as the sum of the MAHs and PAHs measured in the microcosms. Samples for PAHs analysis were prepared by drying 4 ml of the acetone extract or 1 ml of the aqueous phase under a gentle stream of N₂ gas at 30 °C. The dried samples were dissolved in hexane. PAHs were measured using liquid, cool on-column injection with a HP 6890 series GC system and Agilent CP-Sil 5 CB column (0.32 mm x 30 m), equipped with a FID (COC-GC-FID). The FID was set at 330 °C. The oven temperature program was 50 °C, followed by an increase of 18 °C/min to 130 °C and then increased by 4 °C/min to 300 °C and held for 20 minutes. The program was run at a constant pressure of 100 kPa with helium carrier gas. Liquid samples of 1 μL were injected using a 10 μL syringe, flushed 10 times with each ethylacetate and hexane before and after use.

PAH peaks were identified using an Agilent 7890B GC with an Agilent 5977 MSD and a CP-Sil 5 CB column (0.32 mm x 25 m). The oven temperature program was 50 °C, followed by an increase of 18 °C/min to 130 °C and then increased by 4 °C/min to 320 °C and held for 5 minutes, then a decrease of 100 °C to 50 °C and held for 10 minutes. Samples were injected by autosampler and a solvent delay of 4 minutes was used. The program was run with constant flow of 1.6 ml/min and helium carrier gas. An internal calibrant, perfluorotributylamine (PFTBA) was used to improve mass spectral accuracy. PFTBA was injected to the MSD between 64-66 minutes at the end of each

sample run at an oven temperature of 50 °C.(Wang and Prest, 2006) The acquisition type was profile mode, the tune type EI and gain factor set to 1.

Samples for MAHs analysis were prepared by diluting 0.5 ml of the sample (aqueous phase or acetone extract) in 11.5 ml of MilliQ water in 20 ml glass vials, crimp sealed with butyl/PTFE caps (VWR, Netherlands). MAHs were measured on an Agilent 7890A GC with a 5975C MSD and a Grace AT-624 column (0.25 mm x 60 m). Samples were heated to 45 °C for 20 minutes and extracted with a syringe at the same temperature. Headspace samples (250 μ L) were taken with a Gerstael multi-purpose sampler. The injector temperature was 200 °C with a split ratio of 5:1. The oven temperature program was 1 minute at 40 °C, followed by an increase of 10 °C/min to 200 °C then increased by 20 °C/min to 300 °C and held for 1 minute. The program was run with constant flow of 1 ml/min with helium carrier gas and ion source temperature of 200 °C. A solvent delay of 8 minutes was used on acetone-extracted samples while a solvent delay of 4 minutes was used for water samples.

Headspace MAHs and methane concentrations were measured on an Agilent 6850 GC-FID (flame ionized detector) equipped with an Agilent HP-1 columns (0.32 mm x 30 m), as described by van Leeuwen et al.(Leeuwen et al., 2020) Briefly, the FID detector was set at 250 °C and the injector at 200 °C with a split ratio of 5:1. The final oven temperature program was 3 minutes at 40 °C, followed by an increase of 10°C/min to 90°C and held constant for 4 minutes then increased by 10 °C/min to 220 °C. The program was run with constant pressure of 5 psi with helium carrier gas. Headspace samples (0.5 ml) were withdrawn directly from microcosms with a 1 ml glass, Pressure-Lock syringe. Sterile disposable needles were first flushed with N₂/CO₂ (80%/20%).

Table S3.3-2: Concentration of hydrocarbons in well A003a (depth 10.8 m) used to create the microcosm experiments

Hydrocarbon	Concentration (mg/L)
Benzene	15.00
Toluene	16.00
Ethylbenzene	0.48
Xylene	3.50
Naphthalene	4.00

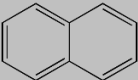
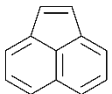
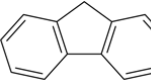

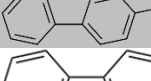
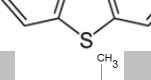
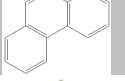
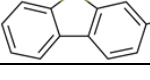
Table S3.3-3: Summary of primers used and thermal amplification profiles for the genes analyzed by qPCR used in this study

Target	Oligonucleotide sequence (5'-3') ^{a,b}	Thermal Profile	No. Cycles	References
16S rRNA gene total bacteria	GCCAGCAGCCGCGTAAT (519F) CCGTC AATCC TTTGAGTTT (907R)	94 °C 3 min	1	519F(Lane, 1991) 907R(Muyzer and Ramsing, 1995)
		94 °C 30 s, 58 °C 30 s, 72 °C 30 s	35	
		72 °C 5 min	1	
		Melt curve from 58 °C to 95 °C with increment 0.5 °C/10 s	1	
16S rRNA gene <i>Peptococcaceae</i>	CCTTCGGGTAGACAGGGAGA (PeptoF) AGCCTCTCTAGAGTGCCCAA (PeptoR)	94 °C 3 min	1	(van der Waals et al., 2017)
		94 °C 30 s, 60 °C 30 s, 72 °C 60 s	35	
		72 °C 2 min	1	
		Melt curve from 60 °C to 95 °C with increment 0.5 °C/10 s	1	
<i>abcA</i>	GCGGTGAGGTATTGACCACT (bc_F) TTCGGGCTGACATATCCTTC (bc_R)	95 °C 3 min	1	(van der Waals et al., 2017)
		95 °C 30 s, 58 °C 30 s, 72 °C 60 s	40	
		72 °C 2 min	1	
		Melt curve from 58 °C to 95 °C with increment 0.5 °C/10 s	1	
<i>bssA</i> - NRB	ACGACGGYGGCATTCTC (bssA_F) GCATGATSGGYACCGACA (bssA_R) FAM CTTCTGGTTCTTCTGCACCTTGACACC (bssA_probe)	95 °C 3 min	1	(Beller et al., 2002)
		95 °C 15 s, 58 °C 60 s	50	
		72 °C 3 min	1	
<i>bssA</i> - SRB	GTSCCATGATGCGCAGC (SRBf) CGACAT- TGAAC TGCACGTGRTCG (SRBr)	95 °C 5 min	1	(Beller et al., 2008)
		95 °C 15 s, 58 °C 60 s	45	
		72 °C 3 min, 95 °C 60 s, 58 °C 60 s	1	

			Melt curve from 58 °C to 95 °C with increment 0.5 °C/5 s	1	
<i>narG</i>	TA(CT) GT(GC) GGG CAG GA(AG) AAA CTG (narGGF) CGT AGA AGA AGC TGG TGC TGT T (narGGR)		94 °C 3 min	1	(López-Gutiérrez et al., 2004)
			94 °C 15 s, 63 °C 30 s, 72 °C 30 s	35	
			72 °C 5 min, 95 °C 60 s, 56 °C 60 s	1	
			Melt curve from 58 °C to 75 °C with increment 0.5 °C/10 s	1	
<i>nirS</i>	TTC(A/G)TCAAGAC(C/G)CA(C/T)CCGAA (nirS4F) CGTTGAACTT(A/G)CCGGT (nirS6R)		94 °C 3 min	1	(Braker et al., 1998)
			94 °C 15 s, 63 °C 30 s, 72 °C 30 s	35	
			72 °C 5 min, 95 °C 60 s, 56 °C 60 s, 58 °C 10 s	1	

^aPrimer names may differ from original publication

^bY = C or T; S = C or G; V = A or C; B = G or T or C; R = A or G

	Molecular Structure	Mol Weight (g/mol)	S-Con	U-Con	NO ₃	NO ₃ -S	NO ₃ -A	SO ₄	ClO ₃
Naphthalene		128.17	37.9	49.8	41.3	35.6	36.0	35.5	33.2
Acenaphthylene		152.19	0.4	6.2	8.1	4.7	0.0	8.5	0.5
Fluorene		166.22	3.8	13.3	13.1	7.8	1.2	10.5	3.4
Phenanthrene		178.23	26.0	27.9	24.6	18.0	10.7	20.1	15.5
2-methyl-9H-fluorene		180.25	4.3	7.9	7.4	5.3	2.4	6.0	3.7
Dibenzothiophene		184.26	4.5	6.6	6.2	4.5	2.2	5.2	3.5
Methyl phenanthrene		192.26	20.7	20.1	17.5	12.9	9.2	14.3	12.1
Methyldibenzothiophene		198.28	10.6	11.6	10.2	7.6	5.0	8.3	6.8

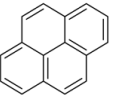
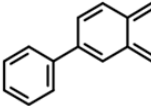
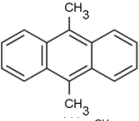
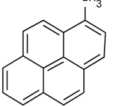
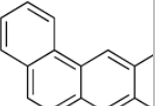
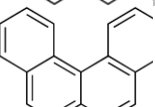
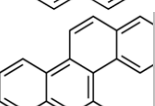
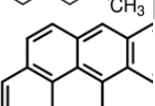
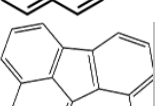
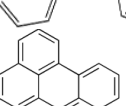
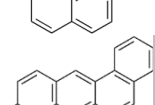
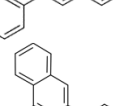
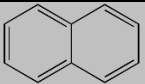
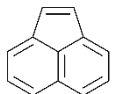
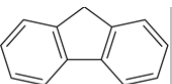

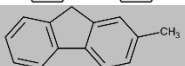
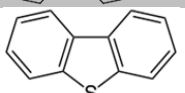
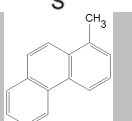
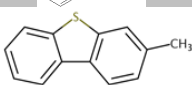
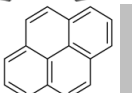
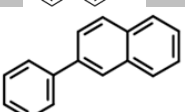
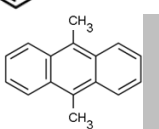
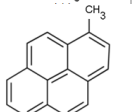
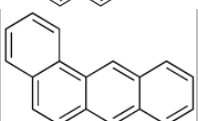
Pyrene		202.26	25.2	21.7	19.2	14.3	10.6	15.5	13.9
2-phenylnaphthalene		204.27	7.7	5.3	4.4	3.2	2.5	3.7	3.6
9,10-Dimethylantracene		206.23	17.2	15.4	13.5	10.0	7.4	11.1	9.7
1-methylpyrene		216.28	17.7	14.9	14.2	10.8	7.9	11.4	9.9
benz[a]anthracene		228.29	11.4	10.2	9.1	7.1	5.0	7.7	9.1
benzo[c]phenanthrene		228.29	8.4	8.3	7.7	5.6	4.0	6.3	5.5
5-methylChrysene		242.32	6.4	5.6	5.1	4.2	2.8	4.7	7.9
Benz[a]pyrene		252.32	8.7	7.0	7.1	5.5	4.4	6.0	5.4
Benzo[fluoranthene,		252.32	3.7	2.6	2.6	2.1	1.7	2.2	2.1
Benzo[ghi]perylene		276.34	5.3	4.5	5.0	4.0	3.2	4.1	3.3
Dibenz(a,h)anthracene		276.34	3.2	2.7	2.6	2.0	1.9	1.8	2.5
Dibenzo[a,e]fluoranthene		302.38	1.2	0.5	0.7	0.5	0.5	0.5	0.6

Table S3.3-4: Mass of PAHs (mg) remaining in microcosms after 4 years. PAHs listed in order of increasing molecular weight. Raw measurements before normalization.

	Molecular Structure	Mol Weight (g/mol)	S-Con	U-Con	NO ₃	NO ₃ -S	NO ₃ -A	SO ₄	ClO ₃
Naphthalene		128.17	37.9	49.8	41.3	35.6	36.0	35.5	33.2
Acenaphthylene		152.19	0.4	6.2	8.1	4.7	0.0	8.5	0.5
Fluorene		166.22	3.8	13.3	13.1	7.8	1.2	10.5	3.4
Phenanthrene		178.23	26.0	27.9	24.6	18.0	10.7	20.1	15.5
2-methyl-9H-fluorene		180.25	4.3	7.9	7.4	5.3	2.4	6.0	3.7
Dibenzothiophene		184.26	4.5	6.6	6.2	4.5	2.2	5.2	3.5
Methyl phenanthrene		192.26	20.7	20.1	17.5	12.9	9.2	14.3	12.1
Methyl dibenzothiophene		198.28	10.6	11.6	10.2	7.6	5.0	8.3	6.8
Pyrene		202.26	25.2	21.7	19.2	14.3	10.6	15.5	13.9
2-phenylnaphthalene		204.27	7.7	5.3	4.4	3.2	2.5	3.7	3.6
9,10-Dimethylanthracene		206.23	17.2	15.4	13.5	10.0	7.4	11.1	9.7
1-methylpyrene		216.28	17.7	14.9	14.2	10.8	7.9	11.4	9.9
benz[a]anthracene		228.29	11.4	10.2	9.1	7.1	5.0	7.7	9.1

Enhanced biodegradation on DNAPL-source zone

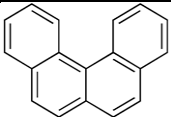
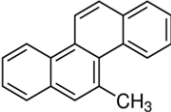
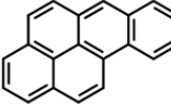
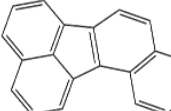
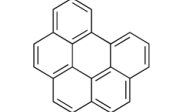
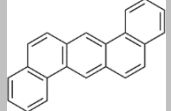
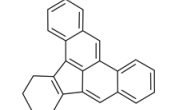
benzo[c]phenanthrene		228.29	8.4	8.3	7.7	5.6	4.0	6.3	5.5
5-methylChrysene		242.32	6.4	5.6	5.1	4.2	2.8	4.7	7.9
Benz[a]pyrene		252.32	8.7	7.0	7.1	5.5	4.4	6.0	5.4
Benzo[fluoranthene,		252.32	3.7	2.6	2.6	2.1	1.7	2.2	2.1
Benzo[ghi]perylene		276.34	5.3	4.5	5.0	4.0	3.2	4.1	3.3
Dibenz(a,h)anthracene		276.34	3.2	2.7	2.6	2.0	1.9	1.8	2.5
Dibenzo[a,e]fluoranthene		302.38	1.2	0.5	0.7	0.5	0.5	0.5	0.6

Table S3.3-5: Mass of VOCs (mg) remaining in microcosms after 4 years. VOCs listed in order of increasing molecular weight.

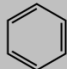
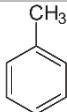
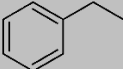
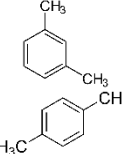
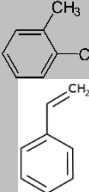
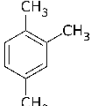
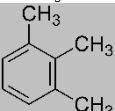
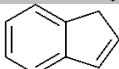
	Molecular Structure	Mol Weight (g/mol)	S-Con	U-Con	NO ₃	NO ₃ -S	NO ₃ -A	SO ₄	ClO ₃
Benzene		78.11	0.3	0.2	0.8	0.8	0.6	0.7	0.8
Toluene		92.14	0.5	1.1	1.3	0.9	0.9	1.0	0.6
Ethylbenzene		106.17	0.8	0.6	1.3	1.1	1.2	1.0	0.5
m/p-Xylene		106.17	2.4	4.5	4.3	3.8	4.0	4.0	3.5
o-Xylene/styrene		106.17 / 104.15	2.2	3.9	4.1	3.7	3.7	3.8	4.0
1,2,4-TMB		120.19	3.9	7.2	6.2	5.7	5.2	5.6	4.7
1,2,3-TMB		120.2	2.3	3.7	3.3	2.9	2.6	2.8	2.5
Indene		116.16	3.7	5.7	5.0	4.3	3.9	4.2	3.7

Table S3.3-6: The volume of tar (ml) calculated using Equations 1 and 2 and the napl-water partitioning coefficients (K_{nw}) from Van Leeuwen et al. 2020.

	Control		Stimulated		
	S-Con	U-Con	NO ₃	NO ₃ -S	NO ₃ -A
Benzene	0.59	8.75	0.10	0.05	0.80
Toluene	0.24	0.53	0.25	0.15	0.47
Ethylbenzene	0.85	3.05	0.78	0.71	1.42
m/p-Xylene	0.45	0.76	0.45	0.53	1.10
o-Xylene	0.41	0.76	0.42	0.83	1.26
Indene	0.46	0.72	0.41	1.38	0.89
123-TMB	0.35	0.57	0.33	0.41	0.74
124-TMB	0.57	1.04	0.59	0.72	1.48
Naphthalene	0.40	0.80	0.46		
Average	0.41	0.74	0.42	0.67	0.99
Average*	0.48	1.89	0.42	0.60	1.02

*Average without benzene and ethylbenzene used in calculations for partitioning coefficients

Table S3.3-7: Direct headspace GC-FID measurements of gaseous methane concentrations in microcosm headspace.

	Sterile	Unstimulated	Nitrate	Nitrate-Succinate	Nitrate-Acetate	Sulfate	Chlorate
	S-Con	U-Con	NO ₃	NO ₃ -S	NO ₃ -A	SO ₄	ClO ₃
Methane (mg/L)	0.0	2.4	2.4	2.2	2.3	2.7	2.1

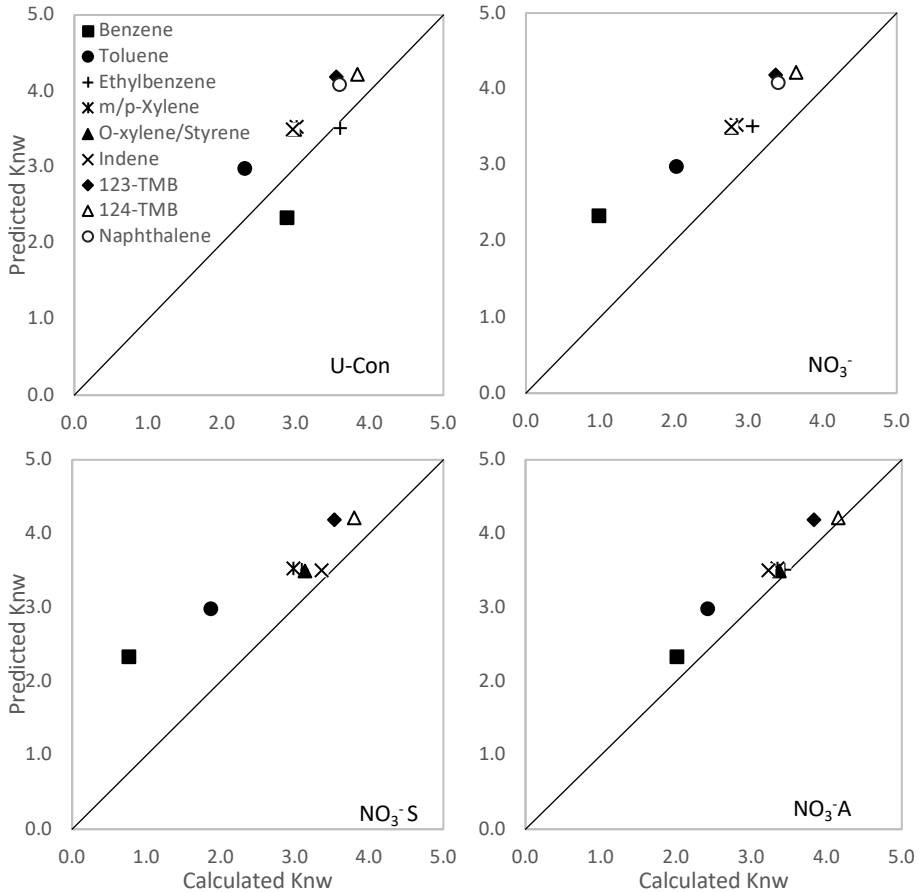


Figure S3.1: Predicted $\text{Log}K_{ow}$ vs. calculated $\text{Log}K_{ow}$ for VOCs. Predicted $\text{Log}K_{ow}$ from partitioning experiments on pure phase tar from the same well as the residual sediment used in the microcosms. (Leeuwen et al., 2020) The solid black line shows the 1:1 ratio of predicted vs. calculated $\text{Log}K_{ow}$

Table S3.3-8: Metabolite concentrations ($\mu\text{g/L}$) measured in microcosms

Metabolite	U-Con	S-Con	NO ₃	NO ₃ -A	NO ₃ -S
Toluene					
Sum	432.6	142.7	318.2	403.9	832.7
Cinnamic acid	15.7	7.4	53.1	36	6.9
Benzoic acid	369.3	112.2	248.3	350.4	805.7
Benzylsuccinic acid	13	12.9	13.9	15.6	18.7
Benzylsuccinic acid - isomers	34.6	10.2	2.9	1.9	1.4
Ethylbenzene					
Sum	471	154.9	257.8	372	836
Benzoylactic acid	10.8	0.9	0.6	2.6	4.4
Benzoylactic acid, P-coumaric acid or Hydroxycinnamate - isomers	90.9	41.8	8.9	19	25.9
Benzoic acid	369.3	112.2	248.3	350.4	805.7
Xylenes					
Sum	621.7	1058.3	449.1	455.5	939.1
3-o-toluoyl propionic acid - isomers	168.1	814.2	30.3	31.9	33.1
Methyl benzoic acid or Acetylphenol - isomer 1	74.6	127.4	166.2	71.6	97.5
Benzoic acid	369.3	112.2	248.3	350.4	805.7
Methylbenzylsuccinic acid - isomer 1	9.7	4.5	4.3	1.6	2.8
Styrene					
Sum	155.8	241	246.2	172.9	219.4
Indenediol or styrene carboxylic acid - isomers	71.5	108.2	75.7	99	119.1
2-ethylhexanol	-	-	-	-	-
Hydroxyphenylacetic acid	-	0.9	-	0.7	-
Methyl benzoic acid or Acetylphenol - isomers	74.6	127.4	166.2	71.6	97.5
Methylbenzylsuccinic acid - isomers	9.7	4.5	4.3	1.6	2.8
Trimethylbenzoic acid					
Sum	187.8	156.4	55.6	55.1	76.1
Tetrahydro-2-indenoic acid, Phenylbutyrate or Trimethylbenzoic acid - isomers	55.6	50.9	13	14.4	16.4
Trimethylbenzoic acid - isomer 1	-	-	-	-	0.7

Dimethyl-benzoic acid or Benzylacetate - isomers	132.2	105.5	42.6	40.7	59
Indene					
Sum	231	372	161	195.2	210.1
2-methylindene - isomers	0.4	7	1.4	2	1.1
Indenediol - isomer 1	-	2.6	-	1.7	-
Indenediol or styrene carboxylic acid - isomers	71.5	108.2	75.7	99	119.1
1H-indene-2-carboxylic acid	13.7	87.1	34.1	31	27.1
1H-indene-2-carboxylic acid - isomers	11.9	40.3	17.6	15.7	17.8
Indyl methyl succinic acid - isomers	3.9	3.1	1.9	1.9	1.7
Dihydro-2-indenoic acid - isomers	17.6	8.8	1.5	6.8	7
Tetrahydro-2-indenoic acid, Phenylbutyrate or Trimethylbenzoic acid - isomers	55.6	50.9	13	14.4	16.4
Carboxylated methyl indene or Dihydro- naphthoic acid - isomer 1	8.8	48.5	7.8	8.8	8
Dihydromethyl indenoic acid, Tetrahydro- naphthoic acid or 2,3- dihydro-1H-indene- acetic acid - isomer 1	39.5	6.8	2.7	4.3	5.8
Tetrahydromethyl indenoic acid or Hexahydro-naphthoic acid - isomer 1	5.3	7.1	2.9	2.7	3.2
Octahydro-2-naphthoic acid or Hexahydromethyl indenoic acid	-	-	-	-	-
Dicyclononane-2- carboxylate (octahydro- 2-indenoic acid)	-	-	-	-	-
2- carboxycyclohexylacetic acid	2.8	1.6	2.4	6.9	2.9
Naphthalene					
Sum	578.7	671.2	265.8	298.5	296.8
Carboxylated methyl indene or Dihydro- naphthoic acid - isomer 1	8.8	48.5	7.8	8.8	8
Dihydromethyl indenoic acid, Tetrahydro- naphthoic acid or 2,3- dihydro-1H-indene- acetic acid - isomer 1	39.5	6.8	2.7	4.3	5.8
Tetrahydromethyl indenoic acid or Hexahydro-naphthoic acid - isomer 1	5.3	7.1	2.9	2.7	3.2

Octahydro-2-naphthoic acid or Hexahydromethyl indenoic acid	-	-	-	-	-
Decahydro-naphthoic acid	0.5	-	-	-	0.1
Naphthaleneacetic acid or methyl-naphthoic acid - isomer 1	161.1	196	53.2	69.1	62.6
1-naphthoic acid	66.8	101.9	9.5	7.3	10.6
2-naphthoic acid	234.2	293.1	178.6	181.3	190.1
Dimethyl-naphthoic acid - isomer 1	34.8	13.6	6.9	13.6	10.4
Hydroxy-naphthoic acid	0.3	-	0.3	0.5	0.4
2-carboxycyclohexylacetic acid	2.8	1.6	2.4	6.9	2.9
2,3-dihydroxynaphthalene	-	-	-	-	-
3-naphthalenedicarboxylic acid - isomer 1	23.9	2.2	1.5	3.1	2.7
Naphthyl-2-methylsuccinate - isomer 1	0.7	0.4	0	0.9	0
Acenaphthene/acenaphthylene					
Sum	41.6	37.3	15.4	19.6	18.7
Acenaphthyleneic acid - isomer 1	26	7.1	4.3	5.7	4.7
Acenaphthyl methylsuccinate - isomer 1	5.1	15.2	2.7	6	4.3
Acenaphthenoic acid - isomer 1	10.5	15	8.4	7.9	9.7
Phenanthrene	15.4	10.9	10.8	12.2	14.1
Phenanthroic acid - isomer 1	9.9	2.7	3	6.8	6.3
P-cresol - isomer 1	5.5	8.2	7.8	5.4	7.8
Aniline					
4-aminobenzoic acid	0.2	-	0.2	0.2	0.5
Phenol					
4-hydroxy benzoic acid	1.1	0.4	1.6	2.1	-
Benzoic acid	369.3	112.2	248.3	350.4	805.7
Fluorene					
Sum	4.7	2.8	2.1	4.3	1.3
Fluorene-carboxylic acid - isomer 1	4.7	2.8	2.1	4.3	0.9
Phenol	-	-	-	-	0.4

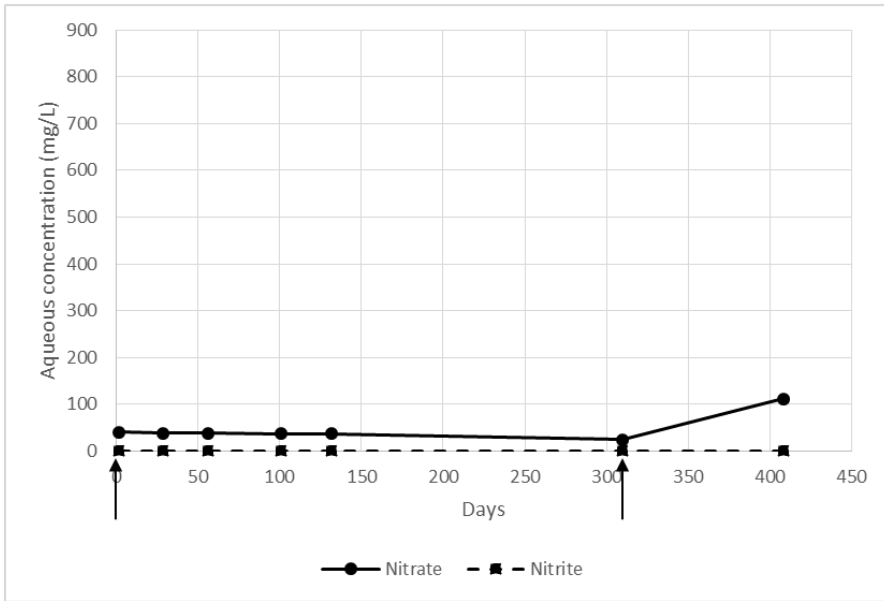


Figure S3.3-10: Anion concentration over time for the S-Con microcosm. Arrows indicate dosing of mercury chloride and sodium azide (for continued sterilization).

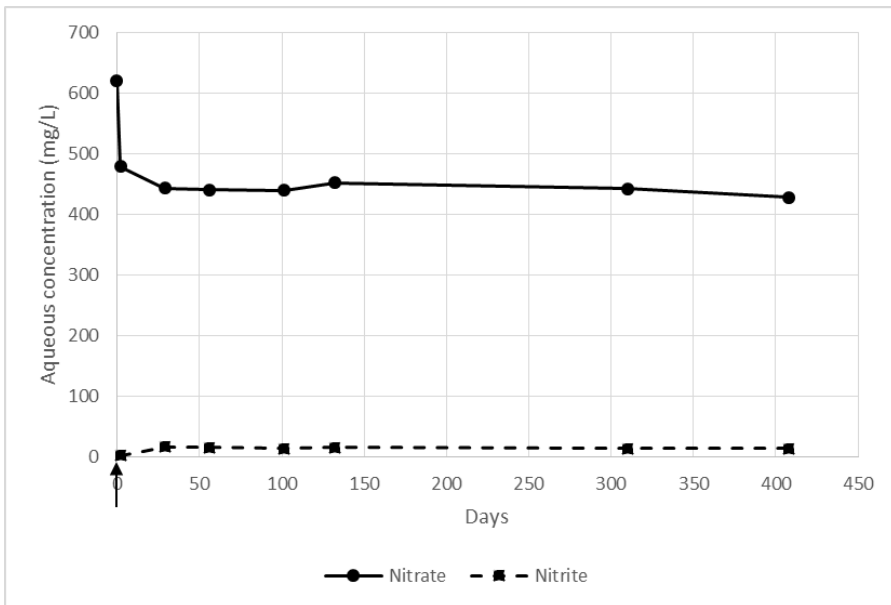


Figure S3.3-11: Anion concentration over time for the Nitrate microcosm.

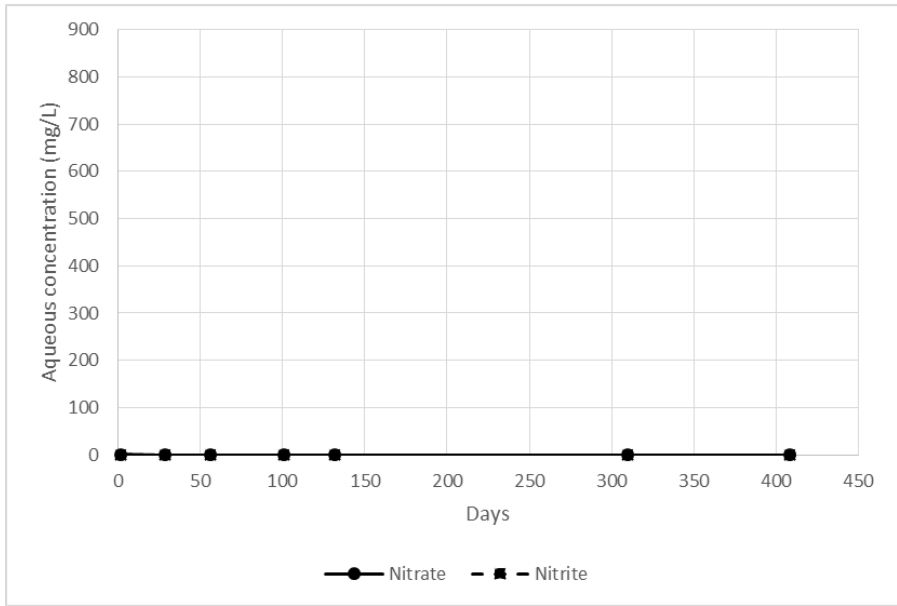


Figure S3.3-12: Anion concentration over time for the U-Con microcosm.

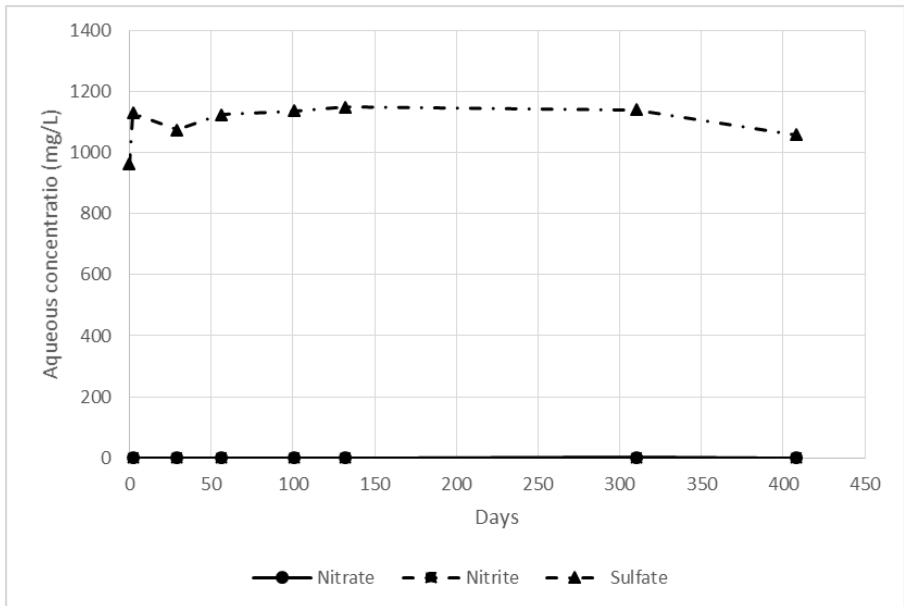


Figure S3.3-13: Anion concentration over time for the Sulfate microcosm

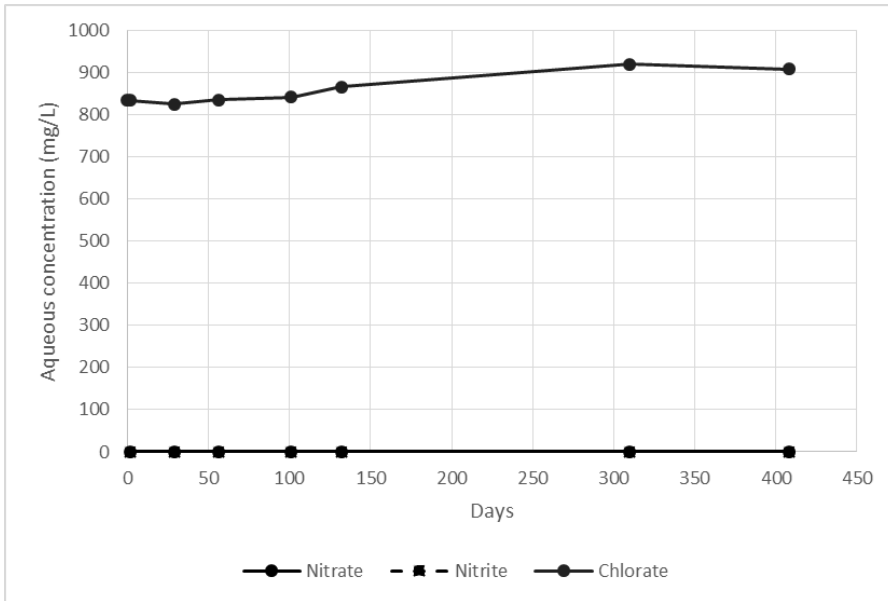


Figure S3-14: Anion concentration over time for the Chlorate microcosm.

4 Anaerobic degradation of benzene and other aromatic hydrocarbons in a tar-derived plume: nitrate versus iron reducing conditions

A version of this chapter is submitted for publication to the journal of contaminant hydrology

Johan A. van Leeuwen, Jan Gerritse, Niels Hartog, Siegmund Ertl, John R. Parsons, S. Majid Hassanizadeh

Abstract

The anaerobic degradation of aromatic hydrocarbons in a plume originating from a Pintsch gas tar-DNAPL zone was investigated using molecular, isotopic and microbial analyses. Benzene concentrations diminished at the relatively small meter scale dimensions of the suboxic nitrate reducing plume fringe. The ratio of benzene to toluene, ethylbenzene, xylenes and naphthalene (BTEXN) in the fringe zone compared to the plume zone, indicated relatively more loss of benzene in the fringe zone than TEXN. This was substantiated by changes in relative concentrations of BTEXN, and multi-element compound specific isotope analysis for $\delta^2\text{H}$ and $\delta^{13}\text{C}$. This was supported by the presence of (*abcA*) genes, indicating the presumed benzene carboxylase enzyme in the nitrate-reducing plume fringe. Biodegradation of most hydrocarbon contaminants at iron reducing conditions in the plume core, appears to be quantitatively of greater significance due to the large volume of the plume core, rather than relatively faster biodegradation under nitrate reducing conditions at the smaller volume of the plume fringe. Contaminant concentration reductions by biodegradation processes were shown to vary distinctively between the source, plume (both iron-reducing) and fringe (nitrate-reducing) zones of the plume. High anaerobic microbial activity was detected in the plume zone as well as in the dense non aqueous phase liquid (DNAPL) containing source zone. Biodegradation of most, if not all, other water-soluble Pintsch gas tar aromatic hydrocarbon contaminants occur at the relatively large dimensions of the anoxic plume core. The highest diversity and concentrations of metabolites were detected in the iron-reducing plume core, where the sum of parent compounds of aromatic hydrocarbons was greater than 10 mg/L. The relatively high concentrations of metabolites suggest a hot spot for anaerobic degradation in the core of the plume downgradient but relatively close to the DNAPL containing source zone.

4.1 Introduction

Groundwater contamination by hydrocarbons is a global problem, mainly caused by spills and leaks related to the production and usage of petroleum products (Einarson and Mackay, 2001; Kueper et al., 2003; Röling and Van Verseveld, 2002). Typically, petroleum products are complex mixtures of hydrocarbons (McGregor et al., 2012; Sandercock and Du Pasquier, 2003; Sjögren et al., 1995). Once they invade the saturated subsurface as dense non-aqueous phase liquid (DNAPL), water soluble compounds start partitioning from the DNAPL into the groundwater, forming contaminated groundwater plumes (Peters and Luthy, 1993). Processes that mainly reduce the actual removal of the dissolved contaminants in the groundwater plume are due to retardation through adsorption to the soil matrix, dilution through dispersion and biodegradation by microorganisms (Aronson and Howard, 1997; Micic et al., 2007; Oka et al., 2011; Rogers et al., 2002; Wiedemeier, Todd H.; Rifai, Hanadi, S.; Newell, Charles J.; Wilsdon, John, 1999). At tar contaminated sites, besides the commonly reported benzene, toluene, ethylbenzene and xylenes (BTEX) in groundwater, other aromatic hydrocarbon compounds such as styrene, trimethylbenzenes, ethyltoluenes, indene, indane, naphthalene, methylnaphthalenes and methylindenes, are encountered (Micic et al., 2007; Schirmer et al., 2006; Zamfirescu and Grathwohl, 2001). For naphthalene, degradation rates are generally low compared to those of BTEX (Gerritse, J; van der Grift, B; Langenhoff, 2004), while sorption dependant attenuation is a more prominent removal process due to a higher K_{oc} coefficient and relatively low water solubility (Rogers et al., 2002; Swartjes et al., 2011).

Biodegradation of one or multiple monocyclic aromatic hydrocarbons compounds has been shown to occur in laboratory and field studies under both oxic and anoxic conditions (da Silva and Corseuil, 2012; Gibson et al., 1968a; Gieg et al., 2009; Grbic-Galic and Vogel, 1987) Biodegradation rates range widely and depend mostly on the molecular structure of the contaminant and the

terminal electron-accepting processes (Foght, 2008; Meckenstock et al., 2016, 2015). Complex mixtures of aromatic hydrocarbon compounds in groundwater systems often lead to sequential attenuation of the individual components (Suarez and Rifai, 1999). Biodegradation rates for some compounds might increase, in different redox zones, while they decrease for others (Suarez and Rifai, 1999; Swartjes et al., 2011). Moreover, in complex mixtures, cometabolism can enhance biodegradation of certain recalcitrant compounds (Swartjes et al., 2011). In contrast, certain compounds can inhibit biodegradation due to toxicity (Swartjes et al., 2011). The complex interplay between multiple contaminant compounds that are present in groundwater plumes, abiotic and biotic attenuation processes, sequential redox conditions, and geohydrological setting makes it difficult to interpret biodegradation processes at contaminated sites.

While field studies have shown that under oxic conditions benzene biodegrades faster than toluene, ethylbenzene or xylenes (Alvarez et al., 1991; Suarez and Rifai, 1999), under anoxic conditions biodegradation of benzene is generally slower than that of other aromatic compounds (Weelink et al., 2010). Biodegradation of benzene under suboxic nitrate-reducing conditions has been observed (Coates et al., 2002a; Vogt et al., 2011), but its occurrence has been erratic in the laboratory as well as at the field scale (Suarez and Rifai, 1999). It has been suggested that benzene biodegradation in shallow aquifers is actually enabled by the presence of low oxygen concentrations, along the fringe of the contaminant groundwater plumes (Aronson and Howard, 1997). Nonetheless, to date a variety of bacteria using nitrate as electron acceptor and capable of benzene degradation, have been isolated in a pure culture (Vogt et al., 2011). More recently, laboratory studies showed strictly anaerobic degradation of benzene or naphthalene under nitrate reducing conditions related to *Peptococcaceae* (members of the order *Clostridiales*) and benzene carboxylase genes (*abcA*) (Atashgahi et al., 2018; Cupples, 2016; Kleemann and Meckenstock, 2011; van der Waals et al., 2017; van der Zaan et al., 2012; Vogt et al., 2011). To our

knowledge, no studies have been published on the relevance of *Peptococcaceae* and the presence of benzene carboxylase genes (*abcA*) throughout contaminated plumes at the field scale.

Therefore, this field study focuses on the biodegradation of a wide range of hydrocarbons that derive from the dissolution of Pintsch gas tar, in a two-aquifer system dominated by denitrifying conditions in the surrounding native groundwater. This was performed to assess the differences and controls on the biodegradation of individual hydrocarbon compounds and benzene in specific in the presence of different electron acceptors. This was done by assessing specific redox conditions, enrichment and depletion of compounds in the contaminant mixture along groundwater direction of flow. Verification of *in situ* biodegradation was done through a combination of compound-specific isotope analysis (CSIA), signature metabolite analysis (SMA)(Griebler et al., 2004) and deoxyribonucleic acid analysis (DNA) of anaerobic aromatics degrading micro-organisms.

4.2 Material and Methods

4.2.1 Site description

The studied field site is located adjacent to the railway station in the city of Amersfoort, The Netherlands. On this site, a manufactured gas plant (MGP) was active from 1910 until 1958. The hydrogeological situation consists of a two-aquifer system. The shallow aquifer from 2 to 12 meter below ground surface (mbgs) consists of medium to silty fine sands, and the deep aquifer from 12 to 85 mbgs of mainly coarse sands with gravel enclosures. The general direction of groundwater flow in the shallow aquifer is to the southeast and to the northwest in the deep aquifer (Figure 4-1). Locally at the MGP site, groundwater flow shifts in the shallow aquifer, due to sheet piling containment measures and absence of the confining layer (Figure 4-1). The hydraulic conductivity of the aquifers varies from $k = 5$ m/d in the shallow aquifer to $k = 15$ m/d in the deep aquifer. The two aquifers are separated by a clay/peat confining layer in the north (Figure 4-2). The clay/peat layer thins out from more than 5 meters thickness in the north, to about 50 cm or less at the MGP site. The aquitard fringe is situated some 50 meters south of the DNAPL source zone (Figure 4-2). In both aquifers, liquid phase tar is detected as free flowing DNAPL as described earlier (Leeuwen et al., 2020).

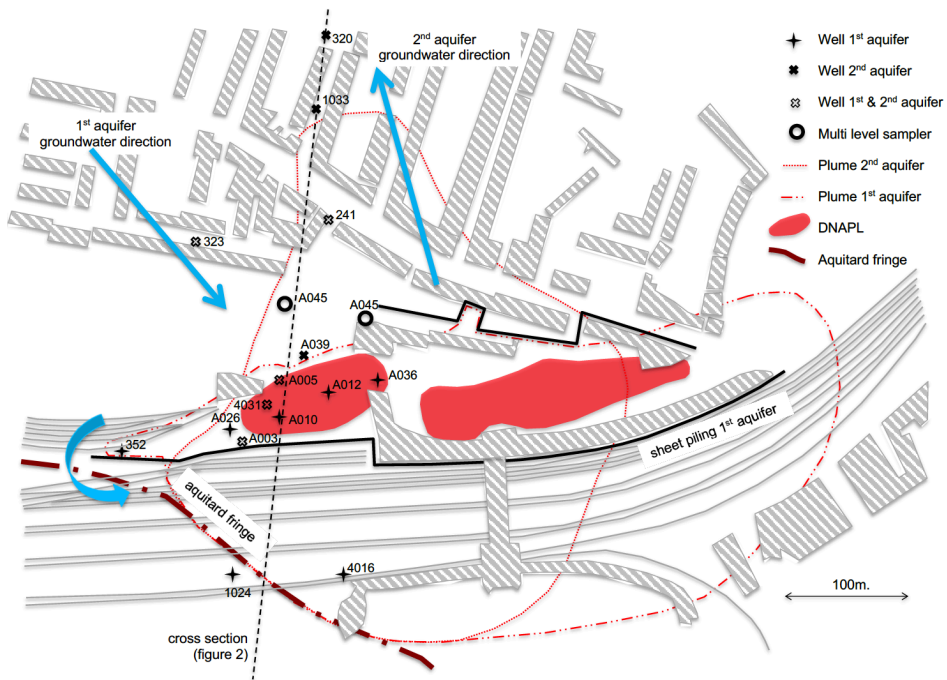


Figure 4-1: Plan view of the investigated site. The four-pointed stars show the locations of groundwater monitoring wells in the shallow aquifer; x-shapes show monitoring well locations, both in shallow and deep aquifers; donut shapes represent multi-level samplers in the deep aquifer. DNAPL source zones are shown in red. The contaminated groundwater plumes are outlined by red dotted lines. Sheet pilings are shown by thick black lines, and directions of groundwater flow by blue arrows.

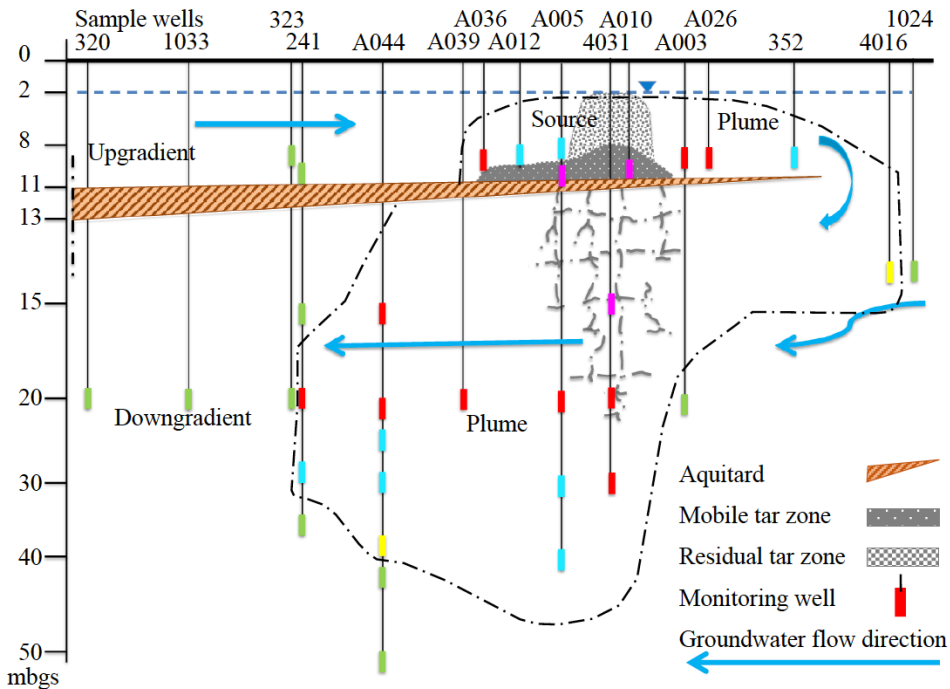


Figure 4-2: Cross section of a site conceptual model (not to scale) showing the two aquifer systems and the thinning aquitard clay/peat layer. Concentrations indicated in colors are measured sum of benzene, toluene, ethylbenzene, xylenes, and naphthalene. Green represents 0 - 100 $\mu\text{g/L}$, yellow 100 - 1,000 $\mu\text{g/L}$, red 10,000 - 100,000 $\mu\text{g/L}$ and magenta 100,000 - 1,000,000 $\mu\text{g/L}$.

The contaminated MGP site was divided into different zones, based on samples from groundwater sampling wells within each zone. The upgradient zone, represents non-impacted groundwater and is used as a reference. The source zone is the area where DNAPL is present and the plume zone is the area where dissolved contaminants are present. The fringe zone represents the area where contaminant concentrations in groundwater are diminishing and mixing with the surrounding groundwater occurs by dispersion. Downgradient is the area in the direction of flow for groundwater and contaminant concentrations below 10 $\mu\text{g/L}$. In Table 4-1, the number of sampling wells in each zone is given.

Table 4-1: Overview of contaminated site zonation and number of groundwater sampling wells per zone. Upgradient: ± 140-meter upgradient from the source zone. Plume zone: No DNAPL presence in sampling well and at least one contaminant > 2 mg/L. Source zone: DNAPL presence within the sampling well. Plume zone: No DNAPL presence in sampling well and at least one contaminant > 2 mg/L. Fringe zone: No DNAPL present in sampling well and each contaminant < 2 mg/L. Downgradient: sample wells are hydrogeological downgradient and each compound < 10 µg/L.

	Upgradient	Source zone	Plume zone	Fringe zone	Downgradient
Groundwater sampling wells	1 well	4 wells	11 wells	6 wells	7 wells

4.2.2 Groundwater sampling

To create a two-dimensional, transect of the groundwater contamination in the two-aquifer system, groundwater samples were obtained from 34 sampling wells. The wells were selected along the groundwater flow direction (Figure 4-1), as well as along a transversal cross section of the plume (Figure 4-2). A comprehensive overview of the sampling wells is given in the supplementary information. To keep the groundwater samples anoxic while sampling, Marprene tubing (Rubber BV, Hilversum) in combination with a peristaltic pump (Watson-Marlow, type 604 U/R, MA, USA) was used. Some wells in the source zone contained DNAPL. To acquire clear groundwater samples, these wells were pumped at a flow rate of 10 L/h until groundwater breakthrough was established. Typically, two to sixty liters of tar was pumped before groundwater break through started (Table 4-2). Unaffected reference well 323 is located 145 meters upgradient in the shallow aquifer.

Table 4-2: Wells sampled in the DNAPL-source zone, with well screen depth in meters below ground surface (mbgs), tar height measured from bottom of the well. Pumped tar volume before groundwater breakthrough (PBGB) is given in liters (L).

Sampling well	A010	A005	A012	A036A	4031	4031
Well screen (mbgs)	2 - 12	10 - 12	10 - 12	10 - 12	16 - 17	20 - 21
Tar height (m)	6	3.8	2.7	2.5	0.3	0.3
PBGB (L)	60	35	10	15	5	2

4.2.3 Aromatic hydrocarbon analysis

For the determination of concentrations of aromatic hydrocarbon compounds in the groundwater samples, a gas chromatographic headspace analyses method was used. Analyses were performed on a Shimadzu GC-2010 gas chromatograph equipped with a PAL auto sampler (Shimadzu Benelux, 's Hertogenbosch, The Netherlands) as previously described (Leeuwen et al., 2020).

4.2.4 Compound specific stable isotope analysis

Fractionation of stable hydrogen ($^2\text{H}/^1\text{H}$) and carbon ($^{13}\text{C}/^{12}\text{C}$) isotopes was determined in duplicate for aromatic hydrocarbons in groundwater samples to gain information on potential enrichment of heavy isotopes due to biodegradation. The 100-mL groundwater samples were preserved using one NaOH tablet per glass bottle, sealed with a PTFE lined butyl-rubber septum and a crimp cap (IVA Analysentechnik GmbH). To trap volatile hydrocarbons, samples (maximum 15 mL) were purged by an IMT PTA-3000 purge-and-trap system at a flow rate of 20 mL/min. The purged compounds were dried by a Nafion water tube and trapped on Tenax. Trapping time and temperature program details are given in the supplementary information.

For hydrogen isotope analysis, the compounds were thermally converted at 1400°C to H_2 by glassy carbon. $^2\text{H}/^1\text{H}$ -ratios of the produced H_2 were determined using a GC-MS-IRMS system consisting of a Thermo scientific Trace GC Ultra (GC), a Thermo scientific ISQ (qMS), a Thermo scientific GC Isolink (interface) and a Thermo scientific Delta V Advantage (IRMS) was used. Both $\delta^{13}\text{C}$ and $\delta^2\text{H}$ values were calculated using evaluation software ISODAT NT 2.0 ($\delta^{13}\text{C}$) and ISODAT 3.0 ($\delta^2\text{H}$). Isotope enrichment factors (ϵ) of BTEX and naphthalene were used in calculations to quantify biodegradation (Kümmel et al., 2016). Degradation was calculated from the enrichment of heavy isotopes in BTEX and naphthalene, by using simplified Rayleigh equation (Elsner, 2010).

$$\delta^H X(t) = \delta^H X(0) + \varepsilon \ln\left(\frac{c(t)}{c(0)}\right) \quad (1)$$

where $\delta^H X(t)$ is δ -value at interval t, starting at the source zone containing DNAPL. Here $\delta^H X(t)$ is defined as:

$$\delta^H X(t) = \left(\frac{H_X / L_X \text{ sample}}{H_X / L_X \text{ standard}} - 1 \right) 1000 \text{ ‰} \quad (2)$$

H = Heavy Isotope, L = Light Isotope, X = Element

The measured $\delta^{13}\text{C}$ -values are referenced to V-PDB (Vienna-Pee-Dee-Belemnite; $^{13}\text{C}/^{12}\text{C} = 0.0112372 \pm 0.0000090$) and the $\delta^2\text{H}$ -values to V-SMOW (Vienna-Standard Mean Ocean Water; $^2\text{H}/^1\text{H} = 0.00015576 \pm 0.0000001$). A δ -value of ‘fresh’ water dissolved contamination is: $\delta^{13}\text{C}(0)$. For hydrogen the same equations 1 and 2 were used.

4.2.5 *Semi-quantitative metabolite analysis*

Putative metabolites of aromatic hydrocarbon degradation were analyzed by liquid chromatography, using a Shimadzu Nexera UHPLC system and a Bruker maXis 4G quadrupole orthogonal accelerated time-of-flight mass spectrometer as described (Leeuwen et al., 2020). Analytes were semi-quantified by using a linear relation between polarity and the molar response factor, where standards with known concentrations were used to define the unknown ones through correlation (Wang et al., 2010).

4.2.6 *Analysis of anions, manganese and iron*

Groundwater samples were analyzed for concentrations of anions (SO_4^{2-} , NO_3^- and NO_2^-) by liquid chromatography (LC) on a Dionex ICS-1500 equipped with an IONPAC AS14 anion exchange column and an A SRSs-Ultra 14 mm suppressor (Dionex Corporation, Sunnyvale CA, USA). Concentrations of dissolved manganese and iron in the groundwater samples were measured by a Perkin-Elmer Avio 500 inductively coupled plasma-optical emission spectrometer (ICP-OES). For both LC and ICP-OES analysis, groundwater was

sampled in 1.5 mL vials with screw caps and silicon PTFE lined septa (Grace). The samples were sterilized in the field by addition of 0.6 mL of a 68% solution of nitric acid (Sigma-Aldrich Chemie N.V., Zwijndrecht, The Netherlands).

4.2.7 DNA extraction and qPCR analysis

For the extraction of DNA, 1-liter groundwater samples were collected from monitoring wells in clean green glass bottles. To prevent the introduction of oxygen, the bottles were filled completely from the bottom up, and let to overflow for a few minutes before sealing with a polypropylene screw cap. The bottles were immediately put-on ice in a cool box and transported to the laboratory. The 1-liter samples were vacuum filtered within 24 hours. For filtration, 47-mm diameter, 0.22 μm pore size, hydrophilic filters were used (Millipore BV, Amsterdam, The Netherlands). DNA was subsequently extracted with the MoBio Powerlyzer kit according to the supplier's protocol (MoBio, CA, USA). DNA extracts were stored at -80°C until analyzed.

Genes of general groups of micro-organisms were detected that signify redox conditions, such as nitrate reducers (*narG*), sulfite reducers (*drsA*), iron (III) reducers (16S rRNA *Geobacteraceae*), methanogens (*mcrA*), and *Archaea* (16S rRNA). Additionally, genes indicating bacteria and enzymes were targeted that are known to metabolize benzene, such as *Peptococcaceae* and benzene carboxylase (*abcA*). Furthermore, toluene degrading benzylsuccinate synthase genes (*bssA*) of sulfate- and iron-reducing, and of nitrate-reducing micro-organisms were analyzed. Furthermore, total bacteria were quantified (16S rRNA). An overview of all analyzed genes encoding and primers, is given in the supplementary information. Assays for qPCR analysis were performed on a CFX96 Real-time PCR machine (Bio-Rad) as described (van der Waals et al., 2017).

4.3 Results and Discussion

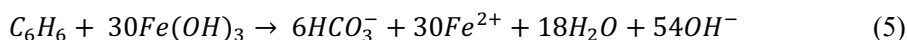
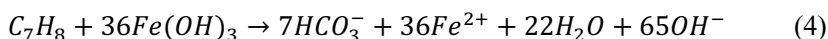
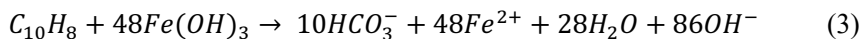
4.3.1 *Distribution of electron acceptors*

Dissolved oxygen concentrations were below 0.5 mg/L, indicating anoxic conditions in all sampled groundwater wells. In groundwater wells surrounding the contaminated area, nitrate (24 - 33 mg/L) and sulfate (31 - 36 mg/L) were present. A comprehensive list of hydrogeochemical data can be found in the supplementary information. Nitrate was depleted in the upgradient part of the source zone. The complete oxidation of 1 mole of benzene or toluene to CO₂, would require reduction of 6 or 7.2 moles of nitrate to N₂, respectively (Burland and Edwards, 1999). The influx of groundwater containing 24 - 33 mg/L nitrate can therefore serve as an electron acceptor for the oxidation of only a relatively small fraction of the contaminant load present as DNAPL in the source zone. Nitrate in the groundwater depletes readily within the contaminated zone.

Sulfate concentrations decreased along the groundwater path of flow and remained low (0.1 – 7.5 mg/L) throughout the plume zone, along the groundwater path of flow. In only 4 out of 34 sampling wells was sulfate below 1 mg/L.

Dissolved iron and manganese were not detected in the uncontaminated upstream reference well. In contrast, dissolved iron and manganese were detected in relatively high concentrations up to 14.6 mg/L, within the contaminated plume and fringe zones. This is an indication of iron(III) and manganese(IV) reduction by bacteria such as *Geobacteraceae*, which are known to use a wide range of aromatic compounds (Nealson, 1994). Dissolved iron and manganese were detected at similar concentrations, which is remarkable, since generally iron is five to ten times more abundant in soil systems than manganese (Nealson, 1994). This observation may be explained by precipitation of ferrous iron with sulfide produced through sulfate reduction. The solubility in water of FeS is negligible, whereas that of MnS is 47 mg/L at 18°C (Nealson, 1994). It was reported that about 60% of the iron (III) had been reduced to iron (II) in the source zone, and

35% of the ferric iron in the plume zone due to biodegradation of aromatic hydrocarbons from a tar contaminated site (Wege, 2005). Stoichiometric relationships for the oxidation of naphthalene, toluene and benzene are as follows:



Stoichiometric relations imply that 2,7 kilograms of ferric iron are needed to biodegrade 1 mole (128 g) of naphthalene. For biodegradation of 1 mole of benzene (78 g) or toluene (92 g) 1.7 and 2 kg of ferric iron are needed, respectively (equation 4 and 5). In the Netherlands, generally 1.5 – 30 grams/dm³ Fe(OH)₃ is present in sandy soils (Vries, 1999). This implies that for every kilogram of naphthalene a soil volume of on average 1.3 m³ is potentially sufficient as electron acceptor. The total dimension of the contaminant plume zone at the investigated site is approximately 3.3 million m³. The contaminated soil volume of the plume at the former MGP site in Amersfoort would potentially hold sufficient Fe(III) as electron acceptor for the biodegradation of 2.5 million kg naphthalene. Although the contaminated area in the shallow aquifer is at a constant inflow (± 25 m/y) of nitrate and sulfate from upgradient, this would contribute 8,500 kg/y of sulfate and 7,300 kg/y of nitrate respectively. Ferric iron is not replenished like nitrate and sulphate and might potentially deplete. However, its reduction coupled to relatively slower biodegradation of most hydrocarbon contaminants within the plume zone appears quantitatively to be of greater significance than at higher biodegradation rates, coupled to nitrate reduction in the fringe zone, due to the volume of soil it relates too.

4.3.2 *Distribution of aromatic hydrocarbons*

In the source zone, the relatively light hydrocarbon compounds partition from the tar into the surrounding groundwater. The liquid DNAPL in the source zone, is

considered to be an instantaneous solute source. The composition of the initial solute mixture (C_0) is determined by averaging the concentrations of partitioned tar compounds to water and is shown in (Figure 4-3) and described by (Leeuwen et al., 2020).

The composition of the initial solute mixture (C_0) is determined by averaging the concentrations of partitioned tar compounds to water and is shown in (Figure 4-3) and described by (Leeuwen et al., 2020). The nine most abundant compounds that have partitioned into the groundwater are:

naphthalene (29%), followed by toluene (22%) and benzene (15%). Other compounds such as 2-methylnaphthalene (2-MN), styrene, indene, xylenes and ethylbenzene were detected varying from 8% down to 2%. The other 15 detected aromatic compounds at lower concentrations than ethylbenzene is not considered here (not shown in Figure 4-3). An overview of all detected compounds per sampling well is given in the supplementary information.

Propagation of the contaminant mixture and dispersion in the groundwater plume, have an effect on concentration decrease along the path of flow. Composition of the aromatic hydrocarbon mix is affected by retardation for each compound. K_{oc} values and retardation values for the nine most abundant aromatic hydrocarbons detected in the contaminant groundwater are given in Table 4-3 (Abraham et al., 1994; Freeze and Cherry, 1979). The K_{oc} values used are obtained from chemical database (gsi-net.com).

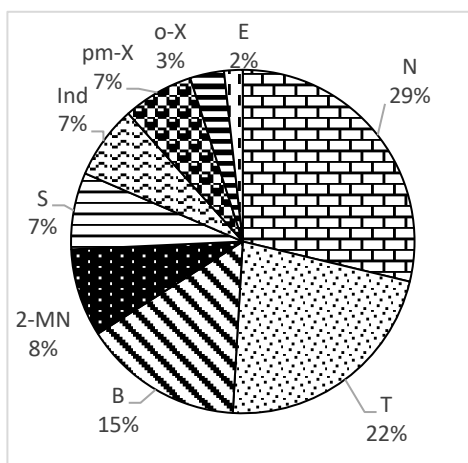


Figure 4-3: Nine most abundant hydrocarbon compounds in the aqueous phase within the DNAPL source zone. Concentrations represent the average of four samples taken from the pool zone. N = naphthalene, T = toluene, B = benzene, 2-MN – 2-methylnaphthalene, S = styrene, Ind = indene, pm-X = para- and meta xylene, o-X = ortho xylene, E = ethylbenzene.

Table 4-3: Log K_{oc} is given for the nine most abundant aromatic hydrocarbons compounds partitioned into the groundwater in the source zone. 2-methylnaphthalene (2-MN), naphthalene (N), para- and meta xylene (pm-X), ethylbenzene (E), ortho xylene (o-X), styrene (S), Indene (Ind), toluene (T), benzene (B). organic carbon content (f_{oc}) = 1%, bulk density 1.8, porosity 0.32.

	Retardation factor	
	Log K_{oc}	R
N	2.91	2.14
2-MN	2.83	1.95
pm-X	2.48	1.42
E	2.48	1.42
o-X	2.46	1.41
S	2.33	1.30
Ind	2.92	2.17
T	2.17	1.21
B	1.73	1.08

In the plume zone, the composition of the contaminant mixture has changed, compared to the source zone. In the source zone naphthalene and toluene were the most abundant compounds (Figure 4-3), whereas in the plume zone, these were ethylbenzene and benzene, with values of 0.56 and 0.71 C/C_0 , respectively (Figure 4-4). One

may attribute this to the retardation effect as the K_{oc} value for ethylbenzene and benzene and other mono- and bicyclic aromatic hydrocarbons is lower than that of naphthalene (Fetter, 1999) (Table 4-3). Another compound from the most abundant hydrocarbon compounds, 2-methylnaphthalene (2-MN), has a relatively high K_{oc} , and is expected to decrease less than naphthalene, based on retardation. However, 2-MN decreased relatively the most of all compounds from the source zone to the plume zone (Figure 4-4). Naphthalene is expected to decrease the most if only retardation played a role. This is indicative for biodegradation of 2-MN within or relatively close ($\pm 10 \text{ m}^1$) to the source zone. Further downgradient ($\pm 50\text{-}150 \text{ m}^1$), from the plume zone to the fringe zone, the highest relative loss was not observed for 2-MN, but for styrene and toluene. Where styrene and toluene decrease the most, naphthalene is decreasing more than benzene, 2-MN and indene. Indicating changing decrease for contaminant compounds along the groundwater path of flow, not related to retardation or dilution through dispersion.

At the boundary of the groundwater plume, where the plume zone transitions into the fringe, the concentration of ethylbenzene is observed to decrease 2.5 times more compared to the upgradient decrease from source to plume.

Overall, the relative decrease of contaminant compound differences from source zone to plume zone compared to fringe zone to downgradient in other ratios than cannot be explained by retardation. This suggests that biodegradation occurs for most contaminant compounds. Moreover, decreases of individual contaminant compounds within the mix, differ along the groundwater path of flow in different zones within the contaminant plume (Figure 4-4).

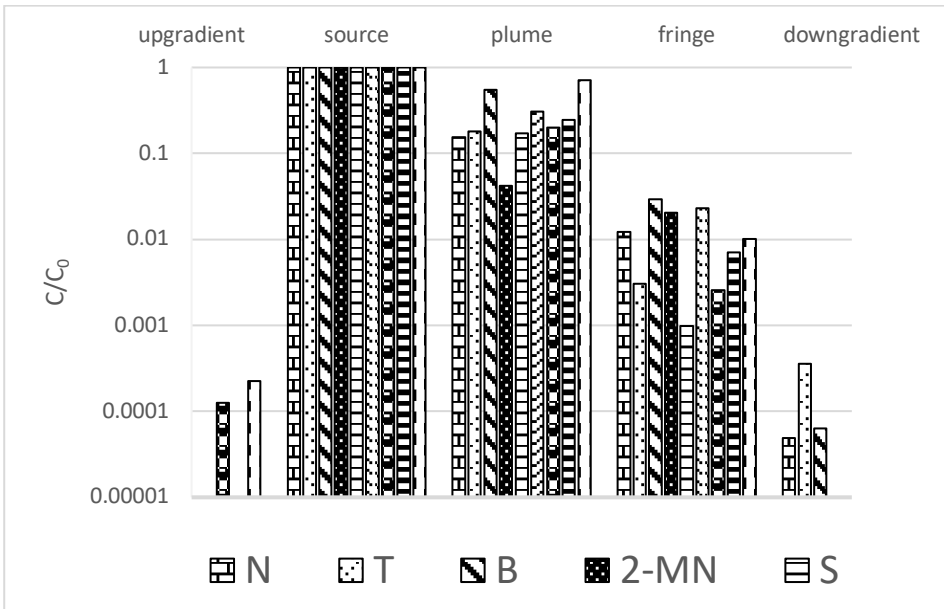


Figure 4-4: Aromatic compounds per contamination zone. From left to right average concentrations sampled in each zone. Sample wells per zone are given in **Error! Reference source not found.** Abbreviations on x-axis represent: N = naphthalene, T = toluene, B = benzene, 2-MN = 2-methylnaphthalene, S = styrene, Ind = indene, pm-X = pm-xylene, o-X = o-xylene, E = ethylbenzene.

To interpret the composition changes of compounds in the complex contaminant mixture along the path of groundwater flow, two-dimensional plots were produced, where the concentration of 1,3,5-trimethylbenzene (1,3,5-TMB) was plotted versus contaminant compounds as presented in Figure 4-4 ($C_{1,3,5-tmb} : C_x$)

using all obtained groundwater samples (Figure 4-5 and Figure 4-6). Where $C_{1,3,5-TMB}$ is the concentration of 1,3,5-TMB and C_x the concentration of a specific aromatic hydrocarbon from the contaminant mix.

Naphthalene, 1,2,3-trimethylbenzene (1,2,3-TMB) and 1,2,4-trimethylbenzene (1,2,4-TMB) show a comparative fit to linear dilution or dispersion only (Figure 4-5). Benzene and toluene show the least fit to linear dilution and benzene as well as toluene concentration decrease relatively more than 1,3,5-TMB at relatively lower concentrations (Figure 4-6). Although soil heterogeneity and retardation effects play a role in groundwater transport of contaminants, relatively for the contaminant mix benzene shows the most deviation from dilution and naphthalene together with trimethylbenzenes the least (Figure 4-5). This indicates that naphthalene and trimethylbenzenes are the most conservative compounds in the contaminant mix. Tri-substituted alkylbenzenes are less vulnerable to microbial degradation than monosubstituted alkylbenzenes (Peng et al., 2021). Moreover 1,3,5-TMB is recognized as the most conservative degrading aromatic hydrocarbon compound (Aamand et al., 1989; Aronson and Howard, 1997; Baedecker et al., 2011; Peng et al., 2021; Richnow et al., 2003). Other contaminant compounds such as xylenes, ethylbenzene, styrene and 2-methylnaphthalene show, however less distinct, decreased relative concentrations corresponding to benzene and toluene versus 1,3,5-TMB. Two-dimensional plots for these other compounds can be found in the supplementary information.

Naphthalene and benzene both non-substituted cyclic aromatic hydrocarbons are also known as anaerobically slow degrading compounds relative to other water soluble tar constituents (Aronson and Howard, 1997; Flanagan et al., 2014; Wiedemeier, Todd H.; Rifai, Hanadi, S.; Newell, Charles J.; Wilsdon, John, 1999). The data obtained from this contaminated groundwater plume show that naphthalene is behaving in accordance, however benzene is not. Benzene concentrations decrease in the same order as toluene concentrations when plotted to the most persistent compound in the mix 1,3,5-TMB (Figure 4-6). Considering

various redox conditions along the path of flow, concentration ratios for benzene (C_B) and toluene (C_T) could be occurring at different conditions and are given in ($C_B:C_T$), Figure 4-7. In the source zone, which is considered an instantaneous point source, concentrations are relatively high for benzene (30,000 $\mu\text{g/L}$) and toluene (32,000 $\mu\text{g/L}$). The majority of samples containing dissolved iron and manganese, yet no nitrate, show a ratio of greater than one for benzene versus toluene (Figure 4-7). This could be explained by relatively more adsorption of toluene to the soil matrix, since benzene has a lower retardation factor. However, some of the samples show a ratio smaller than one for benzene versus toluene (Figure 4-7). These samples relate to suboxic conditions containing nitrate and correlate to the fringe zone. The surrounding groundwater contains nitrate, which mixes in with the contaminated groundwater, due to dispersion. The relatively high toluene versus low benzene concentrations, indicate more loss of benzene than of toluene under the nitrate reducing conditions at the fringe of the contaminant plume. This composition change was also observed in sample locations above the source zone, where an inflow of nitrate containing groundwater from upgradient occurs. The lower ratio of benzene versus toluene in the up- and downgradient locations cannot be explained by retardation effects or dilution through dispersion and therefore indicates greater biodegradation of benzene than toluene at nitrate reducing conditions in the plume fringe.

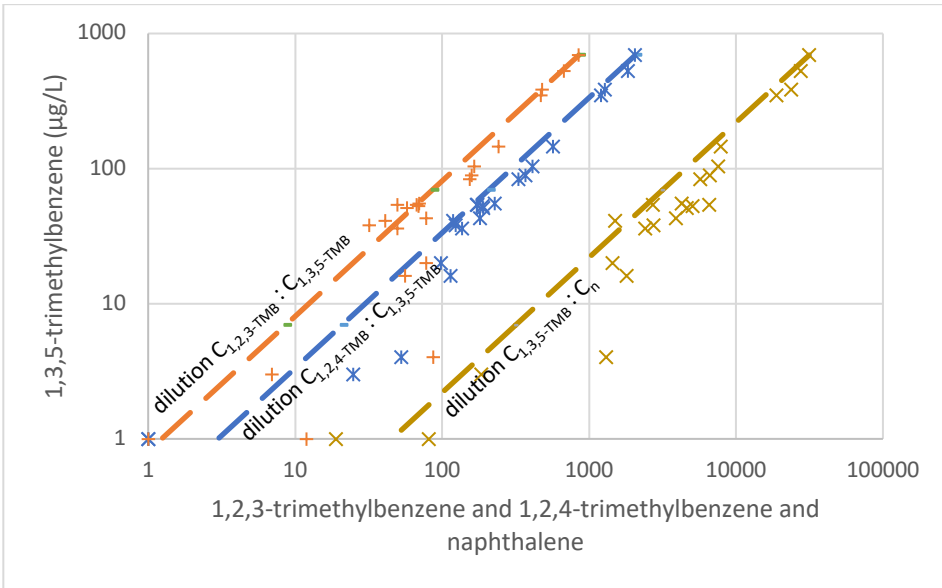


Figure 4-5: Concentrations of 1,3,5-trimethylbenzene ($C_{1,3,5-TMB}$) versus 1,2,3-trimethylbenzene in orange ($C_{1,2,3-TMB}$), 1,2,4-trimethylbenzene in blue ($C_{1,2,4-TMB}$) and naphthalene in ochre (C_n). The dotted line represents 1-D dilution. All three contaminants show a relatively good linear fit considering soil heterogeneity and retardation over the ± 300 -meter sampled trajectory of the groundwater plume.

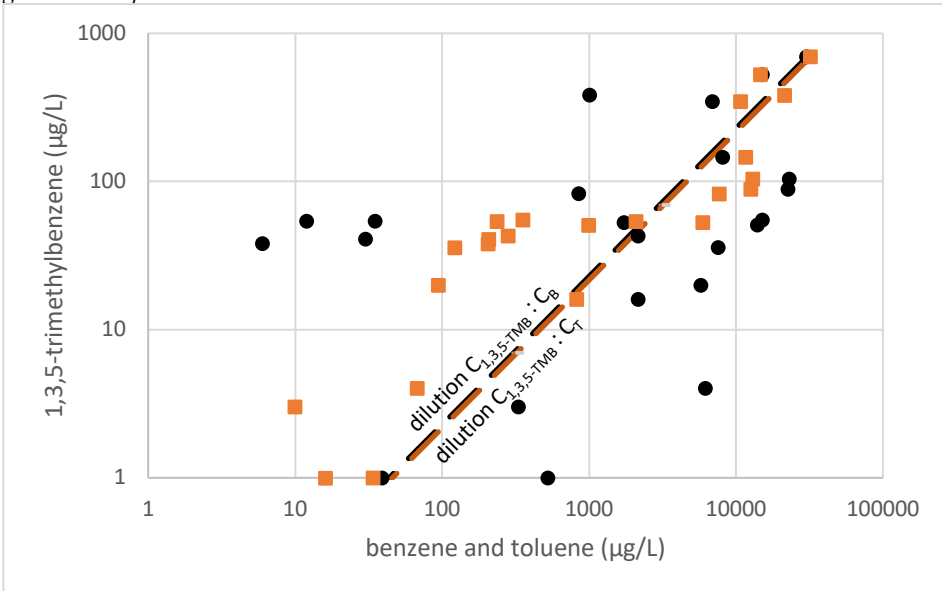


Figure 4-6: Concentrations of 1,3,5-trimethylbenzene ($C_{1,3,5-TMB}$) versus benzene (C_B) and toluene (C_T). The dotted line represents 1-D dilution. Benzene and toluene show a relatively bad linear fit considering soil heterogeneity and retardation over the ± 300 -meter sampled trajectory of the groundwater plume.

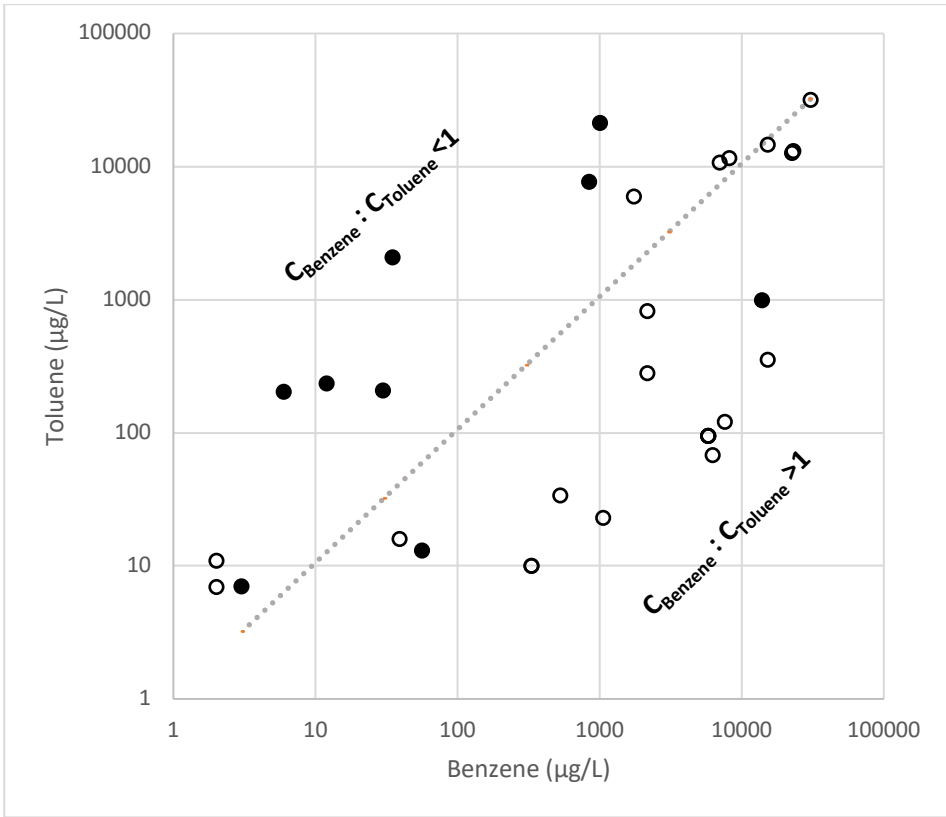


Figure 4-7: Concentrations of benzene versus toluene for all sampled wells, donut shapes represent samples containing no nitrate presence and black dots represents nitrate containing samples. The dotted line represents dilution only ($C_B : C_T = 1$). Ratio of benzene to toluene is smaller when nitrate is present, indicating more loss of benzene than toluene when nitrate is present. No replicate samples have been analyzed.

4.3.3 Multi-element compound-specific isotope fractionation

Fractionation of stable isotopes of hydrogen ($^2\text{H}/^1\text{H}$) and carbon ($^{13}\text{C}/^{12}\text{C}$) was determined for BTEX, indene, and naphthalene in contaminated groundwater samples. To determine direct insight in the reaction mechanisms for biodegradation, hydrogen ($\delta^2\text{H}$) and carbon ($\delta^{13}\text{C}$) enrichments were combined, into two-dimensional compound specific isotope analysis plots. The slope of the linear regression, leads to the apparent reaction mechanism and is expressed as the lambda value (Λ) (Kümmel et al., 2016) (Figure 4-8). Lambda values indicate putative reaction mechanisms of aromatic hydrocarbon degradation pathways

corresponding to carboxylation, fumarate addition, and hydroxylation (Vogt et al., 2016). The Λ -value found for toluene ($\Lambda = 25$) and o,m-xylene ($\Lambda = 20$) both corresponded to anaerobic degradation via succinylation by fumarate addition (Figure 4-8). Benzene isotope fractionation ($\Lambda = 19$), corresponds to degradation via the putative carboxylation reaction mechanism, in which benzene is carboxylated yielding benzoate (Coates et al., 2002a).

The Λ -value for naphthalene has a poor correlation ($R^2 = 0.51$) and does not correspond with a known carboxylation mechanism. This can be explained by masking of kinetic isotope fractionation because of the relatively low solubility of naphthalene, resulting in diffusion controlled degradation rates (Vogt et al., 2018). Another possibility could be that an alternate degradation mechanism is present at this site such as methylation with a yet unknown Λ -value. Two-dimensional plots for indene and naphthalene fractionation of C and H isotopes are given in the supplementary information.

The lowest values for fractionation of hydrogen ($\delta^2\text{H}$) and carbon ($\delta^{13}\text{C}$) isotopes were generally found in samples from the source zone and its proximity. This indicates that a relatively large fraction of the total amount of contaminants in the source zone has not been biodegraded. Small fractionation values of carbon and hydrogen might not reliably be quantified and could be underestimated due to ongoing partitioning of aromatic hydrocarbons from the DNAPL into the bypassing groundwater (Leeuwen et al., 2020). Moreover, the partitioning effect induced by groundwater flow, could be increased by higher mass transfer rates caused by biodegradation (Langevoort, 2009). The ongoing partitioning of relatively light contaminants from the instantaneous source to the groundwater, mixes with the earlier dissolved compounds and started biodegrading in the vicinity of the DNAPL (Leeuwen et al., 2020). Simultaneous biodegradation and

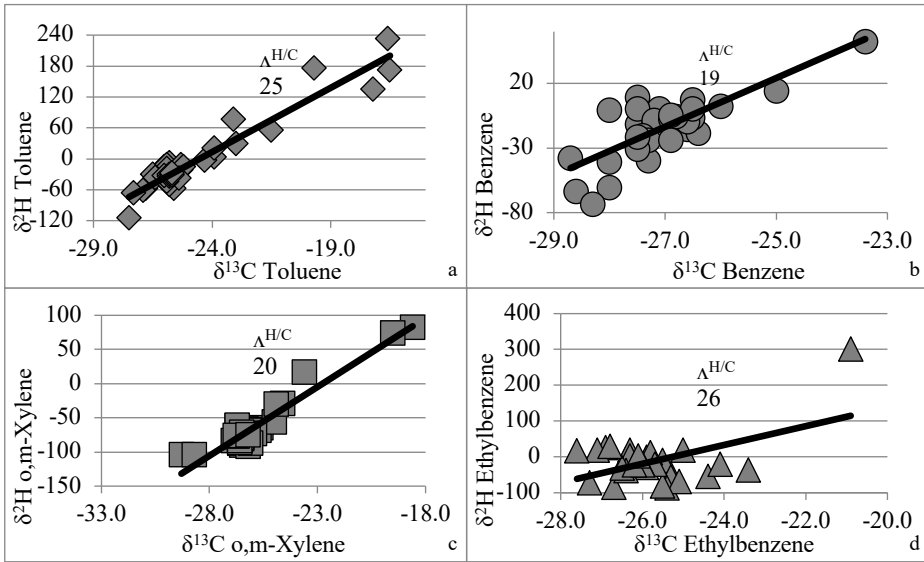


Figure 4-8: Two-dimensional plots for δ^2H and $\delta^{13}C$. Lambda values (Λ) are shown for toluene, benzene, o,m-xylene and ethylbenzene. $\Lambda \cong \epsilon_{\text{bulk H}} / \epsilon_{\text{bulk C}}$.

source partitioning could therefore underestimate the biodegradation effect in the source zone (Vogt et al., 2016).

4.3.4 Metabolites of aromatic hydrocarbon biodegradation

The highest total concentration of metabolites in a single well (545 $\mu\text{g/L}$) was found at the start of the plume (well A026). This well is located approximately 35 meters downgradient of the source zone (Figure 4-1 and Figure 4-2). This suggests that the start of the plume, governed by metal reducing conditions corresponds to a biodegradation hot-spot (Abu Laban et al., 2010; Beller et al., 2008; Jobelius et al., 2011b, 2011a; Klemann and Meckenstock, 2011; Neelson, 1994). In the source zone the second highest concentration of metabolites in a single well (321 $\mu\text{g/L}$) was detected. In the fringe zone, upgradient and downgradient highest total metabolite concentrations for a single well were measured at 40 $\mu\text{g/L}$, 37 $\mu\text{g/L}$ and 50 $\mu\text{g/L}$, respectively.

These findings indicate that biodegradation occurs in the plume zone and in the source zone. The upgradient reference sample, fringe zone and downgradient

samples, all show some metabolite presence, however at relatively low concentrations.

It has been reported that the highest concentrations of metabolites occurred at plume fringes (Abu Laban et al., 2010; Elsner, 2010), while at this MGP site in Amersfoort, The Netherlands, the highest concentrations were detected within the source zone and at the start of the plume. Limited electron acceptor availability at this site may have resulted in metabolite accumulation (Jobelius et al., 2011a). Another explanation for metabolite presence is that the source zone and the start of the plume are the most biologically active zones. Metabolite absence in the fringe zone can be explained by the relatively fast degradation of both parent compounds and their metabolites due to nitrate availability in fringe zone.

Over 40%, of the metabolite concentration detected in the plume zone, were signature metabolites related to toluene degradation. The highest concentration was found for benzylsuccinic acid (211.8 $\mu\text{g/L}$), a signature metabolite for toluene (Callaghan, 2013; Griebler et al., 2004). While in the source zone benzylsuccinic acid was absent.

Although naphthalene showed little scatter when plotted versus o-xylene and is suggested to biodegrade less than benzene and toluene, approximately 25% of the metabolite concentration detected in the plume zone were related to the anaerobic naphthalene degradation. The highest concentration for a naphthalene signature metabolite was found for naphthaleneacetic acid (67.3 $\mu\text{g/L}$), a metabolite known in naphthalene methylation pathway (Safinowski and Meckenstock, 2006). Moreover, nine specific metabolites for naphthalene carboxylation were detected in multiple samples including di-methyl benzoic acid (36.8 $\mu\text{g/L}$), and 2-naphtoic acid (38.1 $\mu\text{g/L}$)(Callaghan, 2013). Naphthalene metabolite concentrations were generally the highest in the plume zone, except for 2-naphtoic acid (61 $\mu\text{g/L}$), which was detected as the highest concentration in the source zone. The other naphthalene metabolites related to carboxylation were also present in the source zone, however at lower concentrations than in the plume zone. This suggests that

the first step in the carboxylation pathway is more apparent in the vicinity of the DNAPL than in the groundwater downgradient (Callaghan, 2013).

In the source and plume zone, other individual metabolites for anaerobic biodegradation were detected related to parent compounds ethylbenzene, indene, naphthalene, acenaphthene, phenanthrene and fluorene (Annweiler et al., 2000; Beller and Spormann, 1998; Callaghan, 2013; Chee-Sanford et al., 1996; Cozzarelli et al., 1990; Gieg and Suflita, 2002; Morasch et al., 2004; Safinowski, 2005; Tischler and Kaschabek, 2012). A few metabolites were found at highest concentrations within the source zone, such as dimethylbenzoic acid, methylbenzoic acid and benzoic acid. Another compound that was detected in groundwater samples, 2-methylindene, could possibly be a compound originating from the tar, or a metabolite formed through biodegradation of indene in the aquifer, similar to methyl naphthalenes (Callaghan, 2013). Furthermore 2-ethylhexanol, a metabolite for anaerobic biodegradation of styrene (Tischler, 2015) and 4-amino benzoic acid a metabolite from aniline (Schnell and Schink, 1991) degradation were detected.

Some metabolites, such as 3-o-toluoylpropionic acid and benzoic acid, were not only detected in the contaminated area, but also up- and downgradient, though in relatively low concentrations. These metabolites could originate from the contaminated zone upgradient, however, it is likely that benzoic acid is also formed during degradation of aromatic compounds in natural organic matter present in the aquifer. A comprehensive overview of all detected metabolites per groundwater sample is given in the supplementary information.

High concentrations of metabolites in the source and plume zone, instead of at the fringe zone, might suggest that they were discharged from the DNAPL. However, since they are thermally relatively unstable, they would have disintegrated at the high temperatures during the Pintsch gas fabrication process (Leeuwen et al., 2020). The presence of carboxylated and succinylated metabolites therefore indicate active anaerobic degradation in the DNAPL

containing source zone and the plume (Aitken et al., 2004; Bian et al., 2015; Callaghan, 2013; Elshahed et al., 2001; Head et al., 2003).

4.3.5 Distribution of microorganisms and enzymes

Gene copies of generic microorganisms, that use specific electron acceptors indicating redox conditions, were analyzed in groundwater samples. Gene copies indicating *Geobacteraceae*, nitrate and sulfate reducing micro-organisms, and methanogenic *Archaea* were found throughout the investigated area at concentrations from 10^3 per mL for methanogens up to 10^7 per mL for total bacteria (Figure 4-9). This suggests that these micro-organisms co-exist, or that different microbial niches exist in a smaller domain than the one-meter filter length of the groundwater sampling wells (Rivett et al., 2008).

Gene copy concentrations of sulfite reducers (*drsA*) and iron reducing *Geobacteraceae* 16S rRNA were one order of magnitude higher in the source zone than observed anywhere else in the aquifer. Total 16S rRNA bacterial and *Archaea* genes in the source zone were two orders of magnitude higher than in the contaminant plume area (Figure 4-9).

In samples from the source zone(s), gene copies of *nirS* and *narG* were two orders of magnitude higher than anywhere else, although no nitrate or nitrite was detected in those samples (Figure 4-9).

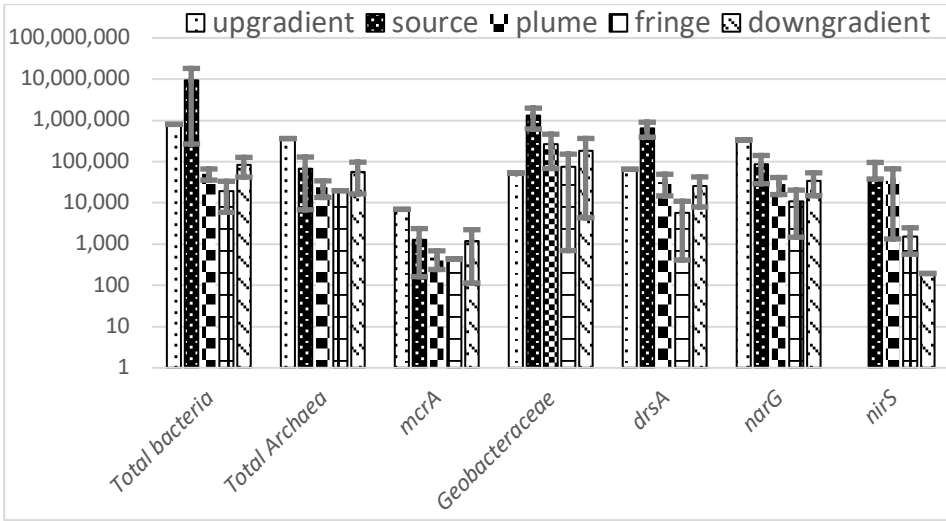


Figure 4-9: Gene copy concentrations in distinct contamination areas, upgradient, source zone, plume area, fringe, downstream for total-, sulfate reducing-, metal reducing- bacteria, and methanogens and archaea.

In addition to detected genes related to use of specific electron acceptors, DNA was targeted for bacteria and enzymes known capable of anaerobic biodegradation of mono- and bicyclic aromatic hydrocarbons, such as *Peptococcaceae* 16S rRNA genes, benzene carboxylase (*abcA* genes) and benzylsuccinate synthase (*bssA* genes) (Figure 4-10). The functional *bssA* genes for anaerobic toluene degradation via succinylation were found throughout the aquifer in relatively high concentrations, suggesting toluene degradation all over the investigated area. The highest gene copy numbers of *bssA* genes for iron and sulfate reducers were detected in the source zone, while the highest concentration of *bssA* genes of nitrate-reducers was detected in the plume zone (Figure 4-10). These results indicate presence of microorganisms capable of toluene degradation by succinylation over the whole contaminated area, at iron, sulfate and nitrate reducing conditions.

The highest concentrations of *Peptococcaceae* 16S rRNA genes were detected in the source zone, but they were also present in the plume zone, and at the fringe of the contaminated area (Figure 4-9). *Peptococcaceae* 16S rRNA genes were

detected in relatively low concentrations from hundreds up to thousands of gene copies per mL groundwater, compared to *bssA* genes. This suggests that *Peptococcaceae*, known to be involved in anaerobic benzene and naphthalene degradation, may have contributed to the anaerobic degradation of benzene and naphthalene at this site (Abu Laban et al., 2010; Kleemann and Meckenstock, 2011; Luo et al., 2014; van der Waals et al., 2017; van der Zaan et al., 2012).

Genes encoding for the benzene carboxylase enzyme (*abcA*), were detected in relatively low concentrations in the source-, and plume zones. The highest concentrations of *abcA* genes were detected at the plume fringe (Figure 4-10). This indicates that the carboxylation reaction mechanism may be involved in benzene degradation in the vicinity of the nitrate containing groundwater at the fringes of the plume.

The lowest concentration of bacterial 16S rRNA gene copy numbers was found at the plume fringe, and downgradient outside the contaminant plume. Although concentrations of gene copies for bacteria and *Archaea* are relatively high in the upgradient reference well, genes indicating aromatic hydrocarbon degrading microorganisms such as benzylsuccinate synthase by sulfate and iron reducers, *Peptococcaceae* and benzene carboxylase (*abcA*) were absent. The absolute amount of biodegraded contaminants is highest in the source zone. This most likely explains why the source zone is teeming with microbial life. In the fringe zone biodegradation is potentially the fastest under nitrate reducing conditions, however concentrations have decreased heavily before arriving that far

downgradient, and thus are merely a polishing step influencing the length of the contaminant plume.

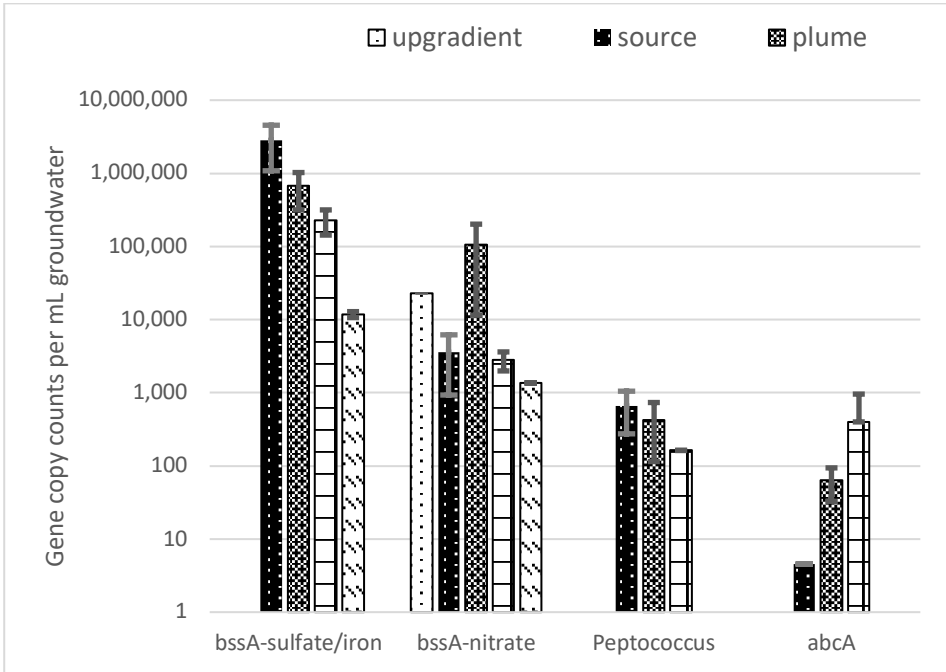


Figure 4-10: Genes indicating microorganisms and enzymes capable of anaerobic toluene and benzene degradation. Gene copies are given for contaminant zone upgradient, source zone, plume area, plume fringe, downstream. For Peptococcaceae, benzene carboxylase (*abcA*) and benzylsuccinate synthase (*bssA*) at sulfate and nitrate reducing conditions.

4.4 Conclusions

The results of this study show that benzene degrades relatively slow compared to other monoaromatic hydrocarbons at the iron reducing core of the groundwater plume but is the fastest degrading component at the suboxic nitrate reducing plume fringe. Biodegradation of benzene was confirmed in the source zone and all along the groundwater path of flow by fractionation of stable isotopes. Changes in stable isotopic ratios for $\delta^2\text{H}$ and $\delta^{13}\text{C}$ indicated biodegradation via the carboxylation mechanism. The concentration ratio of benzene versus toluene, ethylbenzene, xylenes and naphthalene shifted from greater than one at iron reducing conditions to smaller than one at nitrate reducing conditions. Moreover,

benzene carboxylase (*abcA*) genes, were in accordance most abundant at the nitrate reducing plume fringe.

Overall composition of the contaminant compounds changes along the groundwater path of flow in other ratios than can be explained by dispersion nor adsorption. In addition, metabolites of xylenes and trimethylbenzenes were detected in the source zone at their highest concentrations. This indicates active biodegradation in the vicinity of the DNAPL pool zone. The highest numbers of 16S rRNA gene copies for total bacteria, *bssA* of sulfate, iron-reducing *Geobacteraceae*, and *Peptococcaceae*, were detected within the source zone.

The highest diversity and concentrations of most metabolites were detected in the upgradient part of the plume zone, near the source indicating a hotspot for biodegradation.

Most if not all water-soluble aromatic hydrocarbon contaminants biodegrade at the relatively large dimensions of the anoxic plume core. However, relatively slow biodegradation of most hydrocarbon contaminants at iron reducing conditions within the plume zone appears quantitatively to be of greater significance than relatively high biodegradation rates in the nitrate reducing fringe zone.

4.5 Acknowledgements

This work was financially supported by SBNS, Foundation of Dutch Railways for soil remediation. We acknowledge Antoine Booms, Gerhard Winter, Roy Goossen, Patrick Broekhuizen from Aveco de Bondt and Andre Cinjee from Deltares, for sharing their site knowledge, site access and assistance in the field. Special thanks to Fredericke Hannes and Rick Helmus for their support in the laboratory and guidance to interns Thomas Wagner, Olaf Brock, Merijn van Logtenstijn and Panos Panagiotis on metabolite and qPCR analysis.

4.6 Supplementary information

Table S4.1: Overview of analyzed genes encoding for anaerobe microorganisms at varying redox conditions and or involved in degradation of groundwater contaminants.

Function	Target (gene)	Oligonucleotide sequence	Primer	Reference
Total bacteria	16S rRNA gene total bacteria	GCCAGCAGCCGCGTAAT CCGTCAATTCCTTTGAGTTT	519f 907r	Lane et al., 1991 Muyzer and Ramsing 1995
Nitrate reducing	<i>narG</i>	TA(CT)GT(GC)GGGCAG GA(AG)AAACTG CGTAGAAGAAGCTGGTGCTGTT	<i>narGGf</i> <i>narGGr</i>	Lopez-Gutierrez et al. 2004
Sulphate reducing	<i>drsA</i>	ACSCACTGGAAGGACG CGGTGMAGYTCRTCCG	<i>drsAf</i> <i>drsA</i> 500r	Wagner et al. 1998 Dhillon et al. 2003
Iron (III) reducing	16S rRNA gene <i>Geobacter</i>	AAGCGTTGTTCGGAWTTAT GGCACTGCAGGGGTAATA	GEO 564f GEO 840r	Holmes et al. 2002
Carbon dioxide reducing	<i>mcrA</i> Methanogens	GCMATG CARATHGGWATGTC TGTGTGAASCKACDCCACC	ME 1f ME 3r	Hales et al. 1996
Methanogenesis	16S rRNA gene total <i>Archaea</i>	CTGGTTGATCCTGCCAG TCGCGCCTGCTGCGCCCGT	Arch 0025f Arch 364r	Vetriani et al. 1999
Benzene carboxylase	<i>abcA</i>	GCGGTGAGGTATTGACCACT TTCGGGCTGACATATCCTTC	<i>abcA</i> bcf <i>abca</i> ber	Van der Waals et al. 2017
Succinilation of toluene (sulphate reducing)	<i>bssA</i>	ACGACGGYGGCATTCTC	<i>bssA</i> SRBf	Beller et al. 2002
Succinilation of toluene (nitrate reducing)	<i>bssA</i>	GCATGATSGGYACCGACA	<i>bssA</i> SRBr	Beller et al. 2002
Benzene degrading bacteria	16S rRNA gene <i>Peptococcaceae</i> <i>sp.</i>	CCTTCGGGTAGACAGGGAGA AGCCTCTCTAGAGTGCCCAA	Pepto_r Pepto_f	Van der Waals et al. 2015

S4.6.1 Trapping time and temperature program compound specific stable isotope analysis

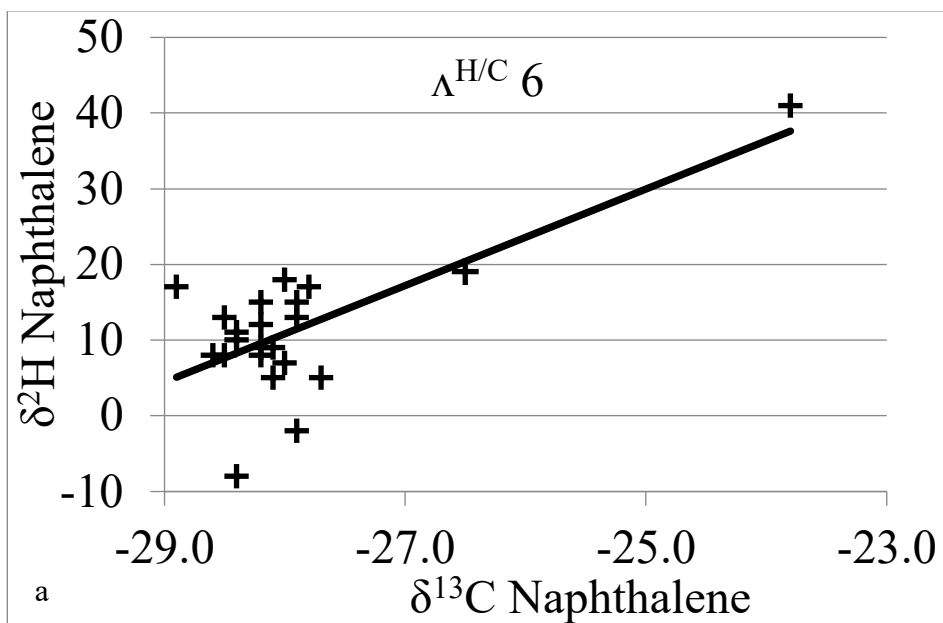
Trapping time was set to 20 minutes at -125°C, with a desorption time of 10 min at 220°C. Gas chromatography mass spectrometry isotope-ratio mass spectrometry (GC-MS-IRMS) was performed on an Agilent 6890 GC with an Agilent PoraPlot Q (length: 25 m, inner diameter: 0.32 mm, particle size: 10 µm). Column flow was set at 2.5 mL/min.

Table S4-2: Temperature program of the Gas-Chromatograph (GC).

Initial Temp. [°C]	35	
Initial Time [min]	25	
Rate [°C/min]	Final temp. [°C]	Final time [min]
10	150	10
10	180	30
10	230	45

After separation of the compounds the column flow were spitted into an Agilent 5973 qMS to identify the compounds and a Finnigan GC II-III interface to oxidize the compounds to CO₂ and measure the ¹³C/¹²C-ratios by a Finnigan Delta S Isotope ratio mass spectrometer.

The oxidation was done by a 960°C hot furnace filled with Ni/Cu/Pt-wires. Water was removed by a Nafion tube and possible other oxidation products, especially N₂O, was reduced by a furnace filled with copper wire at 600°C.



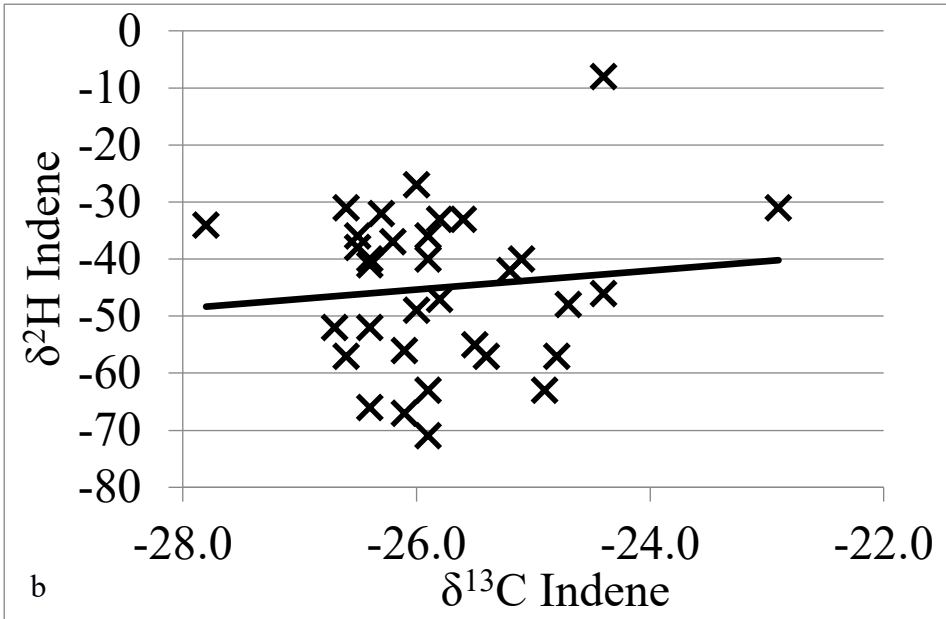


Figure S4-1a-b: Hydrocarbon activation reactions, given in Lambda (Λ) for naphthalene and indene.

Table S4.3: Overview of all detected aromatic hydrocarbon compounds in $\mu\text{g/L}$, analyzed by GC-MS per sampled well.

well name	323	A036	A012	A005	A005	A010	A003	A026	352	4016	1024	A003
screen	8-9	6.8-7.8	7.5-8.5	7.5-8.5	11-12	11-13	9.8-10.8	9.7-10.7	8-9	15-16	15-16	20-21
Sum GC	9	13342	4336	5781	87453	150695	57599	59499	3697	733	9	39
benzene	0	35	6	12	1007	30370	22556	23064	30	331	0	2
toluene	7	2081	204	236	21280	32004	12690	13092	207	10	7	7
ethylbenzene	1	283	72	95	1373	2093	1073	869	14	17	1	1
pm-xylene	1	1283	259	358	5862	7824	2830	3015	50	11	1	1
styrene	0	443	3	129	5686	7800	4234	3836	34	1	0	0
o-xylene	0	454	79	179	2678	3693	1584	1559	60	9	0	1
iso-propylbenzene	0	0	0	4	33	93	15	13	8	9	0	12
n-propylbenzene	0	13	10	16	157	317	32	40	18	1	0	1
3-ethyltoluene	0	80	56	56	509	897	140	149	7	3	0	0
4-ethyltoluene	0	30	21	29	246	483	66	74	46	6	0	0
1,3,5-trimethylbenzene	0	54	38	54	383	692	89	104	41	3	0	0
2-ethyltoluene	0	17	13	28	210	427	65	73	31	14	0	2
1,2,4-trimethylbenzene	0	173	124	174	1278	2067	370	413	119	25	0	0
4-isopropyltoluene	0	0	0	2	19	78	3	3	4	1	0	0
1,2,3-trimethylbenzene	0	50	32	67	481	854	160	166	41	7	0	0
1,3-diethylbenzene	0	0	0	6	51	0	11	11	4	1	0	0
indene	0	1283	138	396	6266	7056	3773	3715	158	39	0	6

1,2,4,5-tetramethylbenzene	0	0	0	12	96	199	12	15	15	3	0	0
2-methylindene	0	13	0	149	1464	1742	313	385	98	15	0	7
naphtalene	0	6609	2755	2726	23870	31492	6652	7587	1510	186	0	0
2-methylnaphtalene	0	322	372	628	7874	10179	562	790	715	4	0	0
1-methylnaphtalene	0	121	155	342	3838	5601	337	465	384	31	0	0
2-ethylnaphtalene	0	0	0	23	722	1374	11	19	42	3	0	0
2,6-dimethylnaphtalene	0	0	0	35	1283	2002	10	21	37	2	0	0
1,6-dimethylnaphtalene	0	0	0	25	786	1358	10	18	26	2	0	0

well name	4031	4031	4031	A005	A005	A005	A039	A044	A044	A044	A044
screen	16-17	20-21	29-30	21-22	30-31	38-39	20-21	17-18	21-22	23-24	29-30
Sum GC	102809	66183	45940	26464	7911	9922	18825	27114	25731	10168	2300
benzene	15116	6945	8150	847	2153	6200	1737	15103	13936	2154	1051
toluene	14653	10798	11667	7654	829	68	5967	356	989	282	23
ethylbenzene	1668	1077	1429	590	436	287	462	3214	2257	688	51
pm-xylene	6061	3908	3323	2209	249	108	1458	1174	1029	306	7
styrene	7341	4812	3778	2937	273	7	973	0	62	106	0
o-xylene	3007	1972	1772	1231	307	93	714	791	727	341	13
iso-propylbenzene	60	35	27	10	21	30	6	55	22	27	18
n-propylbenzene	232	139	52	26	10	17	16	13	15	20	0
3-ethyltoluene	673	418	200	107	11	4	74	223	46	20	0
4-ethyltoluene	357	222	107	50	15	25	36	182	88	36	1
1,3,5-trimethylbenzene	527	347	146	83	16	4	53	55	51	43	0
2-ethyltoluene	318	210	107	63	56	66	36	35	29	60	18
1,2,4-trimethylbenzene	1849	1210	567	331	115	53	189	228	191	181	4
4-isopropylouene	32	22	5	2	0	1	0	0	0	1	0
1,2,3-trimethylbenzene	674	470	244	154	56	87	69	70	58	78	14
1,3-diethylbenzene	79	57	18	8	5	4	0	0	0	10	4
indene	6795	4362	3636	3008	1284	1340	1701	1349	1475	1182	299
1,2,4,5-tetramethylbenzene	144	118	27	12	5	6	0	0	0	6	1
2-methylindene	1616	1079	451	310	136	99	0	0	0	177	34
naphtalene	27739	18969	7887	5742	1804	1310	5079	4266	4644	3902	367
2-methylnaphtalene	6633	4752	1294	623	18	0	180	0	114	284	179
1-methylnaphtalene	4186	2811	766	388	112	105	76	0	0	253	130
2-ethylnaphtalene	812	433	82	22	0	2	0	0	0	3	21
2,6-dimethylnaphtalene	1316	621	120	31	0	3	0	0	0	4	39
1,6-dimethylnaphtalene	923	395	83	25	0	3	0	0	0	3	27

well name	A044	A044	A044	241	241	241	241	323	1033	320
screen	39-40	41-42	53-54	15-16	20-21	29-30	35-36	20-21	21-22	20-21
Sum GC	1139	114	85	29	14985	10375	8	8	9	13
benzene	525	39	56	3	7550	5800	0	0	0	2
toluene	34	16	13	7	121	95	7	7	7	11
ethylbenzene	5	6	2	0	1896	1030	1	1	1	0
pm-xylene	16	5	2	1	743	166	1	1	1	0

styrene	2	1	0	0	5	17	0	0	0	0
o-xylene	32	3	1	0	431	118	0	0	0	0
iso-propylbenzene	11	4	0	0	45	59	0	0	0	0
n-propylbenzene	2	1	0	0	15	23	0	0	0	0
3-ethyltoluene	1	1	0	0	144	3	0	0	0	0
4-ethyltoluene	4	1	1	0	100	60	0	0	0	0
1,3,5-trimethylbenzene	1	1	0	0	36	20	0	0	0	0
2-ethyltoluene	15	1	0	0	34	84	0	0	0	0
1,2,4-trimethylbenzene	1	1	0	0	137	98	0	0	0	0
4-isopropyltoluene	1	0	0	0	6	2	0	0	0	0
1,2,3-trimethylbenzene	12	1	0	0	50	78	0	0	0	0
1,3-diethylbenzene	3	0	0	0	27	14	0	0	0	0
indene	340	13	8	3	932	992	0	0	0	0
1,2,4,5-tetramethylbenzene	1	0	0	0	4	10	0	0	0	0
2-methylindene	29	0	0	0	84	104	0	0	0	0
naphthalene	81	19	0	13	2426	1450	0	0	0	0
2-methylnaphthalene	0	0	0	0	107	4	0	0	0	0
1-methylnaphthalene	21	0	0	0	86	140	0	0	0	0
2-ethylnaphthalene	0	0	0	0	6	6	0	0	0	0
2,6-dimethylnaphthalene	0	0	0	0	0	1	0	0	0	0
1,6-dimethylnaphthalene	0	0	0	0	0	2	0	0	0	0

Table S4-4: Overview of field parameters, terminal electron acceptors, and dissolved nitrite, sulfide, manganese and dissolved iron.

Well	pH	EC (µS/cm)	T (°C)	Redox (mV)	O ₂ (mg/L)	TOC (mg/L)	Cl ⁻ (mg/L)	NO ₂ ⁻ (mg/L)	NO ₃ ⁻ (mg/L)	SO ₄ ²⁻ (mg/L)	S ⁻ (mg/L)	Mn ²⁺ (mg/L)	Fe ²⁺ (mg/L)
323	5.6	322	12.7	152	0.3	6.1	7.29	0.00	24.10	35.6	0.0	0.13	0.04
241	5.4	310	12.6	212	0.2	4.9	5.73	0.00	0.00	0.6	0.0	0.18	0.18
A036	5.0	405		204	0.9	7.2	6.24	0.00	5.13	25.4	0.0	0.78	1.66
A012	5.1	223		87	0.1	4.6	3.41	0.03	3.39	16.9	0.0	0.17	0.31
A005	5.3	58	12.2	210	0.5	2.9	3.96	0.26	3.36	7.4	0.0	0.02	0.08
A005	5.9	363		93	0.0	13.5	14.70	0.02	5.40	7.5	0.0	0.34	0.66
A010	6.4	400		-30	0.0	53.2	2.45	0.00	0.00	2.4	0.0	0.93	0.31
A003a	6.0	144	11.6	8	0.2	7.2	2.29	0.00	0.00	7.1	0.0	0.14	0.84
A026	6.3	182	11.6	33	0.2	14.3	0.69	0.00	0.00	0.2	0.0	0.10	1.00
352	5.3	229	11.6	180	0.1	3.5	17.09	0.46	6.74	23.3	0.0	0.16	0.04
4016	6.0	279	12.1	-11	0.2	3.5	17.85	0.00	0.00	16.3	0.0	2.75	3.30
1024	6.4	563	11.5	78	0.3	1.5	51.80	0.00	9.91	5.7	0.0	0.01	0.03

A003-2	6.4	253	11.6	-23	0.2	3.0	5.76	0.00	0.00	6.9	0.0	1.20	4.00
4031	6.0	194		-41	0.0	7.5	12.45	0.00	0.00	4.8	1.0	0.33	8.60
4031	6.2			-90	0.0	7.4	2.94	0.00	0.00	0.3	0.0	0.92	2.90
4031	6.3	231		-62	0.0	14.6	1.12	0.00	0.00	0.1	0.0	0.76	7.70
A005	5.8	410		153	0.0	5.9	10.73	0.00	0.92	2.9	0.0	0.41	0.82
A005	6.7	316	11.8	-85	0.2	11.7	4.03	0.00	0.00	0.1	0.0	1.20	9.10
A005	6.8	344	11.8	-111	0.1	9.0	11.60	0.00	0.00	1.3	0.0		
A039	6.2	504	11.6	55	0.3	5.8	52.34	0.02	0.00	22.9	0.0	0.67	0.74
A044	6.2	296		1	0.1	10.6	31.10	0.00	0.00	0.0	0.0	0.26	8.52
A044	6.1	256		3	0.1	10.7	30.50	0.10	0.30	0.0	0.0	0.29	4.22
A044	6.1	359		-75	0.1	8.1	5.50	0.00	0.00	1.0	0.0	1.34	11.49
A044	6.7	434		-78	0.1	5.3	3.40	0.00	0.00	1.9	0.0	4.57	5.42
A044	6.8	388		-92	0.2	3.3	1.00	0.00	0.00	0.5	0.0	14.58	3.97
A044	6.6	434		78	0.2	2.5	2.00	0.00	0.00	1.0	0.0	1.81	0.36
A044	6.5	292		129	0.1	1.4	1.40	0.00	3.70	1.7	0.0	0.17	0.00
241	5.7	396	12.3	87	0.1	4.5	10.89	0.00	0.44	7.2	0.0	0.13	1.10
241	6.3	366	12	-32	0.2	4.8	43.13	0.00	0.00	0.0	0.0	0.19	14.50
241	6.2	301	11.8	-30	0.2	6.5	10.49	0.00	0.00	0.0	0.0	0.93	6.40
241	5.6	341	11.5	134	0.2	5.5	24.45	0.00	32.58	31.0	0.0	0.05	0.11
323	7.0	539	12.1	-86	0.2	1.4	14.86	0.00	0.20	10.4	0.0	0.28	1.30
1033	7.1	500		-145	1.1	2.4	0.77	0.00	6.66	0.1	0.0	0.34	11.00
320	7.4	821	11.6	-133	0.2	3.6	83.51	0.00	0.00	38.6	0.0	0.42	4.30
320	7.5	752	11.5	-158	0.1	2.5	42.89	0.00	0.00	10.7	0.0	0.14	5.30
320	6.8	536	11.5	19	0.2	1.6	45.84	0.00	1.15	47.2	0.0	0.19	0.06

5 In-situ biostimulation and bioaugmentation of nitrate-reducing aromatic-hydrocarbon-degrading microbial communities

A version of this chapter is currently prepared to submit for publication

*Johan A. van Leeuwen, Jan Gerritse, Marcelle van der Waals, Niels
Hartog, S. Majid Hassanizadeh*

Abstract

To assess bioremediation potential in contaminated groundwater plumes at high concentrations for aromatic hydrocarbons (50-60 mg/L), long term biostimulation and bioaugmentation field tests were accomplished. The field tests were conducted at a former manufactured gas plant, using a multi well recirculation system in duplicate. Enhanced biodegradation was observed for most aromatic hydrocarbons such as BTEX, naphthalene, indene and styrene. Biostimulation and Bioaugmentation with a laboratory-grown culture in combination with nitrate injections, increased concentration of *Peptococcaceae*, benzene carboxylase (*abcA*). Benzene degradation was successfully enhanced under anaerobic conditions at the field scale by nitrate additions, although an adaptation time of more than one year was observed. Changes in fractionation of ^2H stable isotopes indicated that after adaptation, benzene degradation was faster than toluene.

This study demonstrates the potential for biostimulation through nitrate injections and bioaugmentation at sites contaminated by aromatic hydrocarbons. However, adaptation time for the indigenous contaminant degrading microorganisms can take up to one or year or more.

5.1 Introduction

Contamination of groundwater resources with aromatic hydrocarbons is of major concern worldwide (Einarson and Mackay, 2001). Tar is a viscous liquid, denser than water and composed of many different, primarily aromatic hydrocarbons. The number of different compounds found in tar varies from several hundred up to a thousand (Koolen et al., 2015; Leeuwen et al., 2020; Novotny et al., 1981). Large volumes of tar were often discarded in land pits or on-site as a primary waste product from manufactured gas plants (MGP) (Birak and Miller, 2009; Murphy and Brown, 2005; Thomas and Brinckerhoff, 2014). Pintsch gas tar is a particular waste product from MGP, containing a relatively high content of water

soluble monoaromatic hydrocarbons (Leeuwen et al., 2020). Although monoaromatic hydrocarbons, such as benzene, toluene, ethylbenzene and xylenes (BTEX) are not the most abundant compounds in the tar itself, these compounds are predominant in groundwater, due to partition effects. Moreover, in groundwater contaminated by Pintsch gas tar, along with BTEX, also naphthalene, styrene and indene are known to partition in relatively high concentrations into the aqueous phase (Leeuwen et al., 2020).

Aromatic hydrocarbons can be degraded, under strictly anoxic conditions in the environment, by bacteria that use various terminal electron acceptors such as iron(III), sulfate or nitrate (Foght, 2008; Lovley, 1997; Widdel and Rabus, 2001). A major advantage of anaerobic degradation coupled to sulphate- or nitrate-reduction over aerobic processes is the availability of good electron acceptors in soil (Farhadian et al., 2008). Water-soluble tar aromatics in general can be removed from groundwater by natural attenuation. However, enhanced biodegradation is generally faster and can be more efficient (Farhadian et al., 2008; Suarez and Rifai, 1999). Enhanced biodegradation refers to supporting the natural biodegradation processes by addition of extra terminal electron acceptor and nutrients (biostimulation) and or competent degrading microorganisms (bioaugmentation) to the contaminated aquifer (Scow and Hicks, 2005). Nitrate and sulfate are commonly used additives in field-scale enhanced biodegradation operations (Istok et al., 1997; Langenhoff, 1997; Ponsin et al., 2014; Schreiber and Bahr, 2002; Sublette et al., 2006). Benzene is a known compound in Pintsch gas tar; it is carcinogenic and is often found to be the most persistent compound to biodegradation under anoxic conditions (Chen et al., 2012; Cozzarelli et al., 2010; Leeuwen et al., 2020). Enhanced biodegradation may not always lead to satisfactory results for all aromatic compounds, such as benzene, if specific microorganisms capable of degrading this compound are absent within the contaminated area (Da Silva et al., 2005). Recently, benzene degrading microorganisms such as *Peptococcaceae* and benzene carboxylase, were shown

to be responsible for benzene degradation at nitrate reducing conditions and potentially beneficial to field scale bioaugmentation (van der Waals, 2018).

In-situ bioremediation techniques such as biostimulation and bioaugmentation are more complicated to perform at field scale than laboratory scale testing due to heterogeneity of the subsurface. To overcome heterogeneity effects, impact prospects of engineered bioremediation can typically be tested by push-pull tests. In a push-pull test, *in-situ* microbial activities are determined by injection of a test solution, containing a tracer and one or more reactive solutes. After a certain period, groundwater is extracted and conversion of contaminants is studied (Istok et al., 1997). Lag times after start of enhanced biodegradation with a terminal electron acceptor can vary from several up to 250 days (Krumholz, Lee R.; Caldwell, Matthew E.; Sufflita, 1996; Rogers et al., 2002). If lag times prevail at a contaminated site, groundwater flow can affect the result, to a point of non-detectable concentrations, by dilution, advection and dispersion. In such situations, well to well recirculation tests are more suitable than single well push-pull tests (Ponsin et al., 2014).

In this study, we present the results of enhanced biodegradation of BTEX and other aromatic compounds in groundwater at a Pintsch gas tar contaminated site in the Netherlands. The objective of this study was to assess the efficacy of biostimulation by injection of nitrate, and bioaugmentation by injection of nitrate combined with anaerobic benzene degrading microorganisms in a contaminated shallow sandy aquifer. The extent of enhanced biodegradation of benzene and other tar-aromatics was investigated using several strategies including geochemical analysis, microbial and molecular methods, tracer tests, and compound specific stable isotope analysis in a multi well recirculation field test (Bombach et al., 2010).

5.2 Material and Methods

5.2.1 Site description

The field study site was located at a former manufactured gas plant (MGP), adjacent to the railway station in the city of Amersfoort, the Netherlands. The subsurface was contaminated by mono- and polyaromatic compounds from dumped Pintsch gas tar by operation of a former MGP, that has been active from 1910 to 1958. The contaminated groundwater plume covers an area of approximately 15 hectares (van Leeuwen in preparation). The biostimulation and bioaugmentation study was performed in the shallow aquifer from two, down to twelve meters below ground surface (mbgs). The subsurface consists of medium to silty fine sands ($k = 5\text{-}15\text{ m/d}$). The vadose zone is from zero to two mbgs, and at twelve mbgs a clay-peat aquitard is present (van Leeuwen in preparation). The groundwater direction of flow at the pilot location is locally to the south-east. Free flowing DNAPL, is located, approximately 20 meters upgradient from the pilot test location, and acts as a relentless source of mono- and polycyclic aromatic hydrocarbons, partitioning to the groundwater. Existing sampling wells R003 and R026 were used as upgradient uninfluenced reference wells for contaminant influx into the test field (Figure 5-1). The site is described in more detail by Van Leeuwen *et al.* (Leeuwen et al., 2020).

5.2.2 Multi-well recirculation set-up and operation

The field test was conducted at the highly contaminated section of the contaminant plume, approximately 20 meters downgradient from the DNAPL pool zone.

The multi-well recirculation field test set-up consisted of a duplicate system, sections A and B (Figure 5-1). The purpose of duplicate parallel operating sections was to subsequently compare effects of flushing only, biostimulation and bioaugmentation. Groundwater was pumped from extraction wells AO6 and

BO7, was kept anoxic, and then injected in wells AIN61 and AIN62, and BIN 71 and BIN72 (Figure 5-1). Injection and extraction wells consisted of poly vinyl chloride tubes (diameter 110 mm). Wells were installed in the aquitard embedded in a gravel pack and screened from 10 to 12 mbgs (Figure 5-2). Monitoring wells were positioned along the downgradient path of flow at 5, 10 and 20 meters downgradient of the injection wells. Reference well R204 was located 35 meters downgradient of the test field (Figure 5-1).

A Modflow groundwater model was created to estimate an effective pump rate, without crossover between sections A and B of the test field. The model was divided into two unconfined layers of 10 and 2 meters thick, respectively, representing the silty sands on site, to determine flow regimes for pumping and drift phase(s). Intrinsic groundwater flow without pumping was calculated to be 12 m/yr.

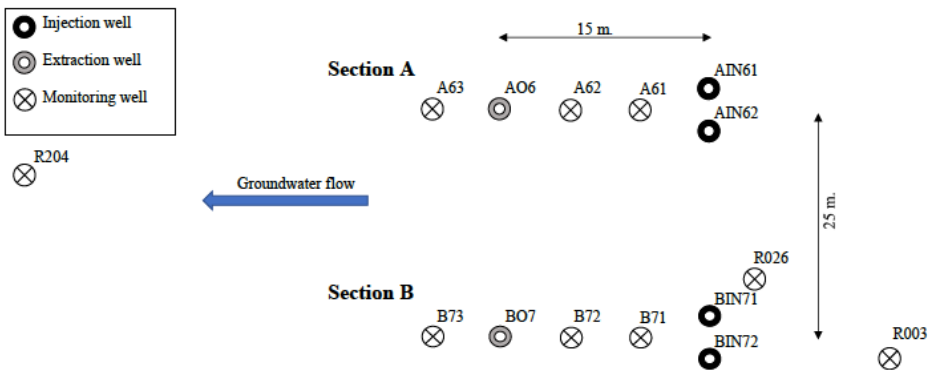


Figure 5-1: Overview of the multi-well recirculation system lay-out. Locations marked with an M, are monitoring filters, locations marked with O are extraction wells and locations marked with IN represent injection wells. Locations R003 and R026 were used as upgradient and R204 as downgradient reference monitoring wells.

The extraction and injection rates were determined at 250 L/h. At this pumping rate, travel time from the injection to the extraction well was calculated to be 21 days.

The field test set-up could be operated in four modes:

- 1) Flushing mode: extraction and injection of groundwater, to establish baseline conditions or act as control,
- 2) Biostimulation mode: Extraction and injection of groundwater, while adding nitrate,
- 3) Bioaugmentation mode: Extraction and injection of groundwater, while adding nitrate and micro-organisms,

Drift mode: Neither extraction nor injection and only natural groundwater flow conditions (Table 5-1).

Table 5-1: Overview of field test operation and sampling schedule. In period I pane A acted as control section (no stimulation only flushing) and section B was biostimulated by sodium-nitrate addition. In period II, section B remained biostimulated and section A acted as bioaugmentation section.

Period	Time (Day)	Action and sampling	Operation Mode section A	Operation Mode section B
I	0	T=0	-	-
I	34	start	flushing	flushing
I	69	T=1	-	-
I	78	stop	flushing	flushing
I	78	start	flushing	biostimulation
I	86	stop	flushing	biostimulation
I	86	-	drift phase	drift phase
I	150	T=2	-	-
I	226	T=3	-	-
I	282	T=4	-	-
I	282	End period I	-	-
II	471	T=5	-	-
II	539	-	drift phase	drift phase
II	539	start	bioaugmentation	biostimulation
II	545	stop	bioaugmentation	biostimulation
II	-	-	drift phase	drift phase
II	580	T=6	-	-
II	601	T=7	-	-
II	638	start	bioaugmentation	biostimulation
II	644	stop	bioaugmentation	biostimulation
II	-	-	drift phase	drift phase
II	653	T=8	-	-
II	697	T=9	-	-
II	708	start	bioaugmentation	biostimulation
II	718	stop	bioaugmentation	biostimulation
II	-	-	drift phase	drift phase
II	723	T=10	-	-
II	794	24 hrs	bioaugmentation	-
II	807	T=11	-	-
II	816	start	bioaugmentation	biostimulation
II	906	T=12	-	biostimulation
II	908	stop	bioaugmentation	biostimulation
II	-	-	drift phase	drift phase
II	959	T=13	-	-
II	1078	T=14	-	-

To prepare baseline conditions in the test area, prior to nitrate addition, initial recirculation of groundwater was executed in flushing mode, in both sections for 43 days (Table 5-1) at a rate of 250 L/h. The aim of control section A during period I, was to study effects of only groundwater recirculation. After the initial recirculation in both sections, groundwater recirculation flow in section B was supplemented with nitrate. In section B, 125 kg of sodium-nitrate stock solution (conc. 250 g/L) was added at a rate of 3.3 L/h to the influent flow (Figure 5-2). To prevent atmospheric oxygen from entering the stock solution tank, a continuous nitrogen/carbon dioxide (95%/5%) gas flow was applied. Nitrate addition resulted in 3 g/L in the 258 m³ injected groundwater. At day 86 the flushing and biostimulation were stopped in both sections and a drift phase was conducted for 196 days (Table 5-1).

The aim of test period II was studying nitrate addition in section B, versus nitrate addition plus bioaugmentation in Section A. The operation was adjusted due to relatively long lag phase of nitrate addition in period I (section B). Therefore, subsequently a second test period II was initiated for an extra 607 days. During test period II, nitrate was added to ± 550 m³ recirculated groundwater in section A and ± 600 m³ in section B, at a concentration of 1.5 g/L. Subsequently, anaerobic benzene degrading micro-organisms were added for bioaugmentation in section A.

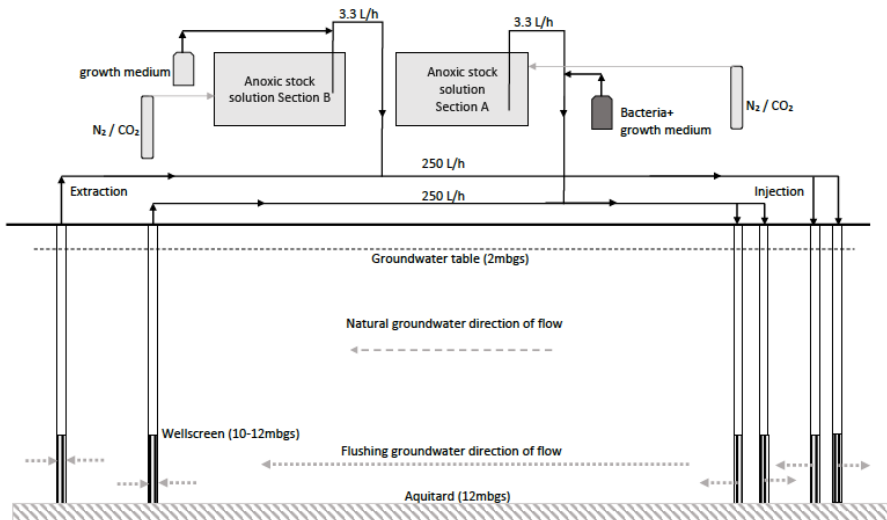


Figure 5-2: Schematic cross section of multi well recirculation test setup for enhanced biodegradation. Two similar sections were operated simultaneously as section A and section B.

5.2.3 Groundwater sampling

In between the injection and extraction wells two monitoring wells were placed at an interval of five meters (Figure 5-1). Groundwater samples were collected throughout the duration of the enhanced biodegradation periods (Table 5-1). A comprehensive overview of samples and performed analyses is given in the supplementary information. Samples were collected from the monitoring wells within the test field and up- and down gradient and from the extraction and injection wells. Groundwater samples were collected by a peristaltic pump (Eijkelkamp12 Vdc-122527, Eijkelkamp, Giesbeek, The Netherlands) using marprene tubing (Rubber BV, Hilversum The Netherlands), to ensure anoxic samples.

5.2.4 *Sample analyses*

Analyses were performed to determine concentrations of mobile aromatics, anions, cations, biodegradation metabolites, DNA and multi element compound specific stable isotope analysis (ME-CSIA).

Groundwater concentrations of mobile aromatic hydrocarbons were measured on a GC-MS (Shimadzu GC-2010). The column used was a Varian VF-624ms (0.25 mm x 30 m) (Varian, CA, USA), as previously described (Leeuwen et al., 2020). Water dissolved elements were analyzed on a ICP-OES as described by van der Waals et al. (van der Waals et al., 2017). For DNA extraction of the microbial community, filters were crushed, and total DNA was extracted using the MoBio Powerlyzer DNA isolation kit (MoBio, CA, USA). DNA was stored at -80°C until further molecular analyses. Quantification of total bacterial 16S rRNA genes, benzene carboxylase (*abcA* genes) and *Peptococcaceae* 16S rRNA genes was performed as described van der Waals et al. (van der Waals et al., 2017). ME-CSIA was done for $^{13}\text{C}/^{12}\text{C}$ and $^2\text{H}/^1\text{H}$ isotopes according to the method previously described (van Leeuwen et al. in preparation).

5.2.5 *Bioaugmentation*

Anaerobic benzene-degrading bacteria were harvested from a denitrifying continuous biofilm reactor (van der Waals et al., 2017; van der Zaan et al., 2012). To determine the effect of bio-augmentation in the field, contaminated groundwater from site was injected in a continuous benzene degrading culture as described van der Waals et al. (van der Waals, 2018). Effluent was pumped from the reactor to the harvest vessel at a rate of 1 l/day. As harvest vessel a 23 L glass bottle (Duran, Wertheim, Germany) was used, with an N_2 / CO_2 (80% / 20% v/v) gas phase and covered with aluminum foil. The harvest vessel was continuously stirred at 100 rpm. After filling the harvest vessel up to 10 liters, the stirrer in the continuous culture was increased from 200 rpm to 500 rpm for 1 hour to disperse biofilm aggregates attached to the glass and metal surfaces in the reactor. The

harvest vessel containing benzene degrading micro-organisms, and a similar vessel containing fresh growth medium only (van der Waals, 2018) were transported from the laboratory to the field site and pumped into the amended injection flow for injection under strictly anoxic conditions. The injected growth medium was used as previously described (van der Waals et al., 2017). Because growth medium was present in the vessel containing benzene degrading micro-organisms harvested in the laboratory, growth medium only was also added to the bio-stimulated system. The micro-organism injections were solely performed into section A. To ensure the only difference between both sections was the added benzene degrading culture. In section B, growth medium only was injected. The growth medium was added at the same rate in the bioaugmentation as well as the biostimulation section at 1.5 L/hr using a Watson/Marlow peristaltic pump type (Watson-Marlow, MA, USA). This augmentation procedure was repeated, five times during period II of the test. The first three injections consisted of 46-liter harvested bio-reactor effluent, the fourth injection of 34 liters and the fifth injection of 16 liters.

5.3 Results

5.3.1 *Test-field set-up and operation*

The multi well recirculation system was operated for 830 days, without major complications. On one occasion, a leaking pump hose caused temporary aeration of the influent for several days. Oxygen levels were raised to approximately 8 mg/L in the injection wells days, however, in the test field dissolved oxygen remained below 0.3 mg/L. It is assumed that this onetime event did not affect the results. Groundwater level rose approximately 50 cm in the injection wells over the test period. Increased water levels in the injection wells might suggest partial well clogging, nevertheless groundwater recirculation was not disrupted.

5.3.2 Aquifer geochemistry and interactions with acceptor

Initially, electric conductivity (EC) of groundwater in the test fields varied from 150 – 334 $\mu\text{S}/\text{cm}$ and redox potential from -237 to +149 mV (Table 5-2). Nitrate, sulfate, dissolved iron and manganese in the groundwater, varied in concentration over the test field area (Table 5-2). In section A, nitrate was varying from 0.1 mg/L up to 0.9 mg/L, but it was below detection limit of 0.01 mg/L in section B. Sulfate was present in all sampling wells initially, varying from 1.4 to 24.8 mg/L. Dissolved iron and manganese varied from 0.04 – 8.7 mg/L and < 0.1 – 2.8 mg/L, respectively.

After applying the flushing mode of anoxic groundwater, by recirculation for 44 days in both sections (section A and B), the EC dropped to a range of 131 – 207 $\mu\text{S}/\text{cm}$. The drop in EC was in parallel with a decrease in nitrate, sulfate and dissolved iron and manganese concentrations (Table 5-2). Redox potential increased slightly to -128 to +166 mV.

Table 5-2: Groundwater geochemistry and acceptor during the field test.

		Initial conditions T=0	After flushing T=1	After nitrate injection in section B T=2 / T=4	After nitrate injection and bioaugmentation T=5 / T=14	Reference upgradient (R003) T=0 / T=14
		(mg/L)	(mg/L)	(mg/L)	(mg/L)	(mg/L)
Section A	NO_3^-	0.1 – 0.9	< 0.1 – 0.6	< 0.1	<0.1 – 3063	<0.1 – 46.7
	SO_4^{2-}	2.8 – 24.8	1.7 – 17.4	9.5 – 40.6	<0.1 – 40.6	0.9 – 38.3
	CH_4^-	–	–	–	<0.1 – 1722	0.9 – 14196
	Fe(II)	0.04 – 1.4	0.02 – 0.1	0.2 – 2.2	<0.1 – 8.0	0.15 – 4.3
	Mn(II)	<0.1 – 0.3	<0.1 – 0.2	<0.1 – 0.3	<0.1 – 1.0	<0.1 – 0.2
	EC	150 – 334	131 – 307	142 – 352	155 – 5100	161 – 207
	redox	-20 – +149	-128 – +166	-208 – +170	-209 – +117	-237 – +26
Section B	NO_3^-	< 0.1	< 0.1 – 2177	< 0.1 – 1848	<0.1 – 3889	idem
	SO_4^{2-}	1.4 – 1.8	1.1 – 3.6	17.7 – 25.5	0.6 – 25.5	
	CH_4^-	–	–	–	0.1 – 960	
	Fe(II)	0.08 – 8.6	< 0.1 – 6.2	< 0.1 – 10.5	<0.1 – 13.7	
	Mn(II)	<0.3 – 2.8	0.1 – 0.3	<0.1 – 1.4	<0.1 – 0.8	
	EC	150 – 205	149 – 201	164 – 3490	228 – 7340	
	redox	+7 – +33	-72 – +42	-38 – +115	-223 – +154	

The range of EC increased in section B to a maximum of 3,490 $\mu\text{S}/\text{cm}$ as a result of the nitrate injection, while in the reference section, EC returned approximately to the same range as initial conditions, before flushing (131 – 307 $\mu\text{S}/\text{cm}$). Concentrations of sulfate, dissolved iron, and manganese returned to initial

concentrations accordingly. However, in section B, dissolved iron increased from < 0.1 to 10.5 mg/L.

In test period II, nitrate was injected in both sections A and B, and its concentration increased to $3,063$ and $3,889$ mg/L, respectively. EC also increased to $5,100$ and $7,340$ $\mu\text{S}/\text{cm}$, accordingly. Sulfate remained within both sections in the range of 1.7 and 24.8 mg/L for section A, and less than < 0.1 up to 40.6 mg/L in section B. Dissolved iron in section A fluctuated from < 0.1 to 8 mg/L and in section B from < 0.1 to 13.7 mg/L. Dissolved manganese was not detected higher than 1 and 0.8 mg/l in section A and B, respectively.

In period II, additionally the methane concentration in the groundwater was measured, and the highest concentration was observed at the contaminated upgradient reference well (14.2 mg/L). Methane was also detected in both sections during the test. While enhanced bioremediation was applied by nitrate supply, methane was detected at a concentration of 1.7 mg/L in section A and 9.6 mg/L within section B.

Concentrations of nitrate remained within the range of initial conditions (0.1 – 0.9 mg/L) during period I in section A. Therefore, we assume that no crossover has occurred from section B to section A (Table 5-2).

In section A, while only flushing mode or drift phase was applied, concentrations of nitrate, iron and EC remained in the range of initial conditions during period I (Figure 5-3). In period II, EC increased from 174 $\mu\text{S}/\text{cm}$ to $4,170$ $\mu\text{S}/\text{cm}$ and nitrate from 0.12 mg/L to $2,175$ mg/L as a result of the nitrate injection. Dissolved iron increased from < 0.1 to 8 mg/L (Figure 5-3).

In section B, nitrate injections were applied in both period I and period II, and as a result EC increased from 198 $\mu\text{S}/\text{cm}$ to $3,930$ $\mu\text{S}/\text{cm}$, and nitrate from < 0.1 mg/L to $2,120$ mg/L. Similar to section A, dissolved iron increased in section B along with nitrate injection. In section B the increase was from 2 mg/L to 20 mg/L (Figure 5-4).

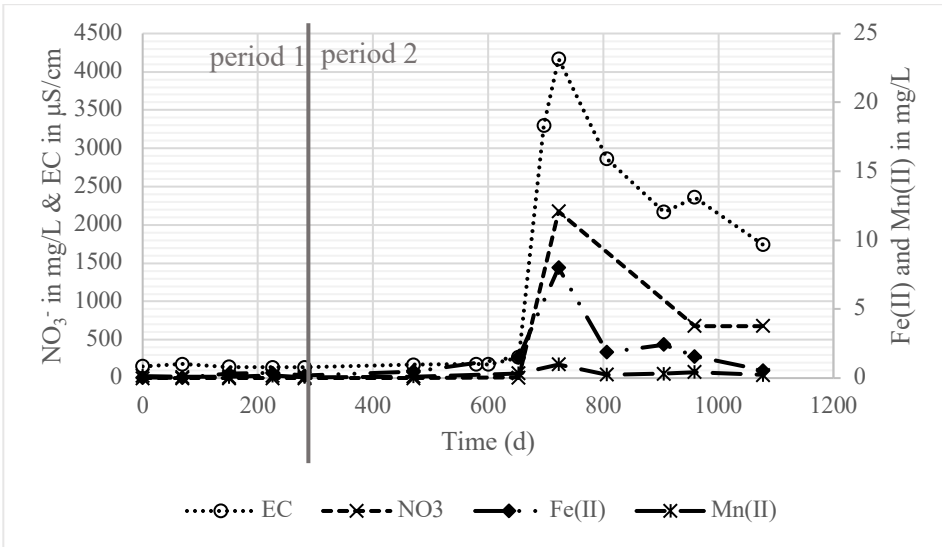


Figure 5-3: Section A, concentrations Fe^{2+} , Mn^{2+} , NO_3^- and EC, in monitoring well A62. Section A served as a negative control in period 1 (only flushing). In period 2, section A was augmented by sodium nitrate and a laboratory grown benzene degrading culture.

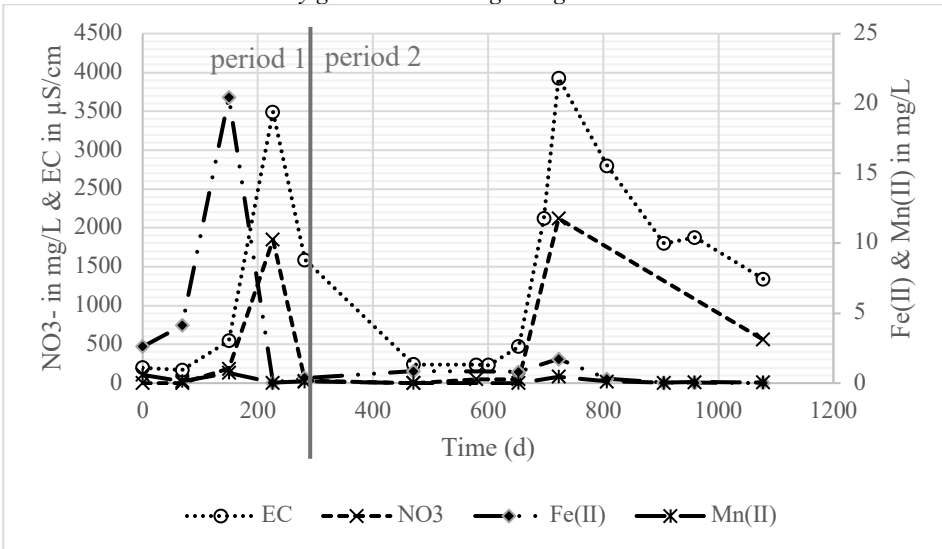


Figure 5-4: Section B, concentrations Fe^{2+} , Mn^{2+} , NO_3^- and EC, in monitoring well B72. Section B served as enhanced biodegradation by sodium nitrate injections in period 1 and period 2.

At concentrations of nitrate higher than 500 mg/L, the ratio of sodium versus nitrate remained similar. This indicates that nitrate consumption is not significant above this threshold. At a nitrate concentration below 500 mg/L, the ratio of nitrate versus sodium changed and a relatively large scatter was observed (Figure 5-5). This indicates that nitrate-reduction was mainly observed below a threshold of 500 mg/L.

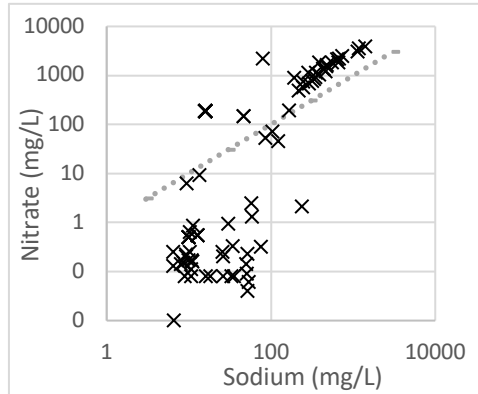


Figure 5-5: Sodium versus nitrate. Nitrate to sodium concentration scatters the most, when nitrate is below 500 mg/L.

After nitrate-supply, nitrite was detected in most of the wells throughout the test at an average of 2.3 mg/L, although never higher than 14 mg/L.

5.3.3 Aromatic hydrocarbons

Benzene and toluene concentrations varied within the test-field initially from 1,520 to 12,980 $\mu\text{g/L}$, and 5,410 to 13,830 $\mu\text{g/L}$, respectively (Table 5-3). Naphthalene varied in concentration from 3,110 to 7,100 $\mu\text{g/L}$. Concentrations of 1,2,3-Trimethylbenzene and 1,2,4-trimethylbenzene were ranging from 80 to 190 $\mu\text{g/L}$ and 230 to 580 $\mu\text{g/L}$, respectively.

After flushing, naphthalene and the trimethylbenzene remained at similar concentrations compared to initial conditions. However, the concentration range of benzene and toluene changed. The high end of the concentration range decreased for benzene from 12,980 $\mu\text{g/L}$ at initial conditions to 6,010 $\mu\text{g/L}$ after flushing and for toluene from 13,980 down to 8,150 (Table 5-3).

Table 5-3: Concentration range at initial conditions and after flushing the test field.

	Initial conditions (T=0)		After flushing (T=1)	
	Lowest conc. (µg/L)	Highest conc. (µg/L)	Lowest conc. (µg/L)	Highest conc. (µg/L)
Benzene	1,520	12,980	3,310	6,010
Toluene	5,410	13,980	3,900	8,150
Naphthalene	3,110	7,100	3,160	7,220
1,2,3-trimethylbenzene	80	190	< 100	200
1,2,4-trimethylbenzene	230	580	190	540

To interpret the result of the enhanced biodegradation tests changes in composition of the contaminant mixture were evaluated. Trimethylbenzenes, naphthalene, benzene and toluene were plotted using all analyzed samples taken from the test field and the upgradient contaminated reference well (Figure 5-6a-d). When all analyses from sections A and B and the contaminated upgradient reference well were combined into one cross plot, the concentrations of 1,2,3-trimethylbenzene (1,2,3-TMB) and 1,2,4-trimethylbenzene (1,2,4-TMB) shows a good linear relationship ($R^2 = 0.93$) (Figure 5-6a). This indicates a dominant effect for dilution, because trimethylbenzenes were relatively persistent, or that they decreased at the same ratio in the aquifer.

When all samples from sections A and B and the contaminated upgradient reference well were combined into one cross plot (Figure 5-6b), concentration of naphthalene versus concentration of 1,2,4-TMB shows a moderate linear fit ($R^2 = 0.64$). This larger scatter could be caused by either adsorption (K_{oc} value for naphthalene is higher than for 1,2,4-TMB), or a combination of adsorption and biodegradation and their differences between the different compounds.

Plots of concentrations benzene and toluene versus concentration of 1,2,4-TMB, respectively (Figure 5-6c-d), both revealed a moderate linear fit, with $R^2 = 0.62$ for benzene and $R^2 = 0.56$ for toluene. Although the linear fit is similar to naphthalene (Figure 5-6b), the observed scatter is larger. Contrary to naphthalene,

benzene and toluene both have a lower K_{oc} value than 1,2,4-TMB. Therefore, it

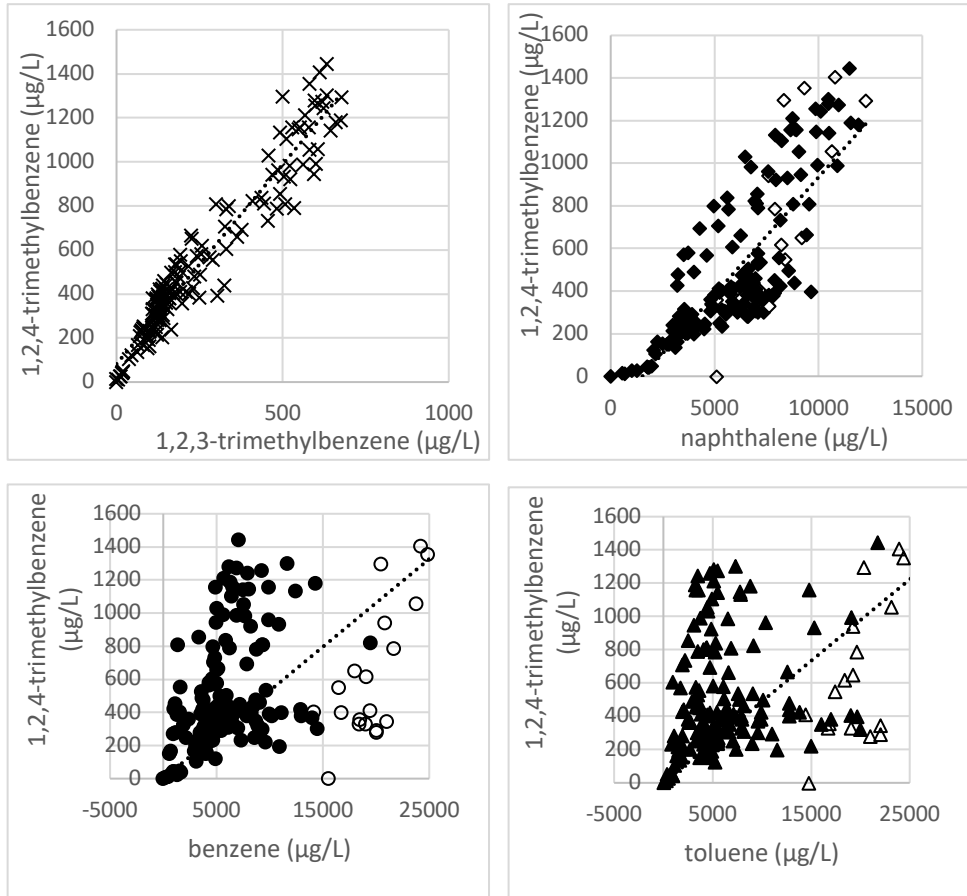


Figure 5-6: Ratios of aromatic hydrocarbons from initial conditions (day 1) until end of test (1078 days). 6a shows a good linear fit ($R^2 = 0.93$) for 1,2,3-trimethylbenzene versus 1,2,4-trimethylbenzene. 6b shows a moderate linear fit ($R^2 = 0.64$) for 1,2,4-trimethylbenzene versus naphthalene. 6c shows a moderate linear fit ($R^2 = 0.62$) for 1,2,4-trimethylbenzene Vs benzene. 6d shows a moderate linear fit ($R^2 = 0.56$) for 1,2,4-trimethylbenzene Vs toluene. Diamonds, circles and triangles with no fill, represent the contaminated upgradient reference well outside the test field.

is likely that the composition change is not caused by adsorption but by biodegradation. The composition change is further illustrated by the difference in samples from the test field, versus the contaminated reference well upgradient. Although concentrations vary upgradient from the test field contaminants remained at similar ratio's (Figure 5-6).

When samples for sections A and section B were plotted separately, into cross plots of benzene versus toluene, differences in ratios appear between the sections (Figure 5-7a-b).

In section A (Figure 5-7a), for some samples a lower toluene than benzene concentration is observed, and for some other samples a higher toluene than benzene concentrations is observed. While in the upgradient reference well the ratio the concentration of benzene versus toluene remains the same. This indicates that sometimes more toluene is lost than benzene and in other cases more benzene is lost in the test field.

In bioaugmented section B (Figure 5-7b), the ratio change was even more distinct, and concentrations of benzene were generally less than toluene.

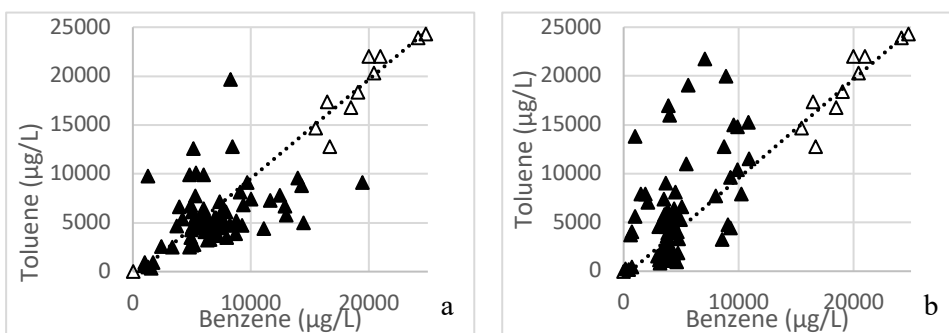


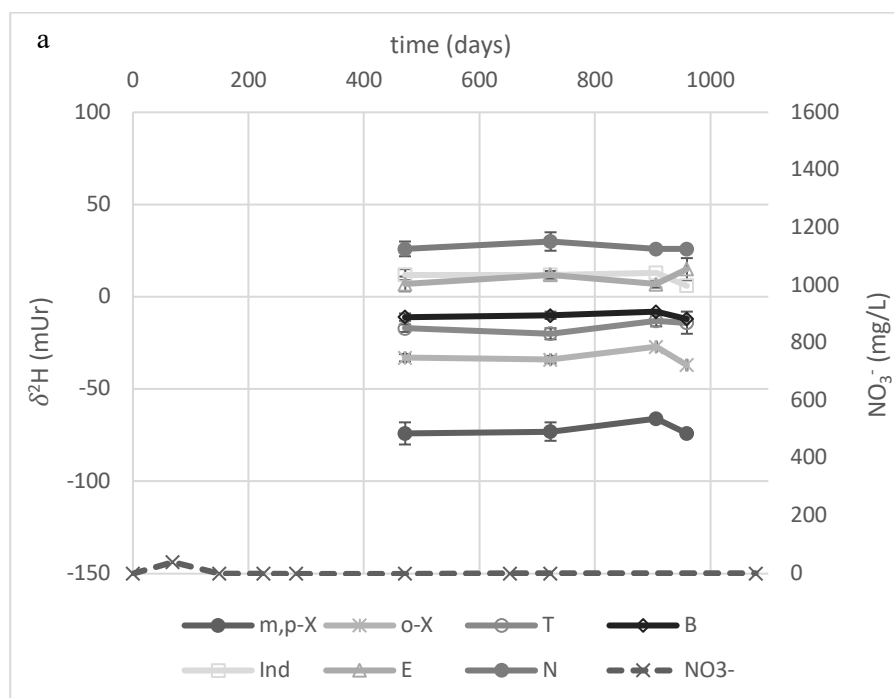
Figure 5-7a-b: Ratio of toluene versus benzene concentrations in section A and in section B, from initial conditions (day 1) until end of test (1078 days). Triangles with no fill, represent contaminated upgradient reference well outside the test field.

5.3.4 Changes in isotopic signatures of aromatic hydrocarbons

Changes in isotopic signatures of $\delta^{13}\text{C}$ and $\delta^2\text{H}$ of aromatic hydrocarbons were determined to reveal actual *in-situ* anaerobic degradation.

In the upgradient reference well R003, variations in isotopic signatures for $\delta^{13}\text{C}$ and $\delta^2\text{H}$ of aromatic hydrocarbons were relatively small (Figure 5-8a-b). These relatively small variations are within the range of the analysis accuracy and therefore not significant. These small and not significant changes in carbon isotope fractionation ($\delta^{13}\text{C}$) indicated that enrichment of $\delta^{13}\text{C}$ isotopes or $\delta^2\text{H}$ did

not occur for the analyzed aromatic hydrocarbons. Remarkable is that not all compounds in the mixture behave in the same way. At 959 days (T=13) for $\delta^2\text{H}$, the isotopic signature becomes heavier for Ethylbenzene, while changing to lighter signature for o-Xylene and m,p-Xylene (Figure 5-8a). For $\delta^{13}\text{C}$, these changes are within the deviation for analysis accuracy and therefore not significant.



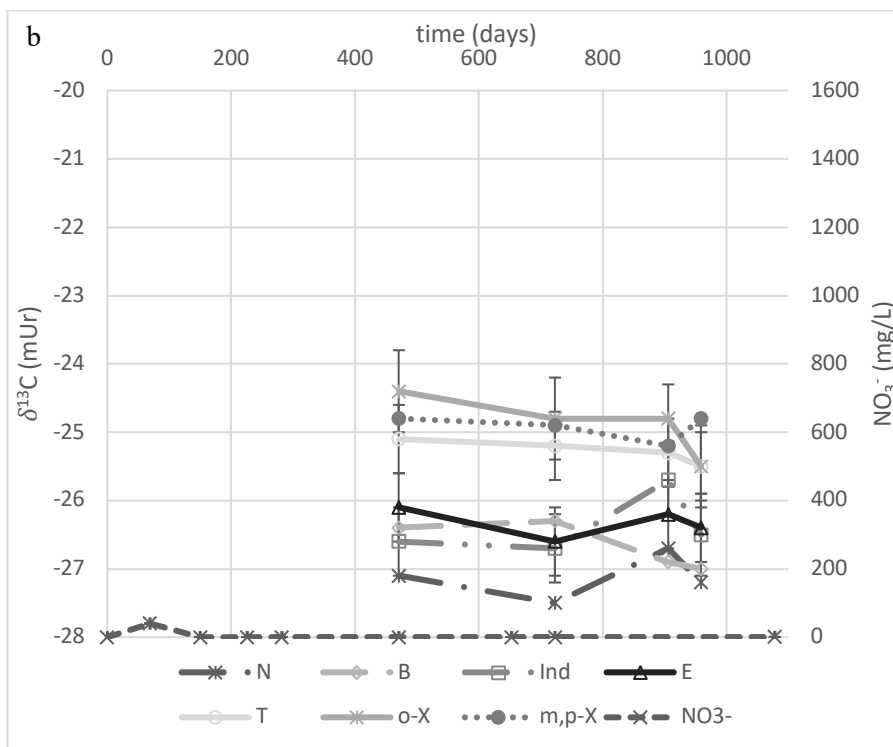


Figure 5-8a-b: Hydrogen **a**) and Carbon **b**) isotope ratio's ($\delta^{13}\text{C}$ and $\delta^2\text{H}$) in the contaminated upgradient reference well R003, at four sampling times for styrene (S), o-xylene (o-X), m,p-xylene (m,p-X), toluene (T), ethylbenzene (E), indene (Ind), benzene (B) and naphthalene (N). Error bars represent deviation in analysis accuracy.

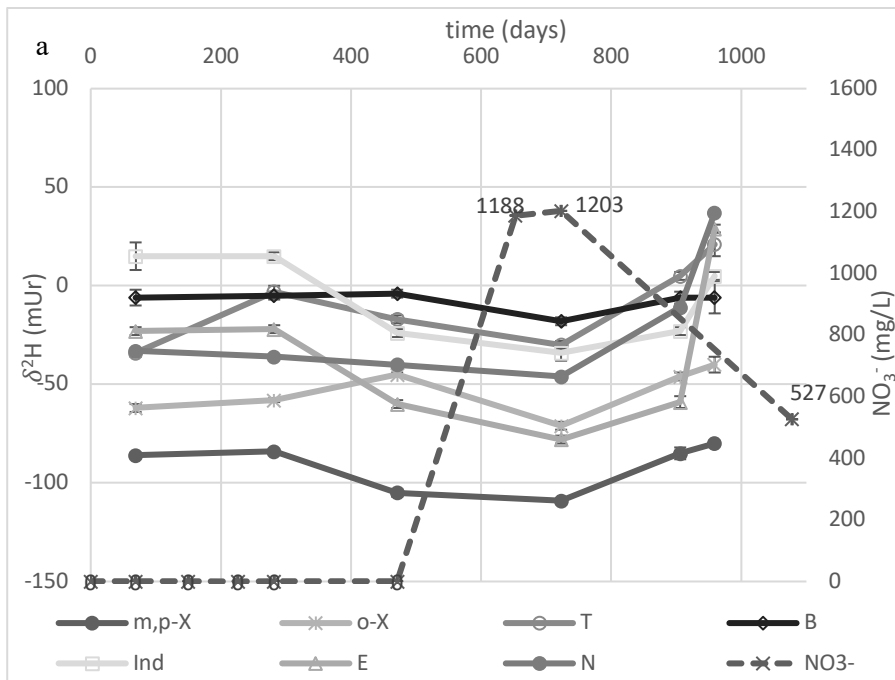
5.3.5 Section A

In period I (T=1 to T=4), when only flushing and a drift phase was applied, section A served as a negative control. Changes were observed in hydrogen ($\delta^2\text{H}$) and carbon ($\delta^{13}\text{C}$) isotope fractionation (Figure 5-9a-b). In period I, when no nitrate was injected, only toluene shows a lighter isotopic signature over time for $\delta^2\text{H}$ and $\delta^{13}\text{C}$. While in period II, when nitrate was present, the isotopic signature of toluene changes less towards a lighter signature, than during period I when nitrate was absent.

After the nitrate injections in combination with a benzene degrading culture was applied during period II, all analyzed aromatic hydrocarbons showed lighter

isotopic signatures over time for $\delta^2\text{H}$ and $\delta^{13}\text{C}$ (Figure 5-8a-b), with the exception of m,p-xylene. No significant lighter isotopic signature for carbon ($\delta^{13}\text{C}$) of m,p-xylene was observed during this time. The greatest shift towards lighter isotopic signatures was observed between 906 and 959 days into the field test.

The largest changes in isotopic signatures over time for $\delta^2\text{H}$ and $\delta^{13}\text{C}$, occurred for ethylbenzene. This shift towards lighter isotopic signatures occurred under nitrate reducing conditions in period II; it changed from -25.3 to -21.1 mUr, which is significantly lighter than in period I (Figure 5-9a-b). For o-xylene, the signature declined in period II from -25.2 to -24.0 mUr; a difference of +1.2 mUr and of the same order as the isotopic signature change in period I with a difference of +1 mUr. Although this change was small, it is still larger than the deviation in analyses accuracy of ± 0.5 mUr.



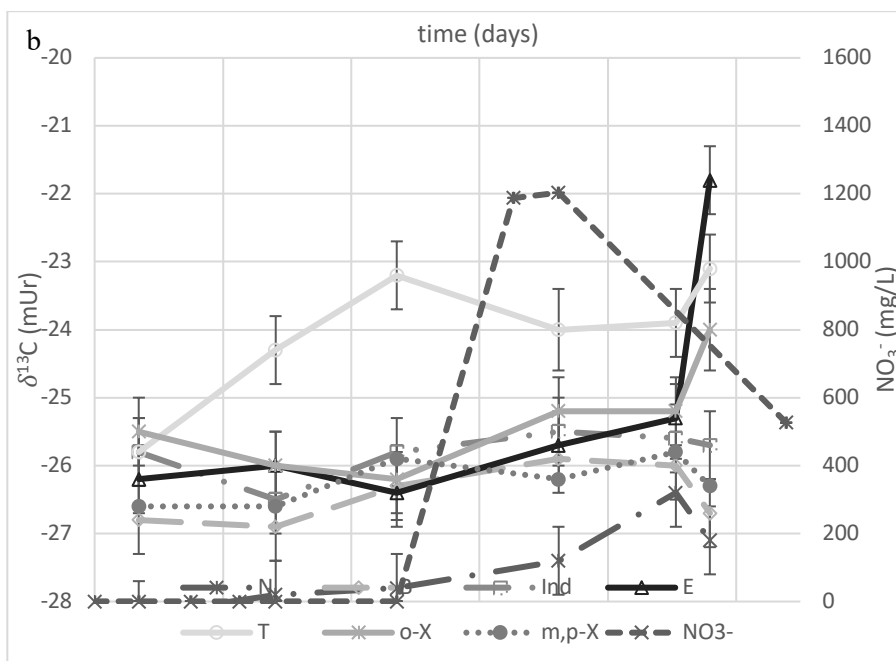


Figure 5-9a-b: Hydrogen *a*) and carbon *b*) isotopic signature ($\delta^{13}\text{C}$ and $\delta^2\text{H}$) in section A (monitoring well A62) at four time intervals for styrene (S), o-xylene (o-X), m,p-xylene (m,p-X), toluene (T), ethylbenzene (E), indene (Ind), benzene (B) and naphthalene (N).

5.3.6 Section B

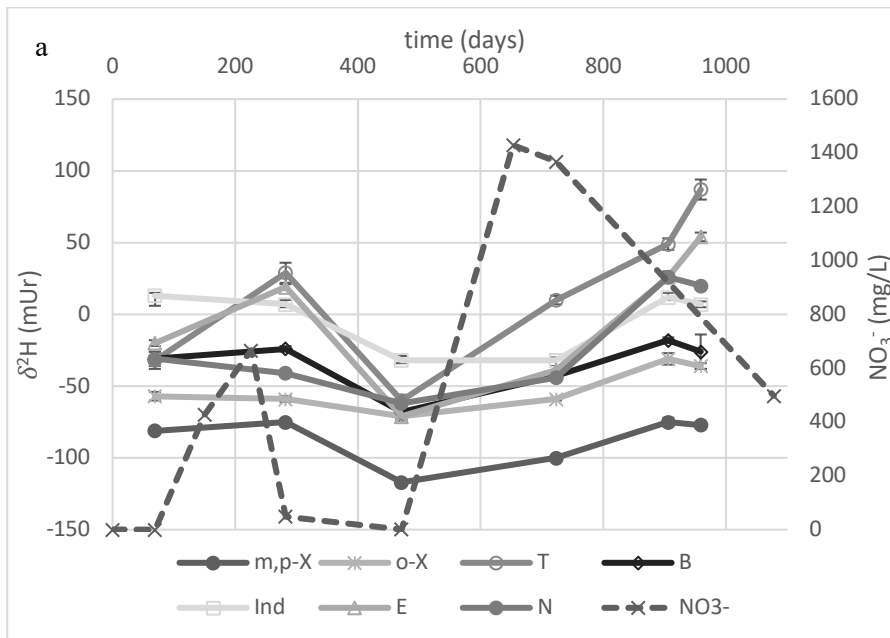
Section B was stimulated by nitrate addition during both test periods I and II. Changes in carbon isotope fractionation ($\delta^{13}\text{C}$) indicated enrichment of ^{13}C isotopes occurred for all analyzed aromatic hydrocarbons, except for m,p-xylene (Figure 5-10a-b). In period I, when nitrate was available, benzene, toluene and ethylbenzene changed towards heavier isotopic signatures.

In period II, enrichment was observed for BTEX, however not for Naphthalene and indene. Enrichment for naphthalene and indene did occur in between the nitrate injection of period I and period II, during a 453 day during drift phase, when nitrate concentrations dropped to values similar to initial conditions.

Significant enrichment of $\delta^2\text{H}$ isotopes were observed for all detected aromatic hydrocarbons. However, there were differences per compound in the mixture between period I and II. In period I, enrichment of $\delta^2\text{H}$ was observed for toluene

and ethylbenzene. In period II, all detected aromatic hydrocarbons showed enrichment in isotopic signatures. Remarkable is that ethylbenzene and toluene still show enrichment when nitrate concentration was declining, while the other compounds tend to show lighter isotopic signatures.

Although benzene and other compounds showed enriched isotopes in correlation with nitrate presence, toluene and ethylbenzene show the largest enrichments from -60 and -71 mUr to +87 and +54 mUr, respectively (Figure 5-10a-b).



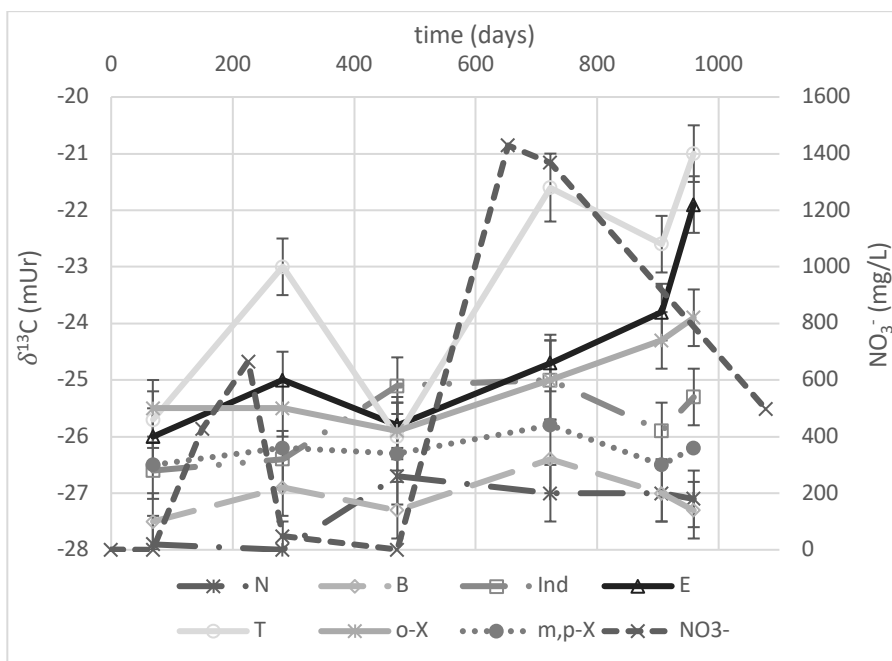


Figure 5-10a-b: Hydrogen *a*) and Carbon *b*) isotopic signature ($\delta^{13}\text{C}$ and $\delta^2\text{H}$) in samples from monitoring well B72 in section B at four time intervals for styrene (S), *o*-xylene (*o*-X), *m,p*-xylene (*m,p*-X), toluene (T), ethylbenzene (E), indene (Ind), benzene (B) and naphthalene (N).

5.3.7 Characterization of biodegradation mechanisms in the test-field

Hydrogen and carbon isotope enrichments were combined into two-dimensional compound-specific isotope plots to obtain insight in the apparent reaction mechanisms in the test field. For benzene (Figure 5-11a) and toluene (Figure 5-11b) lambda (Λ)-values were determined to be $\Lambda = 12$ and $\Lambda = 22$, respectively. A Λ -value of 12 is in agreement with values obtained for putative carboxylation of benzene and a Λ -value of 22 points to the succinylation reaction mechanism for toluene. Two-dimensional compound-specific isotope analysis plots leads to $\Lambda = 15$ for ethylbenzene, $\Lambda = 1,5$ for *m,p*-xylenes and $\Lambda = -12$ for naphthalene. From these analyses, no distinct reaction mechanism could be determined. Additionally, for indene a Λ -value of 0,6 was observed, however no valid data to our knowledge is available to determine a known reaction mechanism for this

compound. The two-dimensional compound-specific isotope analysis plots for ethylbenzene, xylenes, naphthalene and indene are given in the Supplementary information.

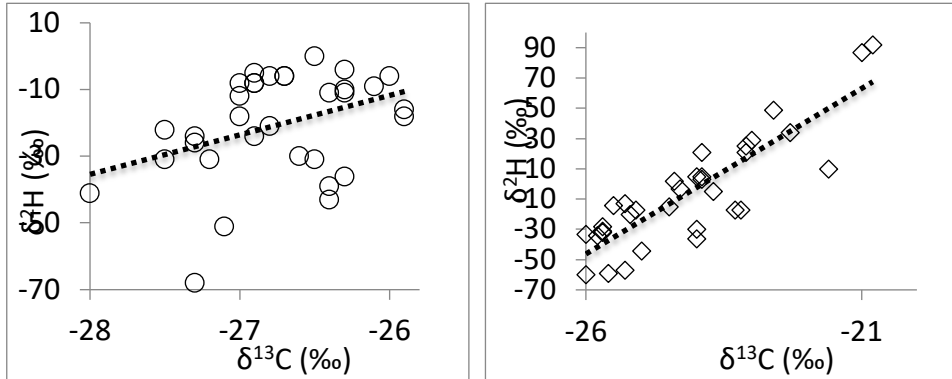


Figure 5-11a-b: Carbon $^{13}\text{C}/^{12}\text{C}$ versus $^2\text{H}/^1\text{H}$ for benzene, gives A -value = 12 (a) and a A -value of 22 for toluene (b).

5.3.8 Micro-organisms in the test-field

In the sections A and section B, gene copies per milliliter for total bacteria 16S rRNA genes were determined. The values varied two orders of magnitude and in some cases more, over the duration of the test period. In groundwater samples from the upgradient contaminated reference well, 16S rRNA genes for total bacteria varied from 10^3 to 10^4 copies per mL. In section A, rRNA genes for total bacteria varied from 10^2 up to 10^7 gene copies per mL. In section B, rRNA genes for total bacteria varied from 10^3 to 10^7 gene copies per mL. A comprehensive overview of 16S rRNA gene copies for total bacteria can be found in the Supplementary information.

In the test field, no obvious temporal variation of bacterial 16S rRNA genes was observed. This suggests that flushing, biostimulation, or bioaugmentation did not affect bacterial concentrations in the sampled groundwater (not shown). However, copies of *Peptococcaceae* 16S rRNA genes did increase in the test field (Figure 5-12 and Figure 5-13). In section A, initially (T=0), *Peptococcaceae*

were detected in both injection wells after installation (AIN61 and AIN62). Initially, *Peptococcaceae* 16S rRNA genes were not detected (< 10 copies / mL) in any of the other wells in section A (Figure 5-12). At the end of test period (T=4), *Peptococcaceae* were not only detected in the injection wells, but also in the extraction well (AO6). Although, increased numbers of *Peptococcaceae* were found in the extraction well, they were not detected in the monitoring wells at this time yet. During nitrate injection and bioaugmentation in test period II, *Peptococcaceae* 16S rRNA genes were throughout the whole of test section A. While *Peptococcaceae* remained absent downgradient of the test field. These results indicate growth of *Peptococcaceae* throughout section A, due to nitrate addition and or bioaugmentation.

Initially, in section B, 25 meters south of section A, 16S rRNA genes of *Peptococcaceae* were detected in all wells (Figure 5-13). This indicates that there is a variation in the population of *Peptococcaceae* on the field test scale. During the test period, where section B was under influence of nitrate injections for 830 days, *Peptococcaceae* 16S rRNA genes increased in the extraction and injection wells from 10^2 to 10^3 copies per mL.

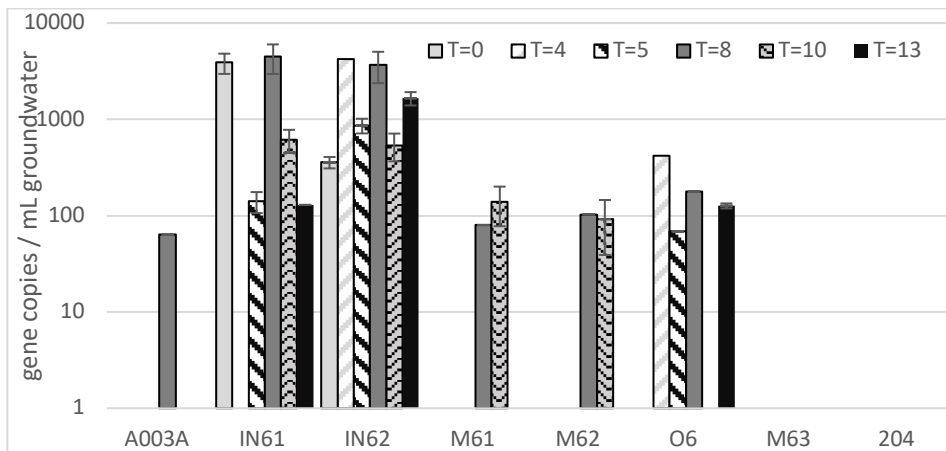


Figure 5-12: Gene Copies of *Peptococcaceae* 16S rRNA genes per mL of groundwater in section A of the test field. T=0 and T=4 represent the only flushing reference control part of the test. After T=5 bioaugmentation started by injecting nitrate and a benzene degrading laboratory grown culture. R003 and R204 are the up- and downgradient sample wells respectively.

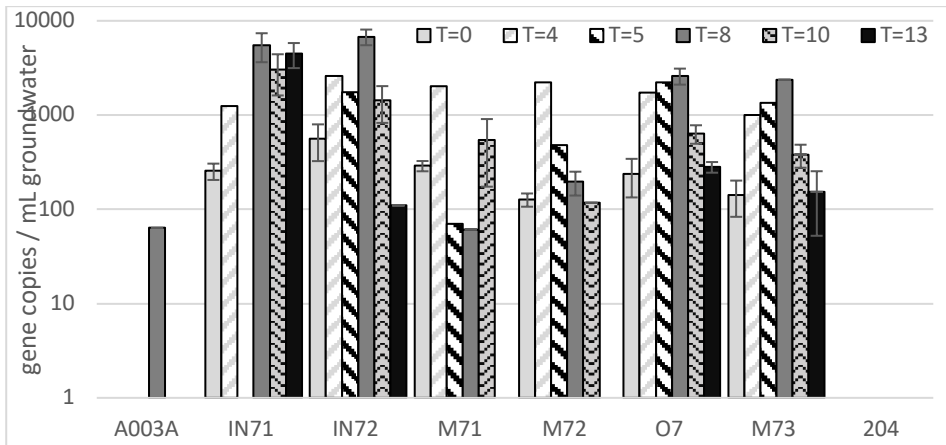


Figure 5-13: Gene copies of *Peptococcaceae* 16S sRNA genes per mL of groundwater in section B of the test field. Section B was stimulated after T=0 and remained so during period I and II of the tests. R003 and R204 are the up- and downgradient sample wells respectively.

Initially, benzene carboxylase genes (*abcA*) were only detected in the contaminated upgradient reference well, but not in any of the wells within the test-field, or downgradient, in monitoring well R204 (Figure 5-14 and Figure 5-15). In section A, an increase of *abcA* genes was observed in the injection and the extraction wells after nitrate injections in combination with bioaugmentation (Figure 5-14). In Section B, benzene carboxylase genes appeared and increased from 10^1 to 10^5 copies per mL in the injection wells, and from 10^1 to 10^3 copies per mL in the other wells (Figure 5-15).

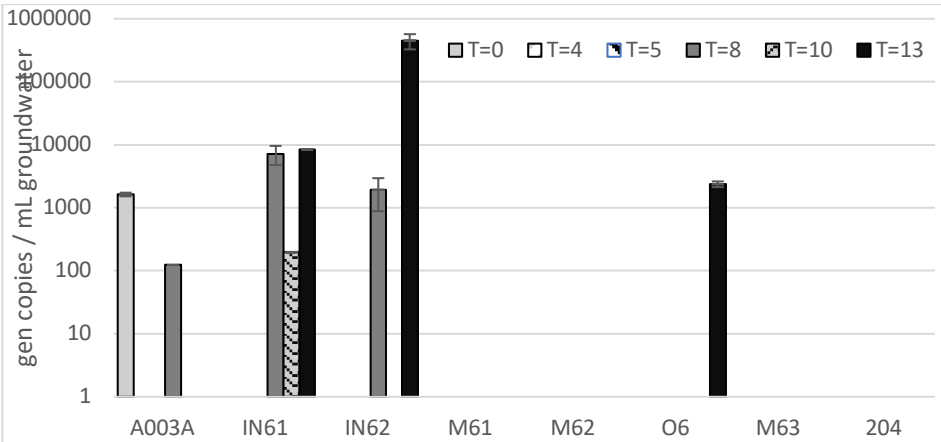


Figure 5-14: Benzene carboxylase gene copies (*abcA*) in section A of the test field. T=0 and T=4 represent the no flushing period I. After T=5 the bioaugmentation was started. R003 and R204 are the up- and downgradient sample wells respectively.

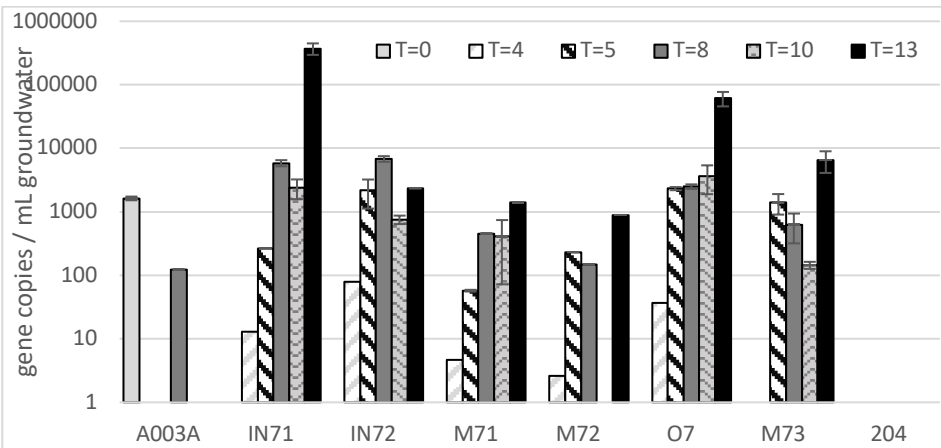


Figure 5-15: Gene copies detecting for benzene carboxylase (*abcA*) in section B of the test field. Biostimulation in section B was started after T=0 and maintained so during period I and II of the tests. R003 and R204 are the up- and downgradient sample wells respectively.

5.4 Discussion

5.4.1 Terminal electron acceptors

The ratio of nitrate versus sodium in the test field revealed a threshold of 500 mg/L for nitrate consumption (Figure 5-5). Nitrate might still have been reduced above this threshold, but due to the high background concentration this could not

be distinguished from our data. Another explanation could be that the nitrate concentrations indicate inhibition caused by relatively high levels of organic compounds in the recirculated groundwater (Dou et al., 2008; Spence et al., 2001). Denitrification was further substantiated by nitrite, detected throughout the test field, at an average of 2.3 mg/L, during most of the test period. Nitrite was not detected higher than 14 mg/L, which is an indication of nitrate reduction, and no inhibition due to accumulation up to toxic levels (Glass et al., 1997).

In both recirculation sections, along with the increased concentrations of nitrate due to injection, an increase of dissolved iron was observed. The dissolved iron was not observed in the influent injection water and it was most distinct at the first nitrate injections. Although it is proposed that nitrate reductase can transfer electrons to ferric iron this does not occur when nitrate is available (Wilson and Bouwer, 1997). Possibly, dissolved iron is measured due to oxidation of iron sulfide minerals coupled to denitrification (Zhang et al., 2009).

5.4.2 Distribution of aromatic hydrocarbons in the test-field

Variation in contaminant composition throughout the test field could have been caused by transport effects, such as retardation in combination with heterogeneities in the subsurface or biodegradation. Trimethylbenzenes (TMB) are known to be relatively persistent compounds at anaerobic conditions (Aronson and Howard, 1997; Blum et al., 2009; “Wiedemeier_et_al-1996-Groundwater_Monitoring_&_Remediation (1).pdf,” n.d.), and were suitable as internal tracer in assessing changing ratios to other aromatic hydrocarbon compounds (Corseuil and Schneider, 2002).

The 2-D plot for naphthalene versus 1,2,4-TMB concentrations (Figure 6b) showed a larger scatter than the plot for 1,2,3-TMB versus 1,2,4-TMB (Figure 6a), which can be explained by a larger retardation value for naphthalene than for 1,2,3-TMB trimethylbenzene. Therefore, transport behavior is masking biodegradation possibly by relatively more adsorption to the soil matrix.

Recalcitrance of naphthalene under nitrate reducing conditions was earlier described to occur, and pure cultures that degrade naphthalene with nitrate are unknown to date (Meckenstock and Mouttaki, 2011). However, an earlier study reported that biodegradation did occur under such conditions in the laboratory (Rockne et al., 2000). Another explanation is that measurable effects take long to appear. Doubling times for naphthalene or benzene degraders such as *Peptococcaceae* are reported in the range of weeks or even months (Meckenstock et al., 2016). Possible causes for long lag times, could be due to either inhibitory effects by other hydrocarbons in the complex groundwater contaminant mixture, or some components for growth are missing and must be synthesized under new created redox conditions (Gitiafroz, 2012).

The decrease in benzene and toluene (Figure 5-6c and Figure 5-6d), is likely caused by biodegradation because both compounds have a smaller retardation value than 1,2,4-TMB.

Remarkable is that the decrease in benzene is more prominent than for toluene in section B (nitrate only) and that toluene decrease is more prominent than benzene in section A (nitrate + bio-augmentation). Section B (nitrate injection only) was exposed to nitrate injections for 830 consecutive days, while section A (nitrate + bioaugmentation) was exposed to nitrate injections for 539 days. More biodegradation of benzene than toluene in relation to nitrate presence was also observed at the fringes of the contaminant plume (van Leeuwen et al. in preparation). Possibly, the differences during the enhanced bioremediation test between benzene and toluene biodegradation in section, A and B, are caused by relatively faster growing toluene degraders versus slower growing benzene degraders at nitrate reducing conditions (Swartjes et al., 2011).

5.4.3 Enrichment of ^{13}C and ^2H isotopes of aromatic hydrocarbons

Isotopic signatures for benzene, toluene, ethylbenzene, o-xylene and naphthalene changed towards heavier signatures and this indicates biodegradation. For m,p-xylene, no significant changes were observed. While enrichment of $\delta^{13}\text{C}$ and $\delta^2\text{H}$ was observed in the test field, in the upgradient reference well no significant enrichment of ^{13}C or ^2H isotopes of aromatic hydrocarbons was observed. During flushing of the field setup some aromatic hydrocarbons compounds, such as indene and o-xylene, are slightly enriched while toluene shows a considerable lighter isotopic signature in the same sample. When the isotopic signature changes to a heavier isotopic signature, this could be explained by intrinsic biodegradation upgradient of the test field. However, a lighter isotopic signature, which indicates a less biodegraded contaminant compound, could only be explained by less biodegraded aromatic compounds arriving by groundwater flow from further upgradient than the used reference well towards the source zone containing DNAPL. Another explanation is mixing of contaminants in the groundwater that was pumped from the extraction into the injection well. That toluene shows enrichment could also be caused by biodegradation while nitrate is absent. In section A, the most changes in isotopic fractionation were detected for naphthalene and ethylbenzene, while in section B these were for toluene, benzene and indene. The difference in degradation of aromatic hydrocarbons in section A versus section B may be explained by the duration of nitrate exposure. In section B the time of exposure to nitrate was one half times longer than in section A (830 versus 539 days, respectively). This could indicate that lag times for microbial populations to adapt to the nitrate injections are relatively long. In section B, the indigenous microbial community had more time to adapt to nitrate reducing conditions and changed to more benzene, toluene and indene degradation.

5.4.4 *Micro-organisms*

The distribution of genes indicating *Peptococcaceae* and benzene carboxylase (*abcA*) initially varied from <1 to several thousand per milliliter groundwater. The variation was most distinct at the macro scale between section A and B, which were 25 meters apart from each other. Note that variations in concentrations of micro-organisms also were observed within each section, where the sample wells were only five meters apart. This indicates that the variation in concentrations of micro-organisms responsible for biodegradation of aromatic hydrocarbons also exist at the smaller micro scale. The distribution of micro-organisms in macro- or micro niches could well be affected by the recirculating groundwater. During the field tests, we observed an increased concentration of gene copies indicating *Peptococcaceae* and benzene carboxylase (*abcA*), while in flushing mode. This could possibly be caused by small amounts of benzene degrading organisms present in the aquifer, multiplying due to groundwater dynamics and therefore mixing of relatively low nitrate concentration from the surrounding groundwater, when creating baseline conditions. Another possibility could be related to detachment of biofilm containing *Peptococcaceae* from soil particles due to the increased flow rate, while operating in flushing mode. During the test period of more than 2.5 years, the number of detections of *Peptococcaceae* 16S rRNA gene copies increased by only one order of magnitude. This indicates a low doubling time of this species (Vogt et al., 2011). The relatively slow growth, may explain the long lag time of 1.5 year observed for benzene degradation after nitrate supply (Da Silva and Alvarez, 2004). Bioaugmentation was applied for 539 days compared to 830 days of nitrate biostimulation of the indigenous culture. In both sections, the micro-organisms potentially important in anaerobic benzene degradation (van der Zaan et al., 2012) increased. It was expected that *Peptococcaceae* 16S rRNA and benzene carboxylase (*abcA*) gene copies would increase more by bioaugmentation in section A, than by biostimulation by only nitrate supply to the indigenous

microbial population in section A. However, the increase of *Peptococcaceae* in section B happened before bioaugmentation had started. This could be an effect of nitrate injection on the indigenous species, probably present at lower than detection limit numbers. In section A, benzene carboxylase gene copies were abundant in the injection wells, but only detected once in one other well. This suggests that transport of micro-organisms and genes from the injection to the monitoring wells was limited. In addition, it is possible that the laboratory-grown bioaugmentation culture was readily outcompeted by the indigenous microbial population in the test field. Note that in the nitrate stimulated section B, benzene decreased more than toluene, while in bioaugmented section A, toluene decreased more than benzene. This could have been caused by the initially higher numbers of *Peptococcaceae* and benzene carboxylase genes in section B. It is clear that nitrate addition has a positive effect on increased biodegradation of most mono aromatic hydrocarbons, with m,p-xylene as an exception. However, it is unclear whether the growth of micro-organisms in the augmented and stimulated section is considered a positive effect of the nitrate injections only. It could have been due to the addition of the benzene degrading culture during bio-augmentation.

5.5 Conclusions

Enhanced anaerobic degradation of aromatic hydrocarbons by biostimulation through nitrate injections was successfully performed *in situ* by means of a multi well recirculation system. Enhanced biodegradation was observed for most aromatic hydrocarbons such as BTEX, naphthalene, indene and styrene. Although bioaugmentation with a laboratory-grown culture in combination with nitrate injections increased benzene degradation, growth of benzene carboxylase (*abcA*) was similar in the not-augmented test field.

Benzene degradation was successfully enhanced under anaerobic conditions at the field scale by nitrate additions, after a lag time of more than one year. Changes in fractionation of ^2H stable isotopes indicated that after adaptation, benzene

degradation was faster than toluene, and degradation was faster than xylenes. Although indigenous microorganisms *Peptococcaceae* and benzene carboxylase were present at relatively low or undetectable levels, their population grew considerably by nitrate additions during the field test. This suggests that benzene degradation was coupled to indigenous micro-organisms.

Biostimulation through nitrate injections could be a viable option for sites contaminated by aromatic hydrocarbons and a more efficient approach than air sparging. However, adaptation time for the indigenous contaminant degrading microorganisms needs to be considered and take up to one or several years. Bioaugmentation can help to shorten adaptation, although this should be substantiated by further studies.

5.6 Acknowledgements

This work was financially supported by SBNS, Foundation of Dutch Railways for soil remediation.

We acknowledge Antoine Booms, Roy Goossen, Patrick Broekhuizen from Aveco de Bondt and Andre Cinjee from Deltares, for sharing their site knowledge and assistance in field work.

5.7 Supplementary information

Table S5-1: Overview sampling rounds and analyses performed during the multi well recirculation test for enhanced bioremediation.

Test period	Sampling round	Time (day)	pH	EC	Redox	GC-MS	LC	ICP-OES	qPCR	IR-GRMS
I	T=0	0	X	X	X	X	X	X	X	-
I	T=1	69	X	X	X	X	X	X	-	X
I	T=2	150	X	X	X	X	X	X	-	-
I	T=3	226	X	X	X	X	X	X	-	-
I	T=4	282	X	X	X	X	X	X	X	X
I	T=5	471	X	X	X	X	X	X	X	X
II	T=6	580	-	-	-	X		-	-	-
II	T=7	601	-	-	-	X		-	-	-
II	T=8	653	X	X	X	X		X	X	-
II	T=9	697	X	X	X	X		-	-	-
II	T=10	723	X	X	X	X		X	X	X
II	T=11	807	X	X	X	-		X	-	-
II	T=12	906	X	X	X	-		X	-	X
II	T=13	959	X	X	X	-		X	X	X
II	T=14	1078	X	X	X	X		X	-	-

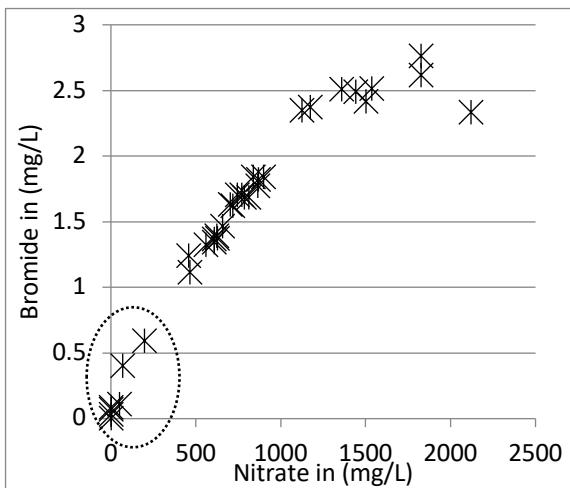


Figure S5-1: Bromide was used as tracer. However, nitrate was mostly consumed below 500mg/L, where concentrations of Br⁻ became to diluted to act as a tracer.

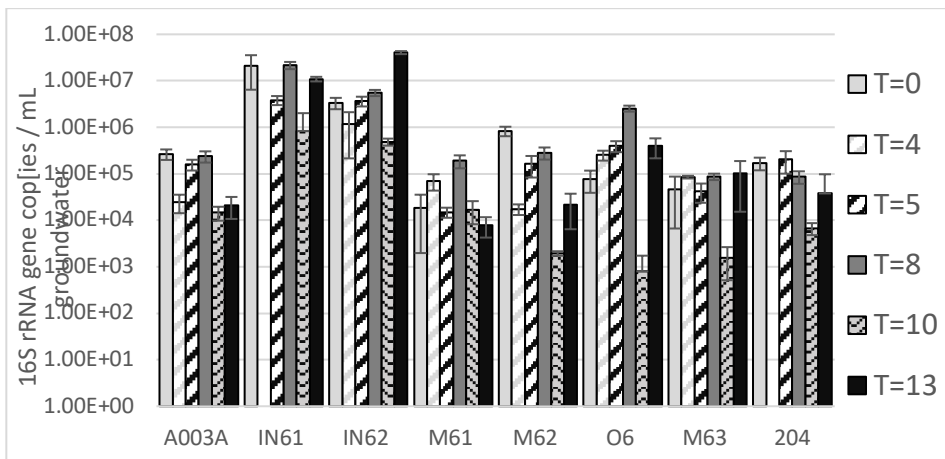


Figure S5-2: Gene copies for 16S rRNA total bacteria in section A of the test-field. T=0 / T=4 represents test-period I, recirculation only. After T=5 period II started, where nitrate+bioaugmentation was injected. A003 and 204 are the up- and downgradient sample wells respectively.

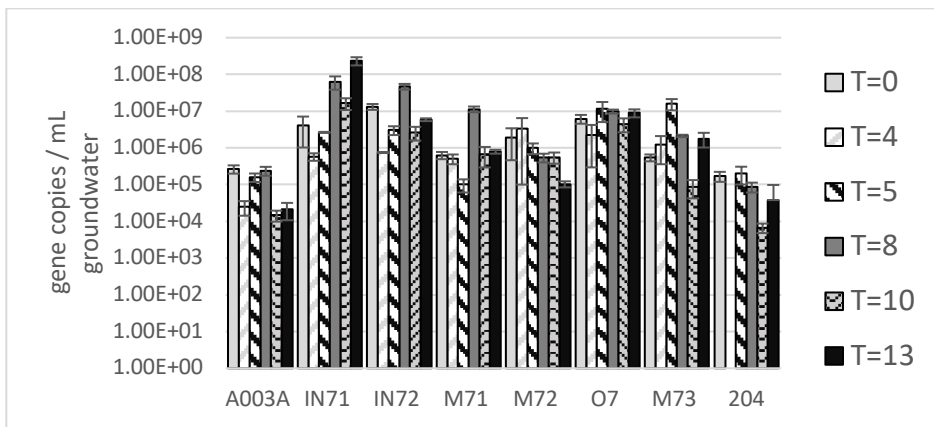


Figure S5-3: Gene copies for 16S rRNA total bacteria in section B of the test-field. Section B was stimulated after T=0 and remained so during period I and II of the test. A003 and 204 are the up- and downgradient sample wells respectively.

6 Discussion, conclusions and outlook

Soil contaminated by dense non aqueous phase liquid (DNAPL) can contaminate the subsurface for decades or longer. This is of major concern because $\pm 60\%$ of our drinking water is derived from aquifers. However, nature is resilient, and the more biological degradation of disposed chemicals is studied, the more chemicals at various conditions seem to be biodegrading. Intrinsic biodegradation in the saturated subsurface is often relatively slow, nevertheless we humans are capable of building with nature and developing remediation techniques by facilitating the responsible micro-organisms. In this study we have conducted a field study on intrinsic anaerobic biodegradation, elongated by various experiments initially in the laboratory and subsequently upscaled field tests. During these experiments we investigated the fate of Pintsch gas tar compounds in a nitrate containing aquifer and the potential for bio-stimulation and bio-augmentation as a means of active bioremediation.

Although Pintsch gas tar is a waste product from manufactured gas plants similar to coal tar, our study revealed that these types of tar differ in physical properties as well as chemical composition. GCxGC-TOF-MS analysis revealed 948 tar components present in the Pintsch gas tar. For the collected tar samples, density ($1.03 - 1.06 \text{ kg/m}^3$) and viscosity ($18.6 - 39.4 \text{ cP}$) are relatively low compared to other coal tars. Analysis showed that phenanthrene is the primary component rather than naphthalene, and that the pintsch gas tar contains a relatively high amount of light molecular aromatic hydrocarbon compounds, such as benzene, toluene, ethylbenzene and xylenes (BTEX). Less commonly reported components, such as styrene, ethyltoluenes, di-ethylbenzene, 1,2,4,5-tetramethylbenzene, were also detected in water extracts from Pintsch gas tar.

Previous research on biodegradation of dissolved tar components shows that most water soluble volatile aromatic hydrocarbons biodegrade at various redox conditions. However, biodegradability of benzene, indene and polycyclic aromatic hydrocarbons such as acenaphthylene and phenanthrene at nitrate reducing conditions is much less understood. Degradation rates of specific aromatic hydrocarbon compounds differ with each redox condition and the microbial culture present. Moreover, inhibition or co-metabolism may affect complex mixtures which are common at tar contaminated sites. From our field study at the Pintsch gas tar contaminated site in Amersfoort, The Netherlands, we learned that all water-soluble Pintsch gas tar compounds biodegrade either at source zone or groundwater plume conditions.

Biodegradation studies at source zone conditions are less abundant and more complex than groundwater plume studies. From our source zone study in the field it was found that biodegradation occurs at these assumed to be toxic conditions. These findings were substantiated by detection of 123 metabolites that indicate active biodegradation for broad range of tar constituents. Besides metabolites from water soluble contaminants such toluene, styrene and trimethylbenzene, also metabolites were found amongst none water soluble tar compounds such as naphthalene, indene, acenaphthylene and phenanthrene. We detected nine metabolites related to anaerobic degradation of indene. From these a biodegradation pathway was composed representing the pathway for carboxylation.

Source zone mimicking microcosms in the laboratory containing tar DNAPL, show more biodegradation of the relatively light molecular polycyclic aromatic hydrocarbons and less to no degradation for the water soluble mono aromatic hydrocarbons. If biodegradation occurs at source zone conditions, where active partitioning creates high concentrations of the water-soluble aromatics in the water phase. Micro-organisms either have to cope with the governing high

concentrations or biodegrade the contaminants at a faster rate. However, in this line of thought it is assumed that conditions are similar throughout the microcosm, which in our experiment was not the case. During our microcosm experiments, prepared with contaminated sediment from site, extra interphases were observed. While in plume mimicking microcosms the main interchanges took place between the water and gas or water and sediment phase. The result of DNAPL in a microcosm, is pure phase tar sticking to the glass of the bottle, mixing in with the sediment and behaving as LNAP floating on the water surface. These effects create extra interphases for partitioning and heterogeneity of contaminant distribution, even within a 200 mL glass bottle. Where partitioning of a complex mixture creates lower concentrations for individual compounds, which may affect a less toxic environment, also the heterogeneous distribution of the DNAPL may contribute to micro niches for micro-organisms. These effects might have contributed to the observed biodegradation, and some might also apply to field conditions, where distribution of DNAPL tends to be erratic. It has been described that bio-enhanced dissolution factors can be greater than the biodegradation rates and resulting in greater fluxes, resulting in an extending groundwater plume. Although stimulation of source zone conditions was successful in the laboratory it is still unsure if bio-stimulation safely can be applied at source zone field conditions and more research is needed to address mobilization of DNAPL due to bio-stimulation and effects of larger contaminant fluxes.

During our investigations on the occurrence and extent of anaerobic biodegradation of aromatic hydrocarbons in the groundwater plume originating from a Pintsch gas tar source zone reduction of specific compounds varied distinctively. It was found that relatively slower biodegradation of most hydrocarbon contaminants at iron reducing conditions within the plume zone appears to be of greater significance than at higher biodegradation rates in the

nitrate reducing fringe zone, except for benzene. In the fringe zone benzene was more strongly degraded than toluene, ethylbenzene, xylenes and naphthalene (BTEXN) compared to the plume zone, and vice versa. The significance of iron-versus nitrate reducing conditions is mainly because of the dimensions of the iron reducing part of the plume, which is relatively much larger than the dimensions of the nitrate reducing plume fringe. Furthermore, the highest diversity and concentrations of metabolites were detected in the iron- reducing plume core, where the sum of parent compounds of aromatic hydrocarbons was greater than 10 mg/L. This diversity and relatively high concentrations of metabolites suggest a hot spot for anaerobic degradation in the core of the plume downgradient but relatively close to the DNAPL containing source zone.

From our enhanced anaerobic degradation field test, biodegradation was observed for most aromatic hydrocarbons such as BTEX, naphthalene, indene and styrene. Benzene degradation was successfully enhanced under anaerobic conditions at the field scale by nitrate additions, after a lag time of more than one year. Although bioaugmentation with a laboratory-grown culture in combination with nitrate injections increased benzene degradation, growth of benzene carboxylase (*abcA*) was similar in the not-augmented test field. Bio-augmentation could shorten adaptation time for micro-organisms to adapt to created nitrate reducing conditions. However, the laboratory culture that we injected in the field, remained in the injection wells, rather than entering and spreading in the sediment. Still transposons could have an enhancement effect on the indigenous cultures, but this is unsure. Spreading of injected bacteria in the subsurface and transposons affecting indigenous micro-organisms in the subsurface could be subject to further research.

Changes in fractionation of ^2H stable isotopes indicated that after adaptation, benzene degradation was faster than toluene, and degradation of benzene was faster than xylenes. Although indigenous microorganisms *Peptococcaceae* and

benzene carboxylase were present at relatively low or undetectable levels, their population grew considerably after nitrate additions during the field test. This suggests that benzene degradation was coupled to indigenous micro-organisms. Biostimulation through nitrate injections could be a viable option for sites contaminated by aromatic hydrocarbons and a more efficient approach than air sparging. However, adaptation time for the indigenous contaminant degrading microorganisms needs to be considered and can take up to one or several years. Bioaugmentation can help to shorten adaptation, although this should be substantiated by further studies.

The effect of bio-augmentation at the field scale is complex and difficult to grasp, soil heterogeneity exists at the meter, centimeter, millimeter and other scales. Little is known about spatial distribution of micro-organisms in the subsurface or how bacteria move through the subsurface. It's hard to imagine or hypothesize the effects of adding laboratory grown and harvested micro-organisms to the field and expect them to multiply and add a measurable contribution to intrinsic biodegradation. Where micro-organisms that have been grown in the laboratory for more than 17 years are set free in a hostile world of competition. Personally, I find bio-augmentation in the field an analogy for a lion release program, where Zoo bred lions do not fear armed and dangerous humans or make friends to a zebra instead of recognizing it as a meal once set free in the savannah. Therefore, this zoo bred creatures have little chance surviving in the wild. Nevertheless bio-augmentation could a feasible and promising technique for bioremediation in the future and if we could find the parameters that lead to success. Further field tests applying bio-augmentation are needed and an interesting subject for future studies.

Curriculum Vitae

Johan van Leeuwen was born on the 30th of June 1971 in Gellicum The Netherlands. He attended University of applied sciences Larenstein in Velp and later Hogeschool van Arnhem and Nijmegen (HAN). Johan started his career as field worker at De Ruiter Milieutechnologie in Halfweg The



Netherlands and later worked as consultant for this company. Then he worked for BAM a 7.2 billion EURO contracting company, where he designed and applied *in-situ* remediation operations. Then Johan moved to Stichting Bodemsanering Nederlandse Spoorwegen (SBNS), where he conducted large scale site restorations.

His special interests are in the study of DNAPL dynamics and biodegradation of chemical waste components in the environment. He enjoys working on translating fundamental science into applications for ecological engineering concepts, such as: 1) the first Dutch direct push injection of nutrients for biological degradation of perchloroethylene. 2) Wind-powered *in-situ* remediation by means of constructed wetlands for PCE dechlorination. 3) Net zero carbon emission *in-situ* remediation of oil contaminated subsurface by using off grid renewable energy sources.

In 2018 Johan started his PhD in the environmental hydrology group at Utrecht university. He will continue working as researcher at Deltares research institute in Utrecht The Netherlands, where he conducts research in the field of contaminated subsurface and wastewater treatment.

References

- Aamand, J., Jørgensen, C., Arvin, E., Jensen, B.K., 1989. Microbial adaptation to degradation of hydrocarbons in polluted and unpolluted groundwater. *J. Contam. Hydrol.* 4, 299–312. doi:10.1016/0169-7722(89)90030-2
- Abraham, M.H., Chadha, H.S., Whiting, G.S., Mitchell, R.C., 1994. Hydrogen bonding. 32. An analysis of water-octanol and water-alkane partitioning and the $\Delta \log p$ parameter of seiler. *J. Pharm. Sci.* 83, 1085–1100. doi:10.1002/jps.2600830806
- Abu Laban, N., Selesi, D., Rattei, T., Tischler, P., Meckenstock, R.U., 2010. Identification of enzymes involved in anaerobic benzene degradation by a strictly anaerobic iron-reducing enrichment culture. *Environ. Microbiol.* 12, 2783–2796. doi:10.1111/j.1462-2920.2010.02248.x
- Aitken, C.M., Jones, D.M., Larter, S.R., 2004. Anaerobic hydrocarbon biodegradation in deep subsurface oil reservoirs. *Nature* 431, 291–294. doi:10.1038/nature02922
- Al-Bashir, B., Cseh, T., Leduc, R., Samson, R., 1990. Effect of soil/contaminant interactions on the biodegradation of naphthalene in flooded soil under denitrifying conditions. *Appl. Microbiol. Biotechnol.* 34, 414–419. doi:10.1007/BF00170071
- Alvarez, P.J.J., Anid, P.J., Vogel, T.M., 1991. Kinetics of aerobic biodegradation of benzene and toluene in sandy aquifer material. *Biodegradation* 2, 43–51. doi:10.1007/BF00122424
- Alvarez, P.J.J., Illman, W.A. (Walter A., 2006. *Bioremediation and natural attenuation: process fundamentals and mathematical models*. Wiley-Interscience. John Wiley & Sons, Inc. Publication, Hoboken, New Jersey.
- Ambrosoli, R., Petruzzelli, L., Minati, J.L., Marsan, F.A., 2005. Anaerobic PAH degradation in soil by a mixed bacterial consortium under denitrifying conditions. *Chemosphere* 60, 1231–1236. doi:10.1016/j.chemosphere.2005.02.030
- American, S., 1898. the manufacture of Pintsch gas. *Sci. Am.* LXXIX, 27.
- Annweiler, E., Michaelis, W., Meckenstock, R.U., 2001a. Anaerobic Cometabolic Conversion of Benzothiophene by a Sulfate-Reducing Enrichment Culture and in a Tar-Oil-Contaminated Aquifer 1. *Appl. Environ. Microbiol.* 67, 5077–5083. doi:10.1128/AEM.67.11.5077-5083.2001
- Annweiler, E., Michaelis, W., Meckenstock, R.U., Meckjenstock, R.U., 2001b. Anaerobic Cometabolic Conversion of Benzothiophene by a Sulfate-Reducing Enrichment Culture and in a Tar-Oil-Contaminated Aquifer 1. *Appl. Environ. Microbiol.* 67, 5077–5083. doi:10.1128/aem.67.11.5077-5083.2001
- Annweiler, E., Richnow, H.H., Antranikian, G., Hebenbrock, S., Garms, C., Franke, S., Francke, W., Michaelis, W., 2000. Naphthalene degradation and incorporation of naphthalene-derived carbon into biomass by the

- thermophile *Bacillus thermoleovorans*. *Appl. Environ. Microbiol.* 66, 518–523. doi:10.1128/AEM.66.2.518-523.2000
- Aronson, D., Howard, P.H., 1997. *Anaerobic Biodegradation of Organic Chemicals in Groundwater: A Summary of Field and Laboratory Studies*. Tech. Rep. 268.
- Atashgahi, S., Hornung, B., Van Der Waals, M.J., Da Rocha, U.N., Hugenholtz, F., Nijse, B., Molenaar, D., Van Spanning, R., Stams, A.J.M., Gerritse, J., Smidt, H., 2018. A benzene-degrading nitrate-reducing microbial consortium displays aerobic and anaerobic benzene degradation pathways. *Sci. Rep.* 8, 1–12. doi:10.1038/s41598-018-22617-x
- Baedecker, M.J., Eganhouse, R.P., Bekins, B.A., Delin, G.N., 2011. Loss of volatile hydrocarbons from an LNAPL oil source. *J. Contam. Hydrol.* 126, 140–152. doi:10.1016/j.jconhyd.2011.06.006
- Balachandran, C., Duraipandiyam, V., Balakrishna, K., Ignacimuthu, S., 2012. Petroleum and polycyclic aromatic hydrocarbons (PAHs) degradation and naphthalene metabolism in *Streptomyces* sp. (ERI-CPDA-1) isolated from oil contaminated soil. *Bioresour. Technol.* 112, 83–90. doi:10.1016/j.biortech.2012.02.059
- Bauer, R.D., Maloszewski, P., Zhang, Y., Meckenstock, R.U., Griebler, C., 2008. Mixing-controlled biodegradation in a toluene plume - Results from two-dimensional laboratory experiments. *J. Contam. Hydrol.* 96, 150–168. doi:10.1016/j.jconhyd.2007.10.008
- Beller, H.R., 2002. Analysis of benzylsuccinates in groundwater by liquid chromatography/tandem mass spectrometry and its use for monitoring in situ BTEX biodegradation. *Environ. Sci. Technol.* 36, 2724–2728. doi:10.1021/es0255271
- Beller, H.R., Kane, S.R., Legler, T.C., Alvarez, P.J.J., 2002. A real-time polymerase chain reaction method for monitoring anaerobic, hydrocarbon-degrading bacteria based on a catabolic gene. *Environ. Sci. Technol.* 36, 3977–3984. doi:10.1021/es025556w
- Beller, H.R., Kane, S.R., Legler, T.C., Mckelvie, J.R., Lollar, B.S., Pearson, F., Balser, L., Mackay, D.M., 2008. Comparative assessments of benzene, toluene, and xylene natural attenuation by quantitative polymerase chain reaction analysis of a catabolic gene, signature metabolites, and compound-specific isotope analysis. *Environ. Sci. Technol.* 42, 6065–6072. doi:10.1021/es8009666
- Beller, H.R., Spormann, a. M., 1998. Analysis of the novel benzylsuccinate synthase reaction for anaerobic toluene activation based on structural studies of the product. *J. Bacteriol.* 180, 5454–5457.
- Berdugo-Clavijo, C., Dong, X., Soh, J., Sensen, C.W., Gieg, L.M., 2012. Methanogenic biodegradation of two-ringed polycyclic aromatic hydrocarbons. *FEMS Microbiol. Ecol.* 81, 124–133. doi:10.1111/j.1574-6941.2012.01328.x

- Bian, X.-Y., Mbadinga, S.M., Liu, Y.-F., Yang, S.-Z., Liu, J.-F., Ye, R.-Q., Gu, J.-D., Mu, B.-Z., 2015. Insights into the Anaerobic Biodegradation Pathway of n-Alkanes in Oil Reservoirs by Detection of Signature Metabolites. *Nat. Rev. Microbiol.* 5, 9801. doi:10.1038/srep09801
- Birak, P.S., Miller, C.T., 2009. Dense non-aqueous phase liquids at former manufactured gas plants: Challenges to modeling and remediation. *J. Contam. Hydrol.* 105, 81–98. doi:10.1016/j.jconhyd.2008.12.001
- Blum, P., Hunkeler, D., Weede, M., Beyer, C., Grathwohl, P., Morasch, B., 2009. Quantification of biodegradation for o-xylene and naphthalene using first order decay models, Michaelis-Menten kinetics and stable carbon isotopes. *J. Contam. Hydrol.* 105, 118–130. doi:10.1016/j.jconhyd.2008.11.009
- Bombach, P., Richnow, H.H., Kästner, M., Fischer, A., 2010. Current approaches for the assessment of in situ biodegradation. *Appl. Microbiol. Biotechnol.* 86, 839–852. doi:10.1007/s00253-010-2461-2
- Braker, G., Fesefeldt, A., Witzel, K.P., 1998. Development of PCR primer systems for amplification of nitrite reductase genes (nirK and nirS) to detect denitrifying bacteria in environmental samples. *Appl. Environ. Microbiol.* 64, 3769–3775.
- Bregnard, Thierry Pierre Alain, Höhener, P., Häner, A., Zeyer, J., 1996. Degradation of weathered diesel fuel by microorganisms from a contaminated aquifer in aerobic and anaerobic microcosms. *Environ. Toxicol. Chem.* 15, 299–307. doi:10.1897/1551-5028(1996)015<0299:DOWDFB>2.3.CO;2
- Bregnard, T.P.A., Höhener, P., Häner, A., Zeyer, J., Ecology, T., Biology, S., 1996. Degradation of Weathered Diesel Fuel By Microorganisms From a. *Environ. Toxicol. Chem.* 15, 299–307.
- Brock, O., 2016. Detection of metabolite biomarkers indicating anaerobic biodegradation of oil-gas tar in soil column and batch experiments and in-situ Internship report.
- Brown, D.G., Gupta, L., Kim, T.H., Keith Moo-Young, H., Coleman, A.J., 2006. Comparative assessment of coal tars obtained from 10 former manufactured gas plant sites in the Eastern United States. *Chemosphere* 65, 1562–1569. doi:10.1016/j.chemosphere.2006.03.068
- Bruce, L., Miller, T., Hockman, B., 1991. Solubility versus equilibrium saturation of gasoline compounds: A method to estimate fuel/water partition coefficients using solubility and Koc. *NWWA/API Conf. Pet. Hydrocarb. Gr. Water.*
- Brzyska, W., Kula, A., 1995. Studies on the thermal decomposition of rare earth element complexes with 2-naphthoic acid. *J. Therm. Anal. Calorim.* 44, 1159–1169. doi:10.1007/BF02547546
- Burchill, P., Herod, A.A., Pritchard, E., 1983. Investigation of nitrogen compounds in coal tar products. 1. Unfractionated materials. *Fuel* 62, 11–19. doi:10.1016/0016-2361(83)90245-4

- Burd, G., Ward, O.P., 1996. Involvement of a surface-active high molecular weight factor in degradation of polycyclic aromatic hydrocarbons by *Pseudomonas marginalis*. *Can. J. Microbiol.* 42, 791–797. doi:10.1139/m96-099
- Burland, S.M., Edwards, E.A., 1999. Anaerobic benzene biodegradation linked to nitrate reduction. *Appl. Environ. Microbiol.* 65, 529–533.
- Butterfield, W.J., 1904. *The Chemistry of Gas Manufacture*, Edition 3., ed. Charles Griffin and Company, Exeter.
- Caldwell, M.E., Suflita, J.M., 2000. Detection of phenol and benzoate as intermediates of anaerobic benzene biodegradation under different terminal electron-accepting conditions. *Environ. Sci. Technol.* 34, 1216–1220. doi:10.1021/es990849j
- Callaghan, A. V., 2013. Metabolomic investigations of anaerobic hydrocarbon-impacted environments. *Curr. Opin. Biotechnol.* 24, 506–515. doi:10.1016/j.copbio.2012.08.012
- Chakraborty, R., Coates, J.D., 2004. Anaerobic degradation of monoaromatic hydrocarbons. *Appl. Microbiol. Biotechnol.* 64, 437–446. doi:10.1007/s00253-003-1526-x
- Chang, S.W., Hyman, M.R., Williamson, K.J., 2002. Cooxidation of naphthalene and other polycyclic aromatic hydrocarbons by the nitrifying bacterium, *Nitrosomonas europaea*. *Biodegradation* 13, 373–381. doi:10.1023/A:1022811430030
- Chang, B. V., Shiung, L.C., Yuan, S.Y., 2002. Anaerobic biodegradation of polycyclic aromatic hydrocarbon in soil. *Chemosphere* 48, 717–724. doi:10.1016/S0045-6535(02)00151-0
- Chee-Sanford, J.C., Frost, J.W., Fries, M.R., Zhou, J., Tiedje, J.M., 1996. Evidence for acetyl coenzyme A and cinnamoyl coenzyme A in the anaerobic toluene mineralization pathway in *Azoarcus toluolyticus* Tol-4. *Appl. Environ. Microbiol.* 62, 964–73.
- Chen, K.-F., Chang, Y.-C., Huang, S.-C., 2012. Biodegradation potential of MTBE and BTEX under aerobic, nitrate reducing, and methanogenic conditions at a gasoline-contaminated site. *Desalin. Water Treat.* 48, 278–284. doi:10.1080/19443994.2012.698825
- Coates, John D., Anderson, R.T., Lovley, D.R., 1996. Oxidation of polycyclic aromatic hydrocarbons under sulfate-reducing conditions. *Appl. Environ. Microbiol.* 62, 1099–1101. doi:10.1128/aem.62.3.1099-1101.1996
- Coates, J D, Anderson, R.T., Lovley, D.R., 1996. Oxidation of Polycyclic Aromatic Hydrocarbons under Sulfate-Reducing Conditions. *Appl. Environ. Microbiol.* 62, 1099–1101.
- Coates, J.D., Chakraborty, R., McInerney, M.J., 2002a. Anaerobic benzene biodegradation - A new era. *Res. Microbiol.* 153, 621–628. doi:10.1016/S0923-2508(02)01378-5
- Coates, J.D., Cole, K.A., Chakraborty, R., O'Connor, S.M., Achenbach, L.A.,

- 2002b. Diversity and ubiquity of bacteria capable of utilizing humic substances as electron donors for anaerobic respiration. *Appl. Environ. Microbiol.* 68, 2445–2452. doi:10.1128/AEM.68.5.2445-2452.2002
- Coates, J.D., Woodward, J., Allen, J., Philp, P., Lovley, D.R., 1997. Anaerobic degradation of polycyclic aromatic hydrocarbons and alkanes in petroleum-contaminated marine harbor sediments. *Appl. Environ. Microbiol.* 63, 3589–3593. doi:10.1128/aem.63.9.3589-3593.1997
- Corseuil, H., Schneider, M., 2002. Natural attenuation rates of ethanol and BTEX compounds in groundwater contaminated with gasohol. *Int. Solid Waste Assoc.* 2121–2128.
- Coulon, F., Pelletier, E., St. Louis, R., Gourhant, L., Delille, D., 2004. Degradation of petroleum hydrocarbons in two sub-Antarctic soils: Influence of an oleophilic fertilizer. *Environ. Toxicol. Chem.* 23, 1893–1901. doi:10.1897/03-484
- Cozzarelli, I.M., Bekins, B.A., Eganhouse, R.P., Warren, E., Essaid, H.I., 2010. In situ measurements of volatile aromatic hydrocarbon biodegradation rates in groundwater. *J. Contam. Hydrol.* 111, 48–64. doi:10.1016/j.jconhyd.2009.12.001
- Cozzarelli, I.M., Eganhouse, R.P., Baedecker, M.J., 1990. Transformation of Monoaromatic hydrocarbons to organic acids in anoxic groundwater environment. *Environ. Geol. Water Sci.* 16, 135–141. doi:10.1007/BF01890379
- Cupples, A.M., 2016. Contaminant-Degrading Microorganisms Identified Using Stable Isotope Probing. *Chem. Eng. Technol.* 39, 1593–1603. doi:10.1002/ceat.201500479
- D’Affonseca, F.M., Prommer, H., Finkel, M., Blum, P., Grathwohl, P., 2011. Modeling the long-term and transient evolution of biogeochemical and isotopic signatures in coal tar-contaminated aquifers. *Water Resour. Res.* 47, 1–22. doi:10.1029/2010WR009108
- Da Silva, M.L.B., Alvarez, P.J.J., 2004. Enhanced anaerobic biodegradation of benzene-toluene-ethylbenzene-xylene- ethanol mixtures in bioaugmented aquifer columns. *Appl. Environ. Microbiol.* 70, 4720–4726. doi:10.1128/AEM.70.8.4720-4726.2004
- da Silva, M.L.B., Corseuil, H.X., 2012. Groundwater microbial analysis to assess enhanced BTEX biodegradation by nitrate injection at a gasohol-contaminated site. *Int. Biodeterior. Biodegrad.* 67, 21–27. doi:10.1016/j.ibiod.2011.11.005
- Da Silva, M.L.B., Ruiz-Aguilar, G.M.L., Alvarez, P.J.J., 2005. Enhanced anaerobic biodegradation of BTEX-ethanol mixtures in aquifer columns amended with sulfate, chelated ferric iron or nitrate. *Biodegradation* 16, 105–114. doi:10.1007/s10532-004-4897-5
- Dean-Ross, D., Moody, J., Cerniglia, C.E., 2002. Utilization of mixtures of polycyclic aromatic hydrocarbons by bacteria isolated from contaminated

- sediment. *FEMS Microbiol. Ecol.* 41, 1–7. doi:10.1016/S0168-6496(02)00198-8
- DobrisAssesment, 1995. Europe's Environment - The Dobris Assessment.
- Dolfing, J., Xu, A., Gray, N.D., Larter, S.R., Head, I.M., 2009. The thermodynamic landscape of methanogenic PAH degradation. *Microb. Biotechnol.* 2, 566–574. doi:10.1111/j.1751-7915.2009.00096.x
- Dou, J., Ding, A., Liu, X., Du, Y., Deng, D., Wang, J., 2010. Anaerobic benzene biodegradation by a pure bacterial culture of *Bacillus cereus* under nitrate reducing conditions. *J. Environ. Sci.* 22, 709–715. doi:10.1016/S1001-0742(09)60167-4
- Dou, J., Liu, X., Hu, Z., 2008. Anaerobic BTEX degradation in soil bioaugmented with mixed consortia under nitrate reducing conditions. *J. Environ. Sci. (China)* 20, 585–92. doi:10.1016/s1001-0742(08)62098-7
- Durant, N.D., Wilson, L.P., Bouwer, E.J., 1995. Microcosm studies of subsurface PAH-degrading bacteria from a former manufactured gas plant. *J. Contam. Hydrol.* 17, 213–237. doi:10.1016/0169-7722(94)00034-F
- Ebihara, T., Bishop, P.L., 2002. Influence of supplemental acetate on bioremediation for dissolved polycyclic aromatic hydrocarbons. *J. Environ. Eng.* 128, 505–513. doi:10.1061/(ASCE)0733-9372(2002)128:6(505)
- Edwards, E. a., Grbic-Galic, D., 1994. Anaerobic degradation of toluene and o-xylene by a methanogenic consortium. *Appl. Environ. Microbiol.* 60, 313–322.
- Egloff, G & Twomey, T.J., 1916. The Effect of temperature on the Formation of Benzene, Toluene, Xylene, Naphtalene and Anthracene from Petroleum at Atmospheric Pressure. *J. Phys. Chem.* 20, 121–150.
- Einarson, M.D., Mackay, D.M., 2001. Peer Reviewed: Predicting Impacts of Groundwater Contamination. *Environ. Sci. Technol.* 35, 66A-73A. doi:10.1021/es0122647
- Electric Power Research Institute, 1993. Chemical and Physical Characteristics of Tar Samples from Selected Manufactured Gas Plant (MGP) Sites; Final Report for Research Project 2879-12; EPRI TR-102184.
- Elkateb, T., Chalaturnyk, R., Robertson, P.K., 2002. an Overview of Soil Heterogeneity Quantification and Implications on.Pdf. *Can. Geotech. J.* 40, 1–15.
- Elshahed, M.S., Gieg, L.M., McInerney, M.J., Suflita, J.M., 2001. Signature metabolites attesting to the in situ attenuation of alkylbenzenes in anaerobic environments. *Environ. Sci. Technol.* 35, 682–689. doi:10.1021/es001571u
- Elsner, M., 2010. Stable isotope fractionation to investigate natural transformation mechanisms of organic contaminants: Principles, prospects and limitations. *J. Environ. Monit.* 12, 2005–2031. doi:10.1039/c0em00277a
- EPA, 2013. Introduction To in Situ Bioremediation of Groundwater, EPA 542-R-13-018.

- Eriksson, M., Dalhammar, G., Borg-Karlson, A.K., 2000. Biological degradation of selected hydrocarbons in an old PAH/creosote contaminated soil from a gas work site. *Appl. Microbiol. Biotechnol.* 53, 619–626. doi:10.1007/s002530051667
- Eriksson, M., Sodersten, E., Yu, Z., Dalhammar, G., Mohn, W.W., 2003. Degradation of polycyclic aromatic hydrocarbons at low temperature under aerobic and nitrate-reducing conditions in enrichment cultures from northern soils. *Appl. Environ. Microbiol.* 69, 275–284. doi:10.1128/AEM.69.1.275-284.2003
- Essaid, H.I., Bekins, B.A., Herkelrath, W.N., Delin, G.N., 2011. Crude oil at the Bemidji site: 25 years of monitoring, modeling, and understanding. *Ground Water* 49, 706–726. doi:10.1111/j.1745-6584.2009.00654.x
- Farhadian, M., Vachelard, C., Duchez, D., Larroche, C., 2008. In situ bioremediation of monoaromatic pollutants in groundwater: A review. *Bioresour. Technol.* 99, 5296–5308. doi:10.1016/j.biortech.2007.10.025
- Fetter, C.W., 1999. *Contaminant Hydrogeology*, 2nd editio. ed. Waveland Press, Inc.
- Flanagan, P. V., Kelleher, B.P., Allen, C.C.R., 2014. Assessment of Anaerobic Biodegradation of Aromatic Hydrocarbons: The Impact of Molecular Biology Approaches. *Geomicrobiol. J.* 31, 276–284. doi:10.1080/01490451.2013.820237
- Foght, J., 2008. Anaerobic biodegradation of aromatic hydrocarbons: Pathways and prospects. *J. Mol. Microbiol. Biotechnol.* 15, 93–120. doi:10.1159/000121324
- Fountain, J.C., 1998. *Technologies for Dense Nonaqueous*. Source 15238.
- Freeze, R.A., Cherry, J.A., 1979. Prentice-Hall, Englewood Cliffs, N.J. *Groundwater* 604.
- Gallacher, C., Thomas, R., Lord, R., Kalin, R.M., Taylor, C., 2017. Comprehensive database of Manufactured Gas Plant tars. Part C. Heterocyclic and hydroxylated polycyclic aromatic hydrocarbons. *Rapid Commun. Mass Spectrom.* 31. doi:10.1002/rcm.7904
- Gallacher, Christopher, Thomas, R., Taylor, C., Lord, R., Kalin, R.M., 2017. Comprehensive composition of Creosote using comprehensive two-dimensional gas chromatography time-of-flight mass spectrometry (GCxGC-TOFMS). *Chemosphere* 178, 34–41. doi:10.1016/j.chemosphere.2017.03.050
- Gerritse, J; van der Grift, B; Langenhoff, A., 2004. *Contaminant Behaviour of Micro-Organics in Groundwater*. John Wiley & Sons inc. doi:10.1036/0071425799
- Geudens, P.J.J., Grootveld, J., 2017. *Dutch Drinking Water Statistics 2017* 130.
- Ghosal, D., Ghosh, S., Dutta, T.K., Ahn, Y., 2016. Current state of knowledge in microbial degradation of polycyclic aromatic hydrocarbons (PAHs): A review. *Front. Microbiol.* 7. doi:10.3389/fmicb.2016.01369

- Ghosh, U., Weber, A.S., Jensen, J.N., Smith, J.R., 2000. Relationship between PCB desorption equilibrium, kinetics, and availability during land biotreatment. *Environ. Sci. Technol.* 34, 2542–2548. doi:10.1021/es9905389
- Ghoshal, S., Pasion, C., Alshafie, M., 2004. Reduction of Benzene and Naphthalene Mass Transfer from Crude Oils by Aging-Induced Interfacial Films. *Environ. Sci. Technol.* 38, 2102–2110. doi:10.1021/es034832j
- Gibson, D.T., Koch, J.R., Kallio, R.E., 1968a. Oxidative Degradation of Aromatic Hydrocarbons by Microorganisms. I. Enzymatic Formation of Catechol from Benzene. *Biochemistry* 7, 2653–2662. doi:10.1021/bi00847a031
- Gibson, D.T., Koch, J.R., Schuld, C.L., Kallio, R.E., 1968b. Oxidative Degradation of Aromatic Hydrocarbons by Microorganisms. II. Metabolism of Halogenated Aromatic Hydrocarbons. *Biochemistry* 7, 3795–3802. doi:10.1021/bi00851a003
- Gieg, L.M., Alumbaugh, R.E., Field, J., Jones, J., Istok, J.D., Suflita, J.M., 2009. Assessing in situ rates of anaerobic hydrocarbon bioremediation. *Microb. Biotechnol.* 2, 222–233. doi:10.1111/j.1751-7915.2008.00081.x
- Gieg, L.M., Suflita, J.M., 2002. Detection of anaerobic metabolites of saturated and aromatic hydrocarbons in petroleum-contaminated aquifers. *Environ. Sci. Technol.* 36, 3755–3762. doi:10.1021/es0205333
- Gitiafroz, R., 2012. Microorganisms and Metabolic Pathways Involved in Anaerobic Benzene Biodegradation under Nitrate-Reducing Conditions By Roya Gitiafroz A thesis submitted in conformity with the requirements for the degree of Doctor of Philosophy Graduate Department of Che.
- Glass, C., Silverstein, J., Oh, J., 1997. Inhibition of denitrification in activated sludge by nitrite. *Water Environ. Res.* 69, 1086–1093. doi:10.2175/106143097x125803
- Gray, N.D., Sherry, A., Hubert, C., Dolfing, J., Head, I.M., 2010. Methanogenic degradation of petroleum hydrocarbons in subsurface environments: Remediation, heavy oil formation, and energy recovery, 1st ed, *Advances in Applied Microbiology*. Elsevier Inc. doi:10.1016/S0065-2164(10)72005-0
- Grbic-Galic, D., Vogel, T.M., 1987. Transformation of toluene and benzene by mixed methanogenic cultures. *Appl. Environ. Microbiol.* 53, 254–260.
- Griebler, C., Safinowski, M., Vieth, A., Richnow, H.H., Meckenstock, R.U., 2004. Combined Application of Stable Carbon Isotope Analysis and Specific Metabolites Determination for Assessing In Situ Degradation of Aromatic Hydrocarbons in a Tar Oil-Contaminated Aquifer. *Environ. Sci. Technol.* 38, 617–631. doi:10.1021/es0344516
- Guillén, M.D., Blanco, J., Canga, J.S., Blanco, C.G., 1991. Study of the Effectiveness of 27 Organic Solvents in the Extraction of Coal Tar Pitches. *Energy and Fuels* 5, 188–192. doi:10.1021/ef00025a032

- Haritash, A.K., Kaushik, C.P., 2009. Biodegradation aspects of Polycyclic Aromatic Hydrocarbons (PAHs): A review. *J. Hazard. Mater.* 169, 1–15. doi:10.1016/j.jhazmat.2009.03.137
- Hasegawa, K., Shiojima, S., Koizumi, A., Ikeda, M., 1983. Hippuric acid and o-cresol in the urine of workers exposed to Toluene. *Int. Arch. Occup. Environ. Health* 52, 197–208. doi:10.1007/BF00526518
- Hatheway, A.W., Group, F., 2012. Remediation of Former Manufactured Gas Plants and Other Coal-Tar Sites. *Remediat. Former Manuf. Gas Plants Other Coal-Tar Sites.*
- Head, I.M., Jones, D.M., Larter, S.R., 2003. Biological activity in the deep subsurface and the origin of heavy oil. *Nature* 426, 344–352. doi:10.1038/nature02134
- Hodges, P.W., Richardson, C.A., 1996. EPA method 3550B, Spine (Phila Pa 1976).
- Istok, J.D., Humphrey, M.D., Schroth, M.H., Hyman, M.R., O'Reilly, K.T., 1997. Single-well, "Push-Pull" Test for In Situ Determination of Microbial Activities. *Ground Water*. doi:10.1111/j.1745-6584.1997.tb00127.x
- Jobelius, C., Anneser, B., Griebler, C., Meckenstock, R.U., Reineke, A., Frimmel, F.H., Zwiener, C., 2011a. Supporting Information to the manuscript Metabolites indicate hot spots of biodegradation and biogeochemical monitoring well gradients in a 45, 1–12.
- Jobelius, C., Ruth, B., Griebler, C., Meckenstock, R.U., Hollender, J., Reineke, A., Frimmel, F.H., Zwiener, C., 2011b. Metabolites indicate hot spots of biodegradation and biogeochemical gradients in a high-resolution monitoring well. *Environ. Sci. Technol.* 45, 474–481. doi:10.1021/es1030867
- Johnston, N., Sadler, R., Shaw, G., Connell, D., 1993. Environmental modification of PAH composition in coal tar containing samples. *Chemosphere* 27, 1151–1158. doi:10.1016/0045-6535(93)90163-Y
- Jonker, M.T.O., Koelmans, A.A., 2002. Extraction of polycyclic aromatic hydrocarbons from soot and sediment: Solvent evaluation and implications for sorption mechanism. *Environ. Sci. Technol.* 36, 4107–4113. doi:10.1021/es0103290
- Jonker, M.T.O., Smedes, F., 2000. Preferential sorption of planar contaminants in sediments from Lake Ketelmeer, The Netherlands. *Environ. Sci. Technol.* 34, 1620–1626. doi:10.1021/es9906251
- Kaliampakos, D., Damigos, D., Karachaliou, T., n.d. Using the "dry-tomb" technique in the remediation of heavily contaminated land.
- Kaplan, I.R., Galperin, Y., Lu, S.T., Lee, R.P., 1997. Forensic environmental geochemistry: Differentiation of fuel-types, their sources and release time. *Org. Geochem.* 27, 289–317. doi:10.1016/S0146-6380(97)87941-7
- Kleemann, R., Meckenstock, R.U., 2011. Anaerobic naphthalene degradation by Gram-positive, iron-reducing bacteria. *FEMS Microbiol. Ecol.* 78, 488–

496. doi:10.1111/j.1574-6941.2011.01193.x
- Koolen, H.H.F., Swarthout, R.F., Nelson, R.K., Chen, H., Krajewski, L.C., Aeppli, C., McKenna, A.M., Rodgers, R.P., Reddy, C.M., 2015. Unprecedented insights into the chemical complexity of coal tar from comprehensive two-dimensional gas chromatography mass spectrometry and direct infusion fourier transform ion cyclotron resonance mass spectrometry. *Energy and Fuels* 29, 641–648. doi:10.1021/ef502428d
- Krauss, M., Singer, H., Hollender, J., 2010. LC-high resolution MS in environmental analysis: From target screening to the identification of unknowns. *Anal. Bioanal. Chem.* 397, 943–951. doi:10.1007/s00216-010-3608-9
- Krumholz, Lee R.; Caldwell, Matthew E.; Suflita, J.M., 1996. Biodegradation of BTEX hydrocarbons under anaerobic conditions, in: Crawford, Ronald L.; Crawford, D. (Ed.), *Bioremediation: Principles and Applications*. Cambridge University Press, New York, pp. 61–99.
- Kueper, B., Wealthhall, G., Smith, J., Leharne, S., Lerner, D., 2003. An illustrated handbook of Dense Non-Aqueous Phase Liquids (DNAPL) transport and fate in the subsurface.
- Kümmel, S., Starke, R., Chen, G., Musat, F., Richnow, H.H., Vogt, C., 2016. Hydrogen Isotope Fractionation As a Tool to Identify Aerobic and Anaerobic PAH Biodegradation. *Environ. Sci. Technol.* 50, 3091–3100. doi:10.1021/acs.est.5b04819
- Lane, D., 1991. 16S/23S rRNA sequencing. *Nucleic Acid Tech. Bact. Syst.*
- Langenhoff, A.A.M., 1997. Biotransformation of toluene, benzene and naphthalene under anaerobic conditions.
- Langenhoff, A.A.M., Zehnder, A.J.B., Schraa, G., 1996. Behaviour of toluene, benzene and naphthalene under anaerobic conditions in sediment columns. *Biodegradation* 7, 267–274. doi:10.1007/BF00058186
- Langevoort, M., 2009. Multiphase flow and enhanced biodegradation of dense non-aqueous phase liquids, *Geologica Ultraiectina*.
- Leahy, J.G., Colwell, R.R., 2019. Microbial degradation of hydrocarbons in the ecosystem. *Microb. Action Hydrocarb.* 54, 343–351. doi:10.1007/978-981-13-1840-5_14
- Lee, C.M., Meyers, S.L., Wright, C.L., Coates, J.T., Haskell, P.A., Falta, R.W., 1998. NAPL compositional changes influence partitioning coefficients. *Environ. Sci. Technol.* 32, 3574–3578. doi:10.1021/es980261x
- Lee, Linda S, Rao, P.S.C., Okuda, I., 1992. Equilibrium partitioning of polycyclic aromatic hydrocarbons from coal tar into water - f_es00035a006-Lee Article.pdf 26.
- Lee, L. S., Rao, P.S.C., Okuda, I., 1992. Equilibrium partitioning of polycyclic aromatic hydrocarbons from coal tar into water. *Environ. Sci. Technol.* 26, 2110–2115. doi:10.1021/es00035a006
- Lee, P.-H., 2000. Use of solvents for PAHs extraction and enhancement of the

- PAHs bioremediation in coal-tar-contaminated soils.
- Leeuwen, J.A. Van, Hartog, N., Gerritse, J., Gallacher, C., Helmus, R., Brock, O., Parsons, J.R., Hassanizadeh, S.M., 2020. The dissolution and microbial degradation of mobile aromatic hydrocarbons from a Pintsch gas tar DNAPL source zone. *Sci. Total Environ.* 722, 137797. doi:10.1016/j.scitotenv.2020.137797
- Liu, L., Endo, S., Eberhardt, C., Grathwohl, P., Schmidt, T.C., 2009. Partition behavior of polycyclic aromatic hydrocarbons between aged coal tar and water. *Environ. Toxicol. Chem.* 28, 1578–1584. doi:10.1897/08-276.1
- Liu, T., Zhang, Z., Dong, W., Wu, X., Wang, H., 2017. Bioremediation of PAHs contaminated river sediment by an integrated approach with sequential injection of co-substrate and electron acceptor: Lab-scale study. *Environ. Pollut.* 230, 413–421. doi:10.1016/j.envpol.2017.06.063
- López-Gutiérrez, J.C., Henry, S., Hallet, S., Martin-Laurent, F., Catroux, G., Philippot, L., 2004. Quantification of a novel group of nitrate-reducing bacteria in the environment by real-time PCR. *J. Microbiol. Methods* 57, 399–407. doi:10.1016/j.mimet.2004.02.009
- Lovley, D.R., 1997. Potential for anaerobic bioremediation of BTEX in petroleum-contaminated aquifers. *J. Ind. Microbiol. Biotechnol.* 18, 75–81. doi:10.1038/sj.jim.2900246
- Lunge, G., 1909. *Coal-Tar and Ammonia* (4th ed.). Gurney and Jackson.
- Luo, F., Gitiafroz, R., Devine, C.E., Gong, Y., Hug, L.A., Raskin, L., Edwards, E.A., 2014. Metatranscriptome of an anaerobic benzene-degrading, nitrate-reducing enrichment culture reveals involvement of carboxylation in benzene ring activation. *Appl. Environ. Microbiol.* 80, 4095–4107. doi:10.1128/AEM.00717-14
- Mahjoub, B., Jayr, E., Bayard, R., Gourdon, R., 2000. Phase partition of organic pollutants between coal tar and water under variable experimental conditions. *Water Res.* 34, 3551–3560. doi:10.1016/S0043-1354(00)00100-7
- Maillacheruvu, K.Y., Pathan, I.A., 2009. Biodegradation of naphthalene, phenanthrene, and pyrene under anaerobic conditions. *J. Environ. Sci. Heal. - Part A Toxic/Hazardous Subst. Environ. Eng.* 44, 1315–1326. doi:10.1080/10934520903212956
- McCarthy, J., Zachara, J., 1989. ES&T Features: Subsurface transport of contaminants. *Environ. Sci. Technol.* 23, 496–502. doi:10.1021/es00063a602
- McGregor, L.A., Gauchotte-Lindsay, C., Nic Daéid, N., Thomas, R., Kalin, R.M., Nic, N., Thomas, R., Kalin, R.M., 2012. Multivariate statistical methods for the environmental forensic classification of coal tars from former manufactured gas plants. *Environ. Sci. Technol.* 46, 3744–3752. doi:10.1021/es203708w
- McRae, C., Sun, C.G., Snape, C.E., Fallick, A.E., Taylor, D., 1999. $\delta^{13}\text{C}$ values

- of coal-derived PAHs from different processes and their application to source apportionment. *Org. Geochem.* 30, 881–889. doi:10.1016/S0146-6380(99)00072-8
- Meckenstock, R.U., Annweiler, E., Michaelis, W., Richnow, H.H., Schink, B., 2000. Anaerobic naphthalene degradation by a sulfate-reducing enrichment culture. *Appl. Environ. Microbiol.* 66, 2743–2747. doi:10.1128/AEM.66.7.2743-2747.2000.Updated
- Meckenstock, R.U., Boll, M., Mouttaki, H., Koelschbach, J.S., Cunha Tarouco, P., Weyrauch, P., Dong, X., Himmelberg, A.M., 2016. Anaerobic degradation of benzene and polycyclic aromatic hydrocarbons. *J. Mol. Microbiol. Biotechnol.* 26, 92–118. doi:10.1159/000441358
- Meckenstock, R.U., Elsner, M., Griebler, C., Lueders, T., Stumpp, C., Aamand, J., Agathos, S.N., Albrechtsen, H.-J.J., Bastiaens, L., Bjerg, P.L., Boon, N., Dejonghe, W., Huang, W.E., Schmidt, S.I., Smolders, E., Sørensen, S.R., Springael, D., Van Breukelen, B.M., 2015. Biodegradation: Updating the Concepts of Control for Microbial Cleanup in Contaminated Aquifers. *Environ. Sci. Technol.* 49, 7073–7081. doi:10.1021/acs.est.5b00715
- Meckenstock, R.U., Mouttaki, H., 2011. Anaerobic degradation of non-substituted aromatic hydrocarbons. *Curr. Opin. Biotechnol.* 22, 406–414. doi:10.1016/j.copbio.2011.02.009
- Meckenstock, R.U., Netzer, F. von, Stumpp, C., Lueders, T., Himmelberg, A.M., Hertkorn, N., Schmitt-Kopplin, P., Harir, M., Hosein, R., Haque, S., Schulze-Makuch, D., 2014. Water droplets in oil are microhabitats for microbial life. *Science* (80-.). 345, 673–676.
- Meckenstock, R.U., Warthmann, R.J., Schäfer, W., 2004. Inhibition of anaerobic microbial o-xylene degradation by toluene in sulfidogenic sediment columns and pure cultures. *FEMS Microbiol. Ecol.* 47, 381–386. doi:10.1016/S0168-6496(03)00303-9
- Mercer, R.M.C. & J.W., 1993. DNAPL Site Evaluation. USEPA Publ. EPA/600/R-, 1–369.
- Meyer, S., Steinhart, H., 2000. Effects of heterocyclic PAHs (N, S, O) on the biodegradation of typical tar oil PAHs in a soil/compost mixture. *Chemosphere* 40, 359–367. doi:10.1016/S0045-6535(99)00237-4
- Micic, V., Straub, K., Blum, P., Kappler, A., 2007. Natural attenuation of naphthalene and benzene at a former gasworks site. *Water Sci. Technol. Water Supply* 7, 145–153. doi:10.2166/ws.2007.077
- Mittal, M., Rockne, K.J., 2008. Indole production by *Pseudomonas stutzeri* strain NAP-3 during anaerobic naphthalene biodegradation in the presence of dimethyl formamide. *J. Environ. Sci. Heal. - Part A Toxic/Hazardous Subst. Environ. Eng.* 43, 1027–1034. doi:10.1080/10934520802059896
- Morasch, B., Hunkeler, D., Zopfi, J., Temime, B., Höhener, P., 2011. Intrinsic biodegradation potential of aromatic hydrocarbons in an alluvial aquifer - Potentials and limits of signature metabolite analysis and two stable isotope-

- based techniques. *Water Res.* 45, 4459–4469. doi:10.1016/j.watres.2011.05.040
- Morasch, B., Schink, B., Tebbe, C.C., Meckenstock, R.U., 2004. Degradation of o-xylene and m-xylene by a novel sulfate-reducer belonging to the genus *Desulfotomaculum*. *Arch. Microbiol.* 181, 407–417. doi:10.1007/s00203-004-0672-6
- Müller, J.B., Ramos, D.T., Larose, C., Fernandes, M., Lazzarin, H.S.C., Vogel, T.M., Corseuil, H.X., 2017. Combined iron and sulfate reduction biostimulation as a novel approach to enhance BTEX and PAH source-zone biodegradation in biodiesel blend-contaminated groundwater. *J. Hazard. Mater.* 326, 229–236. doi:10.1016/j.jhazmat.2016.12.005
- Murphy, B.L., Brown, J., 2005. Environmental forensics aspects of PAHs from wood treatment with creosote compounds. *Environ. Forensics* 6, 151–159. doi:10.1080/15275920590952829
- Musser, M.T., 2003. Ullman's Encyclopedia of Industrial Chemistry, (6th ed.). ed. Wiley-VCH Verlag GmbH & Co. KGaA: Weinheim (2005).
- Muyzer, G., Ramsing, N.B., 1995. Molecular methods to study the organization of microbial communities. *Water Sci. Technol.* 32, 1–9. doi:10.1016/0273-1223(96)00001-7
- Nealson, K.H., 1994. Iron and Manganese in Anaerobic Respiration: Environmental Significance, Physiology, and Regulation. *Annu. Rev. Microbiol.* 48, 311–343. doi:10.1146/annurev.micro.48.1.311
- Novotny, M., Strand, J.W., Smith, S.L., Wiesler, D., Schwende, F.J., 1981. Compositional studies of coal tar by capillary gas chromatography mass spectrometry. *Fuel* 60, 213–220. doi:10.1016/0016-2361(81)90182-4
- Ohlenbusch, G., Zwiener, C., Meckenstock, R.U., Frimmel, F.H., 2002. Identification and quantification of polar naphthalene derivatives in contaminated groundwater of a former gas plant site by liquid chromatography-electrospray ionization tandem mass spectrometry. *J. Chromatogr. A* 967, 201–7. doi:http://dx.doi.org/10.1016/S0021-9673(02)00785-9
- Oka, A.R., Phelps, C.D., Zhu, X., Saber, D.L., Young, L.Y., 2011. Dual biomarkers of anaerobic hydrocarbon degradation in historically contaminated groundwater. *Environ. Sci. Technol.* 45, 3407–3414. doi:10.1021/es103859t
- Peng, L., Lin, Y., Meng, F., Wu, J., Zheng, Y., Sun, T., Wang, G., 2021. Environmental fate and aquatic effects of propylbenzenes and trimethylbenzenes: A review. *Chemosphere* 264, 128533. doi:10.1016/j.chemosphere.2020.128533
- Peters, C. a, Luthy, R.G., 1993. Coal-tar dissolution in water-miscible solvents - experimental evaluation. *Environ. Sci. Technol.* 27, 2831–2843. doi:10.1021/es00049a025
- Peters, C.A., Wammer, K.H., Knightes, C.D., 2000. Multicomponent NAPL

- solidification thermodynamics. *Transp. Porous Media* 38, 57–77.
- Phelps, C.D., Young, L.Y., 1999a. Anaerobic biodegradation of BTEX and gasoline in various aquatic sediments. *Biodegradation* 10, 15–25. doi:10.1023/A:1008303729431
- Phelps, C.D., Young, L.Y., 1999b. Anaerobic biodegradation of BTEX and gasoline in various aquatic sediments. *Biodegradation* 10, 15–25. doi:10.1023/A:1008303729431
- Ponsin, V., Coulomb, B., Guelorget, Y., Maier, J., Höhener, P., 2014. In situ biostimulation of petroleum hydrocarbon degradation by nitrate and phosphate injection using a dipole well configuration. *J. Contam. Hydrol.* 171, 22–31. doi:10.1016/j.jconhyd.2014.10.003
- Qin, W., Fan, F., Zhu, Y., Huang, X., Ding, A., Liu, X., Dou, J., 2017. Anaerobic biodegradation of benzo(a)pyrene by a novel *Cellulosimicrobium cellulans* CWS2 isolated from polycyclic aromatic hydrocarbon-contaminated soil. *Brazilian J. Microbiol.* 49, 258–268. doi:10.1016/j.bjm.2017.04.014
- Rahman, W.U., Khan, M.D., Khan, M.Z., Halder, G., 2018. Anaerobic biodegradation of benzene-laden wastewater under mesophilic environment and simultaneous recovery of methane-rich biogas. *J. Environ. Chem. Eng.* 6, 2957–2964. doi:10.1016/j.jece.2018.04.038
- Ramos, D.T., da Silva, M.L.B., Chiaranda, H.S., Alvarez, P.J.J., Corseuil, H.X., 2013. Biostimulation of anaerobic BTEX biodegradation under fermentative methanogenic conditions at source-zone groundwater contaminated with a biodiesel blend (B20). *Biodegradation* 24, 333–341. doi:10.1007/s10532-012-9589-y
- Raptis, P., Gerritse, J., Van Leeuwen, J., Sutton, N., 2015. A microbial analysis to assess the anaerobic degradation of oil/tar contamination in the subsurface Internship Report.
- Richnow, H.H., Meckenstock, R.U., Reitzel, L.A., Baun, A., Ledin, A., Christensen, T.H., 2003. In situ biodegradation determined by carbon isotope fractionation of aromatic hydrocarbons in an anaerobic landfill leachate plume (Vejen, Denmark). *J. Contam. Hydrol.* 64, 59–72. doi:10.1016/S0169-7722(02)00104-3
- Rittman, Bruce E.; Barden, Michael J.; Lovley, Derek; Luthy, Richard G.; Mackay, Douglas M.; Bekins, Barbara, A.; Firestone, Mary K.; Lester, Stephen; Madsen, Eugene; Mccarthy, Perry L.; Poeter, Eileen; Scifield, Robert; Warrick, Arthur W.; Wilson, John, J., 2000. *Natural Attenuation for Groundwater Remediation, Natural Attenuation for Groundwater Remediation.* doi:10.17226/9792
- Rivett, M.O., Buss, S.R., Morgan, P., Smith, J.W.N., Bemment, C.D., 2008. Nitrate attenuation in groundwater: A review of biogeochemical controlling processes. *Water Res.* 42, 4215–4232. doi:10.1016/j.watres.2008.07.020
- Rixey, W., 1999. Comparison of the fixed-bed and batch leaching characteristics of aromatic compounds in residually trapped crude oils and oily wastes. *J.*

- Hazard. Mater. 64, 137–156. doi:10.1016/S0304-3894(98)00231-3
- Rockne, K.J., Chee-Sanford, J.C., Sanford, R.A., Hedlund, B.P., Staley, J.T., Strand, S.E., 2000. Anaerobic naphthalene degradation by microbial pure cultures under nitrate-reducing conditions. *Appl. Environ. Microbiol.* 66, 1595–1601. doi:10.1128/AEM.66.4.1595-1601.2000
- Rogers, S.W., Ong, S.K., Kjartanson, B.H., Golchin, J., Stenback, G.A., 2002. Natural attenuation of polycyclic aromatic hydrocarbon-contaminated sites: Review. *Pract. Period. Hazardous, Toxic, Radioact. Waste Manag.* 6, 141–155. doi:10.1061/(ASCE)1090-025X(2002)6:3(141)
- Röling, W.F.M., Van Verseveld, H.W., 2002. Natural attenuation: What does the subsurface have in store? *Biodegradation* 13, 53–64. doi:10.1023/A:1016310519957
- Rothermich, M.M., Hayes, L.A., Lovley, D.R., 2002. Anaerobic, sulfate-dependent degradation of polycyclic aromatic hydrocarbons in petroleum-contaminated harbor sediment. *Environ. Sci. Technol.* 36, 4811–4817. doi:10.1021/es0200241
- Safinowski, M., 2005. Anaerobic biodegradation of polycyclic aromatic hydrocarbons.
- Safinowski, M., Griebler, C., Meckenstock, R.U., 2006. Anaerobic cometabolic transformation of polycyclic and heterocyclic aromatic hydrocarbons: Evidence from laboratory and field studies. *Environ. Sci. Technol.* 40, 4165–4173. doi:10.1021/es0525410
- Safinowski, M., Meckenstock, R.U., 2006. Methylation is the initial reaction in anaerobic naphthalene degradation by a sulfate-reducing enrichment culture. *Environ. Microbiol.* 8, 347–352. doi:10.1111/j.1462-2920.2005.00900.x
- Sandercocock, P.M.L., Du Pasquier, E., 2003. Chemical fingerprinting of unevaporated automotive gasoline samples. *Forensic Sci. Int.* 134, 1–10. doi:10.1016/S0379-0738(03)00081-1
- Schirmer, M., Dahmke, A., Dietrich, P., Dietze, M., Gödeke, S., Richnow, H.H., Schirmer, K., Weiß, H., Teutsch, G., 2006. Natural attenuation research at the contaminated megasite Zeitz. *J. Hydrol.* 328, 393–407. doi:10.1016/j.jhydrol.2005.12.019
- Schnell, S., Schink, B., 1991. Anaerobic aniline degradation via reductive deamination of 4-aminobenzoyl-CoA in *Desulfobacterium anilini*. *Arch. Microbiol.* 155, 183–190. doi:10.1007/BF00248615
- Schreiber, M.E., Bahr, J.M., 2002. Nitrate-enhanced bioremediation of BTEX-contaminated groundwater: Parameter estimation from natural-gradient tracer experiments. *J. Contam. Hydrol.* 55, 29–56. doi:10.1016/S0169-7722(01)00184-X
- Scow, K.M., Hicks, K.A., 2005. Natural attenuation and enhanced bioremediation of organic contaminants in groundwater. *Curr. Opin. Biotechnol.* 16, 246–253. doi:10.1016/j.copbio.2005.03.009

- Sharak Genthner, B.R., Townsend, G.T., Lantz, S.E., Mueller, J.G., 1997. Persistence of polycyclic aromatic hydrocarbon components of creosote under anaerobic enrichment conditions. *Arch. Environ. Contam. Toxicol.* 32, 99–105. doi:10.1007/s002449900160
- Sjögren, M., Li, H., Rannug, U., Westerholm, R., 1995. A multivariate statistical analysis of chemical composition and physical characteristics of ten diesel fuels. *Fuel* 74, 983–989. doi:10.1016/0016-2361(95)00056-B
- Solís-González, C.J., Loza-Tavera, H., 2019. Alicyclophilus: current knowledge and potential for bioremediation of xenobiotics. *J. Appl. Microbiol.* 126, 1643–1656. doi:10.1111/jam.14207
- Spence, M.J., Bottrell, S.H., Higgo, J.J.W., Harrison, I., 2001. <Journal of Contaminant Hydrology 53 (2001) 305–318.pdf> 53, 305–318.
- Statistics Canada, 2009. Human Activity and the Environment : Annual Statistics. Minist. responsible Stat. Canada 1–168. doi:1703-5783
- Stringfellow, W.T., Aitken, M.D., 1995a. Competitive metabolism of naphthalene, methylnaphthalenes, and fluorene by phenanthrene-degrading pseudomonads. *Appl. Environ. Microbiol.* 61, 357–362. doi:10.1128/aem.61.1.357-362.1995
- Stringfellow, W.T., Aitken, M.D., 1995b. Competitive metabolism of naphthalene, methylnaphthalenes, and fluorene by phenanthrene-degrading pseudomonads. *Appl. Environ. Microbiol.* 61, 357–362.
- Suarez, M.P., Rifai, H.S., 1999. Biodegradation Rates for Fuel Hydrocarbons and Chlorinated Solvents in Groundwater. *Bioremediat. J.* 3, 337–362. doi:10.1080/10889869991219433
- Sublette, K., Peacock, A., White, D., Davis, G., Ogles, D., Cook, D., Kolhatkar, R., Beckmann, D., Yang, X., 2006. Monitoring subsurface microbial ecology in a sulfate-amended, gasoline-contaminated aquifer. *Gr. Water Monit. Remediat.* 26, 70–78. doi:10.1111/j.1745-6592.2006.00072.x
- Swartjes et al., F.A., 2011. Dealing with contaminated soils, *Soil Use and Management*. Springer (Kluwer Academic Publishers). doi:10.1111/j.1475-2743.1991.tb00867.x
- Teng, Y., Luo, Y., Ping, L., Zou, D., Li, Z., Christie, P., 2010. Effects of soil amendment with different carbon sources and other factors on the bioremediation of an aged PAH-contaminated soil. *Biodegradation* 21, 167–178. doi:10.1007/s10532-009-9291-x
- Thomas, R., Brinckerhoff, P., 2014. The Manufactured Gas Industry in Europe.
- Thomas, R., Churchill, S., 2014. Gas production over the last 200 years : friend or foe ? 8–15.
- Tischler, D., 2015. Microbial Styrene Degradation. *SpringerBriefs Microbiol.* doi:10.1007/978-3-319-24862-2
- Tischler, D., Kaschabek, S.R., 2012. Microbial styrene degradation: from basics to biotechnology. *Microb. Degrad. Xenobiotics* 67–99.
- U.S. Department of Defense, 2009. Cost and Performance Report. *Environ.*

- Secur. Technology Certification Progr.
- USEPA, 1998. Guide to documenting and managing cost and performance information for remediation projects.
- Vaidya, S., Devpura, N., Jain, K., Madamwar, D., 2018. Degradation of chrysene by enriched bacterial consortium. *Front. Microbiol.* 9, 1–14. doi:10.3389/fmicb.2018.01333
- Vaidya, S., Jain, K., Madamwar, D., 2017. Metabolism of pyrene through phthalic acid pathway by enriched bacterial consortium composed of *Pseudomonas*, *Burkholderia*, and *Rhodococcus* (PBR). *3 Biotech* 7, 1–15. doi:10.1007/s13205-017-0598-8
- van der Waals, M.J., 2018. Degradation of fuel components. doi:https://doi.org/10.18174/454763
- van der Waals, M.J., Atashgahi, S., da Rocha, U.N., van der Zaan, B.M., Smidt, H., Gerritse, J., 2017. Benzene degradation in a denitrifying biofilm reactor: activity and microbial community composition. *Appl. Microbiol. Biotechnol.* doi:10.1007/s00253-017-8214-8
- van der Zaan, B.M., Saia, F.T., Stams, A.J.M.M., Plugge, C.M., de Vos, W.M., Smidt, H., Langenhoff, A.A.M.M., Gerritse, J., 2012. Anaerobic benzene degradation under denitrifying conditions: Peptococcaceae as dominant benzene degraders and evidence for a syntrophic process. *Environ. Microbiol.* 14, 1171–1181. doi:10.1111/j.1462-2920.2012.02697.x
- van Logtestijn, M., 2017. Natural vs . stimulated anaerobic biodegradation at the tar contaminated site in Amersfoort Internship report.
- Vewin, 2008. Waterleidingstatistiek 2007.
- Vogt, C., Dorer, C., Musat, F., Richnow, H.-H.H., 2016. Multi-element isotope fractionation concepts to characterize the biodegradation of hydrocarbons - from enzymes to the environment. *Curr. Opin. Biotechnol.* 41, 90–98. doi:10.1016/j.copbio.2016.04.027
- Vogt, C., Kleinstuber, S., Richnow, H.H., 2011. Anaerobic benzene degradation by bacteria. *Microb. Biotechnol.* 4, 710–724. doi:10.1111/j.1751-7915.2011.00260.x
- Vogt, C., Musat, F., Richnow, H.-H., 2018. Compound-Specific Isotope Analysis for Studying the Biological Degradation of Hydrocarbons, Anaerobic Utilization of Hydrocarbons, Oils, and Lipids. doi:10.1007/978-3-319-33598-8_18-1
- Volkman, E.W., Rhodes, E.O., Work, L.T., 1936. Physical Properties of Coal Tars Influence of Tar-Insoluble and Solvent-Insoluble Constituents. *Ind. Eng. Chem.* 28, 721–734. doi:10.1021/ie50318a026
- Vries, F. De, 1999. Karakterisering van Nederlandse gronden naar fysisch-chemische kenmerken.
- Wang, M., Guo, B., Huang, Z., Duan, J., Chen, Z., Chen, B., Yao, S., 2010. Improved compatibility of liquid chromatography with electrospray tandem mass spectrometry for tracing occurrence of barbital homologous residues

- in animal tissues. *J. Chromatogr. A* 1217, 2821–2831. doi:10.1016/j.chroma.2010.02.042
- Wang, Y., Prest, H., 2006. Accurate mass measurement on real chromatographic time scale with a single quadrupole mass spectrometer. *Chromatography* 27, 2–7.
- Wang, Z., 1999. Oil spill identification. *Comments. J. Chromatogr. A* 843, 369–411. doi:10.1021/es60085a010
- Wanior, J., Ripper, J., 1993. GC,13C-NMR and IR study of a mixture of waste oil from the old refinery site Pintsch-Oil GmbH i. L. in Hanau, Germany. *Fresenius. J. Anal. Chem.* 347, 423–429. doi:10.1007/BF00635469
- Ward, F.A., 2015. Organic contaminant transport and fate in the subsurface: Evolution of knowledge and understanding. *Water Resour. Res.* 51, 4861–4902. doi:10.1002/2015WR017121. Received
- Weelink, S.A.B., van Eekert, M.H.A., Stams, A.J.M., 2010. Degradation of BTEX by anaerobic bacteria: Physiology and application. *Rev. Environ. Sci. Biotechnol.* 9, 359–385. doi:10.1007/s11157-010-9219-2
- Wege, R., 2005. Heft 143 Untersuchungs- und Überwachungsmethoden für die Beurteilung natürlicher Selbstreinigungsprozesse im Grundwasser von Ralf Wege.
- Widdel, F., Rabus, R., 2001. Anaerobic biodegradation of saturated and aromatic hydrocarbons. *Curr. Opin. Biotechnol.* 12, 259–276. doi:10.1016/S0958-1669(00)00209-3
- Wiedemeier_et_al-1996-Groundwater_Monitoring_&_Remediation (1).pdf, n.d.
- Wiedemeier, Todd H.; Rifai, Hanadi, S.; Newell, Charles J.; Wilsdon, John, T., 1999. Natural attenuation of fuels and chlorinated solvents in the subsurface. John Wiley & Sons inc.
- Wilson, L.P., Bouwer, E.J., 1997. Biodegradation of aromatic compounds under mixed oxygen/denitrifying conditions: A review. *J. Ind. Microbiol. Biotechnol.* 18, 116–130. doi:10.1038/sj.jim.2900288
- Winter, K., Barton, D., Although, C., 1969. Thermal decomposition of benzoic acid.
- Yuan, S.Y., Chang, B. V., 2007. Anaerobic degradation of five polycyclic aromatic hydrocarbons from river sediment in Taiwan. *J. Environ. Sci. Heal. - Part B Pestic. Food Contam. Agric. Wastes* 42, 63–69. doi:10.1080/03601230601020860
- Zamfirescu, D., Grathwohl, P., 2001. Occurrence and attenuation of specific organic compounds in the groundwater plume at a former gasworks site. *J. Contam. Hydrol.* 53, 407–427. doi:10.1016/S0169-7722(01)00176-0
- Zhang, J., Duke, M.C., Northcott, K., Packer, M., Allinson, M., Allinson, G., Kadokami, K., Tan, J., Allard, S., Croué, J.P., Knight, A., Scales, P.J., Gray, S.R., 2017. Small scale Direct Potable Reuse (DPR) project for a remote area. *Water (Switzerland)* 9. doi:10.3390/w9020094
- Zhang, S., Wang, Q., Xie, S., 2012. Stable isotope probing identifies anthracene

- degraders under methanogenic conditions. *Biodegradation* 23, 221–230. doi:10.1007/s10532-011-9501-1
- Zhang, S.Y., Wang, Q.F., Xie, S.G., 2012. Molecular characterization of phenanthrene-degrading methanogenic communities in leachate-contaminated aquifer sediment. *Int. J. Environ. Sci. Technol.* 9, 705–712. doi:10.1007/s13762-012-0098-7
- Zhang, Y.C., Slomp, C.P., Broers, H.P., Passier, H.F., Cappellen, P. Van, 2009. Denitrification coupled to pyrite oxidation and changes in groundwater quality in a shallow sandy aquifer. *Geochim. Cosmochim. Acta* 73, 6716–6726. doi:10.1016/j.gca.2009.08.026
- Zhang, Z., Lo, I.M.C., 2015. Biostimulation of petroleum-hydrocarbon-contaminated marine sediment with co-substrate: involved metabolic process and microbial community. *Appl. Microbiol. Biotechnol.* 99, 5683–5696. doi:10.1007/s00253-015-6420-9
- Zhang, Z., Lo, I.M.C., Yan, D.Y.S., 2015a. An integrated bioremediation process for petroleum hydrocarbons removal and odor mitigation from contaminated marine sediment. *Water Res.* 83, 21–30. doi:10.1016/j.watres.2015.06.022
- Zhang, Z., Lo, I.M.C., Yan, D.Y.S., 2015b. An integrated bioremediation process for petroleum hydrocarbons removal and odor mitigation from contaminated marine sediment. *Water Res.* 83, 21–30. doi:10.1016/j.watres.2015.06.022
- Zhou, H.W., Luan, T.G., Zou, F., Tam, N.F.Y., 2008. Different bacterial groups for biodegradation of three- and four-ring PAHs isolated from a Hong Kong mangrove sediment. *J. Hazard. Mater.* 152, 1179–1185. doi:10.1016/j.jhazmat.2007.07.116